

PŘÍRODOVĚDECKÁ FAKULTA MASARYKOVY UNIVERZITY

ÚSTAV CHEMIE



SUPRAMOLEKULÁRNÍ CHEMIE VÍCEVAZEBNÝCH HOSTUJÍCÍCH MOLEKUL

Supramolecular chemistry of multitopic guests

Habilitační práce

Vědní obor: Organická chemie

Robert Vícha

Loučka 2017

Bibliografický záznam

Autor: Mgr. Robert Vícha, Ph.D.
Fakulta technologická, Univerzita Tomáše Bati ve Zlíně,
Ústav chemie

Název práce: Supramolekulární chemie vícevazebných hostujících molekul

Klíčová slova: Hostitel-host chemie, klecové uhlovodíky, imidazoliové soli, vysoceafinitní hostující molekuly.

Bibliographic Entry

Author: Mgr. Robert Vícha, Ph.D.
Faculty of Technology, Tomas Bata University in Zlín,
Department of Chemistry

Title of Thesis: Supramolecular chemistry of multitopic guests

Keywords: Host-guest chemistry, cage hydrocarbons, imidazolium salts, high-affinity guests

Prohlášení

Prohlašuji, že jsem svoji habilitační práci vypracoval samostatně s využitím informačních zdrojů, které jsou v práci, případně v příložených původních publikacích, citovány.

Loučka 21. srpna 2017

.....
Mgr. Robert Vícha, Ph.D.

OBSAH

POUŽITÉ ZKRATKY A SYMBOLY	7
I. ÚVOD – CESTA K SUPRAMOLEKULÁRNÍ CHEMII.....	9
II. SÉMANTICKÉ POZNAMKY	13
III. KOMENTÁŘ PUBLIKACÍ.....	17
3.1. Předcucurbiturilové období	17
3.2. Rané období imidazoliových solí	20
3.3. Tritopické ligandy	25
3.4. Od adamantanu ke kubanu.....	31
IV. PŘEDMĚTNÉ PUBLIKACE	37
4.1. <i>Supramolecular Chemistry</i> , 2011 , 23, 663–677.....	37
4.2. <i>Supramolecular Chemistry</i> , 2013 , 25, 349–361.....	53
4.3. <i>Chemistry - A European Journal</i> , 2012 , 18, 13633–13637.....	67
4.4. <i>Rapid Commun. Mass Spectrom.</i> , 2017 , <i>accepted</i>	73
4.5. <i>The Journal of Organic Chemistry</i> , 2016 , 81, 9595–9604.....	83
4.6. <i>Journal of Inclusion Phenomena and Macrocyclic Chemistry</i> , 2016 , 84, 11–20	95
4.7. <i>Chemistry - A European Journal</i> , 2015 , 21, 11712–11718.....	107
4.8. <i>RSC Advances</i> , 2016 , 6, 105146–105153	115
4.9. <i>Organic Letters</i> , 2017 , 19, 2698–2701.....	125
V. ZÁVĚR.....	131
VI. SEZNAM POUŽITÉ LITERATURY	133

VYSVĚTLENÍ POUŽITÝCH ZKRATEK A SYMBOLŮ

<i>Ad</i>	adamantan, 1-adamantyl
<i>CB_n</i>	cucurbit[<i>n</i>]uril
<i>CD</i>	cyklodextrin
<i>CDK</i>	cyklin-dependentní kináza
<i>G / H</i>	host / hostitel (z angl. guest / host)
<i>K</i>	asociační konstanta
<i>NHC</i>	<i>N</i> -heterocyklické karbeny
<i>PC</i>	balící koeficient (z angl. packing coefficient)

I. STRUČNÝ POPIS MÉ CESTY OD ADAMANTANU K SUPRAMOLEKULÁRNÍ CHEMII

V době, kdy jsem začínal intenzívně studovat odbornou literaturu, abych se dozvěděl potřebné informace, či abych získal vzor pro pokusy o sepsání vlastních výzkumných výsledků, jsem byl nadšen tím, jak to jiným autorům pěkně vychází. Oni si vymyslí, že objeví jev A, připraví látku B, nebo něco na ten způsob, pak to jednoduše vyzkouší, vše se chová, jak má, původní hypotézy se potvrdí a nakonec o tom napíše ten článek. Zpočátku mne trochu trápilo, že mně to v laboratoři tak pěkně nefunguje, ale později jsem pochopil, že notná část výsledků je zasazena do širšího rámce *ex post*, zřetelné souvislosti a logická přímočarost se mnohdy vynoří až při sepisování oné publikace. Příběh o tápání a nejistotě, slepých uličkách a nezdařených experimentech, ale bohužel ani o těch momentech, které dělají z vědy lákavé dobrodružství, o chvílích kdy něco konečně pochopíme, kdy se atomy konečně poskládají, jak my chceme, molekuly seřadí a vyrostou vytoužený monokrystal, tento příběh se do odborné literatury, jak se zdá, nehodí. Skutečnost žitá v laboratořích a za psacím stolem je tedy jiná, než ta odborně publikovaná, nikoliv méně vědecká, ale mnohem klikatější, a proto snad i mnohdy poučnější. Protože ale tento text je habilitační prací, tedy snahou o získání pedagogické hodnosti, dovoluji si zdvořile čtenáře žádostivého odborných detailů odkázat na přetištěné předmětné publikace a v následujících kapitolách se budu soustředit na osobní pohled, na motivy a úvahy, které mne během posledních let dovedly až k sepsání tohoto textu.

Ke sloučeninám adamantanu jsem se poprvé dostal během své diplomové práce na PřF MU. Profesor Potáček mi nabídl dvě témata: studium criss-cross cykloadičních reakcí nebo vývoj nového univerzálního postupu přípravy 1-adamantyl(alkyl)ketonů. Druhé zmíněné téma se mělo řešit ve spolupráci s tehdejší výzkumným oddělením firmy Lachema a případný nový postup měl být využit při průmyslové výrobě léčivých substancí, analogů Rimantadinu®. Nerozhodoval jsem se dlouho, vyhrály léčivé látky a ta krásná uhlovodíková klec. Na zvoleném tématu jsem pokračoval i během doktorského studia a výsledkem byla jednoduchá, levná a univerzální metoda pro přípravu 1-adamantyl(alkyl/aryl)ketonů reakcí adamantan-1-karbonylchloridu s příslušným Grignardovým činidlem za katalýzy $Al^{III}/Cu^I/Li^I$. V důsledku postupného rozkladu podniku Lachema se mnou vyvinutá metoda do praxe nezavedla, ale s kolegy ji v laboratoři stále s úspěchem používáme k syntéze výchozích látek pro náš výzkum.

Ještě před ukončením doktorského studia jsem nastoupil jako asistent na Fakultu technologickou Univerzity Tomáše Bati ve Zlíně. Přijetí této pozice jsem podmínil možností nadále pracovat na svých výzkumných tématech, v první řadě pak na dokončení disertační práce. Výsledkem tohoto období byly dvě originální publikace o výše zmíněné metodě přípravy ketonů¹ a detailní rozbor možných

vedlejších produktů.² Podstatnou část teoretické části své disertační práce zabývající se výskytem a původem sloučenin adamantanu v přírodě jsem opublikoval v Chemických Listech.³ Během dopisování disertační práce jsem se porozhlížel, kterým směrem bych se měl se svými deriváty adamantanu vydat, a zaujala mne práce prof. Strnada z Ústavu experimentální botaniky AV ČR v Olomouci na purinových růstových regulátorech. Rozhodl jsem se vytvořit sérii těchto purinů vhodně substituovaných adamantanovým zbytkem a studovat jejich biologickou aktivitu v závislosti na supramolekulární komplexaci s β -cyklodextrinem. Poslední mou publikovanou prací z před-supramolekulárního období je rozbor podmínek a související regioselektivity při elektrofilní aromatické substituci (nitraci) různých 1-adamantylalkyl(aryl)ketonů.⁴ Následující publikace, které jsou již předmětem této habilitační práce, obsahují vždy kromě syntetické části i supramolekulární studie a jsou komentovány v tomto textu.

Kromě hlavního tématu mé vědecké práce, kterým se postupem času stala syntéza a studium supramolekulárního chování vícevazebných hostujících molekul s akcentem na vazebná místa na bázi klecových uhlovodíků, jsem se i nadále mírně věnoval studiu mechanismu vzniku jednoho minoritního vedlejšího produktu vznikajícího při reakci benzylových Grignardových činidel s acylchloridy,⁵ přípravě heterocyklů substituovaných adamantanem⁶ a vzhledem k zaměření většiny výzkumných skupin na FT UTB více či méně na polymery jsem se zapojil do některých výzkumných aktivit kolegů v této oblasti.⁷ Ostatně k aplikacím v komplexních supramolekulárních systémech zahrnujících i modifikované biopolymery směřuje i můj současný hlavní výzkum.

II. NĚKOLIK SÉMANTICKÝCH POZNÁMEK

Ve své práci vycházím z jednoho ze základních konceptů supramolekulární chemie, kterým je vztah mezi dvěma molekulárními entitami označovanými jako hostitel (anglicky „host“) a host (anglicky „guest“). Tento náhled na mezimolekulární vztahy je pak označován jako hostitel-host chemie (anglicky „host-guest chemistry“). Výklad označení jednotlivých partnerů v tomto vztahu vychází z podoby jednoduchých hostitel-host komplexů. Jako hostitel bývá označována zpravidla větší molekula s prostorově vymezeným vazebným místem. Klasickým příkladem je makrocyclická sloučenina s vazebným místem v podobě dutiny. Host je pak molekula zpravidla menší, která v komplexu buď svojí převážnou většinou, či alespoň podstatnou částí preferuje pobyt ve vazebném místě, dutině, hostitele. V biochemii pak tvoří klasický analogický pár proteinový receptor a nízkomolekulární substrát. Jakmile však pokročíme od jednoduchých komplexů se stechiometrií 1:1 ke složitějším agregátům, dostáváme se s těmito pojmy, ve smyslu jejich základních významů, do úzkých. Pokud v komplexu vystupuje více menších molekul obsazujících současně dutinu makrocycly, je ještě vše v pořádku. Jedna hostitelská molekula hostí více hostů. V opačném případě, když jedna molekula hosta disponuje více vazebnými místy, dojde v případě jejich obsazení hostiteli k absurdní situaci, kdy se při jedné příležitosti sejde více hostitelů než hostů. Protože se velkou měrou zabývám právě hosty s více vazebnými místy, dostávám se při popisu vazebného chování do nepřehledných situací, když například musím tvrdit, že zkoumaná molekula je hostem jednoho hostitele a pak, případně současně i druhého hostitele. Mnohem jednodušší mi připadá přijmout obecně platný smysl slov hostitel a host a označovat tak, v uvedeném pořadí, vždy právě tu jednu molekulu, která hostí více jiných molekul, a je jedno zda ve své dutině, nebo například na sobě navlečených. Chápu ovšem, že tento přístup bude narážet na obecné zvyklosti v supramolekulární chemii a proto budu všude tam, kde to bude jen trochu možné, používat neutrální výrazy „makrocycly“ a „ligand“. Oprávněnost použití druhého uvedeného může být zejména anorganickými chemiky zpochybněna. Ovšem v širším smyslu slova a zejména v biochemickém kontextu je termín „ligand“, použitý pro molekulu vázanou například v kavitě makrocycly nebo vazebném místě proteinu, oprávněný a i z hlediska chemické terminologie v pořádku*.

Druhý problém, se kterým se dlouhodobě setkávám, a nutno dodat neúspěšně bojuji, je vyjadřování počtu komponent ve složitějších (než 1:1) supramolekulárních agregátech. Pro nejjednodušší hostitel-host komplex se stechiometrií 1:1 se

* IUPAC. Compendium of Chemical Terminology, 2nd ed. (the "Gold Book"). Compiled by A. D. McNaught and A. Wilkinson. Blackwell Scientific Publications, Oxford (1997). XML on-line corrected version: <http://goldbook.iupac.org> (2006-) created by M. Nic, J. Jirat, B. Kosata; updates compiled by A. Jenkins. ISBN 0-9678550-9-8. <https://doi.org/10.1351/goldbook>.

celkem logicky někdy používá označení „binární komplex“. Jakmile jsou však v komplexu zapojeny více jak dvě molekulární entity, dostává se v literatuře obecně používaná terminologie do sporu s logikou věci, jež má ostatně oporu v jiné oblasti chemie. Dle mého názoru je správné označovat komplexy G:H se stechiometrií 2:1 nebo 1:2 stále jako binární, nikoliv, jak je běžné v literatuře, jako komplexy ternární. Jsou totiž složeny stále jen ze dvou různých stavebních kamenů, jejichž poměr vždy v chemii vyjadřujeme nějakým číselným doplňkem (stechiometrickými koeficienty). Označení takového například 1:2 komplexu pojmem „ternární“ nutně vyžaduje další rozšiřující dovysvětlení rozdílu od, podle mne skučně ternárního, komplexu, například G₁:G₂:H v poměru 1:1:1. To je v literatuře řešeno předřazeným slovem vyjadřujícím heterogenitu uskupení. Komplex G₂@H* je pak označován jako „homo-ternární“ a komplex (G₁,G₂)@H jako „hetero-ternární“. Pokud ovšem zvýšíme komplexitu tohoto problému už jen o jednotku, uvedený systém selže. Nedokáže totiž jednoznačně rozlišit komplex 1:1:1:1 od 1:2:1 (oba komplexy by se označovaly jako hetero-kvartérní). Navíc se nedomnívám, že by zastánci tohoto nepovedeného systému označovali učebnicový příklad supramolekulárního agregátu – dimer kyseliny octové – jakožto homo-binární komplex. V analogii k označování sloučenin binárních (CO, CO₂, H₂O, H₂O₂) a ternárních (NaOH, H₃BO₃, SOCl₂) si dovolím volit v následujícím textu systém označování komplexů tak, že slovem „binární“, „ternární“, „kvartérní“ atd..., budu vyjadřovat počet různých druhů stavebních kamenů a počet těchto komponent budu v nutných případech upřesňovat vyjádřením stechiometrického poměru. Váženému čtenáři se omlouvám za mírné zmatení, neboť v přetisknutých původních pracích jsem byl recenzenty donucen používat výše diskutovaný, dle mého, nevhodný systém.

Poslední poznámku v této kapitole chci věnovat vysvětlení vyjadřování základních geometrických poměrů v komplikovanějších komplexech. Pro jednotlivá vazebná místa vícevazných ligandů používám buď symbol vyjadřující obecnou topicitu (například centrální vazebné místo = C, koncové vazebné místo = T) nebo základní strukturní rys tohoto místa (adamantanové místo = Ad, butylové místo = Bu,...). Polohu makrocycly v komplexu pak vyjadřuji značkou místa v horním indexu. Například ligand **G** se dvěma různými vazebnými místy,

* Pro vyjadřování existence atraktivní interakce mezi molekulárními komponentami supramolekulárních agregátů se v literatuře používá několik symbolů. Někteří autoři vyjadřují existenci inkluzního komplexu matematickým symbolem pro podmnožinu, tedy $G \subset H$ ve významu "G je obsažen v H". Vzhledem k samotnému vlastnímu matematickému významu symbolu („ \subset “ = „je podmnožinou“) mi tento způsob zápisu nepřipadá šťastný; jakpak by mohla být jedna diskrétní molekula podmnožinou jiné? V tomto textu se budu držet častěji používaného symbolu „@“ pro explicitní vyjádření inkluzního komplexu, tedy G@H ve smyslu G je inkludováno v H. V případě nejisté povahy diskutovaného komplexu, případně pro explicitní vyjádření neinkluzní povahy asociátu budu používat symbol „·“, tedy G·H ve smyslu nespécifický agregát G a H.

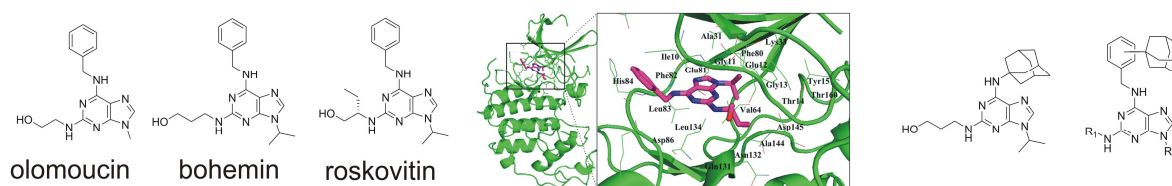
jedním na bázi adamantanu a druhým na bázi butylu může teoreticky tvořit komplex $G@(\beta\text{-CD}^{\text{Ad}}, \text{CB7}^{\text{Bu}})$, tedy s $\beta\text{-CD}$ vázaným na adamantanové místo a CB7 vázaným na místo butylové.



III. KOMENTÁŘ PUBLIKACÍ TVOŘÍCÍCH PODSTATU TÉTO HABILITAČNÍ PRÁCE

3.1 Před cucurbiturilové období

Jak jsem již zmínil v úvodu, prvním impulzem, který mne nasměroval do oblasti supramolekulární chemie, byla snaha o přípravu modifikovaných inhibitorů cyklin-dependentních kináz (CDK) v té době intenzivně studovaných výzkumnou skupinou jejich objevitele, prof. Strnada z Olomouce. Racionální opodstatnění snahy zavést do molekul zmíněných inhibitorů 1-adamantylový substituent spočívá ve dvou již dříve popsanych jevech. Jednak je známo, že adamantan, jakožto uhlovodík $C_{10}H_{16}$, je lipofilní povahy a tudíž může jeho přítomnost v molekule aktivní látky zvýšit prostupnost takto modifikovaných molekul přes buněčné membrány. Zcela opačného efektu, tedy zvýšení rozpustnosti modifikovaného léčiva ve vodném prostředí, lze docílit opět pomocí lipofilního adamantanového substituentu. Deriváty adamantanu jsou známé svou schopností tvořit jedny z nejstabilnějších hostitel-host komplexů s β -cyklodextrinem (β -CD).⁸ Tento makrocyklus, odvozený od α -D-glukózy, zcela biokompatibilní, netoxický a relativně dobře rozpustný ve vodě, je uvedenými vlastnostmi předurčen pro farmaceutické a medicínské aplikace.⁹



Obrázek 1 Známé inhibitory CDK, roskovitine v aktivním místě CDK2 (převzato z referencie¹⁰) a adamantanem modifikované purinové inhibitory CDK.

Všechny aktivní látky, které jsme zamýšleli modifikovat adamantanem, patří do rodiny 2,6,9-trisubstituovaných purinů. Struktury nejznámějších zástupců jsou uvedeny v levé části Obrázku 1. Díky tomu, že jsou známé, alespoň některé, cílové enzymy těchto látek (CDK2, CDK7, CDK9,...) včetně prostorové struktury a orientace inhibitoru v aktivním místě enzymu, je možné navrhnout vhodné polohy pro substituci tak, aby nedošlo k omezení vazby farmakoforu do aktivního místa enzymu. Z krystalografické analýzy komplexu roskovitinu v aktivním místě lidské CDK2, je zřejmé, že roskovitine je zanořen do aktivního místa substituenty na C2 a N9, zatímco $-NHBn$ substituent na C6 směřuje portálem vazebného místa do vnějšího prostředí (Obrázek 1).^{10,11} Tato orientace je společná většině odvozených inhibitorů, a proto jsme se rozhodli zavést adamantanový skelet do substituentu v poloze C6. Na tomto místě je třeba poznamenat, že ve výzkumné skupině prof. Strnada byl již dříve připraven analog s 1-adaman-

tylaminovým substituentem v poloze C6, ale u této látky nebyla pozorována žádná inhibiční aktivita vůči CDK1 ani CDK2,¹² přestože vykazuje nezanedbatelnou cytotoxicitu.¹³ Ztrátu očekávané biologické aktivity lze oprávněně připisat na vrub objemnému adamantanovému substituentu, který je pravděpodobně příliš blízko vlastnímu purinovému farmakoforu a blokuje tak efektivní usazení ve vazebném místě enzymu. Logicky jsme se tedy v naší práci zaměřili na připojení adamantanového skeletu na purin prostřednictvím spojek, které udrží adamantanovou klec dostatečně daleko od portálu aktivního místa. K přípravě stavebních bloků zahrnujících adamantanové vazebné místo pro β -CD, různě dlouhou a různě polární spojku a funkční skupinu vhodnou pro navázání na purinový skelet (aminoskupinu, viz níže) jsme pak využili dosavadní poznatky v oblasti přípravy adamantyl(alkyl/aryl)ketonů a jejich nitrací.

Nutným krokem před samotnou přípravou modifikovaných purinových inhibitorů bylo vytipování vhodných chemických prekurzorů. Protože obvyklou výchozí látkou pro 2,6,9-trisubstituované puriny je 9-alkyl-2,6-dichlorpurin, který postupně reaguje s aminy v poloze C6 a posléze v poloze C2, zaměřili jsme pozornost na přípravu série různě polárních anilinů a benzylaminů, jejichž společným rysem byla přítomnost adamantanové klece. Na těchto aminech jsme dále studovali vliv polarity okolí adamantanové klece na stabilitu supramolekulárních komplexů s β -CD. Postup přípravy série anilinů a benzylaminů je spolu s výsledky příslušných supramolekulárních studií popsány ve dvou publikacích, které jsou součástí této habilitační práce (Publikace 4.1 a Publikace 4.2). Ze supramolekulárního hlediska byla v této době aktuální otázka přesného uspořádání komplexů cyklodextrinů s ligandy obsahujícími objemnou adamantanovou klec a na ni napojený delší substituent. I když to zcela jistě není fundamentální záležitost, určení geometrie komplexů v roztoku a vyřešení související nejistoty, zdali může, a případně za jakých podmínek, adamantanová klec projít skrz kavitu β -CD, mělo zásadní význam pro návrh struktury ligandů i případných polymerů modifikovaných cyklodextriny (nebylo například jasné, zda je třeba napojovat CD jednotku na polymer prostřednictvím primárního nebo sekundárního portálu). Přestože cyklodextrin disponuje vodíkovými atomy v kavitě, není určení prostorové orientace ligandu triviální problém jednak z důvodu relativně malých vzdáleností mezi jednotlivými interními protony kavity a jisté dynamiky ligandu v kavitě a rovněž relativně malé rozdíly v chemických posunech signálů interních vodíkových atomů neusnadňují jednoznačné přiřazení interakčních píků v NOESY/ROESY spektrech. Nám se podařilo jednoznačně určit geometrii našich komplexů kombinací HSQC a NOESY sekvencí, kdy jsme sledovali korelace mezi protony ligandu a uhlíkovými atomy cyklodextrinu. Otázku samotného průchodu adamantanové klece kavitou β -CD jsme poté již neřešili, protože kladná odpověď nepřímo vyplynula z publikace jiných autorů.¹⁴

Poslední část tohoto projektu, tedy navázání připravených aminů na purinový skelet v poloze C6, substituce atomu chloru v poloze C2 3-aminopropan-1-olem a studium biologické aktivity těchto modifikovaných inhibitorů je v podstatě hotova, ale zatím nebyla publikována. Rukopis je ovšem aktuálně připravován k zaslání do redakce k posouzení. Podařilo se nám připravit sérii derivátů purinu s adamantanovým substituentem v poloze 6, které vykazovaly jen málo ovlivněnou biologickou aktivitu v *in vitro* testech inhibice CDK ve srovnání s analogy bez adamantanového substituentu. V některých případech byl dokonce inhibiční účinek nových derivátů vyšší. Při testování cytotoxicity samotných purinů a jejich 1:1 směsí s β -CD proti dvěma liniím nádorových buněk (K-562, MCF-7) jsme sice zaznamenali mírné zvýšení hodnot GI_{50} pro směsi s cyklodextrinem, což se dá vysvětlit nižší dostupností zakomplexovaného purinového derivátu, ale na druhou stranu se pozitivně projevilo vliv komplexace na rozpustnost testovaných látek. Díky tomu jsme mohli pozorovat reálné inhibiční koncentrace i u látek velmi málo rozpustných.

3.2 Rané, řekněme adamantanové, období imidazoliových solí

Již poměrně brzy po zahájení prací na modifikaci výše zmíněných bioaktivních látek pomocí derivátů adamantanu bylo zřejmé, že toto téma nebude natolik silné, aby se mohlo stát jediným dlouhodobým zaměřením mé výzkumné skupiny. Přestože myšlenka cíleného zavedení adamantanového skeletu do struktury inhibitorů CDK vycházející ze znalosti struktury těchto kináz a studium biologické aktivity takto upravených látek byla v pořádku, nemohli jsme v dlouhodobém horizontu konkurovat větším a zavedeným laboratořím. Navíc celkové zaměření Fakulty technologické ve Zlíně nezaručovalo trvalou podporu takovému ryze chemickému a medicíně zaměřenému výzkumnému programu. Proto jsem se začal někdy těsně před rokem 2010 zabývat myšlenkou na rozšíření výzkumných aktivit do oblasti více příbuzné aktivitám jiných výzkumných skupin na FT, konkrétně do oblasti chemie polymerních systémů. Protože jsem se ale nehodlal vzdát, pro mne osobně velmi zajímavého hraničního oboru supramolekulární chemie a snad i proto, že v té době velmi dobře známé supramolekulární vlastnosti adamantanových derivátů tímto směrem přímo ukazovaly, jsem se rozhodl věnovat se syntéze a popisu vlastností nových látek se dvěma (popřípadě i s více) adamantanovými skelety v molekule. Využití takových látek při tvorbě například supramolekulárních hydrogelů s vlastnostmi regulovatelnými pomocí chemických signálů bylo nasnadě.

Aby byly naše více vazebné ligandy široce uplatnitelné, chtěli jsme již od počátku zajistit jejich kompatibilitu (tedy rozpustnost a dlouhodobou stabilitu) s vodným prostředím. Kromě vyloučení hydrolyzovatelných skupin bylo nutné zajistit rozpustnost ligandů ve vodě v koncentracích postačujících k tvorbě požadovaných supramolekulárních struktur. Protože adamantanový skelet je lipofilní a jako takový k rozpustnosti ve vodě nepřispívá, zaměřili jsme od počátku svou pozornost na hydrofilní spojky, kterými jsme hodlali spojovat adamantanová vazebná místa k sobě. Po několika neúspěšných pokusech se spojkami na bázi kyseliny vinné či oligo(oxyethan-1,2-diyly) jsme se zaměřili na deriváty imidazoliových solí. Kromě nesporně polárního charakteru a tím podpořené rozpustnosti ve vodném prostředí, jsou tyto látky zajímavé minimálně ze dvou dalších důvodů. Prvním je již delší dobu známé využití některých imidazoliových solí v oblasti zelené chemie jakožto netěkavých vysoce polárních rozpouštědel (iontové kapaliny) s přesahem využití ke katalýze protických dějů či ke katalýze mezifázového přenosu. Kromě toho mohou imidazoliové soli sloužit jako zdroj tak zvaných *N*-heterocyklických karbenů (NHC), které sice nejsou samy o sobě moc stabilní,*

* Za poznámku stojí skutečnost, že první připravený, při pokojové teplotě stabilní NHC, byl odvozený od 1,3-bis(1-adamantyl)imidazolium-chloridu,¹⁵ přičemž za jeho nereaktivitu jsou zodpovědné právě ony objemné adamantanové substituenty.

ale mohou být využity jako elektron donory při koordinaci kovů či kovových iontů. Takto připravené NHC komplexy byly studovány jako katalyzátory celé řady chemických reakcí. Tato vícepolná atraktivita imidazoliových solí, a zejména úspěšné předběžné pokusy o přípravu adamantanem substituovaných imidazolií, nás přivedly k dlouhodobějšímu a systematictějšímu zájmu o tyto látky.

Až do přípravy prvních adamantanem substituovaných imidazoliových solí jsme uvažovali pouze o supramolekulárních komplexech s cyklodextriny. Nicméně orientace na kationtové ligandy nás postupně přivedla k zájmu i o interakce s hostitelskými molekulami z velmi dynamicky se rozvíjející rodiny cucurbit[*n*]urilů (CB*n*). Homology cucurbit[*n*]urilů kde *n*=7 či 8 totiž, kromě toho, že obdobně jako cyklodextriny, vážou relativně pevně objemné uhlovodíkové klece uvnitř kavity makrocyclu, mohou svými silně elektronegativními portály koordinovat jak anorganické tak organické kationty. V současné době je známa celá řada různých analogů a odvozených struktur, jejichž ucelený přehled publikoval před nedávnem Nau a Assaf.¹⁶ Hledání nejlepší vzájemné komplementarity mezi CB*n*, konkrétně CB7, a vhodným ligandem vyústilo v přípravu derivátu diamantanu nesoucího v polohách 4 a 9 trimethylamoniovou skupinu. Uhlovodíková klec tohoto ligandu totiž velmi přesně vyplňuje kavitu CB7 a navíc umožňuje umístění dvou kationtových substituentů v podélné ose klece s N⁺...N⁺ vzdáleností 7,8 Å, což přibližně odpovídá ideální vzdálenosti dvou volných kationtů vázaných v protilehlých portálech CB7. Komplex tohoto ligandu s CB7 vykazuje dosud nejvyšší známou asociační konstantu s hodnotou $7,2 \times 10^{17} \text{ M}^{-1}$ v čisté D₂O a to jak mezi synteticky připravenými hostitel-host systémy, tak mezi v přírodě zastoupenými vazebnými partnery. Tato krátká odbočka měla čtenáři demonstrovat potenciál kationtových derivátů adamantanu, které sice nedosahují výše zmíněných extrémních hodnot, neboť adamantan je menší než diamantan a nevyplňuje tedy zcela ideálně kavitu CB7 a navíc neumožňuje axiální disubstituci, ale i běžné hodnoty asociační konstanty okolo 10^{12} M^{-1} umožňují konstrukci zajímavých supramolekulárních systémů.

Naše angažmá v supramolekulární chemii imidazoliových solí substituovaných adamantanem exemplárně vypovídá o časté nepřímocarosti výzkumu v přírodních vědách. Důsledkem je pak, alespoň v našem případě, nelogická časová posloupnost zveřejňování výsledků, přičemž mnohé zajímavé výsledky z raných fází našeho výzkumu v této oblasti stále na kompletní systematizaci a zveřejnění (možná marně) čekají.

Původním cílem v raných fázích výzkumu imidazoliových solí bylo připravit sérii ligandů s jedním adamantanovým vazebným místem a jedním dalším místem na bázi lineárních alkylů. Jako doplněk k těmto heteroditopickým ligandům jsme zamýšleli připravit modelové ligandy obsahující pouze adamantanové místo, neboť adamantanem substituované imidazoliové soli nebyly do té doby ze supra-

molekulárního hlediska studovány. Na tuto práci měla navázat studie homoditopických ligandů se dvěma adamantanovými vazebnými motivy a dvěma imidazoli. Ovšem dávno před tím, než jsme dokončili přípravu ucelené série výše zmíněných heteroditopických ligandů, jsme při předběžných studiích homoditopických bisimidazolií pomocí ESI MS zjistili velmi zajímavé chování v plynné fázi, spočívající ve změně fragmentačních drah volného a CB7 komplexovaného ligandu v závislosti na sterickém bránění molekuly ligandu. Nutno podotknout, že v té době se řada odborníků na chování supramolekulárních agregátů v plynné fázi (například prof. Schalley z Berlína*) bavila myšlenkou na rozpoznání vazebných modů, tedy ve smyslu určení pozice makrocyklu na multitopickém ligandu, pomocí MS. V kontextu těchto snah bylo naše zjištění, že způsob fragmentace ligandu komplexovaného v CB7 se mění se sterickým bráněním volnému pohybu makrocyklu po osičce ligandu, pozoruhodné, a proto jsme se rozhodli tyto výsledky velmi rychle systematizovat a sepsat krátké sdělení (viz Publikace 4.3) zaměřené pouze na MS analýzy komplexů našich homoditopických ligandů s CB7. Problematiku jsme se později pokusili rozpracovat podrobnějším rozkrytím mechanismu fragmentace samotných ligandů a popisem role makrocyklu při alternativní fragmentaci. K tomu účelu jsme připravili sérii stericky nebráněných a středně bráněných ligandů selektivně značených ve třech vytipovaných polohách deuteriem. Podrobným, a nutno přiznat, že mnohdy úmorným, rozбором fragmentačních spekter těchto šesti ligandů jsme dospěli k formulaci několika, dle našeho soudu, zajímavých závěrů popsanych v Publikaci 4.4. Nejvýznamnější hypotéza vysvětlující naše pozorování předpokládá dvě vazebné geometrie adamantanového ligandu v kavitě CB7. Netvrdíme, že se nutně jedná o dva odlišné vazebné mody ve smyslu geometrií ležících v lokálních energetických minimech, ale minimálně naznačujeme schopnost adamantanové klece oscilovat uvnitř CB7 mezi pozicemi, z nichž každá vede k jiné fragmentační dráze. Tento projekt, tedy studium fragmentace homoditopických bisimidazolií v plynné fázi pokračuje aktuálně přípravou obdobných ligandů se sterickou zábranou ve středu osičky ligandu a rovněž přípravou série heteroditopických bisimidazolií se dvěma různě stericky náročnými adamantanovými vazebnými motivy.

Na nějaký čas jsme tedy byli nuceni upozadit druhý raný projekt, týkající se heteroditopických imidazoliových solí s jedním adamantanovým ligandem. Nakonec se nám ale podařilo připravit ucelenou sérii žádaných ditopických i příslušných modelových monotopických ligandů. Poněkud mimo původní plán jsme se rozhodli doplnit zamýšlenou jednoduchou studii supramolekulárního chování uvedených ligandů s jednotlivými makrocykly o studii ternárních systémů, tedy systémů obsahujících ligand a dva různé makrocykly. Nutno přiznat,

* <http://www.bcp.fu-berlin.de/en/chemie/chemie/forschung/OrgChem/schalley>

že nikoliv zcela předem plánovaným, ale zato nesmírně důležitým, právě pro chování ve složitějších systémech, strukturním rysem série našich ligandů byla vazba adamantanové klece na imidazolium prostřednictvím dvou různých spojek. První byl methylenový můstek, druhá byla výrazně delší a sestávala z benzenového jádra 1,4-disubstituovaného methylem a karbonylem (struktury viz Schéma 1).

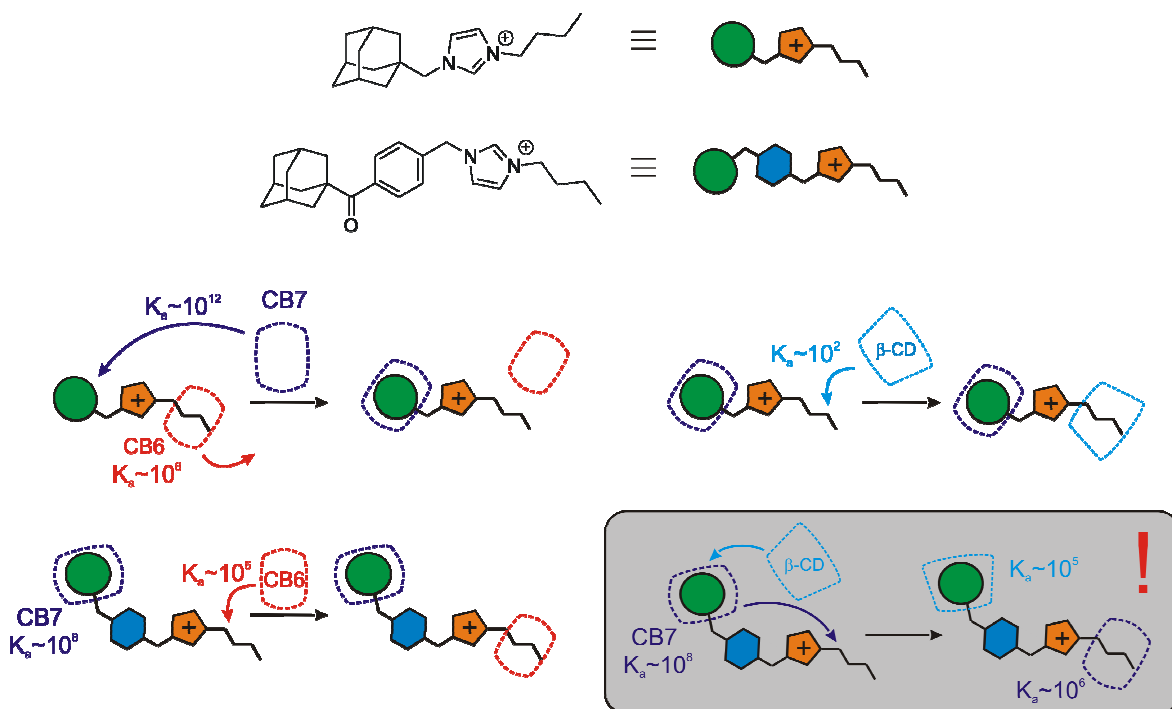


Schéma 1 Chování heteroditopických ligandů v ternárních systémech

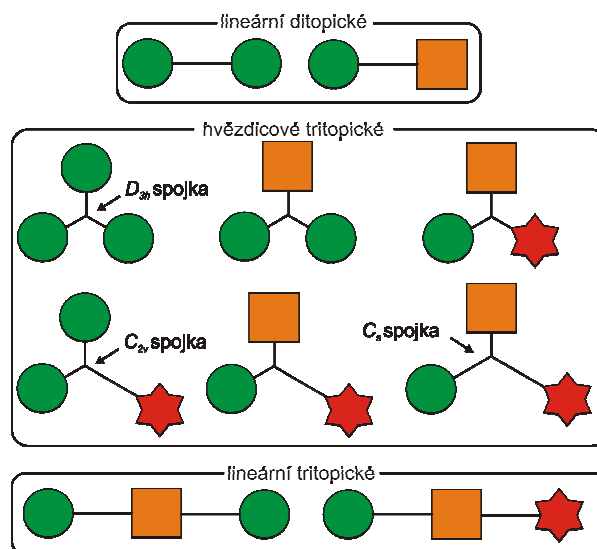
Adamantanová klec sama o sobě vykazuje silnou afinitu k CB7 ($K \sim 10^8 \text{ M}^{-1}$) i k β -CD ($K \sim 10^5 \text{ M}^{-1}$). Pokud se v blízkosti klece nachází kladně nabitá skupina, vzroste asociační konstanta k CB7 až na 10^{12} M^{-1} zatímco afinita k β -CD je přítomností kladného náboje dotčena jen minimálně. Nými připravené ligandy se dvěma vazebnými místy ale pouze jedním imidazoliem, pak dokázaly, v závislosti na délce spojky mezi adamantanem a imidazoliem, komplexovat buď dva makrocykly CB_n v případě dlouhé spojky, nebo pouze jeden makrocyklus v případě spojky krátké. Toto bylo způsobeno tím, že při vazbě CB7 na adamantanové vazebné místo vzdálené od imidazolia se neuplatňovala ion-dipólová interakce portálu CB7 s imidazoliem a takové ligandy tedy mohly relativně pevně vázat i druhý CB_n na butylové místo za vzniku binárních komplexů $\text{G} @ (\text{CB7}^{\text{Ad}}, \text{CB7}^{\text{Bu}})$, případně ternárních komplexů $\text{G} @ (\text{CB7}^{\text{Ad}}, \text{CB6}^{\text{Bu}})$. Díky modelovým ligandům jsme mohli kvantifikovat repulzi mezi dvěma cucurbiturily vázanými na ligand. Na-

proti tomu ligandy s krátkou spojkou umožňovaly vazbu jen jednoho CB_n v souladu s jejich individuálními afinitami k tomu kterému vazebnému místu. Až potom bylo chování studovaných systémů sice velmi zajímavé, ale očekávatelné. Jelikož jsme žili v zajetí představy, že chování ternárních systémů odpovídá superpozici individuálních preferencí jednotlivých vazebných míst a makrocyclů, dočkali jsme se velkého překvapení při titraci komplexu ligandu s dlouhou spojkou a CB_7 ($G@CB_7^{Ad}$) β -cyklodextrinem, u kterého jsme předpokládali vazbu na volné butylové místo. Soutěž cyklodextrinu s CB_7 o vazbu na adamantanové místo se zdála být předem celkem jasně prohraná vzhledem k $1000\times$ vyšší afinitě CB_7 . K našemu údivu však β -CD vytěsnil CB_7 z preferovaného adamantanového místa, zaujal jeho pozici a CB_7 se musel spokojit s nepreferovaným místem butylovým. Z energetického hlediska však bylo toto uspořádání nejvýhodnější a proto výrazně převažující v rovnovážné směsi ve vodném roztoku. Publikace tohoto unikátního chování se poněkud zdržela díky nutnosti objasnit některé aspekty týkající neočekávaných chemických posunů protonů na koncích delších ligandů vzdálených od CB_n a dále jsme byli nuceni všechny NMR titrace provést při vyšším magnetickém poli (16,5 T, 700 MHz pro 1H) z důvodů dosažení potřebné kvality spekter. Výsledky tohoto projektu jsou předmětem Publikace 4.5.

V současné době, majíce k dispozici relativně široké portfolio vazebných motivů, se snažíme dokázat, že výše popsany jev nebyl ojedinělým výstřelkem, ale že racionálním návrhem struktury ligandu lze obdobně se chovající molekuly cíleně připravovat. V dalším kroku chceme tento koncept rozšířit na tritopické ligandy s potenciálním využitím v oblasti chemických senzorů a sond.

3.3 Multitopické ligandy na bázi bisimidazoliových solí

Logickým pokračováním studia vícevazebných ligandů byl přechod od ditopických ligandů k ligandům s více, tedy konkrétně se třemi, vazebnými místy. Zatímco v předchozí kapitole popisované ditopické ligandy mají v podstatě jen dvě možná uskupení, tedy hetero a homoditopické zástupce, u ligandů se třemi vazebnými místy v molekule je situace komplikovanější. Vazebná místa mohou být uspořádána lineárně nebo v hvězdici (s virtuální lokální symetrií planární středové části D_{3h} , C_{2v} nebo C_s) a mohou být stejná nebo různá. Všechna smysluplná uspořádání ditopických a tritopických ligandů jsou uvedena na Obrázku 2. Z odlišných důvodů jsme se zabývali jak lineárním, tak hvězdicovým uspořádáním vazebných motivů. Zatímco hvězdicově uspořádané tritopické ligandy je možné využít pro síťování polymerů modifikovaných vhodnými makrocycly, lineárně uspořádané tritopické ligandy lze využít jako molekulární senzory reagující na chemické podněty. Navzdory časové posloupnosti vydání předmětných publikací bych nejprve věnoval pár slov hvězdicovým homotritopickým ligandům.



Obrázek 2 Možné obecné struktury ditopických a tritopických ligandů

Kromě samotné přípravy c_3 symetrických adamantylovaných trisimidazoliových ligandů nás zajímalo, zda tyto relativně kompaktní molekuly dokáží vázat na všech svých vazebných místech současně tři makrocycly CB7 nebo β -CD a jejich vzájemné kombinace. Pokud by totiž tuto schopnost ligandy neměly, ztratilo by jejich směřování do oblasti supramolekulárního síťování polymerních řetězců smysl a stejně tak dobře by se mohly používat ligandy ditopické. Pokud by se však náš původní záměr ukázal být reálným, dalo by se uvažovat, v systémech s modifikovanými polymery, o dvou funkcích tritopických ligandů. Vzhledem

k přítomnosti tří vazebných míst lze uvažovat zapojení do síťování polymeru pouze u dvou z nich a třetí volné místo využít ke komplexaci a tím k zadržení v systému síťovaného polymeru, nějaké další například bioaktivní nebo stabilizující látky. Druhá funkce tritopického ligandu by mohla spočívat v jemnější kontrole síťovacího procesu pomocí makrocyclických kompetitorů než u ligandů ditopických. V Publikaci 4.6 popsaná pozorování naznačují, že všechny tři místa obou připravených ligandů mohou být současně obsazena jak CB7, β -CD i jejich libovolnými kombinacemi. Kalorimetrické titrační experimenty rovněž nenaznačují, že by pevnost vazby každého dalšího makrocyclu byla znatelně ovlivněna makrocycly již přítomnými. Proto hodláme v blízké budoucnosti využít tyto tritopické ligandy pro studium supramolekulárního síťování modifikovaných biopolymerů.

V první sérii lineárních tritopických ligandů jsme se rozhodli využít poznatky o adamantylovaných imidazoliových solích a zkombinovat tyto vazebné motivy s centrálním bifenylovým motivem. Základní architektura ligandu tedy byla A–B–A. Kladně nabitě jednotky pak byly použity dvě – imidazolium a benzimidazolium (navíc substituované v poloze 2 methylem nebo fenylem). Přestože výsledky této studie jsou předmětem Publikace 4.7, dovoluji si zde, v několika větách, nastínit hlavní zlomové okamžiky výzkumu těchto molekul a nejpodstatnější výsledky. První důležitý moment nastal již při studiu ligandů modelujících samotné centrální vazebné místo. Přestože afinita k β -CD se ukázala být pro oba motivy, tedy jak pro bismidazoliový i pro bisbenzimidazoliový, přibližně stejná (β -CD komplex druhého uvedeného je pouze 2,8× stabilnější), ligand na bázi stericky objemnějšího benzimidazolia vykazoval, na rozdíl od imidazoliového analoga, pomalou výměnu vzhledem k časové škále NMR (500 MHz). Tato skutečnost se projevila zdvojením signálů ligandu inkudovaného v kavitě β -CD s neekvivalentními portály. Při průzkumu chování našich, již tritopických, ligandů v ternárních systémech jsme postupovali tak, že k ligandu byl přidán nadbytek β -CD a směs byla poté titrována roztokem CB7. Bisimidazoliový ligand vytvořil s β -CD komplex se stechiometrií 2:1 (ve prospěch β -CD) s makrocycly na terminálních adamantanových vazebných místech. Po přidání CB7 pak došlo k posunutí jedné β -CD jednotky na centrální bifenylové vazebné místo a jejímu zamčení dvěma CB7 makrocycly na terminálních místech. Analogický ligand odvozený od benzimidazolia dokázal vytvořit již se samotným β -CD komplex se stechiometrií 1:3. Přítomnost β -CD na centrálním vazebném místě byla indikována zdvojením signálů ligandu i β -CD a pomocí DOSY spektroskopie. Přidaný CB7 pak vytěsnil β -CD z terminálních pozic, zatímco centrální β -CD jednotka zůstala na svém místě. Důležitým závěrem práce bylo, kromě zjištění, že sterické bránění vazebného místa může vést paradoxně k lepší schopnosti vázat makrocycly, odhalení funkce CB7 na vysoce afinitních adamantanových terminálních vazebných místech jakožto efektivního supramolekulárního zámku, který znemožňuje dosa-

žení, nebo naopak opuštění centrálního místa jiným makrocyclům. Pokud byl totiž připraven komplex $G@CB7_2^{Ad}$, nedošlo po přidání ani velmi vysokého nadbytku β -CD k jeho navázání do středové pozice. Je ovšem nasnadě, že v dostatečně dlouhém časovém rámci by obsazení středového místa mohlo být pozorováno. Na základě našich experimentů můžeme zodpovědně prohlásit, že čas potřebný pro takový vývoj systému, pozorovatelný pomocí 1H NMR je delší než několik měsíců. Tento jev byl nezávisle pozorován, a tím potvrzen, vědci z jiné skupiny na obdobných tritopických ligandech s terminálními ferrocenovými motivy.¹⁷

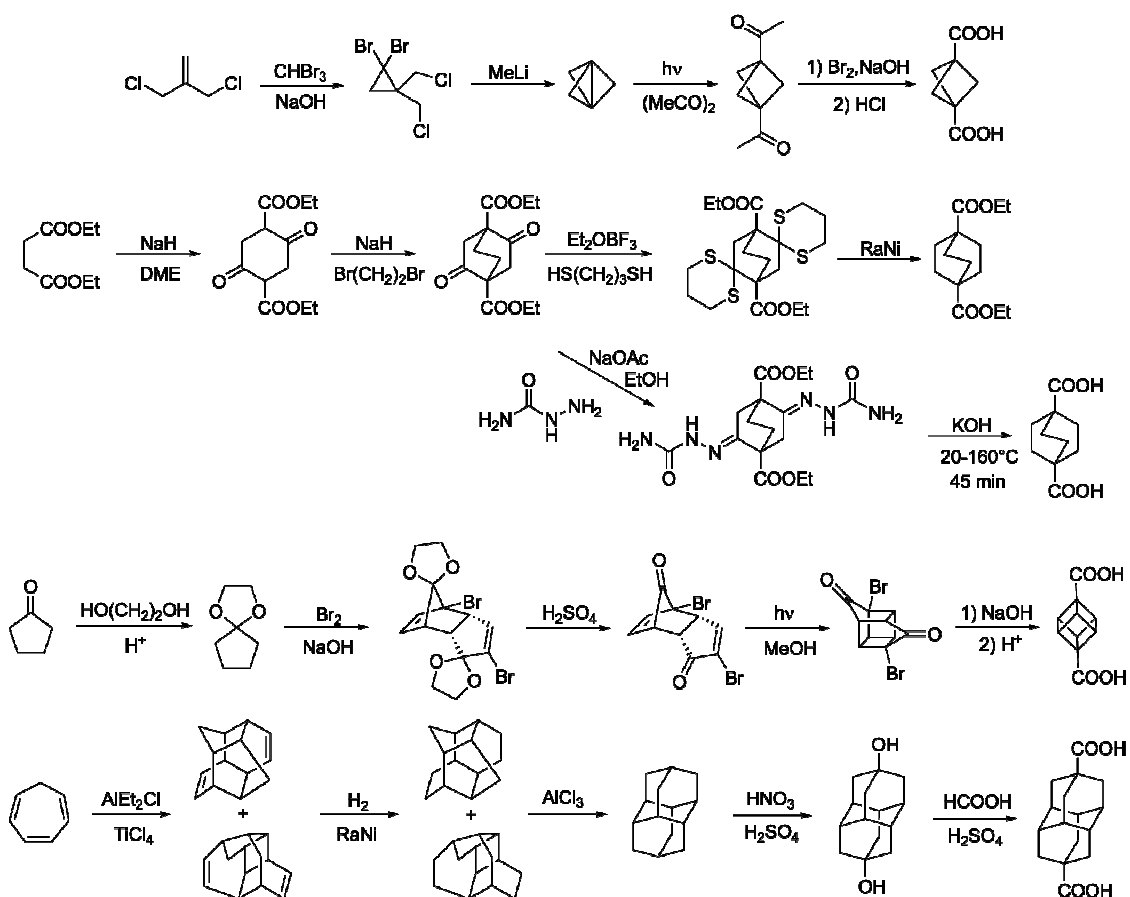
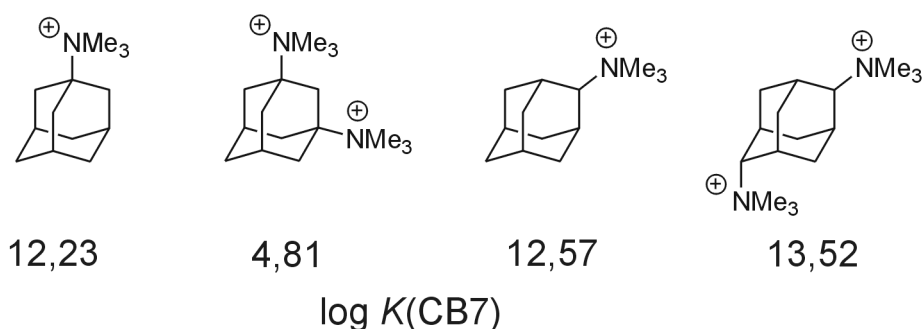


Schéma 2 Syntéza dikarboxylových kyselin bicyclo[1.1.1]pentanu,¹⁸ bicyclo[2.2.2]oktanu,¹⁹ kabanu²⁰ a diamantanu.²¹

V další práci jsme se zaměřili na syntézu a popis lineárních tritopických ligandů s A–B–A uspořádáním vazebných míst obsahujících vhodný klecový uhlovodík v centrální pozici (B). Aby bylo možné klecový uhlovodík zapojit do středu molekuly ligandu je nezbytná disubstituce uhlovodíkové klece. Protože cílové makrocyclky (tedy CB_n a CD) mají kavity „válcovité“, jinými slovy, středy portálů a těžiště celé molekuly makrocyclky leží na přímce, jsou pro konstrukci centrálního motivu vhodné takové uhlovodíky, které lze disubstituovat v ose (vazby k substituentům leží na přímce). Z klecových uhlovodíků relativně dobře synte-

ticky dostupných tomuto předpokladu vyhovují bicyklo[1.1.1]pentan (1,3-disubstituovaný), bicyklo[2.2.2]oktan (1,4-disubstituovaný), kuban (1,4-disubstituovaný) a diamantan (4,9-disubstituovaný). Nevýhodou těchto základních skeletů, jež značně omezuje jejich využití při konstrukci mutlitopických ligandů, je obtížná dostupnost vhodných derivátů využitelných v další syntéze finálních ligandů. Vhodně substituované deriváty těchto uhlovodíků jsou jen omezeně dostupné z komerčních zdrojů, navíc za ceny, které jsou neadekvátní tomu, že k cílovým ligandům je možné dospět jen dalšími několikakrokovými syntézami. Synteticky je možné tyto deriváty připravit zpravidla zdlouhavými postupy (viz Schéma 2). Jediný klecový uhlovodík používaný pro konstrukci ligandů s velmi vysokou afinitou k makrocyclům CB_n , jehož deriváty jsou komerčně dostupné (respektive, dostupné za rozumnou cenu), je adamantan.



Obrázek 3 Vybrané deriváty adamantanu a hodnoty asociačních konstant s $CB7$.

Ve vztahu k uvažovanému využití pro konstrukci centrálních, tedy disubstituovaných, vazebných motivů má tento uhlovodík zásadní nevýhodu plynoucí přímo z jeho struktury. Adamantanový skelet nelze disubstituovat v ose. Vazby ke dvěma substituentům na atomech terciárních uhlíků svírají klasický tetraedrický úhel $107^\circ 27'$. Stejný úhel pak svírají vazby v protilehlých pozicích na atomech sekundárních uhlíků. Vzhledem k tomu, že adamantanová klec téměř přesně vyplňuje kavitu $CB7$ a lze ji tedy teoreticky v kavěte pouze otáčet kolem těžiště, nutně dochází k situaci, kdy při umístění jedné, přímo napojené kladně nabitě skupiny v poloze 1 (například trimethylamoniové) v optimálním středu portálu $CB7$, druhá taková skupina v poloze 3 stericky koliduje s vnitřní stěnou kavity. Situace při disubstituci v polohách 2 a 6 je pouze o málo lepší a to jen proto, že substituenty jsou od sebe více vzdáleny. Nevhodnost těchto geometrických vlastností lze demonstrovat velikostmi interakčních konstant disubstituovaných derivátů s $CB7$ uvedenými na Obrázku 3. Za povšimnutí stojí velmi nízká hodnota K pro komplex $CB7$ s 1,3-bis(trimethylamonio)adamantanem, která naznačuje, že v tomto případě nejde o inkluzní komplex a ligand se pravděpodobně koordinuje k portálu $CB7$ z vnější strany. Rovněž minimální nárůst afinity k $CB7$ po přidání jednoho trimethylamoniového substituentu do polohy 6 v molekule 2-

adamantyl-*N,N,N*-trimethylamonia naznačuje, že obě kladně nabitě skupiny se nemohou současně efektivně vázat v protilehlých portálech CB7.

Pro výše uvedené důvody* jsme od počátku návrhu centrálního vazebného motivu na bázi 1,3-disubstituovaného adamantanu uvažovali o delších flexibilních spojkách mezi adamantanovou klecí a kationtovými skupinami, aby bylo umožněno umístění obou kationtových skupin v blízkosti protilehlých portálů CB n při současném setrvávání adamantanové klece uvnitř kavity makrocyklu. Jako vhodný komerčně dostupný derivát adamantanu se ukázala adamantan-1,3-dioctová kyselina,† kterou bylo možné převést na prekurzor se dvěma ethylenovými můstky sledem redukce a Appelleho bromace. Z tohoto prekurzoru byly připraveny tři ligandy s různými terminálními substituenty, z nichž jeden obsahoval tři vazebná místa na bázi adamantanu v uspořádání A – B – A.

Již při práci na předchozím projektu, kdy se nám podařilo připravit ternární supramolekulární architekturu s jedním cyklodextrinovým makrocyklem zamčeným na centrálním vazebném místě pomocí dvou CB7 na terminálních pozicích, jsme uvažovali o konstrukci ligandu, který by umožňoval inverzní uspořádání, tedy cucurbiturilový makrocyklus v centrální pozici uzavřený dvěma cyklodextriny. Tento cíl se nám nepodařilo dosáhnout v systému s β -CD a CB7, kdy byl pozorován pouze komplex $G@(CB7_2^T, \beta-CD^C)$. Protože však centrální motiv vykazoval vyšší afinitu k CB8 než k CB7, byl ve směsi tritopického ligandu, CB8 a β -CD pozorován požadovaný inverzní komplex $G@(CB8^C, \beta-CD_2^T)$. Takto se nám podařilo demonstrovat, že vhodně zvolenými hodnotami asociačních konstant jednotlivých vazebných míst lze cíleně připravit různé požadované supramolekulární uskupení. Připravený komplex může navíc sloužit jako rozpustný zdroj CB8, který je jinak ve vodném prostředí prakticky nerozpustný. Ternární ligand pak může poskytnout CB8 i pro jinak nepreferovaný komplex s jiným monotopickým ligandem (například T2 na Schématu 3), který v jednoduché směsi CB7/CB8/T2 upřednostňuje CB7. Při vhodném nastavení afinit jednotlivých vazebných míst tak bude z termodynamického hlediska preferovaný komplex s opačným makrocyklem, než v prosté směsi tohoto ligandu s CB7 a CB8 (viz Schéma 3).

* Nutno přiznat anachronismus argumentace 2,6-disubstituovanými deriváty adamantanu, které byly popsány v roce 2016, paralelně s naší prací o centrálním motivu na bázi 1,3-disubstituovaného adamantanu. O 2,6-disubstituci adamantanu jsme nikdy v naší skupině neuvažovali.

† Jsem si vědom toho, že tento název je nesprávně, ovšem i v odborné literatuře velmi často, používán namísto systematického (3-(karboxymethyl)adamantan-1-yl)ethanová kyselina.

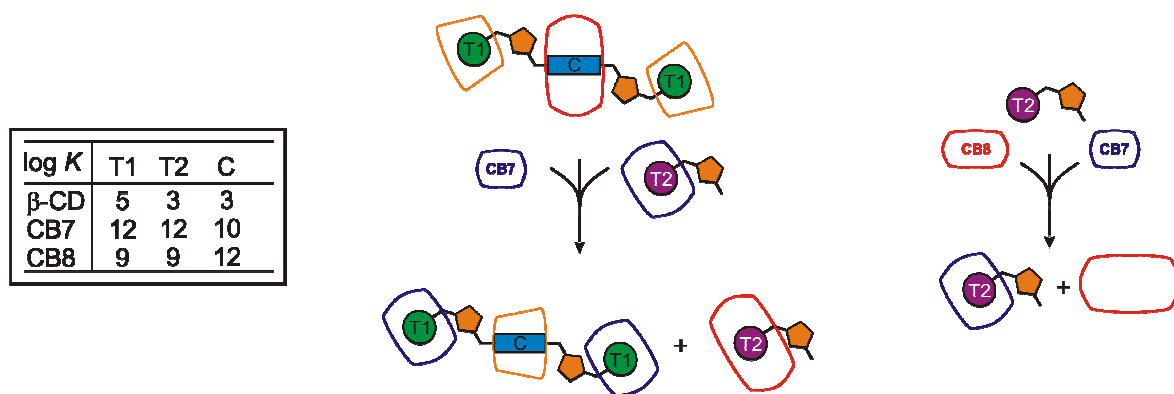


Schéma 3 Tritopický T1–C–T1 nosič CB8 podporující vznik nepreferovaného komplexu.

Jiný příklad reorganizujícího se supramolekulárního systému založeného na hetero-tritopickém ligandu typu A–B–C je schematicky znázorněn na Schématu 4. Molekula ligandu je složená ze tří různých vazebných motivů T1, C a T2. V prvním kroku může vznikat ternární komplex se dvěma různými jednotkami CB_n na terminálních vazebných místech T1 a T2. Tento komplex se po přidání třetího makrocyklu, příkladně β -CD reorganizuje posunutím CB7 makrocyklu na centrální místo, což je spojeno s disociací druhého CB6 z místa T2. V tuto chvíli je systém připraven na detekci nového ligandu, řekněme mu T3. Pokud má ligand T3 hodnotu $\log K$ k CB6 menší než 5 bude se systém vyvíjet tak, jak je naznačeno na Schématu 4, tedy T3 vytvoří komplex s CB7 a tritopický ligand bude preferovat komplex s β -CD^{T1} a CB6^{T2}. Jestliže ovšem bude hodnota $\log K$ komplexu T3@CB6 větší než 7, vznikne právě tento komplex s CB6 nacházejícím se v roztoku a ternární komplex tritopického ligandu zůstane beze změn. Takový systém se může zdát být příliš složitým pro prostou detekci ligandu T3 dokud si ovšem neuvědomíme, že umožňuje odhadnout velikost asociační konstanty T3 k CB6 a tím například zařadit neznámý T3 do užší skupiny struktur. Přípravou takovýchto reorganizujících se systémů se aktuálně zabýváme.

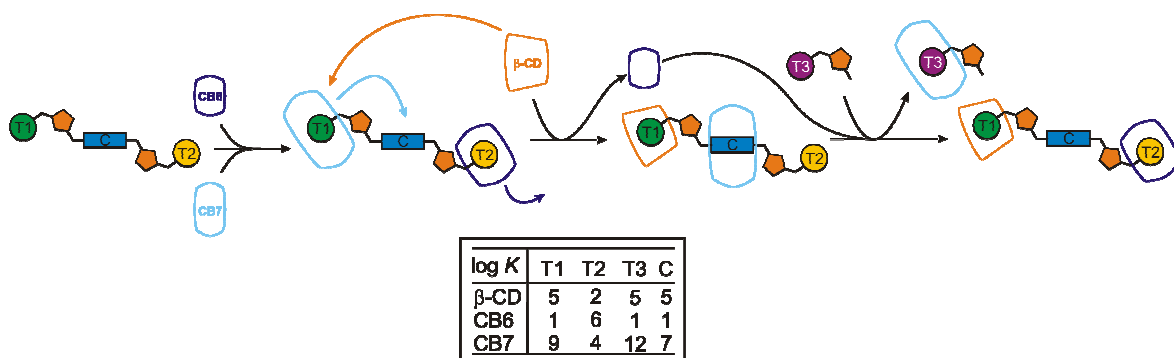
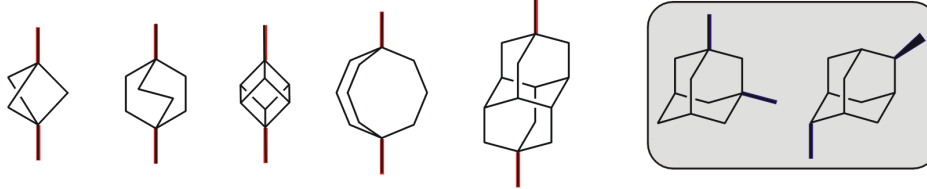


Schéma 4 Tritopický T1–C–T2 ligand vystupující jako molekulární sonda

3.4 Post adamantanové období.

Dalším krokem učiněným při studiu multitopických ligandů byla snaha o rozšíření portfolia vhodných vazebných míst o další strukturní motivy. Limity adamantanového skeletu, detailněji rozebrané výše, lze shrnout do jedné věty. Adamantanový motiv lze plně využít pouze jako terminální vazebné místo, neboť uplatnění na centrální* pozici znesnadňuje nemožnost axiální disubstituce adamantanové klece. Při hledání dalších uhlovodíkových skeletů tedy adjektivum "vhodný" zahrnuje nejen rozumnou syntetickou dostupnost a rozměr odpovídající cílovým makrocyclům, ale rovněž možnost axiální disubstituce. Hned po odhalení velmi vysokých afinit derivátů ferocenu a adamantanu k CB7 byla rodina těchto výjimečných ligandů obohacena o deriváty bicyklo[2.2.2]oktanu a posléze i o jednoduché amoniové deriváty diamantanu.



α [°]			180			109,5
d [Å]	1,93	2,63	2,71	3,43	4,64	2,52 3,55
C/H	5/6	8/12	8/6	11/18	14/18	10/14

Obrázek 4 Uhlovodíkové klece, úhly mezi vazbami k substituentům, vzdálenost mezi C-atomy z nichž tyto vazby vycházejí† a nekrácený poměr mezi počtem C- a H-atomů klece.

Snaha o přípravu nových derivátů uhlovodíkových klecí je ospravedlnitelná dvěma strukturními aspekty. Na jedné straně stojí snaha o maximální vyplnění dutiny makrocyclu, což vede k maximálnímu příspěvku disperzních sil ke stabilizaci komplexu. Na druhé straně je nutné uvažovat o optimální vzdálenosti mezi kationtovými substituenty tak, aby mohly být umístěny v ideálních pozicích v protilehlých portálech CB_n . Protože u uhlovodíkových klecí nelze měnit uvedené parametry nějakou jednoduchou přímočarou homologizací, tak jako například u lineárních uhlovodíků (přičemž i zde lze geometrické parametry měnit pouze skokově v násobcích délek vazeb), je nezbytné zamyslet se nad všemi dostupnými (axiálně disubstituovatelnými) klecemi, vhodné deriváty připravit

* Centrální pozicí se v širším slova smyslu myslí jakákoliv neterminální pozice, tedy například i pozice B, případně C v ligandech typu A–B–B–A případně A–B–C–B–A.

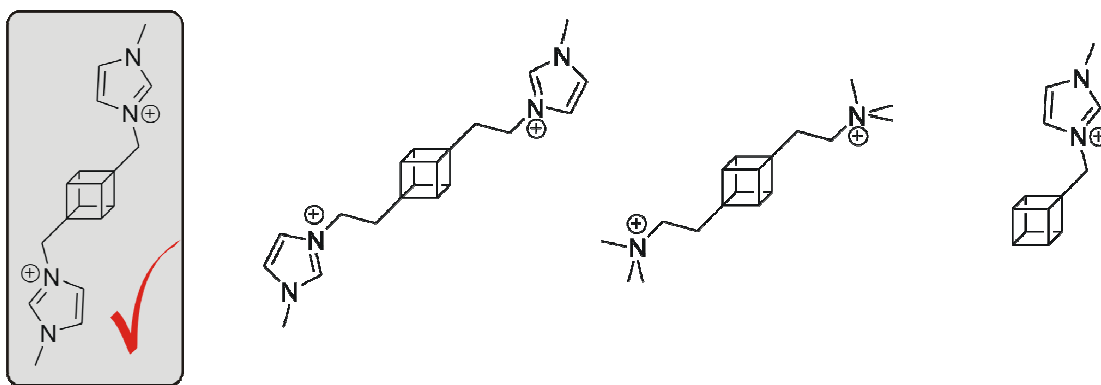
† Spočítáno pro dimetylované deriváty programem Avogadro v1.0.3, optimalizované pomocí molekulové mechaniky s využitím pole MMFF94.

a jejich supra molekulární chování experimentálně ověřit. Poslední vlastnost stojící za zmínku, spíše výhoda než nezbytnost, je malý počet signálů v ^1H NMR spektrech uvažovaných klecí související s jejich vysokou symetrií. Na Obrázku 4 jsou uvedeny struktury a vzdálenosti mezi atomy uhlíku v axiálních pozicích (takové atomy uhlíku, z nichž směřují vazby k dalším substituentům opačným směrem, ale v jedné přímce). Meziportálová vzdálenost u CB_n , tedy vzdálenost mezi rovinami proloženými portálovými atomy kyslíků je $6,1 \text{ \AA}$ (připočteme-li dvojnásobek van der Waalsova poloměru atomu kyslíku dostaneme v literatuře hojně citovanou „výšku“ CB_n soudku $9,1 \text{ \AA}$). Z uvedených struktur se této hodnotě nejvíce blíží klec diamantanu. Připomeňme si, že komplex 4,9-bis(trimethylamonio)adamantanu a CB_7 je dosud nejstabilnější známý nekovaletní komplex dvou monovalentních partnerů. Všechny ostatní uvažované klece mají vzdálenost mezi atomy uhlíku nesoucími substituenty výrazně menší. Z toho plyne nutnost oddálit kationtové skupiny u ligandů odvozených od těchto uhlovodíků pomocí vhodných, například methylenových, můstků. Takto byly připraveny a studovány například trimethylamoniomethylové deriváty bicyklo[2.2.2]oktanu.^{19a}

Protože z našich předchozích experimentů s bisimidazoliiovými solemi odvozenými od bifenyly (Publikace 4.7) vyplynuly poněkud odlišné asociační konstanty k CB_n a CD ve srovnání s trimethylamoniovými analogy (nehledě na další aplikační potenciál imidazoliiových solí zmíněný výše), rozhodli jsme se prozkoumat supramolekulární chování dosud neznámých bisimidazoliiových solí odvozených od bicyklo[2.2.2]oktanu, i přestože analogická bistrimethylamonia byla v té době již popsána. Výsledky tohoto výzkumu zatím nejsou shrnuty do podoby ucelené publikace, a proto nejsou součástí této práce. V ještě méně rozpracované podobě se nachází projekt přípravy vazebných motivů s modulovanou vazebnou afinitou na bázi diamantanu.

Při průzkumu dostupných informací o ligandech na bázi klecových uhlovodíků nás zaujala absence jakýchkoliv kationtových ligandů odvozených od velmi atraktivního uhlovodíku kubanu. Pokud je nám známo, existovala pouze jedna supramolekulární práce popisující neutrální kubanový ligand v systémech s CD.²² Kationtové deriváty kubanu, zřejmě částečně oprávněně, vyvolávají skepsi stran jejich stability, neboť je známo, že již u 1,4-dihydroxymethylkubanu dochází v mírně kyselém prostředí k rozpadu kubanové klece. Rovněž deriváty s amoniiovými skupinami přímo vázanými na kubanovou klec byly shledány jako velmi nestabilní.²³ My jsme se však rozhodli připravit ligandy s kationty na bázi imidazolia, kde je kladný náboj delokalizován po aromatickém heterocyklu a cílové látky by tak mohly být za laboratorní teploty stabilní. Navíc jsme, z geometrických důvodů popsaných výše, vložili mezi imidazoliové kruhy

a kubanovou klec methylenové můstky.* Příprava a supramolekulární chování prvního takto navrženého a posléze připraveného dikationového ligandu odvozeného od kubanu (struktura na Obrázku 5, vlevo) je hlavním obsahem Publikace 4.9. Kromě samotné přípravy a stanovení asociačních konstant s CB7, CB8 a β -CD, se nám podařilo vypěstovat monokrystaly komplexů G@CB7 a G@CB8 a určit jejich strukturu pomocí difrakce Röntgenova záření. Nejzajímavějším strukturním rysem uvedených komplexů je výrazně eliptický tvar portálů CB8 oproti téměř ideálně kruhovému CB7 a zdatelné posunutí imidazoliových kationtů ze středu portálu u komplexu s CB7 ke straně portálů u komplexu s CB8. Tato námi pozorovaná tendence CB8 stabilizovat kationty nikoliv ve středu nýbrž při straně portálu, vytváří další prostor pro případné zvyšování afinity ligandů přidáním více nabitého substituentu. Kationt umístěný při straně portálu ponechává totiž protilehlou část portálu volnou pro další možné ion-dipólové interakce s delšími, vícenásobně nabitými substituenty. Tímto směrem se s velkou pravděpodobností ubírají lovci rekordů hledající nový nejstabilnější komplex. Na druhou stranu ovšem, v nedávné době publikované ligandy na bázi 2,6-disubstituovaného diamantanu, které tvoří nejstabilnější dosud známé komplexy s CB8 (pro uvedenou disubstituci $-\text{N}^+\text{HMe}(\text{CH}_2)_4\text{OH}$ je $K=9,2 \cdot 10^{14} \text{ M}^{-1}$),²⁴ mají atomy dusíku nesoucí kladný náboj umístěny prakticky ve středu eliptického portálu CB8. Eliptický tvar je CB8 vnucen s největší pravděpodobností tvarem diamantanové klece, která leží svou podélnou osou v ekvatoriální rovině CB8.



Obrázek 5 Již popsany a další perspektivní modelové ligandy na bázi kubanu.

Zájem o deriváty kubanu byl rovněž motivován otázkou, zdali je kubanová klec schopna vstoupit do kavity CB6. O tomto homologu CB je známo, že bicyklo[2.2.2]oktan neváže, ale například deriváty 2,3-diazabicyklo[2.2.1]heptanu

* Nadto byl použitý syntetický postup zahrnující transformaci skupiny $-\text{COOH}$ na $-\text{CH}_2\text{OH}$ a dále na $-\text{CH}_2\text{Br}$, který byl poté využit pro substituci na N1 atomu imidazolu v naší laboratoři dobře známý a hojně používaný.

ano.²⁵ Pro posouzení geometrické kompatibility je možné, v prvním přiblížení, použít prosté porovnání objemů kavity příslušného homologu CB a zkoumané klece. Je sice zřejmé, že veškerý objem „velké“ klece nemusí být nutně v případném komplexu přítomen uvnitř kavity a naopak u „malé“ klece mohou být v kavitě přítomny i některé atomy substituentů, ale základní obrázek o prostorových nárocích a z toho plynoucích komplexačních možnostech nám tento přístup může poskytnout. Pro kvantifikaci geometrické podobnosti byl zaveden balící koeficient PC ²⁶ vypočítaný podle prosté rovnice (1)

$$PC = 100 \cdot \frac{V_L}{V_C} \quad (1)$$

kde V_C je objem kavity a V_L je objem ligandu. Hodnoty V_C použité pro výpočty PC uvedených na Obrázku 6 jsou převzaty z práce W. Naua.²⁷ Objem ligandu V_L je možné spočítat z příspěvků jednotlivých atomů a vazeb²⁸ dle rovnice (2)

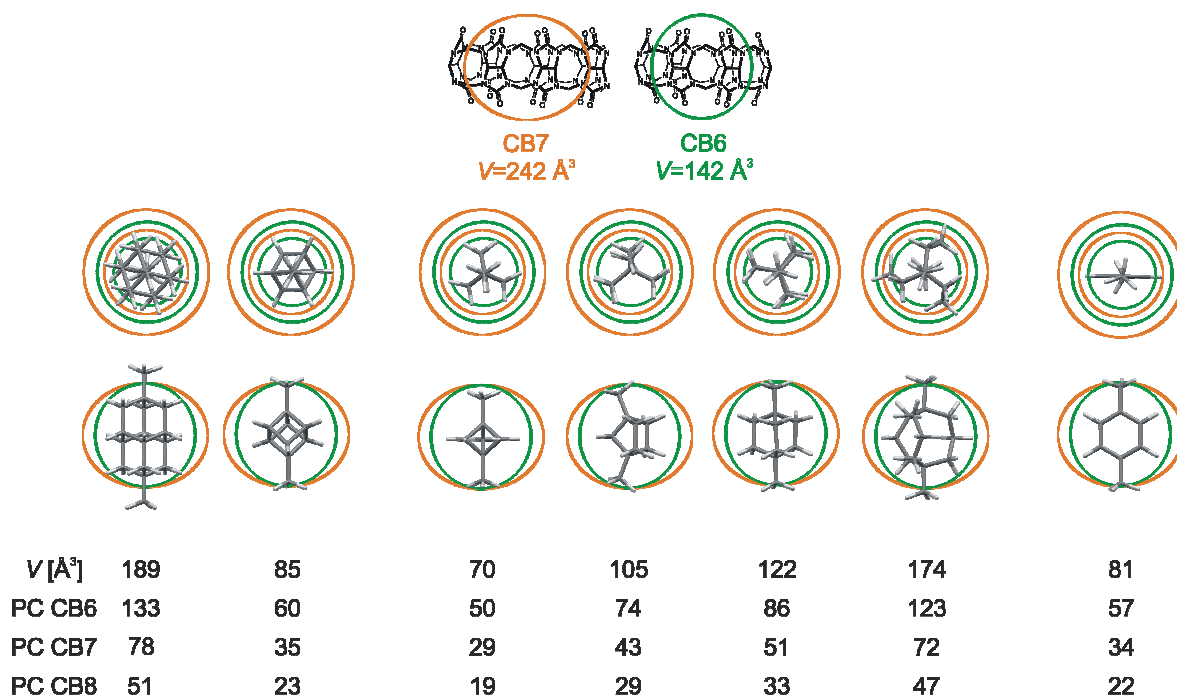
$$V_L = \sum_i n_i \cdot V_{Ai} - 5,92 \cdot N_B - 14,7 \cdot N_{Ar} - 3,8 \cdot N_{Al} \quad (2)$$

kde V_A je van der Waalsův objem atomu příslušného prvku, N_B je počet vazeb (nehledě na jejich řád), N_{Ar} je počet aromatických kruhů a N_{Al} je počet alifatických kruhů a i reprezentuje všechny prvky v molekule.

Hodnoty PC a příslušné objemy základních uhlovodíkových klecí jsou uvedeny na Obrázku 6. Při letmém pohledu se zdá, že hranice ve velikosti klece umožňující komplexaci v kavitě CB₆, leží někde mezi sedmi a osmi těžkými atomy* a z tohoto úhlu pohledu by kuban se svými osmi C-atomy v kleci inkluzní komplexu s CB₆ tvořit neměl. Na druhou stranu, bicyklické deriváty mají výzazně nižší poměr C/H než pentacyklický kuban, který má, mimochodem jako jediný mezi uvažovanými disubstituovanými uhlovodíkovými klecemi, poměr (N_C/N_H)>1. Protože ani H-atomům nelze upřít jisté prostorové nároky, je vysoce kompaktní kubanová klec zřejmě menší než například klec bicyklo[2.2.2]oktanu se stejným počtem atomů uhlíku (ale dvojnásobným počtem atomů vodíku). Objem samotného kubanu, jak je patrné z Obrázku 6, představuje pouze 70% objemu bicyklo[2.2.2]oktanu. Navíc vodíkové atomy jsou u kubanu orientované blíže ekvatoriální rovině CB_n v pomyslném komplexu, tedy v místě, kde je kavity CB_n nejširší, zatímco u bicyklo[2.2.2]oktanu jsou vodíkové atomy poněkud blíže

* Wernerem Nauem publikovaná největší klec tvořící s CB₆ inkluzní komplex je nesubstituovaný 2,3-diazabicyclo[2.2.1]hept-2-en,²⁵ který má objem (90 Å³) i příslušné PC (PC_{CB_6} =63%, PC_{CB_7} =37% a PC_{CB_8} =24%) zřejmě menší než základní uhlovodík díky náhradě dvou uhlíkových atomů menšími atomy dusíku a díky absenci čtyř vodíkových atomů.

portálům. Jiný úhel pohledu zohledňuje hodnoty *PC*. Optimální hodnota *PC* se zdá být někde okolo 55% (45% je například podíl volného prostoru ve vodě) a má se za to, že čistě z geometrického hlediska budou tvořit stabilní inkluzní komplexy ty ligandy jejichž hodnota *PC* pro příslušnou kavitu spadá do intervalu 45–65%.¹⁶ Hodnota *PC* kubanové klece pro CB6 je sice vyšší než optimální, ale pořád bezpečně leží uvnitř výše uvedeného intervalu. Tyto úvahy nás vedly k vyzkoušení schopnosti CB6 inkludovat kubanovou klec. Rovnou můžeme přiznat, že jediný dosud připravený dikationtový ligand odvozený od kubanu (Obrázek 5 vlevo) inkluzní komplex s CB6 za podmínek našich experimentů netvoří. Příčinou může být samotný rozměr klece, přičemž by hlavním omezením byla spíše neschopnost kubanové klece proniknout portálem CB6 než geometrická nekompatibilita s vnitřkem kavity, ale nelze vyloučit ani negativní vliv imidazoliových heterocyklů připojených methylenovým můstkem. V takovém uspořádání se relativně objemné imidazolium nutně dostává do sterické kolize s atomy portálu CB, což může zamezit vzniku inkluzního komplexu. Z těchto důvodů plánujeme pro účely testování s CB6 připravit jiné kationtové deriváty kubanu s kationty více vzdálenými od kubanové klece, případně deriváty pouze jednou substituovaného kubanu (Obrázek 5).



Obrázek 6 Pohled shora a z boku na vybrané klecové uhlovodíky superponované schematickým nákresem kavity CB7 (oranžová) a CB6 (zelená). V pohledu zhora představuje menší kružnice průměr portálu a větší kružnice průměr kavity v ekvatoriální rovině. Nákres je proveden v měřítku dle publikovaných rozměrů CB_n .²⁹ Dimethylované deriváty uhlovodíků zleva: diamantan, kuban, bicyklo[1.1.1]pentan, bicyklo[2.2.1]heptan, bicyklo[2.2.2]oktan, bicyklo[3.3.3]undekan a benzen.

Kromě adamantanu, diamantanu, kubanu, bicyklo[2.2.2]oktanu a potažmo ferocenu, kterým se ale v naší skupině (zatím) nezabýváme, existují minimálně dvě další potenciálně zajímavé axiálně disubstituovatelné uhlovodíkové klece využitelné pro konstrukci vazebných motivů v supramolekulárních systémech. Prvním z nich je bicyklo[1.1.1]pentan a druhým pak bicyklo[3.3.3]undekan. Na Obrázku 6 jsou dobře patrné proporce těchto dvou uhlovodíkových skeletů ve srovnání s jinými, výše zmíněnými a rovněž v porovnání s rozměry kavit CB6 a CB7. Bicyklo[1.1.1]pentan by tak mohl být zajímavým ligandem pro CB6 (přibližně stejně tak vhodným jako je bicyklo[2.2.2]oktan pro CB7), zatímco u vyššího homologu bicyklo[3.3.3]undekanu je oprávněná pochybnost, zdali by vůbec prošel portálem CB7. Každopádně by ale tento nejvyšší homolog typu bicyklo[*n.n.n*] se symetrickou klecí (dle výpočtů konformačního chování i podle ojedinělých případů přípravy a strukturního popisu některých derivátů jsou ramena klecí vyšších homologů flexibilní a samotné klece jsou pak zborcené³⁰) mohl sloužit jako strukturní základ pro konstrukci ligandů pro CB8.

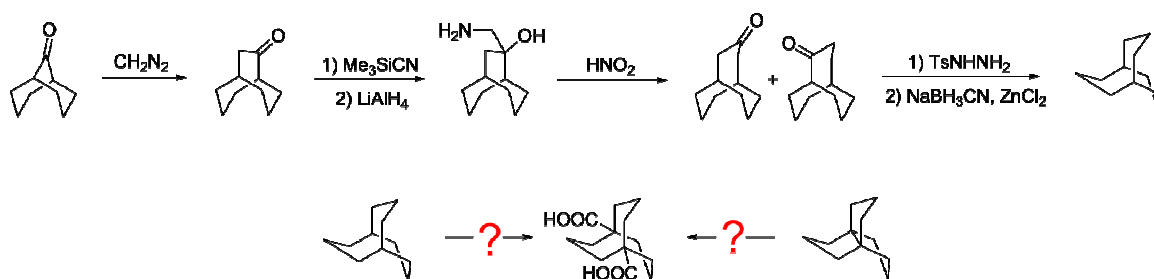


Schéma 5 Příprava bicyklo[3.3.3]undekanu³²

Ze syntetického hlediska je potenciální výchozí derivát pro přípravu ligandů odvozených od bicyklo[1.1.1]pentanu relativně snadno dostupný postupem popsaným na Schématu 2. Naproti tomu, v literatuře popsaná chemie bicyklo[3.3.3]undekanu je překvapivě chudá. Kromě přípravy souvisejícího [3.3.3]propelanu³¹ a samotného bicyklo[3.3.3]undekanu³² (Schéma 5) je popsána příprava jen několika málo derivátů (1,5-diol, 1,5-dimethyl) a rovněž chemická reaktivita zmíněných uhlovodíků v dostupné literatuře nijak rozvedena není. Vzhledem ke značnému potenciálu v oblasti supramolekulární chemie považujeme přípravu vhodných ligandů na bázi bicyklo[3.3.3]undekanu za velkou výzvu.

IV. KOPIE PŘEDMĚTNÝCH PUBLIKACÍ

4.1

Novel adamantane bearing anilines and properties of their supramolecular complexes with β -cyclodextrin.

Robert Vícha*, Michal Rouchal, Zuzana Kozubková, Ivo Kuřitka Petra Branná, Richard Čmelík

Supramolecular Chemistry **2011**, 23, 663–677

Novel adamantane-bearing anilines and properties of their supramolecular complexes with β -cyclodextrin

Robert Vícha^{a*}, Michal Rouchal^a, Zuzana Kozubková^a, Ivo Kuřitka^b, Radek Marek^{c,d}, Petra Branná^a and Richard Čmelík^e

^aDepartment of Chemistry, Faculty of Technology, Tomas Bata University in Zlín, Náměstí T. G. Masaryka 275, 76001 Zlín, Czech Republic; ^bPolymer Centre, Faculty of Technology, Tomas Bata University in Zlín, Náměstí T. G. Masaryka 275, 76001 Zlín, Czech Republic; ^cNational Centre for Biomolecular Research, Masaryk University, Kamenice 5/A4, 62500 Brno, Czech Republic; ^dCentral European Institute of Technology (CEITEC), Masaryk University, Kamenice 5/A4, 62500 Brno, Czech Republic; ^eInstitute of Analytical Chemistry of the ASCR, v.v.i., Veveř 97, 60200 Brno, Czech Republic

(Received 26 October 2010; final version received 13 May 2011)

Several novel anilines bearing 1-adamantyl substituents that are useful for drug modification were synthesised from the corresponding 1-adamantyl (nitrophenyl) ketones. The host–guest systems of these prepared ligands with β -cyclodextrin (β -CD) were studied using electrospray ionisation mass spectrometry, NMR spectroscopy, titration calorimetry and semi-empirical calculations. The complexes with 1:1 stoichiometry were found to predominantly exist as pseudorotaxane-like threaded structures with the adamantane cage sitting deep in the cavity of β -CD close to the wider rim. Such geometry was observed for all examined amines and is independent of their structure and/or presence of protic substituents.

Keywords: adamantane; amines; cyclodextrins; host–guest systems

1. Introduction

Since the first description of the antiviral activity of 1-adamantylamine in 1964 (1), various compounds containing the adamantane scaffold have been shown to exhibit antiviral (2), anticancer (3) and antimicrobial (4) activities; such compounds have also been described as hypoglycaemic (5), proapoptotic (6) and neuroprotective (7) agents, as well as possible treatments for hypertension, vascular inflammation (8) and tuberculosis (9). Adamantane-bearing compounds can also serve as cannabinoid receptor ligands (10). This well-founded interest is related to a unique property of the adamantane cage that can improve the characteristics of biologically active compounds. As a result of its high lipophilicity, adamantane should increase the rate of transfer of a modified drug through cell membranes and thus facilitate the distribution of the drug. On the other hand, the formation of supramolecular complexes with β -cyclodextrin (β -CD) (11) significantly increases drug's solubility in water. CD drug carrier systems have been studied extensively in terms of solubility, bioavailability and stability (12). This attention has yielded several commercial pharmaceutical products based on CD host–guest complexes (12). The adamantane-bearing amines are suitable candidates for drug modification, e.g. as ligands in preclinically tested (3) platinum derivative LA-12 (Figure 1, left) or as building blocks for displacement of C6 substituent in purvalanol-like promising anticancer drugs (Figure 1, right). However,

the steric hindrance of bulky adamantane may lead to attenuation of the desired activity if the scaffold is introduced too close to the active site of the drug (13), hence the need for preparation and property investigation of new suitable adamantane-bearing building blocks is justified.

Although inclusion complexes of β -CD with 1-adamantyl-based compounds have been studied for a long time, previous efforts have focused on small ionic guests (14). Some structural data have also been published for more complex ligands (15). In most of these cases, the nature of the inclusion complexes is determined by the structure of host and/or guest molecule. It is reasonable to suppose that the geometry and stability of host–guest complexes are affected by substituents adjacent to the adamantane cage. Therefore, we have prepared several new potential building blocks with modulated polarity and variable linker length between the adamantane and benzene ring units. The host–guest complexes of these prepared anilines and β -CD were investigated using electrospray ionisation mass spectrometry (ESI-MS), ¹H and ¹³C NMR spectroscopy, and titration calorimetry.

2. Results and discussion

2.1 Synthesis of amines

The nitro intermediates were prepared following previously described procedures, including the ketone

*Corresponding author. Email: rvicha@ft.utb.cz

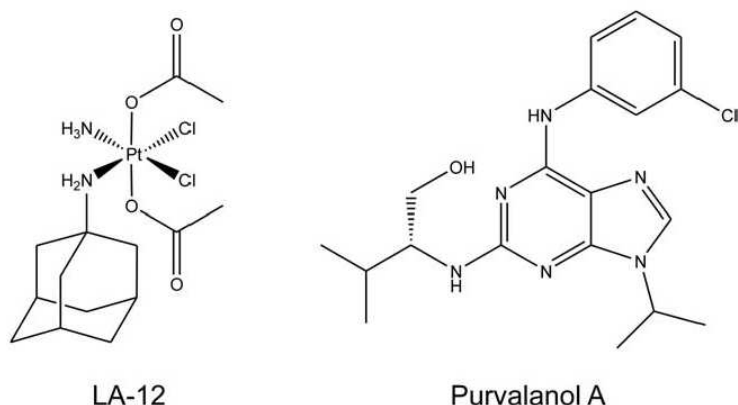


Figure 1. Structural formulas for selected promising anticancer drugs.

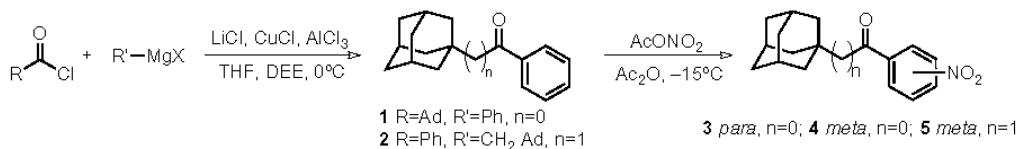
preparation (*16*) and nitration with acetyl nitrate (*17*) as shown in Scheme 1. Regioisomers were separated by column chromatography, and compounds **3–5** were used as starting materials for further reactions.

Aminoketones **6–8** were prepared in methanolic HCl solution using iron powder as a reducing agent. The iron powder used in this reaction was obtained from iron pentacarbonyl decomposition (purchased from commercial source); use of iron fillings or turnings led to considerably longer reaction times. Amines **6–8** are rather unstable at room temperature as a free base (but may be stored for several months at -10°C) and decompose to dark brown oily products within a few days. Unfortunately, transformation to their corresponding solid hydrochloride salts via introduction of dry gaseous hydrogen chloride into diethyl ether or hexane solution only provided oily, brownish products.

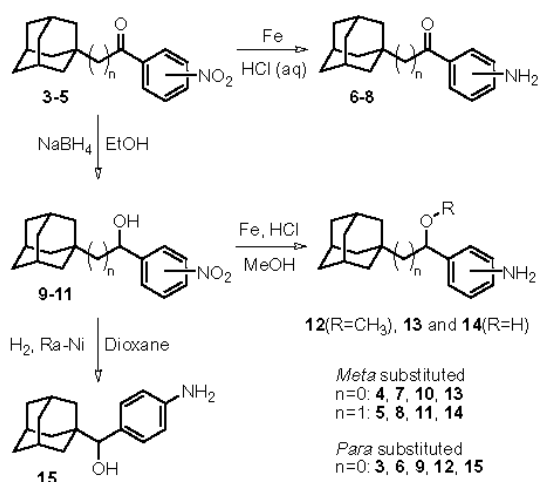
Aminoalcohols **13–15** were prepared from nitroketones in two steps. Selective reduction using NaBH_4 proved to be very effective in our case, and we obtained nitroalcohols **9–11** in excellent yields ($\sim 95\%$) in 30 min. Reduction of the nitro group was carried out using iron powder in a methanol/HCl (1/1, v/v; conc. HCl was used) mixture. Amines **13** and **14** were isolated either as free bases (pH adjustment followed by extraction) or directly as hydrochloride salts. Attempted preparation of aminoalcohol **15** in the same manner failed due to undesirable nucleophilic substitution, and methoxyamine **12** was isolated in 85% yield. Therefore, catalytic hydrogenation

on Ra–Ni was employed in the preparation of amine **15** (Scheme 2). Attempts to prepare aminoalcohols from compounds **3–5** in one step using less selective reducing agents such as LiAlH_4 or $\text{H}_2/\text{Ra-Ni}$ were not successful, and complex mixtures were obtained.

Amines with non-polar hydrocarbon spacers between the adamantane and benzene ring moieties (**25–27**) were also prepared in two (via 1,3-dithianes) or three (via 1,3-dithiolanes) steps. This synthesis involved the formation of the corresponding *S,S*-acetals, followed by the reduction of the nitro group by iron powder in alcohol/HCl mixture and reduction/desulphurisation with H_2 on Ra–Ni catalyst (Scheme 3). Although the yields of the first step were excellent (about 90% of isolated products **16–20**), the following steps were accompanied by some difficulties. Nitrodithiane **18** was treated with Ra–Ni in ethanol under hydrogen atmosphere and was successfully desulphurised. The nitro group was also reduced under these conditions, but an undesirable substitution occurred, and the corresponding *N*-ethyl derivative was identified as the main product. Dithiane **16**, however, afforded required amine **27** under the same conditions. Although the isolated yield was not excellent, no side products were detected by either TLC or GC analysis. Due to the very poor solubility of dithioacetals in hexane, reduction with H_2 could not be performed without the use of a more polar solvent. We attempted the reduction of dithiane **18** in a dioxane/hexane mixture (1/1, v/v), but under such conditions, the nitro group was reduced to an amino group, while the dithiane



Scheme 1. Reaction pathway leading to 1-adamantyl (nitrophenyl) ketones.

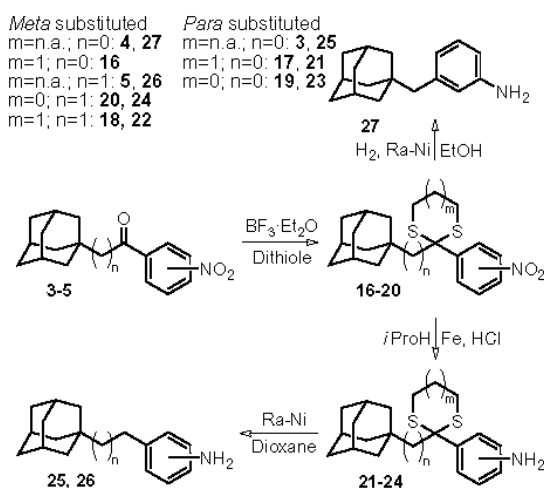


Scheme 2. Synthesis of aminoketones and aminoalcohols.

ring did not react. As a result, the corresponding aminodithiane derivative was isolated. Similarly, nitrodithiane **17** afforded the corresponding aminodithiane in an ethanol/hexane reaction medium. Thus, a two-step procedure was necessary for the smooth transformation of nitrodithianes to the required amines. Iron in *i*PrOH/HCl and Ra-Ni in dioxane were used for nitro group reduction and desulphurisation, respectively (Scheme 3).

2.2 ESI-MS analysis

Solutions of individual amines, as well their 1:1 mixtures with β -CD, were studied by ESI-MS. The dominant ions corresponding to the amines were the pseudomolecular



Scheme 3. Synthesis of anilines with non-polar linker.

ions $[M + H]^+$, accompanying the signals at m/z values about two times as high (exactly $[2 \times (M + H) - 1]^+$ or $[2 \times M + 23]^+$). The latter ions were observed when a polar functional group (oxo or hydroxy) was present in the amine molecule, as shown for amine **13** in Figure 2(a). These signals are assumed to be related to associates of dimer linked via hydrogen bonds with a proton or sodium cation, respectively. The formation of analogous dimers in the solid state has been observed for aminoalcohol **15** (**18**). In the amine/ β -CD mixtures, the protonated amine and sodium adduct of β -CD, as well as protonated β -CD-amine complex, were detected for all examined amines (Table 1). Figure 2(b) shows a typical spectrum of an equimolar mixture of β -CD and amine **27**. The tandem mass spectrum of the protonated complex showed a characteristic fragmentation pattern, which confirms its identity. The ions at m/z 1136, 974, 811, 649 and 487 resulted from the successive losses of amine and glucose residues of the β -CD moiety (Figure 2(c)).

2.3 The geometry of host-guest complexes

The β -CD is a heptamer built up from glucopyranose units linked by α -1,4-glycosidic bonds with a very well-known structure (**19**) that it is often described as a doughnut with rims of differing diameters. The larger diameter corresponds to the secondary rim where secondary hydroxyl groups at C2 and C3 are located; primary hydroxyl groups at C6 are placed on the opposite smaller primary rim due to the non-alternating orientation of the glucose units. The interior of the cavity has steric constraints due to H3 and H5 protruding into the cavity (**14c**). Schematics with the relevant dimensions of β -CD and the prepared amines are displayed in Figure 3.

The internal diameter of the cavity is likely to be slightly smaller than the diameter of the nearly ball-shaped adamantane moiety, which cannot pass through it easily but still fit well in the interior of the β -CD cavity. As a result, two distinct complexes may form. The adamantane moiety can be located either at the primary rim region or at the secondary rim region. In a solution, a reasonable orientation of a short and, in most cases, charged, substituent bound to adamantane is outside the β -CD cavity (**14c**, **15a**). Occupancy of the primary rim was observed only when the secondary rim was blocked. Higher thermodynamic stabilities were calculated for complexes with the adamantane unit sitting in the secondary rim (**14c**). However, it is reasonable to suppose that a non-polar substituent of appropriate length may thread through the cavity of β -CD. Thus, four possible arrangements of 1:1 adamantane and β -CD complexes should be considered. These arrangements are illustrated in Figure 4.

All examined systems obey the fast exchange mode on the NMR timescale, and thus only one set of signals was

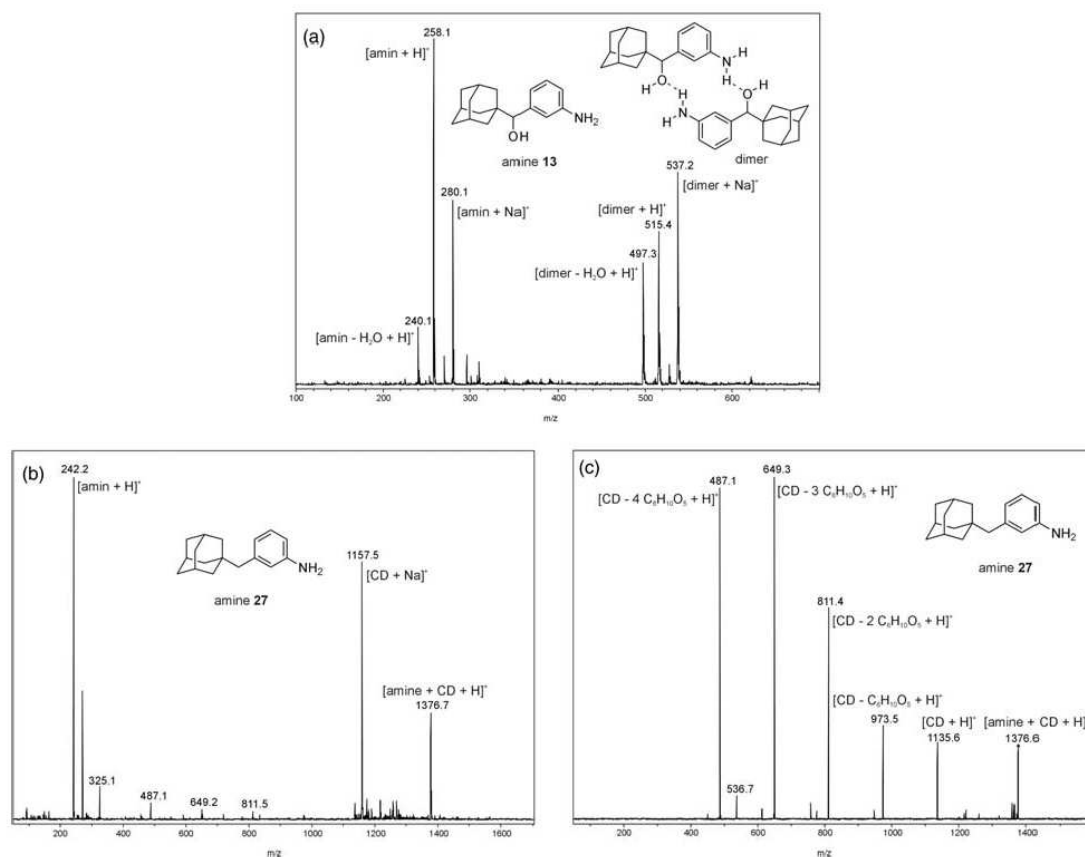


Figure 2. ESI-MS data for amine 13 (a), equimolar mixture of amine 27 with β-CD (b), and MS² spectrum of amine 27-β-CD complex, target mass = 1377 m/z (c).

Table 1. Results of MS analyses – ionic species observed for amine with and without the presence of β-CD.

Amine	Exact mass					
	[Amine + H] ⁺		[2-amine + Na] ⁺		[β-CD + amine + H] ⁺	
	Calc.	Found	Calc.	Found	Calc.	Found
6	256.2	256.1	533.4	533.3	1390.6	1390.6
7	256.2	256.1	533.4	533.3	1390.6	1390.6
8	270.2	270.1	561.4	561.3	1404.6	1404.6
12	272.2	272.1	565.4	–	1406.6	1406.6
13	258.2	258.1	537.4	537.2	1392.6	1392.6
14	272.2	272.1	565.4	565.4	1406.6	1406.7
15	258.2	258.1	537.4	537.2	1392.6	1392.6
21	346.2	346.1	714.4	–	1480.6	1480.7
22	360.2	360.2	742.4	–	1494.6	1494.7
24	346.2	346.3	714.4	–	1480.6	1480.8
25	242.2	242.8	505.4	–	1376.6	1376.7
26	256.2	256.3	533.4	–	1390.6	1390.7
27	242.2	242.1	505.4	–	1376.6	1376.6

observed in all cases. Unfortunately, the shifts observed upon complexation for the host and guest protons were small ($<10^{-2}$ ppm), and determination of thermodynamic parameters from NMR titrations was generally impossible.

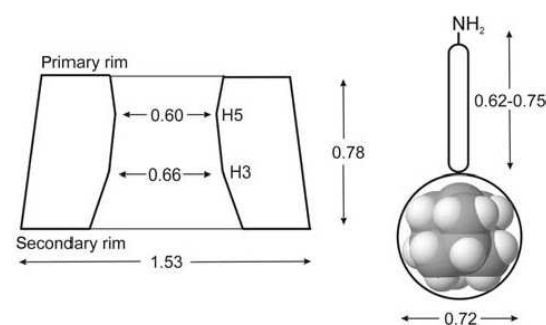


Figure 3. Schematic representations of β-CD and the prepared guest molecules with dimensions shown in nanometres.

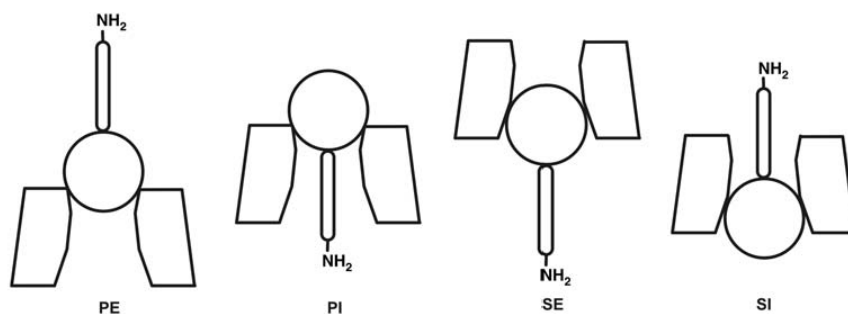


Figure 4. Schematic representations of possible geometries of host–guest systems under consideration. S, secondary; P, primary; I, internal; E, external. (Previously published (14) geometric parameters were considered.)

We observed reproducible complexation-induced shifts of the well-resolved ^1H NMR signals only for guest **14**. Although the Job plot for the H5 protons (Figure S1) of the adamantane guest indicates a 1:1 stoichiometry, the analysis of titration data was unsatisfactory. The fitting of experimental data to the theoretical rectangular hyperbola using the standard least square regression procedure (MicroCal ORIGIN) led to an estimation of association constant being $\sim 40\text{M}^{-1}$, but the systematic discrepancy between the theoretical data and best-fit curve is too high (Figure S2). We attribute this discrepancy to the influence of higher ordered, hydrogen-bonded complexes on the observed chemical shifts. Nevertheless, the downfield shifts for guest protons H4–6 (on the adamantane cage) and upfield shifts for H1, H2^{A,B}, H14 and H16–18 were clearly observed (Figure S3).

The observed NOE interactions between guest protons bound to the adamantane cage (H4–6 for guest **14**) and inner hydrogen atoms of the CD cavity suggest the formation of an inclusion complex with adamantane positioned inside the β -CD cavity. The observation of relatively strong NOE interactions between guest protons H2 and β -CD-H5, together with weak (if any) interactions with β -CD-H3, indicates the occupancy of the secondary rim of β -CD by the adamantane cage. Additionally, in the case of all hydroxylated guests (**13**–**15**), the NOE interactions between the inner β -CD hydrogen atoms and H6_{ax} of adamantane are significantly weakened or completely missing from the spectra, whereas those with H6_{eq} are observed. A portion of the NOESY spectrum of a mixture of amine **14** and β -CD is shown in Figure 5 (top). However, ^1H NMR signals of β -CD inner protons H3 and protons H6 of the secondary rim were significantly overlapped in dimethyl sulphoxide (DMSO) solution, and interpretation of the observed cross-peaks in standard NOESY spectrum became ambiguous. Therefore, we applied a 2D ^1H – ^{13}C gs-HMQC–NOESY experiment to increase the spectral resolution by employing a carbon frequency in an indirect

dimension to assign the individual NOE contacts unequivocally. A schematic of the host–guest complex **7**– β -CD and its observed interactions are depicted in Figure 5 (bottom). Both the observed interactions of adamantane protons H4 and H5 with β -CD carbons C3 and the absence of interactions between these same protons and β -CD carbons C5 indicate a positioning of the adamantane cage inside the β -CD cavity with bridgehead-substituted carbon C2 located close to the secondary rim of β -CD. In addition, observed interactions of phenyl protons H13 and H17 with β -CD carbons C6 and C5 support the proposed structural model in which the aromatic part of the guest protrudes from the secondary rim of β -CD (Figure 5). According to the notation in Figure 4, the observed arrangement of the examined host–guest complexes is assigned as SI.

The binding properties of prepared guests **6**–**8**, **13**–**15** and **25**–**27** were studied using isothermal titration calorimetry. All three aminoalcohols **13**–**15** exhibited additional heat release during both titration and dilution experiments; therefore, thermodynamic parameters could not be determined. This observation may be reasonably attributed to additional equilibria related to the dissociation of dimers and/or higher associates of guest molecules. In addition, dilution data of these aminoalcohols did not fit the theoretical curve using a simple ‘dissociation’ model, which takes into account only dimer dissociation. Therefore, it is reasonable to assume additional equilibria involving higher-ordered associations. Anilines **25** and **27** exhibited some exothermic process that very slowly equilibrated. This slow equilibration thwarted the collection of usable data. The obtained values of binding constants, enthalpies, entropies and stoichiometries of the complexes for aminoketones **6**–**8** and amine **26** are listed in Table 2. For the typical raw data, integrated values of heat released and the fitted curve for guest **7**, see Supplementary data, Figure S4.

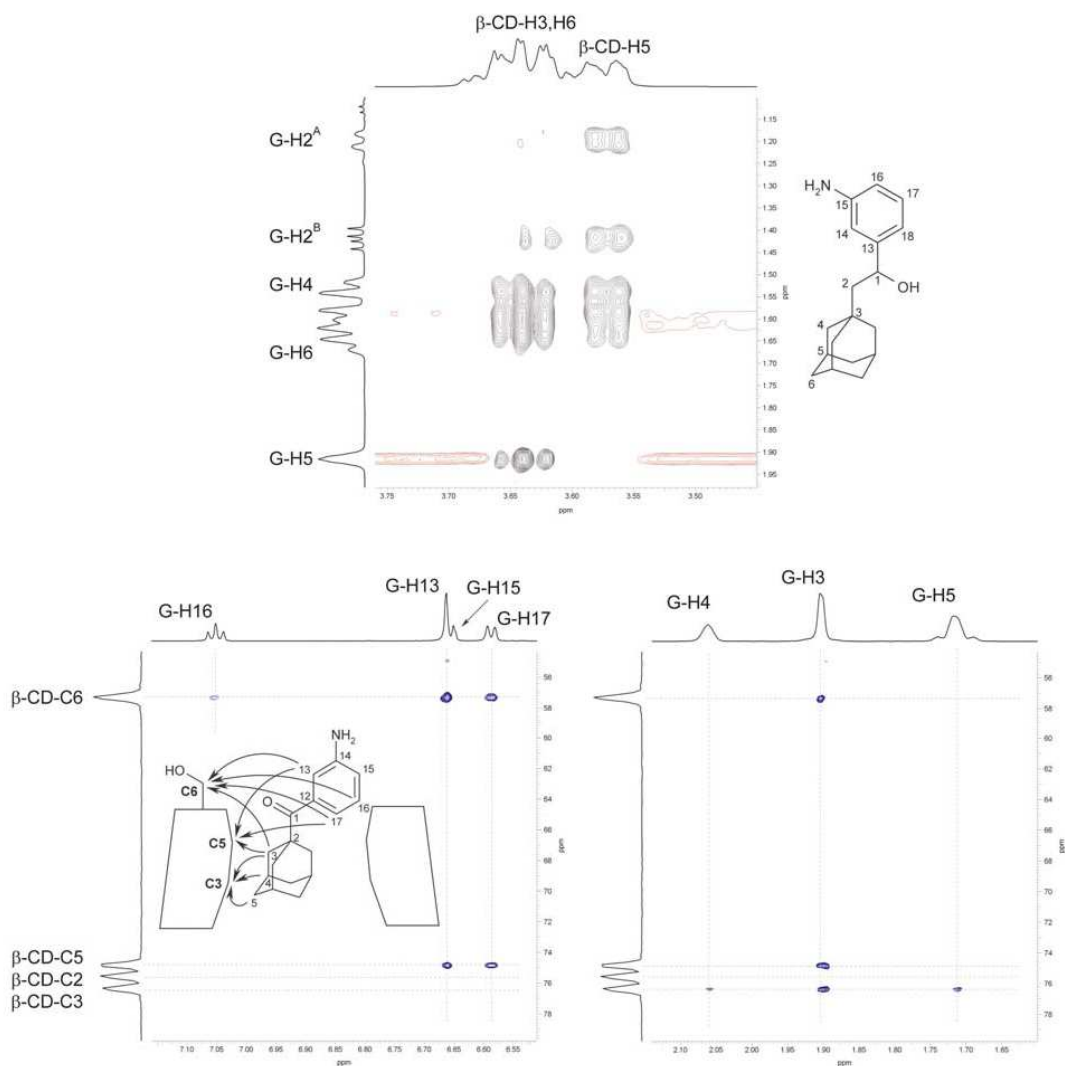


Figure 5. A portion of the NOESY spectrum of a 1:1 mixture of guest **14** with β -CD (top); A portion of the gs-HMQC-NOESY spectrum of a 1:1 mixture of guest **7** with β -CD (bottom). Detailed comment may be found in the text. Signals of host and guest nuclei are labelled as β -CD and G, respectively.

Table 2. Thermodynamic parameters for inclusion complex formation of guest molecules and β -CD derived from calorimetric titration experiments in DMSO/water (3/1, v/v) mixture at 30°C.

Guest	K [M^{-1}]	ΔH [$kJ\ mol^{-1}$]	ΔS [$J\ K^{-1}\ mol^{-1}$]	n
6	186 ± 23	35 ± 14	71	1.1 ± 0.4
7	226 ± 25	46 ± 15	105	1.0 ± 0.3
8	313 ± 55	38 ± 17	75	1.0 ± 0.4
26	694 ± 28	44 ± 3	88	0.93 ± 0.05

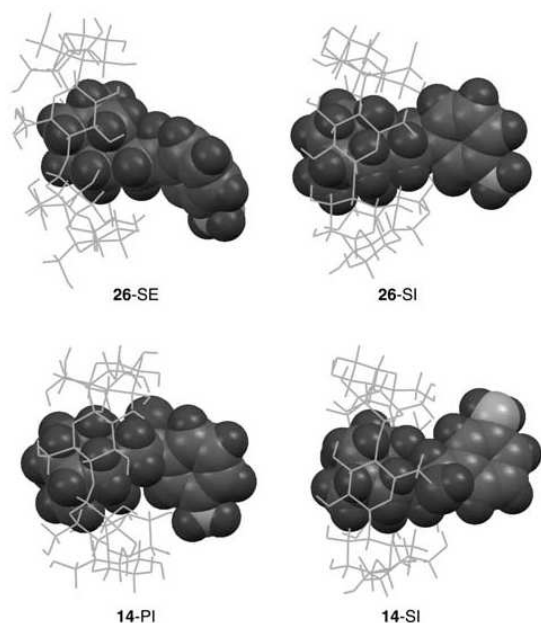


Figure 6. Minimised structures of complexes of β -CD with amine **26** and **14**, respectively.

2.4 Computation

To support the structural conclusions about host–guest complexes formulated from NMR analysis, we performed the modelling of these complexes for amines **14** and **26** with β -CD at a semi-empirical level of theory. Semi-empirical PM3 method (20) proved to perform well across a diverse group of macrocycles, particularly for CDs (21). Moreover, the PM3 method was selected among available semi-empirical methods because of its superiority to AM1 in dealing with hydrogen-bonded molecules (22). Although PM3 method chosen for our preliminary calculations appeared to be a powerful tool in conformational studies of supramolecular systems, computed relative energies should be handled with the full awareness of the weakness of semi-empirical methods in relative energy estimations and interpreted along with the corroborating experimental data. An exhaustive, up-to-date theoretical study may

require equilibrium geometries generated by PM3, combined with single-point energy calculations at higher levels of theory, preferably density functional theory (DFT) which accounts thermochemistry better than semi-empirical methods, as these sequential methods are reported in the recent literature and successfully applied for the CDs (23).

A series of calculations, described in detail in the Experimental section, yielded geometries and energies for several examined positions. The most energetically favoured geometries for amines **14** and **26**, for both directions of their virtual threading through the β -CD cavity, are depicted in Figure 6, and selected geometric parameters and energies are collected in Table 2. In the case of amine **14**, the adamantane cage occupies the secondary or primary rim with distances of $Cg1-Og$ being shorter than 0.16 nm, with the benzene ring positioned on the opposite side of the β -CD. In respect to the orientations defined in Figure 4, they may be called as SI and PI, respectively. In the case of amine **26**, the respective threading resulted in geometries with adamantane located close to the secondary rim with the $Cg1-Og$ being shorter than 0.12 nm, i.e. SE and SI. For both examined amines, the complex with SI geometry was the most populated in the thermodynamic equilibrium.

The calculations were performed for molecules *in vacuo*, neglecting the fact that complex formation might be driven by differences in solvation energies of the host–guest complex and its building blocks. Moreover, the large number of possible orientations of the β -CD's hydroxyl groups is beyond our consideration. Although only one initial conformation of the CD was used for each minimisation, the method provides a consistent indicator of the hydrogen bond stabilisation effect as well. To assess the importance of hydrogen bonding in the complex formation, a modelling experiment was performed. Non-polar parent hydrocarbon (PH) (24) was virtually threaded through the β -CD's cavity in the same way as described above with the amines. Hence, we obtained analogous results for PH and amines **14** and **26**, as shown in Table 3. Although partial stabilisation of this complex geometry via intermolecular hydrogen bonds was expected, it is not clearly manifested here. Therefore, we suggest only a

Table 3. Selected geometric parameters and free energies for complexes of amines **14**, **26** and **PH** with β -CD.

Structure	d [nm] ^a	l [nm]	α [°]	β [°]	Stabilisation energy [kJ/mol]
14-SI	+0.0295	0.0227	142.48	50.31	613.62
14-PI	0.1534	0.1534	163.49	90.00	604.14
26-SI	+0.0656	0.0622	16.10	71.47	655.29
26-SE	+0.1173	0.1158	36.74	80.83	633.66
PH-SI	+0.0930	0.0856	139.54	66.99	668.04
PH-SE	+0.2223	0.2199	30.25	81.57	650.19

For the definition of $Cg1$, $Cg2$, Og and P , see the experimental part. d is $Cg1-Og$ distance, l is $Cg1-P$ distance, α is $Cg1-Og-Cg2$ angle, β is $Cg1-Og-P$ angle.

^aThe positive or negative sign implies location of adamantane cage in cavity close to the secondary or primary rim, respectively.

small contribution of intermolecular H-bonds to the stabilisation of the complex in the gas phase.

3. Conclusions

Ten new anilines-bearing adamantane with linkers of varying polarity and length were synthesised and fully characterised using spectral methods. The inclusion complexes of these anilines with β -CD were detected using ESI-ion trap MS, and their structures were determined by 2D NMR experiments in dimethyl sulphoxide. In agreement with our experimental NMR data and molecular modelling, the most populated inclusion complex between β -CD and adamantane guests with a long, uncharged substituent may be characterised as a pseudorotaxane-like structure in which the adamantane group is sitting deep in the CD cavity close to the wider secondary rim of the β -CD and the substituent protrudes from the primary rim. Association constants of the prepared amines and β -CD were estimated to be on the order of 10^2 M^{-1} by isothermal calorimetric titrations. These binding properties allowed us to consider the use of these prepared amines in further research on drug modification.

4. Experimental section

4.1 General

All starting compounds, reagents and solvents were purchased from commercial sources in analytical quality and were used without further purification. Adamantane-1-carbonyl chloride (**16**) was prepared following a previously published procedure. Melting points were measured on a Kofler block and are uncorrected. Elemental analyses (C, H, N, S) were performed on a Thermo Fisher Scientific FlashEA 1112. Retention times were determined using TLC plates (Alugram Sil G/UV) from Macherey-Nagel and petroleum ether/ethyl acetate as mobile phase. Three compositions of mobile phases were used (v/v): system a (1/1), system b (4/1) and system c (8/1). NMR spectra were recorded on a Bruker Avance 500 spectrometer operating at frequencies of 500.13 MHz (^1H) and 125.77 MHz (^{13}C), and a Bruker Avance 300 spectrometer operating at frequencies of 300.13 MHz (^1H) and 75.77 MHz (^{13}C). ^1H and ^{13}C NMR chemical shifts were referenced to the signal of solvent (^1H : $\delta(\text{residual CHCl}_3) = 7.27 \text{ ppm}$, $\delta(\text{residual DMSO-}d_5) = 2.50 \text{ ppm}$; ^{13}C : $\delta(\text{CDCl}_3) = 77.23 \text{ ppm}$, $\delta(\text{DMSO-}d_6) = 39.52 \text{ ppm}$). The mixing time for NOESY (**25**) experiment was adjusted to 500 ms, and the spin-lock for ROESY was adjusted to 400 ms. The assignment of ^1H signals for β -CD was described previously (**19d**). The 2D ^1H - ^{13}C gs-HMQC-NOESY spectrum (**26**) was measured at resonance frequencies of 600.15 MHz (^1H) and 150.67 MHz (^{13}C). The HMQC step was adjusted for

$^1J_{\text{H C}} = 145 \text{ Hz}$ with a subsequent NOE transfer of 700 ms. The spectrum was recorded in phase-sensitive mode using the echo-antiecho protocol (**27**). The IR spectra were recorded in a KBr disc with a Mattson 3000 FT-IR instrument. GC-MS analyses were run on a Shimadzu QP-2010 instrument using a Supelco SLB-5ms (30 m, 0.25 mm) column. Helium was employed as a carrier gas in a constant linear flow mode (38 cm s^{-1}); $100^\circ\text{C}/7 \text{ min}$, $25^\circ\text{C}/\text{min}$ to 250°C , hold for the required time. Only peaks of relative abundance exceeding 5% are listed. The electrospray mass spectra were recorded with an Esquire LC ion trap mass spectrometer (Bruker Daltonics, Bremen, Germany) equipped with an ESI source. Sample solutions ($8.8 \mu\text{M}$ in methanol/water, 1/1, v/v) were introduced into the ion source at a flow rate of $3 \mu\text{L}/\text{min}$ via a metal capillary held at high voltage ($\pm 3.5 \text{ kV}$). The other instrumental conditions were as follows: drying gas temperature, 250°C ; drying gas flow, $5 \text{ dm}^3/\text{min}$ and nebuliser pressure, 41.37 kPa . Nitrogen was used as both nebulising gas and drying gas. The nozzle-skimmer potential and octopole potential were modified and optimised before each experiment. Isothermal titration calorimetry measurements were done in a DMSO/ H_2O (3/1, v/v) solvent mixture using a VP-ITC MicroCal instrument at 30°C . The concentrations of host in the cell and guest in microsyringe were approximately 7.0 and 0.6 mM, respectively. The raw experimental data were analysed using MicroCal ORIGIN software. The heats of dilution were taken into account for each guest compound. Data were fitted to a theoretical titration curve using the 'one set of binding sites' model.

4.2 Quantum chemical methods

All theoretical calculations were carried out using the SPARTAN'08 software package (**28**). First, the initial geometries of amines **14** and **26** and β -CD were optimised with the PM3 method without imposing any symmetrical restrictions. A hypothetical PH, 1-(1-adamantyl)-2-phenylethane, was used as a non-polar reference to evaluate the effect of hydrogen bonding. This hypothetical parent was constructed and optimised using the same procedure as that used for the amines. The input geometry for the optimisation of β -CD was based on available crystallographic data determined by XRD (**19b**). Initial approximations of amine-CD complexes were then constructed using the optimised structures of both host and guest molecules. As in the case of their constituents, no restrictions were imposed on the complexes. To characterise the mutual orientations of the molecules, the following values were defined: the centre of mass of the four bridgehead carbons in adamantane skeleton (Cg1), the centre of mass of the seven glycosidic oxygen atoms in β -CD (Og), centre of mass of the six carbons of the benzene ring (Cg2) and the best least squares plane of the seven

glycosidic oxygen atoms in β -CD (*P*). The sign in the half-space according to *P* was defined to be positive close to wider secondary rim and negative close to narrower primary rim. Initially, the amine was positioned along the molecular sevenfold axis of β -CD at 11 Cg1–Og distances ranging from 1.0 to –1.0 nm in increments of 0.2 nm. The resulting geometries were optimised. These optimised geometries represent the sequential local minima for an amine passing through the CD cavity. The stabilisation energy of complex formation was calculated as the difference between the energy of the complex and the sum of energies of the guest and host calculated independently. The geometry with the absolute minimum energy could in this way be described as the geometry of inclusion complex. On the other hand, the rotation of the guest molecule within the CD's cavity was not tested, as it is known that the optimisation process automatically finds the best relative rotational orientation of the guest and host molecules (29). Under real condition, one could expect water-filled central cavity in CDs that must be displaced if a guest is to enter which would stabilise any interaction due to hydrophobic effects. Therefore, it is expected that basic considerations for this virtual experiment are not compromised by neglecting of water molecules in calculations. Because both the CD and the amine have non-equivalent sides following the threading route, two distinct threading processes must be performed with each amine. It was decided to arrange the threading process as adamantane-on into the secondary and primary rim of the CD, respectively.

4.3 General procedure for nitro ketones reduction to amino ketones 6–8

The ketone (1.05 mmol) was dissolved in methanol (30 ml) and 6 ml of hydrochloric acid/water (v/v, 1/1) was added. Into the refluxed and well-stirred mixture, a portions of an iron powder (2.33 mmol) were added successively. The reaction was stopped when TLC indicated the consumption of all starting material. The mixture was poured onto a 5% solution of NaOH (40 ml) and extracted several times with diethyl ether. Combined organic layers were washed with brine and dried over sodium sulphate. The crude product was obtained after evaporation of the solvent *in vacuo*.

4.3.1 1-Adamantyl-(4-aminophenyl)methanone (6) was purified by column chromatography (silica gel, system a) to yield 257 mg (96%) of a yellow crystalline powder. Mp 79–81°C, R_f 0.17 (system b), anal. calcd for $C_{17}H_{21}NO$: C, 79.96%; H, 8.29%; N, 5.49%; found C, 80.05%; H, 8.12%; N, 5.63%. 1H NMR ($CDCl_3$): δ 1.78 (m, 6H, $CH_2(Ad)$), 2.07 (m, 9H, $CH_2 + CH(Ad)$), 6.69 (d, $J = 8.6$ Hz, 2H, Ph), 7.72 (d, $J = 8.6$ Hz, 2H, Ph) ppm. ^{13}C NMR ($CDCl_3$):

δ 28.6 (CH), 37.0 (CH_2), 39.9 (CH_2), 46.9 (C), 114.4 (CH), 129.3 (C), 131.0 (CH), 148.2 (C), 206.5 (CO) ppm. IR (KBr): 3469 (m), 3347 (s), 2898 (s), 2847 (m), 1629 (s), 1586 (s), 1557 (m), 1517 (w), 1442 (m), 1322 (m), 1271 (s), 1241 (m), 1171 (s), 1112 (m), 986 (w), 929 (w), 841 (m), 751 (w), 643 (w), 614 (m), 511 (w) cm^{-1} . GC-MS (EI, 70 eV); m/z (%): 65 (8), 79 (9), 92 (9), 93 (7), 120 (100), 121 (8), 135 (11), 255 (M^+ , 8).

4.3.2 1-Adamantyl-(3-aminophenyl)methanone (7) was purified by column chromatography (silica gel, system a) to yield 236 mg (88%) of a colourless crystalline powder. Mp 97–100°C, R_f 0.20 (system b), anal. calcd for $C_{17}H_{21}NO$: C, 79.96%; H, 8.29%; N, 5.49%; found C, 79.89%; H, 8.35%; N, 5.37%. 1H NMR ($CDCl_3$): δ 1.75 (m, 6H, $CH_2(Ad)$), 1.99 (m, 6H, $CH_2(Ad)$), 2.07 (m, 3H, $CH(Ad)$), 3.73 (bs, 2H, NH_2), 6.72–6.77 (m, 2H, Ph), 6.91 (d, $J = 7.6$ Hz, 1H, Ph), 7.16 (t, $J = 7.6$ Hz, 1H, Ph) ppm. ^{13}C NMR ($CDCl_3$): δ 28.4 (CH), 36.8 (CH_2), 39.3 (CH_2), 47.1 (C), 113.7 (CH), 116.8 (CH), 117.3 (CH), 128.9 (CH), 141.2 (C), 146.3 (C), 210.9 (CO) ppm. IR (KBr): 3474 (m), 3381 (s), 2900 (s), 2850 (m), 1662 (s), 1626 (m), 1593 (m), 1494 (m), 1446 (m), 1321 (m), 1295 (w), 1219 (m), 1180 (w), 991 (w), 793 (w), 731 (m), 682 (w), 649 (w) cm^{-1} . GC-MS (EI, 70 eV); m/z (%): 41 (8), 55 (6), 65 (13), 67 (9), 77 (8), 79 (24), 81 (7), 91 (7), 92 (18), 93 (23), 107 (12), 120 (20), 135 (100), 136 (11), 227 (6), 255 (M^+ , 24), 256 (5).

4.3.3 2-(1-Adamantyl)-1-(3-aminophenyl)ethanone (8) was purified by column chromatography (silica gel, system b) to yield 289 mg (92%) of a pale orange crystalline powder. Mp 66–68°C, R_f 0.25 (system c), anal. calcd for $C_{18}H_{23}NO$: C, 80.26%; H, 8.61%; N, 5.20%; found C, 80.11%; H, 8.49%; N, 5.23%. 1H NMR ($CDCl_3$): δ 1.65 (m, 12H, $CH_2(Ad)$), 1.95 (m, 3H, $CH(Ad)$), 2.67 (s, 2H, CH_2CO), 3.80 (s, 2H, NH_2), 6.86 (d, 1H, $J = 6.9$ Hz, Ph), 7.20–7.33 (m, 3H, Ph) ppm. ^{13}C NMR ($CDCl_3$): δ 29.0 (CH), 34.1 (C), 37.0 (CH_2), 43.2 (CH_2), 51.5 (CH_2), 114.3 (CH), 119.3 (CH), 119.5 (CH), 129.4 (CH), 140.4 (C), 146.8 (C), 200.7 (CO) ppm. IR (KBr): 3459 (m), 3405 (m), 3328 (m), 2899 (s), 2846 (s), 1660 (s), 1627 (m), 1595 (m), 1453 (m), 1326 (m), 1287 (m), 1197 (w), 1162 (w), 1143 (w), 1096 (w), 991 (w), 903 (w), 884 (w), 777 (w), 691 (w), 677 (w) cm^{-1} . GC-MS (EI, 70 eV); m/z (%): 41 (8), 55 (5), 65 (18), 77 (7), 79 (12), 91 (10), 92 (42), 93 (19), 106 (6), 107 (10), 120 (100), 121 (14), 135 (20), 241 (5), 251 (6), 269 (M^+ , 51), 270 (10).

4.4 General procedure for nitro ketones reduction to nitro alcohols 9–11

The corresponding ketone (0.84 mmol) was dissolved in warm ethanol (5 ml) and solution was cooled in ice bath. A

small portion of starting material formed a soft precipitate. The sodium borohydride (40 mg, 1.04 mmol) was added into this dispersion in one portion at 0°C. The reaction mixture was vigorously stirred and temperature was allowed to reach 20°C. After the consumption of all starting material (according to TLC), the mixture was poured onto 1 M HCl (10 ml) and a pale yellow solid precipitated. Mixture was extracted twice with diethyl ether (10 ml), collected organic portions were washed with brine and dried over Na₂SO₄. Crude product was obtained after removing of the solvent *in vacuo*.

4.4.1 1-Adamantyl-(4-nitrophenyl)methanol (9) was purified by crystallisation from methanol to yield 233 mg (96%) of a pale yellow crystals. Mp 191–192°C, *R_f* 0.11 (system b), anal. calcd for C₁₇H₂₁NO₃: C, 71.06%; H, 7.37%; N, 4.87%; O, 16.70; found C, 71.34%; H, 7.45%; N, 4.98%. ¹H NMR (CDCl₃): δ 1.47–1.72 (m, 12H, CH₂(Ad)), 2.01 (m, 4H, CH(Ad), OH), 4.33 (s, 1H, CHOH), 7.44 (d, *J* = 8.1 Hz, 2H, Ph), 8.18 (d, *J* = 8.5 Hz, 2H, Ph) ppm. ¹³C NMR (CDCl₃): δ 28.4 (CH), 37.1 (CH₂), 37.7 (C), 38.3 (CH₂), 82.3 (CH), 122.8 (CH), 128.8 (CH), 147.5 (C), 148.8 (C) ppm. IR (KBr): 3565 (s), 3112 (w), 3081 (w), 2908 (s), 2848 (s), 1600 (m), 1506 (s), 1450 (w), 1346 (s), 1312 (m), 1216 (w), 1168 (w), 1105 (m), 1038 (m), 977 (w), 938 (w), 855 (m), 830 (w), 800 (w), 760 (w), 720 (s), 701 (w), 637 (w), 740 (m) cm⁻¹. GC-MS (EI, 70 eV); *m/z* (%): 41 (8), 44 (14), 55 (6), 67 (8), 77 (8), 79 (18), 91 (5), 93 (17), 107 (10), 121 (6), 122 (14), 135 (100), 136 (12), 287 (M⁺, 4).

4.4.2 1-Adamantyl-(3-nitrophenyl)methanol (10) was purified by column chromatography (silica gel, system b) to yield 234 mg (97%) of a colourless crystalline powder. Mp 104–106°C, *R_f* 0.20 (system b), anal. calcd for C₁₇H₂₁NO₃: C, 71.06%; H, 7.37%; N, 4.87%; found C, 70.83%; H, 7.18%; N, 4.55%. ¹H NMR (CDCl₃): δ 1.27–1.71 (m, 12H, CH₂(Ad)), 1.99 (m, 3H, CH(Ad)), 2.10 (s, 1H, OH), 4.33 (s, 1H, CHOH), 7.49 (m, 1H, Ph), 7.59 (m, 1H, Ph), 8.12 (m, 2H, Ph) ppm. ¹³C NMR (CDCl₃): δ 28.9 (CH), 32.9 (C), 37.2 (CH₂), 43.3 (CH₂), 54.7 (CH₂), 70.3 (CH), 120.9 (CH), 122.4 (CH), 129.6 (CH), 132.1 (CH), 148.6 (C), 149.0 (C) ppm. IR (KBr): 3543 (m), 3432 (m), 3106 (w), 3092 (w), 2906 (s), 2848 (s), 1525 (s), 1475 (w), 1448 (w), 1349 (s), 1312 (w), 1286 (w), 1194 (w), 1126 (w), 1088 (w), 1036 (m), 1021 (m), 982 (w), 930 (w), 909 (w), 896 (w), 813 (m), 722 (m), 693 (m), 661 (w), 618 (w) cm⁻¹. GC-MS (EI, 70 eV); *m/z* (%): 41 (10), 55 (7), 67 (10), 77 (13), 78 (5), 79 (26), 81 (6), 91 (7), 93 (22), 105 (5), 107 (12), 135 (100), 136 (11).

4.4.3 2-(1-Adamantyl)-1-(3-nitrophenyl)ethanol (11) was purified by column chromatography (silica gel,

system c) to yield 220 mg (87%) of a colourless crystalline powder. Mp 68–69°C, *R_f* 0.51 (system c), anal. calcd for C₁₈H₂₃NO₃: C, 71.73%; H, 7.69%; N, 4.65%; found C, 71.56%; H, 7.44%; N, 4.83%. ¹H NMR (CDCl₃): δ 1.50 (d, *J* = 2.6, 1H, AdCH^AH^B), 1.59–1.79 (m, 12H, CH₂(Ad)), 1.88 (d, *J* = 3.6 Hz, 1H, AdCH^AH^B), 2.02 (m, 3H, CH(Ad)), 5.05 (m, 1H, PhCHOH), 7.52 (t, *J* = 7.9 Hz, 1H, Ph), 7.70 (d, *J* = 7.6 Hz, 1H, Ph), 8.13 (d, *J* = 8.3 Hz, 1H, Ph), 8.23 (s, 1H, Ph) ppm. ¹³C NMR (CDCl₃): δ 28.9 (CH), 32.9 (C), 37.2 (CH₂), 43.3 (CH₂), 54.7 (CH₂), 70.3 (CH), 120.9 (CH), 122.4 (CH), 129.6 (CH), 132.1 (CH), 148.6 (C), 149.0 (C) ppm. IR (KBr): 3380 (bs), 3090 (w), 3072 (w), 2899 (s), 2845 (s), 1525 (s), 1445 (m), 1349 (s), 1314 (w), 1199 (w), 1160 (w), 1103 (m), 1066 (m), 1014 (w), 969 (w), 827 (w), 802 (w), 740 (m), 722 (m), 698 (m), 676 (m) cm⁻¹. GC-MS (EI, 70 eV); *m/z* (%): 41(17), 43(5), 53(5), 55(12), 65(5), 67(22), 69(7), 77(21), 78(11), 79(35), 80(5), 81(21), 91(20), 92(11), 93(43), 94(8), 95(6), 105(13), 106(8), 107(28), 121(8), 134(6), 135(100), 136(14), 149(58), 150(15), 152(22), 266(17), 283(14).

4.5 General procedure for nitro alcohols reduction to amino alcohols 12–15

The alcohols **13** and **14** and methoxy compound **12** were prepared from corresponding nitro alcohols in the same way as the ketones **6–8**.

4.5.1 4-[1-Adamantyl(methoxy)methyl]anilinium chloride (12-HCl) crystallised as the hydrochloride salt directly from reaction mixture and no further purification was necessary. Yield: 275 mg (85%) of a gold-yellow plate crystals. Mp > 350°C, *R_f* (free base) 0.27 (system b), anal. calcd for C₁₈H₂₆ClNO: C, 70.22%; H, 8.51%; N, 4.55%; found C, 69.94%; H, 8.37%; N, 4.75%. ¹H NMR (DMSO-*d*₆): δ 1.34–1.60 (m, 12H, CH₂(Ad)), 1.89 (m, 3H, CH(Ad)), 3.08 (s, 3H, OCH₃), 3.71 (s, 1H, CHCOCH₃), 7.27–7.36 (m, 4H, Ph), 10.28 (bs, 3H, NH₃⁺) ppm. ¹³C NMR (DMSO-*d*₆): δ 27.5 (CH), 36.5 (CH₂), 37.7 (CH₂), 56.9 (CH₃), 90.8 (CH), 122.0 (CH), 129.3 (CH), 131.0 (C), 137.8 (C) ppm. IR (KBr): 3437 (bs), 2905 (s), 2847 (s), 2562 (s), 1625 (m), 1578 (m), 1556 (m), 1507 (s), 1452 (m), 1360 (w), 1347 (w), 1316 (w), 1241 (w), 1175 (w), 1133 (w), 1085 (s), 997 (w), 826 (w), 529 (m) cm⁻¹. GC-MS (IE, 70 eV); *m/z* (%): 120 (7), 121 (6), 136 (100), 137 (9), 271 (M⁺, 2).

4.5.2 1-Adamantyl-(3-aminophenyl)methanol (13): Crude material was purified by column chromatography (silica gel, system a) to yield 254 mg (94%) of a pale yellow crystalline powder. Mp 137–139°C, *R_f* 0.11 (system b), anal. calcd for C₁₇H₂₃NO: C, 79.33%; H, 9.01%; N, 5.44%; found C, 79.57%; H, 9.15%; N, 5.72%.

^1H NMR (CDCl_3): δ 1.49–1.66 (m, 12H, $\text{CH}_2(\text{Ad})$), 1.97 (m, 3H, $\text{CH}(\text{Ad})$), 3.62 (bs, 2H, NH_2), 4.12 (s, 1H, CHOH), 6.60–6.67 (m, 3H, Ph), 7.10 (t, $J = 7.6$ Hz, 1H, Ph) ppm. ^1H NMR ($\text{DMSO}-d_6$): δ 1.37–1.63 (m, 12H, $\text{CH}_2(\text{Ad})$), 1.89 (m, 3H, $\text{CH}(\text{Ad})$), 3.86 (d, $J = 3.8$ Hz, 1H, CHOH), 4.77 (d, $J = 3.8$ Hz, 1H, CHOH), 4.85 (s, 2H, NH_2), 6.34–6.41 (m, 2H, Ph), 6.46 (s, 1H, Ph), 6.89 (t, $J = 7.6$ Hz, 1H, Ph) ppm. ^{13}C NMR (CDCl_3): δ 28.6 (CH), 29.9 (C), 37.3 (CH_2), 38.5 (CH_2), 83.2 (CH), 114.3 (CH), 114.8 (CH), 118.7 (CH), 128.5 (CH), 142.8 (C), 145.9 (C) ppm. IR (KBr): 3394 (m), 2901 (s), 2847 (m), 2359 (w), 1606 (m), 1490 (w), 1457 (m), 1302 (w), 1125 (w), 1036 (m), 885 (w), 750 (m), 730 (m), 700 (m), 667 (w), 585 (w), 418 (w) cm^{-1} . GC-MS (EI, 70 eV); m/z (%): 41 (8), 55 (7), 65 (5), 67 (10), 77 (16), 79 (24), 81 (7), 91 (6), 92 (5), 93 (25), 94 (17), 107 (13), 120 (6), 121 (54), 122 (13), 135 (100), 136 (11), 257 (M^+ , 20), 258 (4).

4.5.3 2-(1-Adamantyl)-1-(3-aminophenyl)ethanol (14): Crude material was purified by washing with hexane to yield 234 mg (82%) of a colourless crystalline powder. Mp 142–145°C, R_f 0.57 (system a), anal. calcd for $\text{C}_{18}\text{H}_{25}\text{NO}$: C, 79.66%; H, 9.28%; N, 5.16%; found C, 79.73%; H, 9.52%; N, 5.38%. ^1H NMR (CDCl_3): δ 1.50 (d, $J = 2.6$ Hz, 1H, $\text{AdCH}^{\text{A}}\text{H}^{\text{B}}$), 1.59–1.79 (m, 12H, $\text{CH}_2(\text{Ad})$), 1.88 (d, $J = 3.6$ Hz, 1H, $\text{AdCH}^{\text{A}}\text{H}^{\text{B}}$), 2.02 (m, 3H, $\text{CH}(\text{Ad})$), 5.05 (m, 1H, PhCHOH), 7.52 (t, $J = 7.9$ Hz, 1H, Ph), 7.70 (d, $J = 7.6$ Hz, 1H, Ph), 8.13 (d, $J = 8.3$ Hz, 1H, Ph), 8.23 (s, 1H, Ph) ppm. ^{13}C NMR (CDCl_3): δ 28.9 (CH), 32.9 (C), 37.2 (CH_2), 43.3 (CH_2), 54.7 (CH_2), 70.3 (CH), 120.9 (CH), 122.4 (CH), 129.6 (CH), 132.1 (CH), 148.6 (C), 149.0 (C) ppm. IR (KBr): 3380 (bs), 3090 (w), 3072 (w), 2899 (s), 2845 (s), 1525 (s), 1445 (m), 1349 (s), 1314 (w), 1199 (w), 1160 (w), 1103 (m), 1066 (m), 1014 (w), 969 (w), 827 (w), 802 (w), 740 (m), 722 (m), 698 (m), 676 (m) cm^{-1} . GC-MS (EI, 70 eV); m/z (%): 41 (8), 55 (5), 65 (5), 67 (7), 77 (17), 79 (11), 81 (5), 91 (7), 92 (5), 93 (15), 94 (72), 95 (7), 107 (6), 120 (6), 121 (20), 122 (100), 123 (9), 135 (7), 253 (5), 271 (M^+ , 28), 272 (6).

4.5.4 1-Adamantyl-(4-aminophenyl)methanol (15): The nitroalcohol **9** (259 mg, 0.90 mmol) was dissolved in ethanol (40 ml) under H_2 atmosphere and large excess of Ra–Ni was added portionwise until starting material disappeared. Ra–Ni was filtered off, the filtrate was diluted with water and extracted several times with diethyl ether. Collected organic portions were washed with brine, dried over Na_2SO_4 and evaporated *in vacuo*. Crude material was purified by column chromatography (silica gel, system a) to yield 227 mg (98%) of a pale yellow crystalline powder. Mp 143–146°C, R_f 0.41 (system a), anal. calcd for $\text{C}_{17}\text{H}_{23}\text{NO}$: C, 79.33%; H, 9.01%; N, 5.44%; found C, 79.09%; H, 9.23%; N, 5.28%. ^1H NMR

(CDCl_3): δ 1.48–1.67 (m, 12H, $\text{CH}_2(\text{Ad})$), 1.97 (m, 3H, $\text{CH}(\text{Ad})$), 3.53 (bs, 2H, NH_2), 4.11 (s, 1H, CHOH), 6.64 (d, $J = 8.3$ Hz, 2H, Ph), 7.06 (d, $J = 8.1$ Hz, 2H, Ph) ppm. ^{13}C NMR (CDCl_3): δ 28.8 (CH), 29.9 (C), 37.5 (CH_2), 38.5 (CH_2), 83.1 (CH), 114.5 (CH), 128.9 (CH), 131.8 (C), 145.8 (C) ppm. IR (KBr): 3378 (m), 2905 (s), 2847 (m), 1615 (m), 1514 (m), 1447 (w), 1265 (m), 1175 (w), 1128 (w), 1046 (m), 844 (w), 811 (w), 572 (m), 535 (w), 481 (w) cm^{-1} . GC-MS (EI, 70 eV); m/z (%): 77 (9), 79 (7), 93 (7), 94 (12), 120 (9), 121 (38), 122 (100), 123 (8), 135 (5), 257 (M^+ , 4).

4.6 General procedures for nitrodithianes 16–18 and nitrodithiolanes 19, 20 formation

The ketone (0.35 mmol) was dissolved in dichloromethane (2 ml) and corresponding dithiol (1,2-ethanedithiol or 1,3-propanedithiol; 0.55 mmol) was added. The solution was cooled in ice bath to 0°C and stirred for 30 min. After this period, boron trifluoride-diethyl ether (1.00 mmol) was added dropwise and the mixture was stirred at room temperature until TLC indicated complete disappearance of the starting material. The mixture was diluted with CH_2Cl_2 (20 ml) and washed three times with 5% solution of NaOH (10 ml). The organic layer was washed twice with brine, dried over Na_2SO_4 and evaporated *in vacuo*.

4.6.1 2-(1-Adamantyl)-2-(3-nitrophenyl)-1,3-dithiane (16) was purified by crystallisation from hexane/ CH_2Cl_2 to yield 121 mg (92%) of yellow needles. Mp 191–193°C, R_f 0.42 (system c), anal. calcd for $\text{C}_{20}\text{H}_{25}\text{NO}_2\text{S}_2$: C, 63.96%; H, 6.71%; N, 3.73%; S, 17.08%; found C, 64.23%; H, 6.55%; N, 3.37%; S, 17.12%. ^1H NMR (CDCl_3): δ 1.58 (m, 6H, $\text{CH}_2(\text{Ad})$), 1.83 (m, 8H, $\text{CH}_2(\text{Ad})$, SCH_2CH_2), 1.97 (m, 3H, $\text{CH}(\text{Ad})$), 2.45 (m, 2H, $\text{SCH}^{\text{A}}\text{H}^{\text{B}}$), 2.67 (m, 1H, SCH^{C}), 2.71 (m, 1H, SCH^{D}), 7.57 (t, $J = 7.9$ Hz, 1H, Ph), 8.15 (d, $J = 8.3$ Hz, 1H, Ph), 8.33 (d, $J = 7.9$ Hz, 1H, Ph), 8.85 (s, 1H, Ph) ppm. ^{13}C NMR (CDCl_3): δ 25.4 (CH_2), 27.8 (CH_2), 28.9 (CH), 36.8 (CH_2), 37.6 (CH_2), 41.7 (C), 70.2 (C), 122.0 (CH), 127.4 (CH), 128.7 (CH), 138.6 (CH), 141.0 (C), 148.7 (C) ppm. IR (KBr): 2904 (s), 2846 (s), 1521 (s), 1469 (w), 1447 (w), 1420 (w), 1351 (s), 1310 (w), 1273 (w), 1172 (w), 1093 (w), 1010 (w), 979 (w), 940 (w), 892 (w), 813 (w), 787 (w), 726 (m), 694 (m) cm^{-1} . GC-MS (EI, 70 eV); m/z (%): 41 (11), 55 (5), 67 (8), 77 (6), 79 (20), 81 (5), 91 (6), 93 (17), 107 (10), 120 (5), 135 (100), 136 (12), 224 (43), 225 (6), 240 (10), 375 (M^+ , 3).

4.6.2 2-(1-Adamantyl)-2-(4-nitrophenyl)-1,3-dithiane (17) was purified by crystallisation from hexane/ CH_2Cl_2 to yield 120 mg (91%) of yellow needles. Mp 218–220°C, R_f 0.51 (system b), anal. calcd for $\text{C}_{20}\text{H}_{25}\text{NO}_2\text{S}_2$: C,

63.96%; H, 6.71%; N, 3.73%; S, 17.08%; found C, 63.84%; H, 6.52%; N, 3.46%; S, 16.95%. ^1H NMR (CDCl_3): δ 1.57 (m, 6H, $\text{CH}_2(\text{Ad})$), 1.83 (m, 8H, $\text{CH}_2(\text{Ad})$, SCH_2CH_2), 1.97 (m, 3H, $\text{CH}(\text{Ad})$), 2.46 (m, 2H, $\text{SCH}^{\text{A}}\text{H}^{\text{B}}$), 2.67 (m, 1H, SCH^{C}), 2.71 (m, 1H, SCH^{D}), 8.20 (m, 4H, Ph) ppm. ^{13}C NMR (CDCl_3): δ 25.3 (CH_2), 27.8 (CH_2), 28.9 (CH), 36.8 (CH_2), 37.6 (CH_2), 41.7 (C), 70.4 (C), 122.9 (CH), 133.6 (CH), 146.1 (C), 146.6 (C) ppm. IR (KBr): 2908 (s), 2848 (s), 1598 (m), 1515 (s), 1447 (w), 1413 (w), 1349 (s), 1308 (s), 1283 (w), 1264 (w), 1110 (m), 1066 (w), 1011 (w), 976 (w), 930 (w), 855 (m), 839 (m), 794 (w), 727 (m), 696 (w) cm^{-1} . GC-MS (EI, 70 eV); m/z (%): 41 (9), 77 (5), 79 (17), 81 (5), 91 (5), 93 (14), 107 (8), 135 (100), 136 (12), 210 (5), 224 (21), 240 (5), 375(M^+ , 4).

4.6.3 2-(1-Adamantylmethyl)-2-(3-nitrophenyl)-1,3-dithiane (**18**) was purified by crystallisation from hexane to yield 125 mg (92%) of yellow needles. Mp 174–176°C, R_f 0.60 (system b), anal. calcd for $\text{C}_{21}\text{H}_{27}\text{NO}_2\text{S}_2$: C, 64.74%; H, 6.99%; N, 3.60%; S, 16.46%; found C, 64.58%; H, 7.17%; N, 3.87%; S, 16.72%. ^1H NMR (CDCl_3): δ 1.36 (m, 6H, $\text{CH}_2(\text{Ad})$), 1.51 (m, 6H, $\text{CH}_2(\text{Ad})$), 1.78 (m, 3H, $\text{CH}(\text{Ad})$), 1.94 (m, 2H, SCH_2CH_2), 2.04 (s, 2H, AdCH_2), 2.64 (m, 4H, SCH_2), 7.54 (t, $J = 7.9$ Hz, 1H, Ph), 8.13 (d, $J = 7.9$ Hz, 1H, Ph), 8.33 (d, $J = 9.2$ Hz, 1H, Ph), 8.86 (s, 1H, Ph) ppm. ^{13}C NMR (CDCl_3): δ 24.8 (CH_2), 28.1 (CH), 28.9 (CH), 36.1 (C), 36.8 (CH_2), 44.0 (CH_2), 57.6 (C), 59.8 (CH_2), 122.2 (CH), 125.1 (CH), 129.3 (CH), 136.0 (CH), 145.7 (C), 148.7 (C) ppm. IR (KBr): 3083 (w), 2899 (s), 2845 (s), 2672 (w), 1573 (w), 1523 (s), 1470 (w), 1448 (w), 1422 (m), 1350 (s), 1311 (m), 1281 (w), 1270 (m), 1101 (m), 1091 (w), 1079 (w), 1032 (w), 996 (w), 863 (w), 802 (m), 776 (w), 733 (m), 707 (w), 687 (m) cm^{-1} . GC-MS (EI, 70 eV); m/z (%): 41 (11), 55 (11), 67 (13), 69 (5), 77 (8), 79 (28), 81 (10), 91 (10), 93 (24), 107 (18), 135 (100), 136 (13), 239 (43), 315 (7), 389 (M^+ , 6).

4.6.4 2-(1-Adamantyl)-2-(4-nitrophenyl)-1,3-dithiolane (**19**) was purified by crystallisation from hexane/ CH_2Cl_2 to yield 115 mg (91%) of colourless needles. Mp 185–189°C, R_f 0.51 (system b), anal. calcd for $\text{C}_{19}\text{H}_{23}\text{NO}_2\text{S}_2$: C, 63.12%; H, 6.41%; N, 3.87%; S, 17.74%; found C, 63.41%; H, 6.51%; N, 4.12%; S, 17.45%. ^1H NMR (CDCl_3): δ 1.57 (m, 6H, $\text{CH}_2(\text{Ad})$), 1.79 (m, 6H, $\text{CH}_2(\text{Ad})$), 1.99 (m, 3H, $\text{CH}(\text{Ad})$), 2.98 (m, 2H, $\text{SCH}^{\text{A}}\text{H}^{\text{B}}$), 3.27 (m, 2H, $\text{SCH}^{\text{A}}\text{H}^{\text{B}}$), 7.97 (m, 2H, Ph), 8.10 (m, 2H, Ph) ppm. ^{13}C NMR (CDCl_3): δ 29.0 (CH), 36.6 (CH_2), 38.8 (CH_2), 39.9 (CH_2), 41.3 (C), 86.4 (C), 121.6 (CH), 132.0 (CH), 146.8 (C), 151.6 (C) ppm. IR (KBr): 2903 (s), 2845 (m), 1600 (m), 1515 (s), 1447 (w), 1400 (w), 1345 (s), 1308 (w), 1145 (w), 1110 (m), 1014 (w), 979 (m), 853 (m), 842 (m), 809 (w), 728 (m), 697 (m), 638 (w), 503 (w)

cm^{-1} . GC-MS (EI, 70 eV); m/z (%): 41 (6), 67 (7), 77 (5), 79 (18), 81 (5), 91 (5), 93 (17), 107 (10), 135 (100), 136 (13), 196 (10), 210 (8), 361(M^+ , 3).

4.6.5 2-(1-Adamantylmethyl)-2-(3-nitrophenyl)-1,3-dithiolane (**20**) was purified by crystallisation from hexane/ CH_2Cl_2 to yield 110 mg (84%) of a pale yellow crystal. Mp 142–148°C, R_f 0.51 (system c), anal. calcd for $\text{C}_{20}\text{H}_{25}\text{NO}_2\text{S}_2$: C, 63.96%; H, 6.71%; N, 3.73%; S, 17.08%; found C, 63.98%; H, 6.58%; N, 3.95%; S, 16.82%. ^1H NMR (CDCl_3): δ 1.30 (m, 6H, $\text{CH}_2(\text{Ad})$), 1.51 (m, 6H, $\text{CH}_2(\text{Ad})$), 1.80 (m, 3H, $\text{CH}(\text{Ad})$), 2.52 (s, 2H, CCH_2Ad), 3.06 (m, 2H, $\text{SCH}^{\text{A}}\text{H}^{\text{B}}$), 3.38 (m, 2H, $\text{SCH}^{\text{A}}\text{H}^{\text{B}}$), 7.46 (t, $J = 7.9$ Hz, 1H, Ph), 8.07 (d, $J = 7.9$ Hz, 1H, Ph), 8.15 (d, $J = 7.9$ Hz, 1H, Ph), 8.71 (s, 1H, Ph) ppm. ^{13}C NMR (CDCl_3): δ 28.8 (CH), 35.5 (C), 36.8 (CH_2), 38.9 (CH_2), 43.6 (CH_2), 58.3 (CH_2), 72.5 (C), 122.2 (CH), 123.0 (CH), 128.7 (CH), 134.1 (CH), 148.0 (C), 149.1 (C) ppm. IR (KBr): 3077 (w), 2921 (s), 2902 (s), 2888 (s), 2841 (s), 1524 (s), 1447 (w), 1348 (s), 1314 (w), 1277 (w), 1100 (w), 898 (w), 804 (w), 736 (m), 685 (m), 588 (w) cm^{-1} . GC-MS (EI, 70 eV); m/z (%): 41 (8), 55 (8), 67 (9), 79 (23), 93 (18), 107 (9), 135 (35), 149 (6), 180 (6), 226 (100), 227 (12), 228 (10), 375(M^+ , 2).

4.7 General procedure for preparation of aminodithianes **21** and **22**

The corresponding nitrodithiane (0.44 mmol) was dissolved in dioxane (7 ml) and a suspension of Ra–Ni in hexane was added to this solution. The mixture was stirred and refluxed under hydrogen atmosphere. Further portions of Ra–Ni were added until TLC indicated complete disappearing of the starting material. The Ra–Ni was filtrated off, resulting solution was diluted with water (14 ml) and extracted with diethyl ether (6 \times 15 ml) and hexane (1 \times 20 ml). Collected organic portions were washed with water (3 \times 30 ml), brine (3 \times 15 ml) and dried over Na_2SO_4 .

4.7.1 2-(1-Adamantyl)-2-(4-aminophenyl)-1,3-dithiane hydrochloride (**21-HCl**) was precipitated from hexane solution of crude **21** by introducing dry HCl. Yield: 146 mg (87%) of a colourless crystalline powder. Mp 140–145°C, R_f (free base) 0.24 (system b), anal. calcd for $\text{C}_{20}\text{H}_{28}\text{ClNS}_2$: C, 62.88%; H, 7.39%; N, 3.67%; S, 16.79%; found C, 62.73%; H, 7.19%; N, 3.62%; S, 16.98%. ^1H NMR (CDCl_3): δ 1.42–1.60 (m, 8H, $\text{CH}_2(\text{Ad}) + \text{CH}_2(\text{dithiane})$), 1.75 (m, 6H, $\text{CH}_2(\text{Ad})$), 1.92 (m, 3H, $\text{CH}(\text{Ad})$), 2.34 (m, 2H, $\text{CH}_2(\text{dithiane})$), 2.72 (m, 2H, $\text{CH}_2(\text{dithiane})$), 7.43 (d, $J = 8.6$ Hz, 2H, Ph), 7.92 (d, $J = 8.6$ Hz, 2H, Ph), 10.34 (bs, 3H, NH_3) ppm. ^{13}C NMR (CDCl_3): δ 24.7 (CH_2), 27.0 (CH_2), 28.0 (CH), 36.3 (CH_2),

37.0 (CH₂), 41.6 (C), 69.8 (C), 122.4 (CH), 130.8 (C), 133.1 (CH), 136.5 (C) ppm. IR (KBr): 3466 (bs), 2905 (s), 2848 (s), 2597 (m), 1614 (w), 1541 (s), 1504 (m), 1447 (w), 1417 (w), 1359 (w), 1344 (w), 1306 (w), 1279 (w), 1024 (w), 978 (w), 836 (w), 789 (w), 526 (w) cm⁻¹. GC-MS (EI, 70 eV); *m/z* (%): 41 (7), 77 (5), 79 (9), 91 (5), 93 (7), 106 (10), 120 (20), 135 (10), 136 (28), 210 (100), 211 (13), 212 (9), 345 (M⁺, 1).

4.7.2 2-(1-Adamantylmethyl)-2-(3-aminophenyl)-1,3-dithiane (**22**) was purified by column chromatography (silica gel, system b) to yield 106 mg (67%) of a pale yellow crystalline powder. Mp 127–132°C, *R_f* 0.38 (system b), anal. calcd for C₂₁H₂₉NS₂: C, 70.14%; H, 8.13%; N, 3.90%; S, 17.83; found C, 70.33%; H, 7.94%; N, 4.25%; S, 18.08%. ¹H NMR (CDCl₃): δ 1.40–1.58 (m, 12H, CH₂(Ad)), 1.78 (m, 3H, CH(Ad)), 1.85–1.96 (m, 4H, SCH₂CH₂ + CCH₂Ad), 2.57 (m, 2H, SCH^AH^B), 2.78 (m, 2H, SCH^AH^B), 3.68 (bs, 2H, NH₂), 6.58 (d, *J* = 7.9 Hz, 1H, Ph), 7.14 (t, *J* = 7.9 Hz, 1H, Ph), 7.37–7.39 (m, 2H, Ph) ppm. ¹³C NMR (CDCl₃): δ 25.2 (CH₂), 28.2 (CH₂), 29.0 (CH), 36.0 (C), 37.0 (CH₂), 43.6 (CH₂), 59.6 (CH₂), 113.9 (CH), 116.7 (CH), 120.6 (CH), 129.2 (CH), 143.3 (C), 146.6 (C) ppm. IR (KBr): 3443 (w), 3358 (w), 2363 (w), 1730 (w), 1614 (s), 1598 (s), 1489 (m), 1471 (w), 1448 (s), 1417 (w), 1346 (m), 1313 (m), 1277 (w), 1102 (w), 993 (w), 881 (w), 781 (m), 768 (w), 710 (w), 694 (w), 667 (w), 457 (w) cm⁻¹. GC-MS (EI, 70 eV); *m/z* (%): 41 (17), 53 (5), 55 (14), 65 (7), 67 (17), 77 (13), 79 (44), 81 (13), 91 (25), 92 (5), 93 (36), 106 (7), 107 (19), 117 (10), 118 (30), 119 (7), 135 (100), 136 (30), 210 (81), 211 (11), 212 (8), 224 (6), 251 (5), 252 (13), 253 (7), 284 (10), 285 (70), 286 (15), 359 (M⁺, 26), 360 (7).

4.8 General procedure for preparation of amino dithiolanes 23 and 24

The corresponding nitrodithiolane (3.37 mmol) was dissolved in *i*PrOH (125 ml) and hydrochloric acid/water (1/1, *v/v*, 20 ml) and an iron powder (424 mg, 7.59 mmol) was added. Into the well-stirred and refluxed mixture, further portions of an iron powder (424 mg, 7.59 mmol) were added until TLC indicated complete disappearing of the starting material. The mixture was poured onto a 5% solution of NaOH (120 ml) and extracted several times with diethyl ether. Combined organic layers were washed three times with water (3 × 15 ml) and dried over Na₂SO₄ overnight. The crude product was obtained after evaporation of the solvent *in vacuo*.

4.8.1 2-(1-Adamantyl)-2-(4-aminophenyl)-1,3-dithiolane (**23**) was purified by column chromatography (silica gel, CHCl₃) to yield 827 mg (74%) of a pale orange

crystalline powder. Mp 121–124°C, *R_f* 0.31 (system b), anal. calcd for C₁₉H₂₅NS₂: C, 68.83%; H, 7.60%; N, 4.22%; S, 19.34; found C, 68.73%; H, 7.45%; N, 4.53%; S, 19.02%. ¹H NMR (CDCl₃): δ 1.56 (m, 6H, CH₂(Ad)), 1.81 (m, 6H, CH₂(Ad)), 1.96 (m, 3H, CH(Ad)), 2.99 (m, 2H, SCH^AH^B), 3.23 (m, 2H, SCH^AH^B), 3.64 (s, 2H, NH₂), 6.58 (d, *J* = 8.6 Hz, 2H, Ph), 7.55 (d, *J* = 8.6 Hz, 2H, Ph) ppm. ¹³C NMR (CDCl₃): δ 29.1 (CH), 36.8 (CH₂), 38.4 (CH₂), 40.0 (CH₂), 41.4 (C), 87.3 (C), 113.2 (CH), 131.9 (CH), 133.2 (C), 145.0 (C) ppm. IR (KBr): 3417 (w), 2902 (s), 2370 (m), 2341 (m), 1622 (m), 1507 (m), 1280 (w), 1186 (w), 977 (w), 835 (w), 652 (w), 531 (w) cm⁻¹. GC-MS (EI, 70 eV); *m/z* (%): 79 (6), 93 (5), 124 (5), 136 (20), 196 (100), 197 (12), 198 (9), 331 (M⁺, 1).

4.8.2 2-(1-Adamantylmethyl)-2-(3-aminophenyl)-1,3-dithiolane (**24**) was purified by column chromatography (silica gel, system b) to yield 1013 mg (87%) of a pale yellow crystalline powder. Mp 115–120°C, *R_f* 0.29 (system b), anal. calcd for C₂₀H₂₇NS₂: C, 69.51%; H, 7.88%; N, 4.05%; S, 18.56; found C, 69.64%; H, 8.15%; N, 4.27%; S, 18.33%. ¹H NMR (CDCl₃): δ 1.35 (m, 6H, CH₂(Ad)), 1.53 (m, 6H, CH₂(Ad)), 1.80 (s, 3H, CH(Ad)), 2.44 (s, 2H, AdCH₂C), 3.10 (m, 2H, SCH^AH^B), 3.32 (m, 2H, SCH^AH^B), 3.65 (s, 2H, NH₂), 6.52 (d, *J* = 7.9 Hz, 1H, Ph), 7.05 (t, *J* = 7.9 Hz, 1H, Ph), 7.18 (m, 2H, Ph) ppm. ¹³C NMR (CDCl₃): δ 28.9 (CH), 35.4 (C), 36.9 (CH₂), 38.5 (CH₂), 43.2 (CH₂), 58.4 (CH₂), 73.7 (C), 113.8 (CH), 115.0 (CH), 118.7 (CH), 128.6 (CH), 145.8 (C), 146.9 (C) ppm. IR (KBr): 3420 (w), 3345 (w), 2896 (s), 2844 (s), 1615 (m), 1597 (m), 1489 (m), 1445 (m), 1416 (w), 1363 (w), 1346 (w), 1313 (m), 1273 (w), 1103 (w), 994 (w), 781 (m), 694 (m), 452 (w) cm⁻¹. GC-MS (EI, 70 eV); *m/z* (%): 41 (6), 55 (6), 67 (6), 79 (17), 81 (5), 91 (8), 93 (13), 107 (6), 135 (23), 136 (12), 196 (100), 197 (12), 198 (9), 345 (M⁺, 5).

4.9 General procedure for preparation of anilines 25 and 26

The corresponding aminodithiolane (2.37 mmol) was dissolved in dioxane (10 ml) and large excess of Ra-Ni was added. The mixture was stirred and refluxed under an Ar atmosphere. If repeated GC analysis showed no significant progress, further portions of Ra-Ni were added until the starting material was completely consumed. Ra-Ni was filtered off, the filtrate was diluted with water and extracted several times with diethyl ether. Collected organic portions were washed with brine, dried over Na₂SO₄ and evaporated *in vacuo*. The desired crude product obtained as orange oil was subsequently converted to the hydrochloride.

4.9.1 4-(1-Adamantylmethyl)anilinium chloride (**25-HCl**): The crude product was dissolved in hexane/-

diethyl ether and **25-HCl** precipitated when dry HCl was introduced into solution. Yield: 579 mg (88%) of a colourless microcrystalline powder. Mp 178–188°C, R_f (free base) 0.28 (system b), anal. calcd for $C_{17}H_{24}ClN$: C, 73.49%; H, 8.71%; N, 5.04%; found C, 73.22%; H, 8.53%; N, 4.81%. 1H NMR (DMSO- d_6): δ 1.43 (m, 6H, $CH_2(Ad)$), 1.57 (m, 6H, $CH_2(Ad)$), 1.90 (m, 3H, $CH(Ad)$), 2.38 (s, 2H, $AdCH_2Ph$), 7.19 (d, $J = 7.9$ Hz, 2H, Ph), 7.31 (d, $J = 7.9$ Hz, 2H, Ph), 10.43 (bs, 3H, NH_3^+) ppm. ^{13}C NMR (DMSO- d_6): δ 27.9 (CH), 32.9 (C), 36.4 (CH_2), 41.6 (CH_2), 49.5 (CH_2), 122.5 (CH), 129.4 (C), 131.3 (CH), 137.7 (C) ppm. IR (KBr): 2902 (s), 2848 (s), 1613 (w), 1573 (w), 1509 (m), 1450 (w), 1314 (w), 1205 (w), 817 (w), 601 (m), 526 (w), 485 (m) cm^{-1} . GC-MS (EI, 70 eV); m/z (%): 41 (6), 55 (5), 67 (7), 77 (12), 79 (23), 81 (5), 91 (6), 93 (18), 106 (100), 107 (20), 135 (69), 136 (8), 241 (M^+ , 35), 242 (7).

4.9.2 3-[2-(1-Adamantyl)ethyl]anilinium chloride (26-HCl): The crude product was dissolved in hexane and **26-HCl** precipitated when dry HCl was introduced into solution. Yield: 491 mg (71%) of a colourless microcrystalline powder. Mp 142–150°C, R_f (free base) 0.25 (system b), anal. calcd for $C_{18}H_{26}ClN$: C, 74.07%; H, 8.98%; N, 4.80%; found C, 73.86%; H, 9.17%; N, 4.63%. 1H NMR (DMSO- d_6): δ 1.30 (m, 2H, $AdCH_2$), 1.52 (m, 6H, $CH_2(Ad)$), 1.65 (m, 3H, $CH_2(Ad)$), 1.94 (s, 3H, $CH(Ad)$), 2.55 (m, 2H, $PhCH_2$), 7.22 (m, 3H, Ph), 7.36 (t, $J = 7.9$ Hz, 1H, Ph), 10.37 (bs, 3H, NH_3^+) ppm. ^{13}C NMR (DMSO- d_6): δ 28.1 (CH), 28.2 (CH_2), 32.0 (C), 36.6 (CH_2), 41.7 (CH_2), 46.0 (CH_2), 120.3 (CH), 122.7 (CH), 127.8 (CH), 129.5 (CH), 131.8 (C), 145.1 (C) ppm. IR (KBr): 3429 (w), 2901 (s), 2845 (s), 2676 (w), 2605 (m), 2362 (w), 1964 (w), 1598 (m), 1576 (w), 1518 (w), 1490 (m), 1451 (m), 1359 (w), 1314 (w), 1243 (w), 1101 (w), 1046 (w), 790 (w), 691 (m), 524 (w), 437 (w) cm^{-1} . GC-MS (EI, 70 eV); m/z (%): 41 (15), 53 (7), 55 (11), 67 (15), 77 (23), 78 (6), 79 (42), 80 (5), 91 (16), 93 (34), 94 (7), 105 (5), 106 (46), 107 (67), 119 (22), 120 (49), 121 (7), 135 (59), 136 (7), 149 (8), 255 (M^+ , 100), 256 (21).

4.9.3 3-(1-Adamantylmethyl)anilinium chloride (27-HCl) was prepared according to the procedure used for previous amines. The nitrothiane **16** (338 mg, 0.90 mmol) was dissolved in ethanol (40 ml) under H_2 atmosphere and large excess of Ra-Ni was added portionwise until starting material disappeared. The crude product was dissolved in hexane and **27-HCl** precipitated when dry HCl was introduced into solution. Yield: 188 mg (75%) of a colourless microcrystalline powder. Mp 182–187°C, R_f (free base) 0.42 (system b), anal. calcd for $C_{17}H_{24}ClN$: C, 73.49%; H, 8.71%; N, 5.04%; found C, 73.62%; H, 8.51%; N, 5.24%. 1H NMR (DMSO- d_6): δ 1.44 (m, 6H, $CH_2(Ad)$), 1.50–1.66 (m, 6H,

$CH_2(Ad)$, 1.91 (m, 3H, $CH(Ad)$), 2.38 (s, 2H, $AdCH_2Ph$), 7.07–7.11 (m, 2H, Ph), 7.20 (d, $J = 7.9$ Hz, 1H, Ph), 7.37 (t, $J = 7.9$ Hz, 1H, Ph), 10.14 (bs, 3H, NH_3^+) ppm. ^{13}C NMR (DMSO- d_6): δ 27.9 (CH), 32.9 (C), 36.4 (CH_2), 41.6 (CH_2), 49.8 (CH_2), 120.3 (CH), 124.4 (CH), 128.7 (CH), 129.6 (CH), 131.8 (C), 139.4 (C) ppm. IR (KBr): 3421 (m), 2901 (s), 2846 (s), 2604 (m), 1602 (w), 1578 (m), 1518 (w), 1487 (m), 1452 (m), 1105 (w), 795 (m), 742 (w), 716 (w), 694 (m) cm^{-1} . GC-MS (EI, 70 eV); m/z (%): 41 (6), 67 (8), 77 (8), 79 (19), 91 (5), 93 (16), 106 (11), 107 (13), 135 (100), 136 (11), 241 (M^+ , 35), 242 (7).

Acknowledgements

This work was supported by Tomas Bata Foundation to R.V., Ministry of Education, Youth and Sports of Czech Republic (Grant No. MSM7088352101 to R.V. and I.K., MSM0021622413 and LC06030 to R.M.) and institutional research plan AV0Z40310501 to R.C.

References

- (1) Davies, W.L.; Grunert, R.R.; Haff, R.F.; McGahen, J.W.; Neumayer, E.M.; Paulshock, M.; Wats, J.C.; Wood, T.R.; Hermann, E.C.; Hoffmann, C.E. *Science* **1964**, *144*, 862–863.
- (2) (a) Stamatou, G.; Foscolos, G.B.; Fytas, G.; Kolocouris, A.; Kolocouris, N.; Pannecouque, C.; Witvrouw, M.; Padalko, E.; Neyts, J.; de Clercq, E. *Bioorg. Med. Chem.* **2003**, *11*, 5485–5492. (b) Wagner, C.E.; Mohler, M.L.; Kang, G.S.; Miller, D.D.; Geisert, E.E.; Chang, Y.-A.; Fleischer, E.B.; Shea, K.J. *J. Med. Chem.* **2003**, *46*, 2823–2833. (c) Tataridis, D.; Fytas, G.; Kolocouris, A.; Fytas, C.; Kolocouris, N.; Foscolos, G.B.; Padalko, E.; Neyts, J.; De Clercq, E. *Bioorg. Med. Chem. Lett.* **2007**, *17*, 692–696. (d) Zoidis, G.; Fytas, C.; Papanastasiou, I.; Foscolos, G.B.; Fytas, G.; Padalko, E.; de Clercq, E.; Naesens, L.; Neyts, J.; Kolocouris, N. *Bioorg. Med. Chem.* **2006**, *14*, 3341–3348. (e) Makarova, N.V.; Borekova, E.I.; Moiseev, I.K.; Pavlova, N.I.; Zemtsova, M.N.; Nikolaeva, S.N.; Vladyko, G.V. *Pharm. Chem. J.* **2001**, *35*, 480–484. (f) Motomaya, A.E.; Alimbarova, L.M.; Shokova, É.A.; Kovalev, V.V. *Pharm. Chem. J.* **2006**, *40*, 68–72.
- (3) (a) Long, J.; Manchandia, T.; Ban, K.; Gao, S.; Miller, C.; Chandra, J. *J. Cancer Chemother. Pharmacol.* **2007**, *59*, 527–535. (b) Roubalová, E.; Kvardová, V.; Hrstka, R.; Bořilová, Š.; Michalová, E.; Dubská, L.; Müller, P.; Sová, P.; Vojtěšek, B. *Invest. New Drugs* **2010**, *28*, 445–453.
- (4) (a) El-Emam, A.A.; Al-Deeb, O.A.; Al-Omar, M.; Lehmann, J. *Bioorg. Med. Chem.* **2004**, *12*, 5107–5113. (b) Kadi, A.A.; El-Brollosy, N.R.; Al-Deeb, O.A.; Habib, E.E.; Ibrahim, T.M.; El-Emam, A.A. *Eur. J. Med. Chem.* **2007**, *42*, 235–242.
- (5) (a) Koo, K.D.; Kim, M.J.; Kim, S.; Kim, K.-H.; Hong, S.Y.; Hur, G.-C.; Yim, H.J.; Kim, G.T.; Han, H.O.; Kwon, O.H.; Kwon, T.S.; Koh, J.S.; Lee, C.-S. *Bioorg. Med. Chem. Lett.* **2007**, *17*, 4167–4172. (b) Villhauer, E.B.; Brinkman, J.A.; Naderi, G.B.; Burkey, B.F.; Dunning, B.E.; Prasad, K.; Mangold, B.L.; Russell, M.E.; Hughes, T.E. *J. Med. Chem.* **2003**, *46*, 2774–2789. (c) Ahrén, B.; Landin-Olsson, M.;

- Jansson, P.-A.; Svensson, M.; Holmes, D.; Schweizer, A. *J. Clin. Endocr. Metab.* **2004**, *89*, 2078–2084.
- (6) (a) Farhana, L.; Dawson, M.L.; Leid, M.; Wang, L.; Moore, D.D.; Liu, G.; Xia, Z.; Fontana, J.A. *Cancer Res.* **2007**, *67*, 318–327. (b) Farhana, L.; Dawson, M.L.; Fontana, J.A. *Cancer Res.* **2005**, *65*, 4909–4917. (c) Parrella, E.; Gianni, M.; Fratelli, M.; Barzago, M.M.; Raska Jr., I.; Diomedea, L.; Kurosaki, M.; Pisano, C.; Carminati, P.; Merlini, L.; Dallavalle, S.; Tavecchio, M.; Rochette-Egly, C.; Terao, M.; Garattini, E. *Mol. Pharmacol.* **2006**, *70*, 909–924. (d) Wanner, R.; Henseleit-Walter, U.; Wittig, B.; Kolde, G. *J. Mol. Med.* **2002**, *80*, 61–67.
- (7) (a) Jensen, L.S.; Bølcho, U.; Egebjerg, J.; Strømgaard, K. *Chem. Med. Chem.* **2006**, *1*, 419–428. (b) Schlesinger, F.; Tammerna, D.; Krampfl, K.; Büfler, J. *Br. J. Pharmacol.* **2005**, *145*, 656–663. (c) Wang, Y.; Eu, J.; Washburn, M.; Gong, T.; Chen, H.-S.V.; James, W.L.; Lipton, S.A.; Stamler, J.S.; Went, G.T.; Porter, S. *Curr. Alzheimer Res.* **2006**, *3*, 201–204.
- (8) (a) Hwang, S.H.; Morisseau, Ch.; Do, Z.; Hammock, B.D. *Bioorg. Med. Chem. Lett.* **2006**, *16*, 5773–5777. (b) Anandan, S.-K.; Do, Z.N.; Webb, H.K.; Patel, D.V.; Gless, R.D. *Bioorg. Med. Chem. Lett.* **2009**, *19*, 1066–1070. (c) Kim, I.-H.; Morisseau, Ch.; Watanabe, T.; Hammock, B.D. *J. Med. Chem.* **2004**, *47*, 2110–2122. (d) Hwang, S.H.; Tsai, H.-J.; Liu, J.-Y.; Morisseau, Ch.; Hammock, B.D. *J. Med. Chem.* **2007**, *50*, 3825–3840.
- (9) (a) Lee, R.E.; Protopopova, M.; Crooks, E.; Slayden, R.A.; Terrot, M.; Barry, III, C.E. *J. Comb. Chem.* **2003**, *5*, 172–187. (b) Nayyar, A.; Monga, V.; Malde, A.; Coutinho, E.; Jain, R. *Bioorg. Med. Chem.* **2007**, *15*, 626–640.
- (10) (a) Lu, D.; Meng, Z.; Thakur, G.A.; Fan, P.; Steed, J.; Tartal, C.L.; Hurst, D.P.; Reggio, P.H.; Deschamps, J.R.; Parrish, D.A.; George, C.; Järbe, T.U.C.; Lamb, R.J.; Makriyannis, A. *J. Med. Chem.* **2005**, *48*, 4576–4585. (b) Stern, E.; Muccioli, G.G.; Bosier, B.; Hamtiaux, L.; Millet, R.; Poupaert, J.H.; Hénichart, J.-P.; Depreux, P.; Goossens, J.-F.; Lambert, D.M. *J. Med. Chem.* **2007**, *50*, 5471–5484.
- (11) (a) Cromwell, W.C.; Byström, K.; Efting, M.R. *J. Phys. Chem.* **1985**, *89*, 326–332. (b) van Bommel, K.J.C.; Metselaar, G.A.; Verboom, W.; Reinhoudt, D.N. *J. Org. Chem.* **2001**, *66*, 5405–5412.
- (12) (a) Uekama, K.; Hirayama, F.; Irie, T. *Chem. Rev.* **1998**, *98*, 2045–2076, and references therein. (b) Brewster, M.E.; Loftsson, T. *Adv. Drug Deliv. Rev.* **2007**, *59*, 645–666. (c) Okáčová, L.; Vetchý, D.; Franc, A.; Rabišková, M. *Chem. Listy.* **2011**, *105*, 34–40.
- (13) (a) Otyepka, M.; Kryštof, V.; Havlíček, L.; Siglerová, V.; Strnad, M.; Koča, J. *J. Med. Chem.* **2000**, *43*, 2506–2513. (b) Barbari, M.; Uršič, S.; Pilepić, V.; Zorc, B.; Hergold-Brundić, A.; Nagl, A.; Grdiša, M.; Pavličić, K.; Snoeck, R.; Andrei, G.; Balzarini, J.; de Clercq, E.; Mintas, M. *J. Med. Chem.* **2005**, *48*, 884–887.
- (14) (a) Bistri, O.; Mazeau, K.; Auzély-Velty, R.; Sollogoub, M. *Chem. Eur. J.* **2007**, *13*, 8847–8857. (b) Rüdiger, V.; Eliseev, A.; Simova, S.; Schneider, H.-J.; Blandamer, M.J.; Cullis, P.M.; Meyer, A.J. *J. Chem. Soc. Perkin Trans. 2.* **1996**, 2119–2123. (c) Carrazana, J.; Jover, A.; Meijide, F.; Soto, V. H.; Tato, J.V. *J. Phys. Chem. B.* **2005**, *109*, 9719–9726. (d) Hamilton, J.A.; Sabesan, M.N. *Acta Crystallogr., Sect. B: Struct. Sci.* **1982**, *38*, 3063–3069. (e) Weickenmeier, M.; Wenz, G. *Macromol. Rapid Commun.* **1996**, *17*, 731–736.
- (15) (a) Leclercq, L.; Schmitzer, A.R. *J. Phys. Org. Chem.* **2009**, *22*, 91–95. (b) Leggio, C.; Anselmi, M.; di Nola, A.; Galantini, L.; Jover, A.; Meijide, F.; Pavel, N.V.; Tellini, V.H.S.; Tato, J.V. *Macromolecules.* **2007**, *40*, 5899–5906. (c) Ohga, K.; Takashima, Y.; Takahashi, H.; Kawaguchi, Y.; Yamaguchi, H.; Harada, A. *Macromolecules.* **2005**, *38*, 5897–5904. (d) Tellini, V.H.S.; Jover, A.; Galantini, L.; Meijide, F.; Tato, J.V. *Acta Crystallogr., Sect. B: Struct. Sci.* **2004**, *60*, 204–210. (e) Taura, D.; Taniguchi, Y.; Hashizume, A.; Harada, A. *Macromol. Rapid Commun.* **2009**, *30*, 1741–1744. (f) Liu, H.; Zhang, Y.; Hu, J.; Li, C.; Liu, S. *Macromol. Chem. Phys.* **2009**, *210*, 2125–2137.
- (16) Vícha, R.; Potáček, M. *Tetrahedron* **2005**, *61*, 83–85.
- (17) Vícha, R.; Kuřitka, I.; Rouchal, M.; Ježková, V.; Zierhut, A. *ARKIVOC* **2009**, *XII*, 60–80.
- (18) Rouchal, M.; Nečas, M.; Vícha, R. *Acta Crystallogr. Sect. E: Struct. Rep. Online* **2009**, *65*, o1018.
- (19) (a) Dodziuk, H. In *Cyclodextrins and their Complexes*; Dodziuk, H., Ed.; Wiley: Weinheim, Chapter 1 and references therein. (b) Seidel, R.W.; Koleva, B.B. β -Cyclodextrin 10.41-hydrate *Acta Crystallogr., Sect. E: Struct. Rep. Online.* **2009**, *65*, o3162–o3163. (c) Schneider, H.-J.; Hacket, F.; Rüdiger, V.; Ikeda, H. *Chem. Rev.* **1998**, *98*, 1755–1785–2006.
- (20) Stewart, J.J.P. *J. Comput. Chem.* **1989**, *10*, 221–264.
- (21) Britto, M.; Nascimento, Jr, C.S.; Dos Santos, H.F. *Quim. Nova* **2004**, *27*, 882–888.
- (22) Zheng, Y.J.; Merz, K.M. *J. Comput. Chem.* **1992**, *13*, 1151–1169.
- (23) Yang, E.C.; Zhao, X.J.; Hua, F.; Hao, J.K. *J. Mol. Struct.: THEOCHEM* **2004**, *712*, 75–79.
- (24) Rouchal, M.; Nečas, M.; Vícha, R. *Acta Crystallogr. Sect. E: Struct. Rep. Online* **2010**, *66*, o1736.
- (25) Jeener, J.; Meier, B.H.; Bachmann, P.; Ernst, R.R. *J. Chem. Phys.* **1979**, *71*, 4546–4553.
- (26) Martin, G.E.; Crouch, R.C. *J. Nat. Prod.* **1991**, *54*, 1–70.
- (27) Kay, L.E.; Keifer, P.; Saarinen, T. *J. Am. Chem. Soc.* **1992**, *114*, 10663–10665.
- (28) SPARTAN'08, Version 1.2.0; Wavefunction, Inc. Irvine, CA, 2008.
- (29) Jursic, B.S.; Zdravkovski, Z.; French, A.D. *J. Mol. Struct.: THEOCHEM* **1996**, *366*, 113–117.

4.2

Adamantane-bearing benzylamines and benzylamides:
novel building blocks for supramolecular systems
with finely tuned binding properties towards β -cyclodextrin

Michal Rouchal, Alena Matelová, Fabiana Pires de Carvalho, Robert Bernat, Dragan Grbić, Ivo Kuřitka, Martin Babinský, Radek Marek, Richard Čmelík, Robert Vícha*

Supramolecular Chemistry **2013**, 25, 349–361

Adamantane-bearing benzylamines and benzylamides: novel building blocks for supramolecular systems with finely tuned binding properties towards β -cyclodextrin

Michal Rouchal^a, Alena Matelová^a, Fabiana Pires de Carvalho^a, Robert Bernat^a, Dragan Grbić^a, Ivo Kuřitka^b,
Martin Babinský^c, Radek Marek^c, Richard Čmelík^d and Robert Vícha^{a*}

^aDepartment of Chemistry, Faculty of Technology, Tomas Bata University in Zlín, Náměstí T. G. Masaryka 275, 762 72 Zlín, Czech Republic; ^bPolymer Centre, Faculty of Technology, Tomas Bata University in Zlín, Náměstí T. G. Masaryka 275, 762 72 Zlín, Czech Republic; ^cCEITEC – Central European Institute of Technology, Masaryk University, Kamenice 5, 625 00 Brno, Czech Republic; ^dInstitute of Analytical Chemistry, v. v. i., Academy of Sciences of the Czech Republic, Veveří 97, 602 00 Brno, Czech Republic

(Received 19 October 2012; final version received 31 December 2012)

Novel building blocks for the synthesis of supramolecular components based on adamantane-bearing benzylamines were prepared. The binding properties of these amines and the corresponding acetamides towards β -cyclodextrin (β -CD) were studied using mass spectrometry, NMR spectrometry, isothermal titration calorimetry and semi-empirical calculations. It was found that all of the examined guests predominantly formed 1:1 inclusion complexes in an enthalpy-driven manner with association constants of the order of 10^2 – 10^3 M⁻¹. Stronger binding to the β -CD cavity was observed for guests with a longer spacer between the adamantane and benzene moieties and/or a 1,4-disubstituted benzene ring.

Keywords: adamantane; amines; cyclodextrins; binding properties; host–guest systems

1. Introduction

Many examples of host–guest systems based on the interactions between adamantane-bearing guests and β -cyclodextrin (β -CD) can be found in the recent literature. The geometric and electronic properties of both the host and guest components play important roles in the complexation process. The non-polar adamantyl moiety, C₁₀H₁₅, consists of three fused cyclohexane rings in a classical chair conformation and has an almost ideal spherical shape with an atom-to-atom diameter of 7.2 Å. β -CD is a macrocycle composed of seven glucopyranoside units in the ⁴C₁ conformation connected *via* α -1,4-glycosidic bonds. Its geometry is usually described as bottomless cap or doughnut with a wide secondary rim (occupied by secondary OH groups at the C2 and C3 positions) and a narrow primary rim (occupied by primary OH groups at the C6 positions). The hydrophobic cavity is lined with H5, H3 and glycosidic O-atoms and has an internal diameter of approximately 6.5 Å (1).

Although there are rare instances of the binding of some guests on the CD portal (2) or outside the CD cone (3), we are unaware of any demonstration of such binding modes for adamantane-based guests. Owing to the lipophilic character of both the adamantane scaffold and the CD cavity, in conjunction with their complementary geometries, adamantane and β -CD primarily form inclusion complexes in solution, with the adamantane cage more or less buried inside the CD cavity.

These interactions have been used to construct cyclic or linear supramolecular co-polymers consisting of β -CD dimers and homo-ditopic adamantane-based guest dimers (4). In addition, the formation of hydrogels from adamantane-based hetero-ditopic units and β -CD has been described (5). Comb-shaped assemblies based on a CD-modified polyacrylate backbone with reversibly grafted adamantane-terminated polyacrylate chains have been studied (6). The hydrophilic β -CD duplex has been used for the non-covalent cross-linkage of adamantane-grafted chitosan (7). The interactions between ditopic adamantane guests and tritopic β -CD hosts (8), as well as the aggregation of functionalised dendrons leading to tubular vesicles, have been studied (9). The formation of microcapsules for the pH-driven drug release based on the interaction between CD-grafted dextran and 1-adamantyl-grafted poly(aspartic amide) has been described (10). Furthermore, the interactions between the chains of modified dextran and poly[methyl vinyl ether-*alt*-(maleic anhydride)] (11), poly(ethylene glycol) (12), polyacrylate (13) or hyaluronic acid (14) have been studied, and the developed systems have then been used for the formation of multilayer films (15). Because of the strong binding between the adamantane scaffold and β -CD, simple adamantane derivatives (mostly AdNH₂ or AdCOOH, Ad = 1-adamantyl) are used to control supramolecular aggregation (16). Although the above-mentioned papers primarily describe the results of basic binding behaviour studies, it is easy to imagine future applications including

*Corresponding author. Email: rvicha@ft.utb.cz

drug delivery and controlled release, viscosity control and sensors. Some very interesting examples of the interactions between the adamantane cage and β -CD on a macroscopic scale have recently been published (17). In addition, some immunosorbents based on the interactions between modified polymers have already been developed for chromatographic applications (18a) and solid phase extraction material (18b).

Furthermore, the ability of the adamantane moiety to form inclusion complexes with β -CD is frequently used in drug design to produce novel biologically active adamantylated compounds with enhanced transport properties and/or cytotoxicity (19). However, a reduction of the desired biological activity has been clearly documented when the introduced adamantane scaffold lacked a sufficiently long spacer between adamantane and the active site of the drug (20).

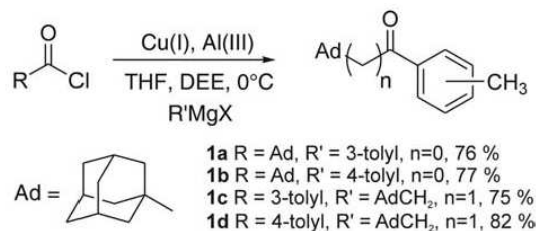
It should be noted that approximately one-half of the papers mentioned above describe guest components based on AdNH_2 . Other frequently used adamantane building blocks are AdOH , AdCH_2OH , 2-(1-adamantyl)ethylamine, AdCH_2COOH and 1-(1-adamantyl)-2-bromoethanone. It is reasonable to suppose that the electronic and steric properties of the linkage between adamantane and, for example, polymer backbone or pharmacophore can significantly affect binding to the CD cavity. For these reasons, novel adamantane building blocks are required. Considering the appropriate amino derivatives that are widely used as adamantane building blocks, we describe in this paper a convenient synthetic method for benzylamines that bear an adamantane moiety, which can be used for the synthesis of fine-tuned components for supramolecular assemblages or drug modification. Thermodynamic data of the host-guest interactions of the corresponding acetamides with β -CD based on calorimetric and NMR titrations, as well as the complex geometry, are discussed.

2. Results and discussion

2.1. Chemistry

The starting materials for this study, ketones **1a–d**, were prepared in satisfactory yields according to a previously described procedure (21) using acyl chlorides and the corresponding Grignard reagents in the presence of a catalytic amount of metal halide (Scheme 1).

Radical bromination of ketones **1** using 1.0 equiv. of *N*-bromosuccinimide (NBS) in dry tetrachloromethane at 80–85°C for the required time (monitoring by TLC) provided bromoketones **2** in approximately 70% yield. The reaction was initiated with a catalytic amount of benzoyl peroxide and irradiation with a tungsten lamp. In all cases, the starting material was not consumed completely when 1.0 equiv. of NBS was used. However, the addition of up to 1.2 equiv. of brominating agent did



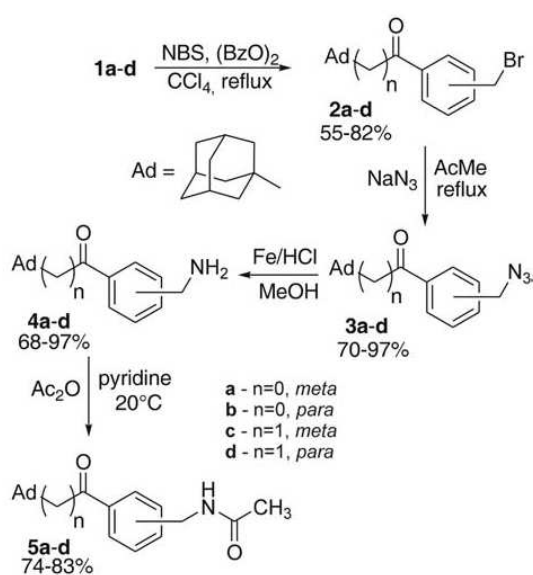
Scheme 1. Synthesis of starting ketones.

not increase the yield of product **2** significantly. Higher amounts of NBS led to the formation of undesired geminal dibromoderivatives.

In the second step, bromoketones **2** were treated with sodium azide (10.0 equiv.) in dry acetone according to the conditions described by Seong (22), and the desired azidoketones **3** were isolated in good to excellent yield.

Several types of reducing agents [e.g. triphenylphosphine (23), triethylphosphite (24), propane-1,3-dithiol (25), zinc in acetic acid (26), FeCl_3/NaI in MeCN (27), complex hydrides (28), $\text{FeSO}_4/\text{NH}_3$ in MeOH (29) and Na_2S in MeOH (30)] under various reaction conditions were unsuccessfully utilised for the preparation of benzylamines **4**. Finally, compounds **4a–d** were smoothly prepared *via* the reaction of the corresponding azidoketones **3** with carbonyl iron powder as a reducing agent in a methanol:hydrochloric acid solution at room temperature. The benzylamines **4b–d** were isolated either as the free bases after adjusting the pH and extracting or as the hydrochlorides *via* treatment of the methanol solution of the corresponding amine with dry gaseous hydrogen chloride. Compound **4a** was isolated in excellent yield (97%) as a free base, but attempts to isolate the corresponding hydrochloride resulted in a colourless liquid. Moreover, the free base of compound **4a** was rather unstable, in contrast to benzylamines **4b–d**, and began to solidify within a few minutes at room temperature. This instability of amine **4a**, together with some difficulties accompanying the isothermal titration calorimetry (ITC) experiments with amines **4** (see discussion below), led us to transform amines **4** into the corresponding acetamides **5**. In addition, the adamantylated amines **4** were intended to be linked to the final supramolecular components *via* an amide bond, which is better mimicked by amides **5**. Amides **5** were prepared *via* the smooth reaction of amines **4** with acetic anhydride in pyridine at room temperature. The entire synthetic pathway is depicted in Scheme 2.

The ability of the prepared amines **4** and amides **5** to form supramolecular complexes with β -CD and the properties of the complexes were further studied. Qualitative ESI-MS analysis was used to detect the supramolecular aggregates in solution and to study their



Scheme 2. Reaction pathway leading to adamantylated amides.

fragmentation in the gas phase. The thermodynamic parameters of the complexation reactions were determined using NMR and ITC titrations, and the spatial arrangement of the aggregates was studied through 2D NMR spectrometry and theoretical calculations.

2.2. Mass spectrometry

The individual guests **4** and **5**, as well as their equimolar mixtures with β -CD, were studied in the gas phase with a mass spectrometer equipped with an electrospray ionisation source (ESI-MS). The pseudomolecular ions $[M + H]^+$ predominated in the first-order mass spectra of all of the examined guests. In the case of amine **4c** and

all the examined amides **5a–d**, the signals of the proton associates were accompanied by signals at an m/z ratio twice as high minus unity (Table 1). We assigned these signals to H-bonded dimers associated with a single proton. Subsequent analyses of the ligand–cyclodextrin mixtures revealed that the protonated guest, a sodium adduct of β -CD and the protonated 1:1 host–guest aggregates were present in the gas phase. With amide **5a**, an additional aggregate of the amide with β -CD and Na^+ was observed and successfully trapped. As illustrated for the equimolar mixture of amide **5d** with β -CD in Figure 1(a), some further minor signals were observed and assigned to the products of either host or guest cleavage during the ESI process. In accordance with the well-known dissimilar stabilities of $[\beta\text{-CD} + H]^+$ and $[\beta\text{-CD} + Na]^+$, the corresponding aggregates of **5**- β -CD with H^+ and with Na^+ displayed markedly different fragmentation patterns during treatment under collision-induced dissociation (CID) conditions. Although the positive ion $[\beta\text{-CD} + H]^+$ lost the neutral amide **5** to produce the singly positively charged ion $[\beta\text{-CD} + H]^+$, which subsequently released four glucose units to produce signals at m/z 973, 811, 649 and 487 as demonstrated with further tandem mass spectrometry (Figure 1(b)), the sodium adduct $[\beta\text{-CD} + Na]^+$ lost the neutral amide **5** to yield solely the sodium adduct of β -CD at m/z 1157, and further fragmentation products were not detected. In addition, the supramolecular aggregates of amides **5** were also observable in the negative-ion mode (Figure 1(c)). In this case, the ions $[\beta\text{-CD} - 2H]^{2-}$, $[5-H]^-$, $[\beta\text{-CD} - H]^-$ and $[5\text{-}\beta\text{-CD} - H]^-$ were usually observed. The fragmentation of the supramolecular aggregate $[5\text{-}\beta\text{-CD} - H]^-$ led exclusively to the release of neutral amide **5** to yield the $[\beta\text{-CD} - H]^-$ ion (Figure 1(d)). The MS data obtained clearly demonstrate that all of the studied amides **5** and amines **4b–d** form 1:1 supramolecular aggregates with β -CD in methanol–water solution, which were successfully transferred and detected in the gas phase using ESI.

Table 1. Important signals observed in the positive-ion mode ESI mass spectra.

Compound	Exact mass							
	Ligand analysis						Mixture analysis	
	Single + H		Dimer + H		Single + Na		β -CD + amine + H	
Calc.	Found	Calc.	Found	Calc.	Found	Calc.	Found	
4b	270.2	270.1	539.4	–	292.2	–	1404.6	1404.6
4c	284.2	284.1	567.4	567.4	306.2	306.0	1418.6	1418.5
4d	284.2	284.1	567.4	–	306.2	–	1418.6	1418.6
5a	312.2	312.1	623.4	623.3	334.2	334.1	1446.6	1446.5
5b	312.2	312.2	623.4	623.5	334.2	334.2	1446.6	1446.8
5c	326.2	326.3	651.4	651.5	348.2	348.2	1460.6	1460.7
5d	326.2	326.3	651.4	651.5	348.2	348.3	1460.6	1460.7

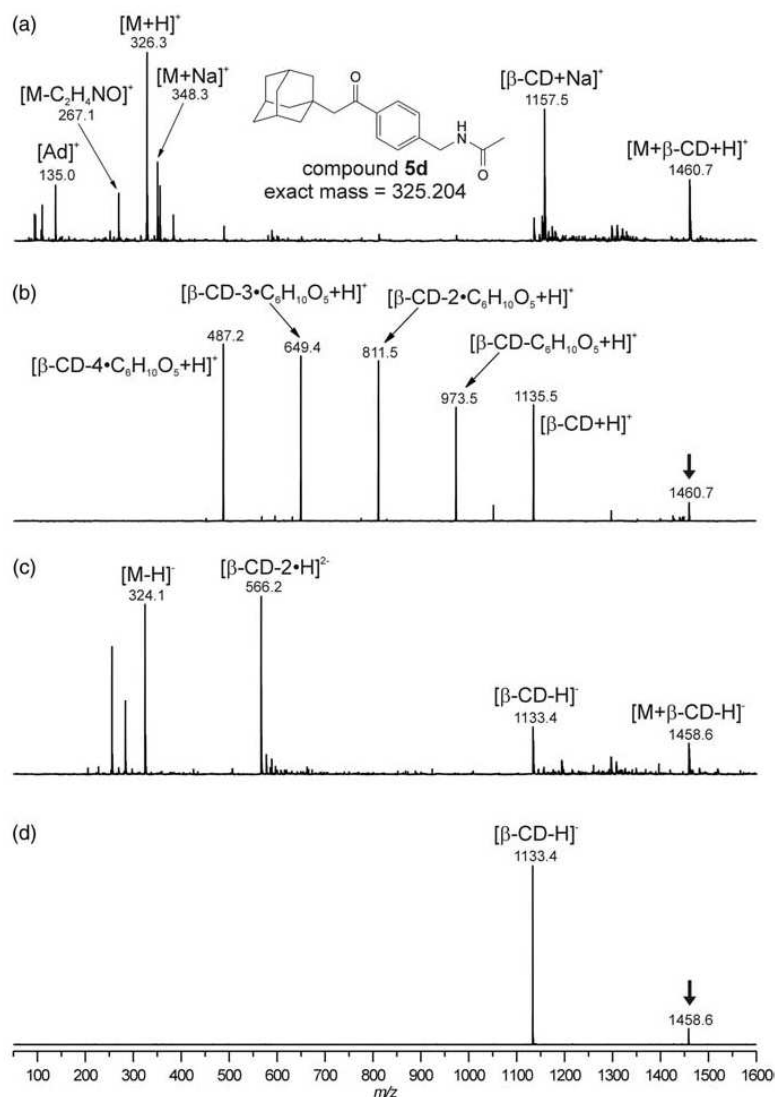


Figure 1. ESI-MS spectra of the mixtures of **5d** and β-CD in the positive-ion (a) and negative-ion (c) mode; ESI-MS/MS spectra of ions at m/z 1460 (b) and 1458 (d). Precursor ions are marked with a bold downward arrow.

2.3. Binding thermodynamics

NMR spectrometry was used to determine the stoichiometry of the complexes and the binding constants K . All of the examined host–guest systems follow the fast exchange mode on the NMR timescale. The complexation-induced shifts (CIS) were clearly seen in the spectra of the host–guest systems in a D₂O:[D₆]DMSO mixture. As it is shown for amide **5d** in Figure 2 (left), the complexation caused a deshielding of the adamantane hydrogen atoms at positions 2, 3 and 4 (for atom numbering, see Figure 3) and a shielding of hydrogen atoms at positions 5, 8 and 9. Nevertheless, the NMR data were often compromised by

the very small CIS of the signals of the shielded H-atoms and overlapping of the signals of the deshielded H-atoms. Therefore, all of the NMR titration data are based only on the unambiguously observed signal of the H-atom at position 3. The stoichiometry of the studied complexes was estimated using the Job method (31) as applied to the NMR data. The prepared amides **5** form 1:1 complexes with β-CD under the experimental conditions, as clearly demonstrated for amide **5d** in Figure 2 (right).

Considering the 1:1 stoichiometry of the studied complexes, the NMR titration data were fitted to the theoretical rectangular hyperbola (Equation (1)), and the

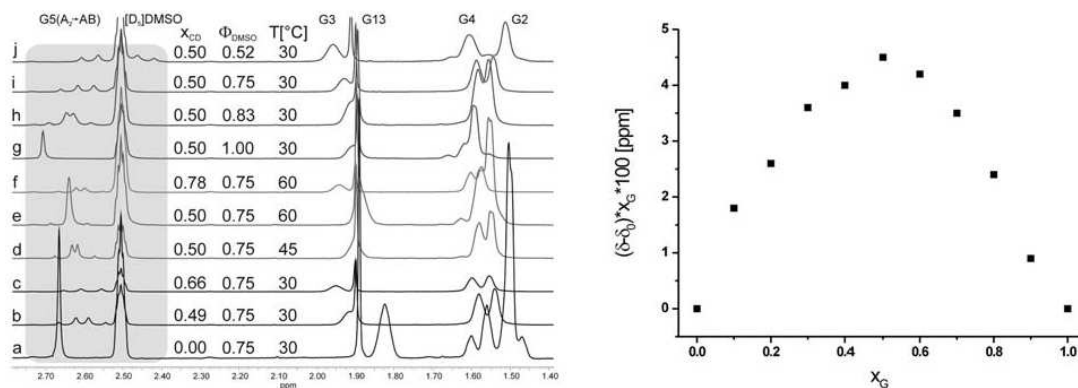


Figure 2. Stacking plot of a portion of the 1H NMR spectra (left) and Job plot (right) for amide **5d** and β -CD mixture. Significant parameters [x_{CD} (molar fraction of CD), Φ_{DMSO} (volume fraction of DMSO) and temperature] are given above each line. Signals of the host and guest nuclei are labelled as H for β -CD and G for guest. The assignment of signals corresponds with the atom numbering in Figure 3.

values of CIS_{max} and K were obtained using a standard least squares regression process (for further details, see Section 4).

$$CIS = \frac{CIS_{max} \cdot K \cdot c_{\beta-CD}}{1 + K \cdot c_{\beta-CD}} \quad (1)$$

The calculated K values are listed in Table 2. It should be noted that satisfactory fits to a theoretical model were not accomplished for amines **4**. We attributed this failure

to the formation of higher order aggregates within the wide range of initial concentrations in the studied solutions. The only successful NMR titration was done with amine **4d**. The comparison of the binding constant value for amine **4d** and the corresponding amide **5d** implies a marginal role of the free amino group in complex stabilisation *via* hydrogen bonding. Further thermodynamic parameters were obtained from ITC experiments. Standard treatment of the ITC data for amides **5a–e** (using a one-binding-site model with three parameters, n , K and ΔH) did not lead to

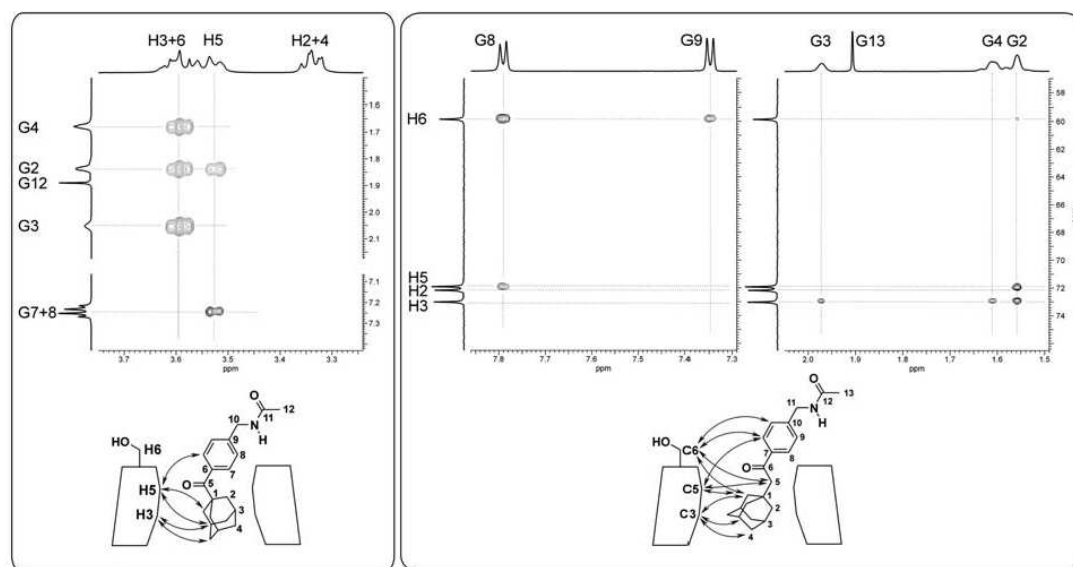


Figure 3. A portion of the ROESY spectrum of a 1:1 mixture of guest **5b** with β -CD (left frame) and a portion of the gs -HMQC-ROESY spectrum of a 1:1 mixture of guest **5d** with β -CD (right frame). Signals of the host and guest nuclei are labelled as H for β -CD and G for guest.

Table 2. Thermodynamic parameters of complexations.

Compound	NMR K (M^{-1})	ITC			
		K (M^{-1})	$-\Delta H$ ($kJ mol^{-1}$)	$-\Delta S$ ($J mol^{-1} K$)	n
5a	538 + 70	128 + 4	26.3 + 0.6	46	1 ^a
5b	767 + 75	258 + 9	28.1 + 0.7	46	1 ^a
5c	1206 + 107	219 + 5	31.0 + 0.4	59	1 ^a
5d	1721 + 34	329 + 3	35.2 + 0.2	67	1 ^a
5d		329 + 20	35.3 + 4	68	1.00 + 0.09
5d^b	439 + 30		(28) ^c	(34) ^c	
4d	1142 + 128				

Note: $T = 303 K$.

^aThe stoichiometry was predicted to be 1:1 using the ITC data treatment parameter $n - 1$.

^b $T = 333 K$.

^cSee Section 4.

satisfactory results. Only iteration of the data for compound **5d** converged to reasonable values. However, we have previously shown predominantly 1:1 stoichiometry using NMR data under essentially the same conditions as those used for the calorimetric titrations. Therefore, we decided to fix the iteration parameter at $n = 1$. Thus, we obtained the thermodynamic parameters given in Table 2. Comparison of the thermodynamic parameters obtained for amide **5d** with and without a fixed n (Table 2) suggests that the presumption of 1:1 aggregates was justified. The slightly higher entropy loss in the case of amides **5c** and **5d** can be attributed to the more constrained guest conformation inside the CD cavity. These data allow us to conclude that all of the examined guests bind in an enthalpy-driven manner. The elongation of the spacer between the adamantane moiety and the benzene ring leads to the formation of more stable aggregates. Further fine tuning of the binding strength can be accomplished by choosing appropriate substitution on the benzene ring. The *para*-substituted amides form more stable complexes; *meta*-substituted amides form less stable complexes.

The common simple adamantane derivatives, independently on their charge, displayed association constants with β -CD around 10^4 . Typically, for $AdCOO^-$ and $AdNH_3^+$, K was estimated to be of 1.6×10^4 and $8.3 \times 10^3 M^{-1}$, respectively (32). For compounds with the adamantane cage linked to some bulkier moiety or polymer backbone, weaker binding was reported. For example, *N*-(1-adamantyl)pyridinium bromide binds the β -CD with $K = 1.9 \times 10^3 M^{-1}$ (4a). Nevertheless, these values were obtained in pure or buffered water. Owing to low solubility of our ligands in water, we carried out all titrations in $H_2O:DMSO$ (1:3, v:v) mixture in which the contribution of hydrophobic effect is significantly weakened. We carried out calorimetric titration of $AdNH_2 \cdot HCl$ in phosphate buffer (pH 7.00) and in $H_2O:DMSO$ mixture to be able to estimate the solvent influence on the K value. The respective association constants are 1.5×10^4 and $2 \times 10^2 M^{-1}$. As can be seen,

the binding is of two orders stronger in water. We believe that this trend is applicable also for our new ligands to sound their binding strength towards β -CD in water similar to other conventional adamantane derivatives.

When carrying out the NMR titration of amide **5d** with β -CD, we observed a large separation between the signals of the initially enantiotopic hydrogen atoms at position 5 (for C-atom numbering, see Figure 3) with an increased proportion of β -CD as the spin system was changed from A_2 to AB (Figure 2(a)–(c)). We attempted to understand the nature of this phenomenon by carrying out additional measurements. Increasing the temperature led to coalescence at approximately $60^\circ C$ (Figure 2(d),(e)). However, when we increased the proportion of β -CD, while concomitantly holding the mixture at $60^\circ C$, the signal split again (Figure 2(f)). Finally, lines g–j in Figure 2 demonstrate the increased signal separation observed with increasing proportions of water in the mixed solvent. All of these observations suggest that the signal splitting could be attributed to the amount of complexed amide in the mixture. We postulate that amide **5d** (similar but significantly smaller signal splitting was also observed with amide **5c**) predominantly adopts a particular conformation within the β -CD cavity, which belongs to the C_1 symmetry point group and is fixed *via* interactions with β -CD. In such a situation, the hydrogen atoms at carbon 5 become non-equivalent due to the adjacent strongly anisotropic carbonyl group (see the calculated model in Figure 4). These observations clearly indicate that particular guest conformations may be locked inside a suitable cavity *via* weak van der Waals interactions and/or a steric hindrance.

2.4. Complex geometry

Owing to geometrical properties of the β -CD cavity (i.e. wider secondary rim, narrower primary rim and central constriction caused by H3 and H5 H-atoms), there are four principal arrangements of an inclusion complex of adamantane guest with β -CD. The adamantane cage can

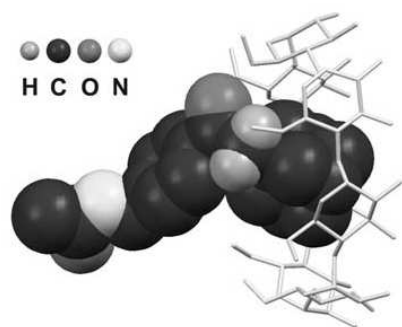


Figure 4. A calculated model of the **5d**- β -CD inclusion complex. H-atoms are omitted for clarity with the exception of AdCH_2 , which were commented in the text.

occupy secondary (S) or primary (P) rim and in both cases, the residue of the guest molecule can either thread the cavity in a pseudorotaxane manner (I – interior) or protrude to the outer environment (E – exterior) (33, 34). As the adamantane cage better fits the wider secondary rim, the positioning of adamantane-based guest molecule in the primary rim has been rarely reported. Although the host–guest complex of 1-adamantylammonium and modified β -CD with the PE geometry was observed only when the secondary rim was blocked by the positively charged aminogroup (33), the PI arrangement has not been reported to the best of our knowledge. The adamantane-based guests with long non-polar substituent adopt predominantly the SI geometry (34, 35c). However, when the SI arrangement was obstructed by either host (e.g. the cyclodextrins are frequently linked to the polymer backbone *via* C6 carbon) or guest (e.g. two adamantane cages linked with a short spacer) form, the preferable geometry was reported to be of SE (4a,b, 35).

Although the distinguishing of S and P binding mode is reasonable from a geometrical point of view, it should be noted that the adamantane cage is usually deeply buried into the CD cavity with the centre of gravity of 10 adamantane carbons being close to the best plane of seven etheric oxygen atoms of β -CD. In addition, the analyses of NOE data including only adamantane H-atoms can be rather confused by means of significant sterically driven deviation of the three-folded axes of adamantane substituent from the seven-folded axes of cyclodextrin ring.

The 2D NMR ROESY spectra indicate that all of the examined amides **5** interact with the β -CD unit predominantly by inclusion within the internal cavity. We clearly observed interactions between the inner H-atoms at carbons 3 and 5 with adamantane H-atoms 2, 3 and 4. The additional cross-peaks that relate to interactions between the aromatic guest H-atoms and the H-atoms at position 5 in CD indicate that the aromatic part of the guest molecule protrudes from the primary rim of cyclodextrin.

A partial ROESY spectrum of an equimolar mixture of amide **5b** with β -CD and a schematic drawing of the suggested complex geometry including the observed interactions is depicted in Figure 3 (left). Furthermore, we attempted to support this arrangement by applying a 2D ^1H - ^{13}C *gs*-HMQC-ROESY experiment. As Figure 3 (right) shows for amide **5d**, the interactions between CD carbon 3 and the amide H-atoms 2, 3 and 4, between CD carbon 5 and the amide H-atoms 2 and 8 and between CD carbon 6 and the amide H-atoms 2, 8 and 9 were clearly observed. These data led us to suggest a very similar arrangement for the **5d**- β -CD complex (Figure 3, right) as that discussed above for amide **5b**.

Finally, the geometry of the inclusion complexes was calculated in a manner described previously (34). The particular amide was positioned stepwise along the seven-fold axis of β -CD to simulate threading the guest molecule through the CD cavity. The geometries were initially optimised using a semi-empirical PM3 method, and single point energies were subsequently calculated at DFT level of theory. The arrangement with the maximum difference between the energy of the complex and sum of the energies of the guest and host calculated separately was considered to be the closest to the predominant actual complex geometry. A typical result obtained for amide **5d** is depicted in Figure 4. The calculated geometry agrees well with the experimental data.

3. Conclusion

In conclusion, we described a convenient synthetic method leading to versatile adamantane-bearing building blocks, which could be subsequently used to prepare components for supramolecular systems. In addition to full characterisation of all of the novel compounds by spectral methods, we studied the binding behaviour of four guests towards β -CD using mass spectrometry, NMR and calorimetric titrations. The association constants were found to be of the order of 10^2 – 10^3 M^{-1} , and a relationship between the guest structure and the binding strength was clearly observed. Binding of the guest into the β -CD cavity was improved with a longer non-polar spacer separating the adamantane scaffold from the rest of the molecule and/or a ‘linear’ arrangement (i.e. *para* substitution of the central benzene ring) of the guest molecule.

4. Experimental section

4.1. General

All solvents, reagents and starting compounds (except those mentioned below) were of analytical grade, purchased from commercial sources and used without further purification. Adamantane-1-carbonyl chloride and 3-methylbenzoyl chloride were prepared according to a previously published procedure (21). Melting points were

measured on a Kofler block and are uncorrected. Elemental analyses (C, H and N) were determined with a Thermo Fisher Scientific Flash EA 1112. Retention times were determined using TLC plates (Alugram Sil G/UV from Macherey-Nagel) and petroleum ether/ethyl acetate was used as the mobile phase. Four systems of mobile phases were used (v/v): system a (1/1); system b (4/1); system c (8/1) and system d (16/1). NMR spectra were recorded at 25°C on a Bruker Avance 500 spectrometer operating at frequencies of 500.13 MHz (^1H) and 125.77 MHz (^{13}C) and a Bruker Avance 300 spectrometer operating at frequencies of 300.13 MHz (^1H) and 75.77 MHz (^{13}C). ^1H and ^{13}C NMR chemical shifts were referenced to the signal of the solvent [^1H : $\delta(\text{residual CHCl}_3) = 7.27$ ppm, $\delta(\text{residual } [\text{D}_5]\text{DMSO}) = 2.50$ ppm; ^{13}C : $\delta(\text{CDCl}_3) = 77.23$ ppm, $\delta([\text{D}_6]\text{DMSO}) = 39.52$ ppm]. The mixing time for the NOESY experiment was adjusted to 700 ms and the spin-lock for ROESY was adjusted to 400 ms. The 2D ^1H - ^{13}C gs-HMQC-ROESY spectrum (36) was measured at resonance frequencies of 600.15 MHz (^1H) and 150.67 MHz (^{13}C). The HMQC step was adjusted for $^1J_{\text{H-C}} = 145$ Hz with a subsequent ROESY spin-lock of 400 ms. The spectrum was recorded in phase-sensitive mode using the echo-antiecho protocol (37). NMR titration experiments were carried out as follows. The solution of guest was titrated with stock solution of β -CD. Complexation-induced shifts (CIS) were calculated as $\text{CIS} = |\delta_{\text{observed}} - \delta_{\text{free guest}}|$. According to Benesi-Hildebrand approach, CIS values were plotted against total concentration of β -CD ($c_{\beta\text{-CD}}$) and data were fitted to a theoretical rectangular hyperbole (Equation (1)) via the routine least square regression process using MicroCal Origin software. The CIS_{max} describes coordinate of horizontal asymptote with the meaning of chemical shift of particular ^1H in the complexed guest molecule ($\text{CIS}_{\text{max}} = |\delta_{\text{complexed guest}} - \delta_{\text{free guest}}|$) and K (an association constant) is the slope for the $\text{CIS} = 0$. For further details, see (31) and references therein. The values of ΔH and ΔS were calculated from NMR data using the van't Hoff equation with $-\Delta H/R$ as the slope and $\Delta S/R$ as the intercept of the straight line obtained from linear regression of the plot of $\ln K$ versus $1/T$. The IR spectra were recorded with a Mattson 3000 FT-IR using a KBr disc. GC-MS analyses were run on a Shimadzu QP-2010 instrument using a Supelco SLB-5 ms (30 m, 0.25 mm) column with He as the carrier gas in constant linear flow mode (38 cm s^{-1}), 100°C for 7 min, 25°C min^{-1} to 250°C, then held for the required time. Only the peaks with relative abundances exceeding 5% are listed. The electrospray mass spectra were recorded with an Esquire LC ion-trap mass spectrometer (Bruker Daltonics, Bremen, Germany) equipped with an ESI source. Sample solutions were prepared immediately before each experiment by mixing β -CD and the individual amine:amide (8.8 μM in methanol:water, 1:1,

v/v). Clear mixtures were introduced into the ion source at a flow rate of 3 $\mu\text{l}/\text{min}$ via a metal capillary held at high voltage ($\pm 3.5 \text{ kV}$). The other instrumental conditions were as follows: the drying gas temperature was 250°C, the drying gas flow was 5 l/min, and the nebuliser pressure was 41.37 kPa. Nitrogen was used for nebulisation and drying. The nozzle-skimmer potential and octopole potential were modified and optimised before each experiment. The tandem mass spectra were collected using CID with He as the collision gas after isolation of the required ions. The ITC measurements were carried out in a DMSO:H₂O (3:1, v/v) solvent mixture using a VP-ITC MicroCal instrument at 30°C. The concentrations of the host in the cell and the guest in the microsyringe were approximately 0.9–1.5 and 9–17 mM, respectively. The raw experimental data were analysed with MicroCal ORIGIN software. The heats of dilution were taken into account for each guest compound. The data were fitted to a theoretical titration curve using the 'one set of binding sites' model.

4.2. General procedure for ketones 1 preparation

Ketones **1a–d** were prepared from the corresponding Grignard reagent and acyl chloride in the presence of a catalyst (21). In all cases, the desired product and a Grignard dimer as a co-product were observed. The dimers were separated from the mixture by column chromatography (system b). The spectral data for ketones **1b** (yield 77%) and **1a** (yield 76%) correspond with the literature (21, 38).

4.2.1. 2-(1-Adamantyl)-1-(4-methylphenyl)ethanone (1d)

Compound **1d** was isolated as colourless crystals in the yield of 82%. M.p. 62–64°C, R_f 0.37 (system d), anal. calcd for $\text{C}_{19}\text{H}_{24}\text{O}$: C, 85.03%; H, 9.01%; found C, 84.87%; H, 8.95%. ^1H NMR (CDCl_3): δ 1.66 (m, 12H, $\text{CH}_2(\text{Ad})$), 1.95 (m, 3H, $\text{CH}(\text{Ad})$), 2.41 (s, 3H, PhCH_3), 2.69 (s, 2H, CH_2CO), 7.24 (d, $J = 7.9$ Hz, 2H, Ph), 7.85 (d, $J = 8.0$ Hz, 2H, Ph) ppm. ^{13}C NMR (CDCl_3): δ 21.7(CH_3), 28.9(CH), 37.0(CH_2), 43.2(CH_2), 51.3(C), 128.7(CH), 129.3(CH), 136.7(C), 143.6(C), 200.0(CO) ppm. IR (KBr): 3066(w), 3027(w), 2899(s), 2846(s), 1659(s), 1604(s), 1571(w), 1449(m), 1323(m), 1308(m), 1268(s), 1183(m), 1152(w), 1119(m), 1017(w), 975(w), 842(w), 813(m), 761(m), 582(w) cm^{-1} . GC-MS (EI, 75eV); m/z (%): 41(11), 55(6), 65(14), 67(6), 77(9), 79(13), 91(47), 92(8), 93(9), 105(7), 119(100), 120(9), 135(11), 253(46), 254(9), 268(M^+ , 8).

4.2.2. 2-(1-Adamantyl)-1-(3-methylphenyl)ethanone (1c)

Compound **1c** was isolated as colourless liquid in the yield of 75%. R_f 0.17 (system a), anal. calcd for $\text{C}_{19}\text{H}_{24}\text{O}$: C, 85.03%; H, 9.01%; found C, 85.22%; H, 8.92%. ^1H NMR (CDCl_3): δ 1.66 (m, 12H, $\text{CH}_2(\text{Ad})$), 1.95 (m, 3H,

CH(Ad)), 2.42 (s, 3H, PhCH₃), 2.71 (s, 2H, COCH₃), 7.30–7.35 (m, 2H, Ph), 7.73–7.76 (m, 2H, Ph) ppm. ¹³C NMR (CDCl₃): δ 21.6(CH₃), 28.9(CH), 34.1(C), 37.0(CH₂), 43.2(CH₂), 51.4(COCH₃), 125.9(CH), 128.4(CH), 129.0(CH), 133.6(CH), 138.4(C), 139.2(C), 200.6(CO) ppm. IR (KBr): 2902(s), 2847(s), 2674(w), 2657(w), 1671(s), 1602(w), 1584(w), 1450(m), 1343(w), 1317(w), 1267(s), 1237(w), 1190(w), 1151(w), 1098(w), 1041(w), 804(w), 777(w), 754(m), 693(m) and 607(w) cm⁻¹. GC-MS (EI, 75 eV); *m/z* (%): 41(8), 55(5), 65(11), 67(5), 77(7), 79(11), 91(43), 92(8), 93(9), 119(100), 120(9), 134(5), 135(17), 250(5), 253(15), 268(M⁺, 24) and 269(5).

4.3. General procedure for the synthesis of benzylbromides 2a–d

The corresponding ketone **1** (47.1 mmol) was dissolved in 100 ml of dry tetrachloromethane, and NBS (8.54 g, 48.0 mmol) was added in one portion to this solution. The reaction was initiated by the addition of a catalytic amount of benzoyl peroxide and irradiation with a tungsten lamp. The mixture was stirred and refluxed for 8 h, and the reaction progress was monitored by TLC during this time. After this period, the succinimide was filtered off, and the filtrate was evaporated under vacuum. The desired product was obtained after purification of the crude product by column chromatography (system c).

4.3.1. 1-Adamantyl-[3-(bromomethyl)phenyl]methanone (2a)

Compound **2a** was isolated as colourless liquid in the yield of 80%. The oily material slowly crystallised at –15°C. M.p. 48–50°C, *R_f* 0.42 (system c), anal. calcd for C₁₈H₂₁BrO: C, 64.87%; H, 6.35%; found C, 64.78%; H, 6.21%. ¹H NMR (CDCl₃): δ 1.76 (m, 6H, CH₂(Ad)), 2.01 (m, 6H, CH₂(Ad)), 2.09 (m, 3H, CH(Ad)), 4.50 (s, 2H, CH₂Br), 7.34–7.50 (m, 3H, Ph), 7.54 (s, 1H, Ph) ppm. ¹³C NMR (CDCl₃): δ 28.3(CH), 33.0(CH), 36.7(CH₂), 39.3(CH₂), 47.2(C), 127.1(CH), 127.9(CH), 128.6(CH), 130.8(CH), 137.9(C), 140.4(C), 209.8(CO) ppm. IR (KBr): 2905(s), 2850(s), 2678(w), 2657(w), 1664(s), 1598(w), 1452(m), 1344(w), 1276(m), 1214(m), 1194(w), 1175(m), 1104(w), 1004(m), 802(w), 763(w), 733(w), 695(m), 625(w), 568(w) cm⁻¹. GC-MS (EI, 75 eV); *m/z* (%): 41(8), 55(6), 67(8), 77(7), 79(22), 81(6), 89(7), 90(10), 91(10), 93(18), 107(10), 118(5), 135(100), 136(11) and 332(M⁺, <1).

4.3.2. 1-Adamantyl-[4-(bromomethyl)phenyl]methanone (2b)

Compound **2b** was isolated as colourless crystals in the yield of 72%. M.p. 60–62°C, *R_f* 0.49 (system c), anal.

calcd for C₁₈H₂₁BrO: C, 64.87%; H, 6.35%; found C, 64.59%; H, 6.23%. ¹H NMR (CDCl₃): δ 1.76 (m, 6H, CH₂(Ad)), 2.02 (m, 6H, CH₂(Ad)), 2.09 (m, 3H, CH(Ad)), 4.50 (s, 2H, CH₂Br), 7.42 (d, *J* = 7.9 Hz, 2H, Ph), 7.54 (d, *J* = 7.9 Hz, 2H, Ph) ppm. ¹³C NMR (CDCl₃): δ 28.3(CH), 32.7(CH₂), 36.7(CH₂), 39.3(CH₂), 47.2(C), 127.8(CH), 128.8(CH), 139.7(C), 139.9(C), 209.6(CO) ppm. IR (KBr): 2924(s), 2905(s), 2852(s), 2658(w), 1669(s), 1605(w), 1453(w), 1403(w), 1274(m), 1243(m), 1226(m), 1176(w), 1108(m), 988(m), 951(w), 930(w), 846(w), 788(w), 683(w), 619(m), 595(w) and 557(w) cm⁻¹. GC-MS (EI, 75 eV); *m/z* (%): 43(6), 67(5), 77(5), 79(13), 89(6), 93(13), 107(8), 118(15), 135(100), 136(11) and 332(M⁺, <1).

4.3.3. 2-(1-Adamantyl)-1-[3-(bromomethyl)phenyl]ethanone (2c)

Compound **2c** was isolated as colourless liquid in the yield of 82%. *R_f* 0.45 (system c), anal. calcd for C₁₉H₂₃BrO: C, 65.71%; H, 6.68%; found C, 65.58%; H, 6.65%. ¹H NMR (CDCl₃): δ 1.65 (m, 12H, CH₂(Ad)), 1.94 (m, 3H, CH(Ad)), 2.71 (s, 2H, CH₂CO), 4.52 (s, 2H, CH₂Br), 7.42 (t, *J* = 7.6 Hz, 1H, Ph), 7.56 (d, *J* = 7.6 Hz, 1H, Ph), 7.86 (t, *J* = 7.6 Hz, 1H, Ph), 7.95 (s, 1H, Ph) ppm. ¹³C NMR (CDCl₃): δ 28.8(CH), 32.8(CH₂), 34.1(C), 36.9(CH₂), 43.1(CH₂), 51.4(CH₂), 128.5(CH), 128.9(CH), 129.1(CH), 133.3(CH), 138.4(C), 139.4(C), 199.6(CO) ppm. IR (KBr): 2901(s), 2846(s), 1673(s), 1600(w), 1449(m), 1312(w), 1168(w), 1216(w), 1143(w), 1094(w), 807(w), 762(w) and 692(s) cm⁻¹. GC-MS (EI, 75 eV); *m/z* (%): 41(12), 55(7), 65(5), 67(9), 77(11), 79(21), 81(6), 89(14), 90(31), 91(26), 92(9), 93(16), 105(7), 107(8), 118(21), 119(26), 133(8), 135(40), 136(5), 196(19), 198(20), 253(11), 267(100), 268(21), 346(M⁺, 3) and 348(M⁺ + 2, 3).

4.3.4. 2-(1-Adamantyl)-1-[4-(bromomethyl)phenyl]ethanone (2d)

Compound **2d** was isolated as colourless crystals in the yield of 55%. M.p. 85–88°C, *R_f* 0.22 (system d), anal. calcd for C₁₉H₂₃BrO: C, 65.71%; H, 6.68%; found C, 65.48%; H, 6.52%. ¹H NMR (CDCl₃): δ 1.66 (m, 12H, CH₂(Ad)), 1.96 (m, 3H, CH(Ad)), 2.71 (s, 2H, CH₂CO), 4.51 (s, 2H, CH₂Br), 7.48 (d, *J* = 8.6 Hz, 2H, Ph), 7.93 (d, *J* = 8.6 Hz, 2H, Ph) ppm. ¹³C NMR (CDCl₃): δ 28.9(CH), 32.4(CH₂), 34.2(C), 37.0(CH₂), 43.2(CH₂), 51.5(CH₂), 129.1(CH), 129.3(CH), 138.9(C), 142.5(C), 199.7(CO) ppm. IR (KBr): 2900(s), 2846(m), 2672(w), 2657(w), 1670(s), 1604(w), 1571(w), 1446(w), 1411(w), 1346(w), 1322(w), 1286(w), 1262(m), 1204(w), 1179(w), 1152(w), 1094(w), 1015(w), 977(w), 861(w), 816(w), 782(w), 709(w), 667(w) and 601(m) cm⁻¹. GC-MS (EI, 75 eV);

m/z (%): 40(5), 41(41), 43(6), 51(6), 53(15), 55(24), 63(11), 64(5), 65(24), 66(5), 67(26), 69(6), 77(35), 78(12), 79(59), 80(8), 81(17), 89(33), 90(78), 91(92), 92(24), 93(41), 104(16), 105(20), 107(16), 118(70), 119(100), 120(9), 133(22), 134(21), 135(45), 136(5), 169(6), 197(20), 199(19), 253(43), 254(9), 267(89) and 268(21).

4.4. General procedure for the synthesis of azides 3a–d

The appropriate bromide (2.72 mmol) was dissolved in 10 ml of dry acetone, and sodium azide (1.77 g, 27.2 mmol) was added to this solution in one portion. The reaction mixture was refluxed under an Ar atmosphere until TLC indicated the complete disappearance of the starting material (6–8 h). Subsequently, the mixture was diluted with water and extracted six times with diethyl ether. The combined organic layers were dried over sodium sulphate. Evaporation of the solvent under vacuum followed by purification *via* column chromatography (system c) provided the desired product.

4.4.1. 1-Adamantyl-[3-(azidomethyl)phenyl]methanone (3a)

Compound **3a** was isolated as colourless liquid in the yield of 73%. R_f 0.24 (system d), anal. calcd for $C_{18}H_{21}N_3O$: C, 73.19%; H, 7.17%; N, 14.23%; found C, 73.08%; H, 7.32%; N, 14.17%. 1H NMR ($CDCl_3$): δ 1.76 (m, 6H, CH_2 (Ad)), 2.01 (m, 6H, CH_2 (Ad)), 2.09 (m, 3H, CH(Ad)), 4.39 (s, 2H, CH_2N_3), 7.41–7.51 (m, 4H, Ph) ppm. ^{13}C NMR ($CDCl_3$): δ 28.3(CH), 36.7(CH_2), 39.3(CH_2), 47.2(C), 54.7(CH_2), 126.9(CH), 127.0(CH), 128.7(CH), 129.8(CH), 135.7(C), 140.6(C) and 205.2(CO) ppm. IR (KBr): 2905(s), 2851(s), 2678(w), 2659(w), 2098(s), 1672(s), 1601(w), 1584(w), 1452(m), 1344(m), 1273(m), 1245(m), 1194(w), 1172(m), 1104(w), 999(m), 972(w), 935(w), 887(w), 803(w), 782(w), 732(w), 711(w) and 650(w) cm^{-1} .

4.4.2. 1-Adamantyl-[4-(azidomethyl)phenyl]methanone (3b)

Compound **3b** was isolated as colourless crystals in the yield of 70%. M.p. 35–36°C, R_f 0.45 (system c), anal. calcd for $C_{18}H_{21}N_3O$: C, 73.19%; H, 7.17%; N, 14.23%; found C, 73.36%; H, 7.26%; N, 13.95%. 1H NMR ($CDCl_3$): δ 1.76 (m, 6H, CH_2 (Ad)), 2.02 (m, 6H, CH_2 (Ad)), 2.09 (m, 3H, CH(Ad)), 4.39 (s, 2H, CH_2N_3), 7.35 (d, $J = 7.9$ Hz, 1H, Ph), 7.58 (d, $J = 7.9$ Hz, 1H, Ph) ppm. ^{13}C NMR: δ 28.4(CH), 36.8(CH_2), 39.3(CH_2), 47.2(C), 54.6(CH_2), 128.8(CH), 128.0(CH), 137.8(C), 139.7(C) and 204.8(CO) ppm. IR (KBr): 2910(s), 2851(s), 2098(s), 1657(s), 1605(w), 1452(w), 1428(w), 1408(w), 1344(w), 1295(w), 1270(w), 1233(w), 1173(w), 1103(w),

987(w), 950(w), 927(w), 834(w), 799(w), 738(w) and 685(w) cm^{-1} . GC-MS (EI, 75 eV); m/z (%): 55(8), 67(10), 77(14), 79(21), 81(6), 91(6), 93(20), 107(10), 118(7), 135(100), 136(10), 239(10), 267($M^+ - N_2$, 2) and 295(M^+ , 1).

4.4.3. 2-(1-Adamantyl)-1-[3-(azidomethyl)phenyl]ethanone (3c)

Compound **3c** was isolated as colourless crystals in the yield of 97%. The analytical sample was further crystallised from hexane. M.p. 60–62°C, R_f 0.22 (system d), anal. calcd for $C_{19}H_{23}N_3O$: C, 73.76%; H, 7.49%; N, 13.58%; found C, 73.65%; H, 7.23%; N, 13.78%. 1H NMR ($CDCl_3$): δ 1.66 (m, 12H, CH_2 (Ad)), 1.94 (m, 3H, CH(Ad)), 2.72 (s, 2H, CH_2CO), 4.42 (s, 2H, CH_2N_3), 7.44–7.52 (m, 2H, Ph) and 7.89–7.92 (m, 2H, Ph) ppm. ^{13}C NMR ($CDCl_3$): δ 28.9(CH), 34.1(C), 37.0(CH_2), 43.1(CH_2), 51.5(CH_2), 54.6(CH_2), 128.0(CH), 128.5(CH), 129.2(CH), 132.4(CH), 136.1(C), 139.6(C) and 199.9(CO) ppm. IR (KBr): 2905(s), 2847(s), 2099(s), 1673(s), 1602(w), 1449(m), 1344(w), 1311(w), 1266(m), 1189(w), 1148(w), 1095(w), 979(w), 925(w), 806(w), 757(w), 723(w), 695(m), 695(w), 649(w) and 610(w) cm^{-1} .

4.4.4. 2-(1-Adamantyl)-1-[4-(azidomethyl)phenyl]ethanone (3d)

Compound **3d** was isolated as colourless solid in the yield of 77%. M.p. 25–27°C, R_f 0.33 (system b), anal. calcd for $C_{19}H_{23}N_3O$: C, 73.76%; H, 7.49%; N, 13.58%; found C, 73.82%; H, 7.12%; N, 13.55%. 1H NMR ($CDCl_3$): δ 1.66 (m, 12H, CH_2 (Ad)), 1.95 (m, 3H, CH(Ad)), 2.72 (s, 2H, CH_2CO), 4.42 (s, 2H, CH_2N_3), 7.40 (d, $J = 8.3$ Hz, 2H, Ph), 7.96 (d, $J = 8.3$ Hz, 2H, Ph) ppm. ^{13}C NMR ($CDCl_3$): δ 28.9(CH), 34.2(C), 36.2(CH_2), 43.2(CH_2), 51.5(CH_2), 54.5(CH_2), 128.2(CH), 127.1(CH), 138.9(C), 140.4(C), 199.8(CO) ppm. IR (KBr): 2903(s), 2847(s), 2099(s), 1671(s), 1608(m), 1573(w), 1504(w), 1450(w), 1412(w), 1345(w), 1287(w), 1262(m), 1209(w), 1178(w), 1149(w), 1014(w), 978(w), 915(w), 851(w), 813(w) and 764(w) cm^{-1} . GC-MS (EI, 75 eV); m/z (%): 41(16), 51(7), 53(5), 55(9), 67(12), 76(6), 77(39), 78(6), 79(26), 81(8), 91(21), 92(9), 93(20), 103(6), 104(28), 105(13), 107(9), 132(100), 133(11), 135(32), 252(6), 253(23), 264(9), 280(6), 281($M^+ - N_2$, 75) and 282(16).

4.5. General procedure for the synthesis of benzylamines 4a–d

The corresponding azide (1.88 mmol) was dissolved in 20 ml of methanolic HCl (1–2 M), and iron powder (203 mg, 3.64 mmol) was added to this solution in one portion. The reaction mixture was stirred at room temperature, and another portion of carbonyl iron (3.64 mmol) was added until

the starting material had completely disappeared (according to TLC). The solvent was then removed under vacuum, 30 ml of 7% NaOH (water solution) was added, and the water layer was extracted with diethyl ether (5 × 10 ml). The collected organic portions were washed with brine (3 × 10 ml), dried over sodium sulphate and evaporated under vacuum. The purified product (column chromatography, system d) was generally isolated as a colourless liquid, which was subsequently converted to the hydrochloride.

4.5.1. 1-Adamantyl-[3-(aminomethyl)phenyl]methanone (**4a**)

Compound **4a** was isolated as colourless liquid in the yield of 97%. R_f 0.25 (system a). GC-MS (EI, 75 eV); m/z (%): 41(5), 67(8), 77(11), 79(19), 91(5), 93(18), 106(10), 107(12), 134(14), 135(100), 136(11), 241(22), 252(7) and 269(M^+ , 2).

4.5.2. 1-Adamantyl-[4-(aminomethyl)phenyl]methanone hydrochloride (**4b**)

Compound **4b** was isolated as colourless crystalline powder in the yield of 68%. M.p. 200–204°C, R_f (free base) 0.79 (MeOH:CHCl₃, 3:1, v:v), anal. calcd for C₁₈H₂₄ClNO: C, 70.69%; H, 7.91%; N, 4.58%; found C, 70.48%; H, 7.85%; N, 4.32%. ¹H NMR ([D₆]DMSO, 2.50 ppm): δ 1.69 (m, 6H, CH₂(Ad)), 1.90 (m, 6H, CH₂(Ad)), 2.01 (m, 3H, CH(Ad)), 4.05 (s, 2H, CH₂NH₃), 7.57 (m, 4H, Ph) and 8.52 (s, 3H, NH₃) ppm. ¹³C NMR ([D₆]DMSO, 39.5 ppm): δ 27.2(CH), 35.7(CH₂), 38.1(CH₂), 41.5(CH₂), 45.8(C), 126.8(CH), 128.4(CH), 135.8(C), 138.7(C) and 208.5(CO) ppm. IR (KBr): 3034(w), 2906(s), 2849(w), 1733(w), 1690(s), 1613(w), 1595(w), 1493(m), 1452(m), 1382(w), 1343(w), 1273(w), 1240(m), 1178(w), 1103(w), 1070(w), 989(m), 931(w), 849(m) and 636(m) cm⁻¹. GC-MS (free base) (EI, 75 eV); m/z (%): 79(18), 81(5), 89(7), 91(5), 93(16), 105(5), 106(6), 107(10), 134(21), 135(100), 136(11), 252(10) and 269(M^+ , 2).

4.5.3. 2-(1-Adamantyl)-1-[3-(aminomethyl)phenyl] ethanone hydrochloride (**4c**)

Compound **4c** was isolated as a pale yellow crystalline powder in the yield of 91%. M.p. 163–167°C, R_f (free base) 0.27 (system a), anal. calcd for C₁₉H₂₆ClNO: C, 71.34%; H, 8.19%; N, 4.38%; found C, 71.12%; H, 8.08%; N, 4.53%. ¹H NMR (CDCl₃): δ 1.60 (m, 12H, CH₂(Ad)), 1.88 (s, 3H, CH(Ad)), 2.64 (s, 2H, CH₂CO), 4.18 (s, 2H, CH₂NH₂), 7.36 (t, $J = 7.6$ Hz, 1H, Ph), 7.71 (d, $J = 7.6$ Hz, 1H, Ph), 7.79 (d, $J = 7.6$ Hz, 1H, Ph) and 8.09 (m, 1H, Ph), 8.63 (bs, 3H, NH₃) ppm. ¹³C NMR (CDCl₃): δ 28.9(CH), 34.2(C), 36.9(CH₂), 43.5(CH₂), 51.5(CH₂), 129.2(CH), 129.3(CH), 133.6(CH), 134.0(CH), 139.3(C) and 200.7(CO) ppm. IR

(KBr): 3340(w), 2901(s), 2847(m), 1671(s), 1600(w), 1451(m), 1317(m), 1267(m), 1190(w), 1148(w), 807(w), 757(w), 695(m) and 469(m) cm⁻¹. GC-MS (free base) (EI, 75 eV); m/z (%): 41(6), 55(5), 67(6), 77(21), 79(19), 91(10), 93(11), 104(8), 105(11), 106(22), 107(7), 118(19), 119(5), 134(100), 135(27), 253(14), 266(67) and 267(14).

4.5.4. 2-(1-Adamantyl)-1-[4-(aminomethyl)phenyl] ethanone hydrochloride (**4d**)

Compound **4d** was isolated as a colourless crystalline powder in the yield of 85%. M.p. 220–222°C, R_f (free base) 0.24 (MeOH:CHCl₃, 3:1, v:v), anal. calcd for C₁₉H₂₆ClNO: C, 71.34%; H, 8.19%; N, 4.38%; found C, 71.48%; H, 8.13%; N, 4.72%. ¹H NMR ([D₆]DMSO, 2.50 ppm): δ 1.58 (m, 12H, CH₂(Ad)), 1.88 (m, 3H, CH(Ad)), 2.74 (s, 2H, CH₂CO), 4.08 (s, 2H, CH₂NH₃), 7.65 (s, 2H, Ph), 7.98 (s, 2H, Ph) and 8.66 (bs, 3H, NH₃) ppm. ¹³C NMR ([D₆]DMSO, 39.5 ppm): δ 28.0(CH), 33.4(C), 36.2(CH₂), 41.6(CH₂), 42.2(CH₂), 50.4(CH₂), 128.3(CH), 129.0(CH), 138.2(C), 138.9(C), 199.3(CO) ppm. IR (KBr): 2901(s), 2847(s), 2674(w), 2611(w), 1670(s), 1611(m), 1450(m), 1417(w), 1264(m), 1218(w), 1179(w), 1121(w), 1100(w), 1009(w), 983(w), 915(w), 825(w), 668(w) and 587(w) cm⁻¹. GC-MS (free base) (EI, 75 eV); m/z (%): 41(8), 55(7), 67(7), 77(15), 79(19), 89(20), 91(15), 92(5), 93(12), 104(7), 105(24), 106(15), 107(6), 134(100), 135(24), 253(62), 254(12), 266(42) and 267(10).

4.6. General procedure for the synthesis of acetamides 5

The corresponding benzylamine **4** (0.9 mmol) was dissolved in 45 ml of pyridine, and 0.15 ml of acetic anhydride was added to this solution. The mixture was stirred for 12 h at room temperature and then poured onto crushed ice. The water layer was extracted with diethyl ether (5 × 10 ml), and the combined organic layers were dried over sodium sulphate and evaporated under vacuum. The desired acetamide **5** was obtained after purification of the crude product by column chromatography (system a).

4.6.1. N-[3-(1-adamantylcarbonyl)benzyl]acetamide (**5a**)

Compound **5a** was isolated as a colourless crystalline powder in the yield of 83%. M.p. 105–110°C, R_f 0.31 (system a), anal. calcd for C₂₀H₂₅NO₂: C, 77.14%; H, 8.09%; N, 4.50%; found C, 76.95%; H, 8.18%; N, 4.22%. ¹H NMR (CDCl₃): δ 1.74 (m, 6H, CH₂(Ad)), 1.98–2.07 (m, 12H, CH₂(Ad) + CH(Ad) + CH₃CO), 4.42 (d, $J = 5.6$ Hz, 2H, CH₂NH), 6.10 (bs, 1H, NH), 7.34–7.43 (m, 4H, Ph) ppm. ¹³C NMR (CDCl₃): δ 23.4(CH₃), 28.3(CH), 36.7(CH₂), 39.3(CH₂), 43.6(CH₂), 47.1(C), 126.1(CH), 126.5(CH), 128.4(CH), 129.7(CH), 138.6(C), 140.3(C), 170.2(NHCO) and 210.4(CO) ppm. IR (KBr):

3250(s), 3074(s), 2905(s), 2851(s), 2678(w), 2658(w), 1679(s), 1642(s), 1563(s), 1440(m), 1373(m), 1349(w), 1299(m), 1274(m), 1249(m), 1193(w), 1172(w), 1101(w), 1032(m), 996(m), 896(w), 790(m), 733(w), 705(m), 689(w), 640(w) and 496(w) cm^{-1} . GC-MS (EI, 75 eV); m/z (%): 43(5), 67(6), 77(5), 79(14), 93(13), 106(5), 107(9), 135(100), 136(9), 178(5), 311(M^+ , 9).

4.6.2. *N*-[4-(1-adamantylcarbonyl)benzyl]acetamide (**5b**)

Compound **5b** was isolated as a colourless crystalline powder in the yield of 55%. M.p. 114–117°C, R_f 0.30 (system a), anal. calcd for $\text{C}_{20}\text{H}_{25}\text{NO}_2$: C, 77.14; H, 8.09; N, 4.50; found C, 77.42; H, 7.93; N, 4.37. ^1H NMR (CDCl_3): δ 1.69–1.79 (m, 6H, $\text{CH}_2(\text{Ad})$); 1.99 (m, 6H, $\text{CH}_2(\text{Ad})$); 2.04 (s, 3H, COCH_3); 2.07 (m, 3H, $\text{CH}(\text{Ad})$); 4.44 (d, $J = 5.6$ Hz, 2H, PhCH_2NH); 6.08 (bs, 1H, NH); 7.28 (d, $J = 7.9$ Hz, 2H, Ph); 7.51 (d, $J = 7.9$ Hz, 2H, Ph) ppm. ^{13}C NMR (CDCl_3): $\delta = 23.3$ (CH_3), 28.3 (CH), 36.7 (CH_2), 39.3 (CH_2), 43.5 (CH_2), 47.1 (C), 127.4 (CH), 127.8 (CH), 138.9 (C), 140.7 (C), 170.3 (NHCO) and 209.8 (CO) ppm. IR (KBr): 3250 (s), 3085 (s), 2904 (s), 2848 (s), 2658 (m), 1686 (s), 1646 (s), 1612 (m), 1548 (s), 1452 (s), 1421 (m), 1406 (w), 1375 (m), 1344 (w), 1292 (s), 1273 (s), 1237 (s), 1180 (m), 1122 (m), 1099 (m), 989 (s), 931 (m), 837 (w), 742 (s), 687 (m), 641 (s), 595 (s) and 495 (s) cm^{-1} . GC-MS (EI, 75 eV); m/z (%): 43(6), 67(7), 79(20), 89(5), 91(5), 93(15), 107(10), 135(100), 176(8), 311(M^+ , 9).

4.6.3. *N*-[3-(1-adamantylmethylcarbonyl)benzyl]acetamide (**5c**)

Compound **5c** was isolated as a colourless crystalline powder in the yield of 74%. M.p. 115–120°C, R_f 0.30 (system a), anal. calcd for $\text{C}_{21}\text{H}_{27}\text{NO}_2$: C, 77.50; H, 8.36; N, 4.30; found C, 77.24; H, 8.28; N 4.57. ^1H NMR (CDCl_3): δ 1.59–1.70 (m, 12H, $\text{CH}_2(\text{Ad})$); 1.94 (m, 3H, $\text{CH}(\text{Ad})$); 2.04 (s, 3H, COCH_3); 2.69 (s, 2H, AdCH_2CO); 4.48 (d, $J = 5.3$ Hz, 2H, PhCH_2NH); 6.17 (bs, 1H, NH); 7.37–7.48 (m, 2H, Ph) and 7.81–7.83 (m, 2H, Ph) ppm. ^{13}C NMR (CDCl_3): $\delta = 23.3$ (CH_3), 28.9 (CH), 34.2 (C), 37.0 (CH_2), 43.2 (CH_2), 43.6 (CH_2), 51.5 (CH_2), 127.5 (CH), 127.9 (CH), 129.0 (CH), 132.4 (CH), 139.0 (C), 139.4 (C), 170.4 (NHCO) and 200.3 (CO) ppm. IR (KBr): 3251 (s), 3077 (s), 2990 (w), 2905 (s), 2846 (s), 2674 (w), 2660 (w), 1672 (s), 1644 (s), 1600 (m), 1553 (s), 1437 (s), 1371 (m), 1290 (m), 1251 (m), 1026 (m), 803 (w), 760 (m), 582 (w) and 515 (m) cm^{-1} . GC-MS (EI, 75 eV); m/z (%): 43(18), 55(5), 67(11), 73(5), 77(23), 79(33), 81(8), 89(8), 90(7), 91(18), 43(18), 92(6), 93(22), 104(3), 105(18), 105(35), 107(17), 118(26), 119(11), 134(13), 135(100), 136(11), 148(20), 149(9), 172(7), 176(73), 177(8), 190(10), 253(93), 254(19), 266(65), 267(14) and 325(M^+ , 5).

4.6.4. *N*-[4-(1-adamantylmethylcarbonyl)benzyl]acetamide (**5d**)

Compound **5d** was isolated as a colourless crystalline powder in the yield of 43%. M.p. 84–88°C, R_f 0.27 (system a), anal. calcd for $\text{C}_{21}\text{H}_{27}\text{NO}_2$: C, 77.50; H, 8.36; N, 4.30; found C, 77.38; H, 8.41; N 3.98. ^1H NMR (CDCl_3): $\delta = 1.59$ –1.70 (m, 12H, $\text{CH}_2(\text{Ad})$); 1.94 (m, 3H, $\text{CH}(\text{Ad})$); 2.04 (s, 3H, COCH_3); 2.68 (s, 2H, AdCH_2CO); 4.47 (d, $J = 5.9$ Hz, 2H, PhCH_2NH); 6.16 (bs, 1H, NH); 7.32 (d, $J = 8.3$ Hz, 2H, Ph) and 7.88 (d, $J = 5.9$ Hz, 2H, Ph) ppm. ^{13}C NMR (CDCl_3): $\delta = 23.3$ (CH_3), 28.9 (CH), 34.2 (C), 37.0 (CH_2), 43.2 (CH_2), 43.5 (CH_2), 51.5 (CH_2), 127.8 (CH), 129.0 (CH), 138.3 (C), 143.5 (C), 170.3 (NHCO) and 200.5 (CO) ppm. IR (KBr): 3261 (s), 3079 (s), 2903 (s), 2844 (s), 2673 (w), 2655 (w), 1652 (m), 1609 (m), 1561 (s), 1426 (m), 1371 (s), 1350 (w), 1286 (s), 1263 (s), 1214 (m), 1100 (m), 1027 (s), 983 (m), 915 (w), 813 (m), 771 (m), 623 (w), 585 (s) and 511 (m) cm^{-1} . GC-MS (EI, 75 eV); m/z (%): 41(8), 43(16), 77(14), 79(20), 93(13), 105(17), 106(15), 135(17), 176(55), 253(10), 266(100) and 267(22).

Acknowledgements

This work was supported by the Internal Founding Agency of Tomas Bata University in Zlín, project IGA/FT/2012/016 to A.M., M.R. and R.V., the project 'CEITEC – Central European Institute of Technology' (CZ.1.05/1.1.0/02/0068) from the European Regional Development Fund to R.M. and M.B. and institutional research plan RVO:68081715 to R.C.

References

- (1) Carrazana, J.; Jover, A.; Mejjide, F.; Soto, V.H.; Tato, J.V. *J. Phys. Chem. B* **2005**, *109*, 9719–9726.
- (2) (a) Chelli, S.; Majdoub, M.; Jouini, M.; Aeiyaich, S.; Maurel, F.; Chane-Ching, K.I.; Lacaze, P.-C. *J. Phys. Org. Chem.* **2007**, *20*, 30–43. (b) Carmona, T.; González-Álvarez, M.J.; Mendicuti, F.; Tagliapietra, S.; Cravotto, M.K. *J. Phys. Chem. C* **2010**, *114*, 22431–22440.
- (3) Lahiani-Skiba, M.; Boulet, Y.; Youm, I.; Bounoure, F.; Vêrité, P.; Arnaud, P.; Skiba, M. *J. Incl. Phenom. Macrocycl. Chem.* **2007**, *57*, 211–217.
- (4) (a) Ohga, K.; Takashima, Y.; Takahashi, H.; Kawaguchi, Y.; Yamaguchi, H.; Harada, A. *Macromolecules* **2005**, *38*, 5897–5904. (b) Leggio, C.; Anselmi, M.; Di Nola, A.; Galantini, L.; Jover, A.; Mejjide, F.; Pavel, N.V.; Tellini, V.H.S.; Tato, J.V. *Macromolecules* **2007**, *40*, 5899–5906. (c) Hasegawa, Y.; Miyauchi, M.; Takashima, Y.; Yamaguchi, H.; Harada, A. *Macromolecules* **2005**, *38*, 3724–3730.
- (5) Krishan, R.; Gopidas, K.R. *J. Phys. Chem. Lett.* **2011**, *2*, 2094–2098.
- (6) Bertrand, B.; Stenzel, M.; Fleury, E.; Bernard, J. *Polym. Chem.* **2012**, *3*, 377–383.
- (7) Bistri, O.; Mazeau, K.; Auzély-Velty, R.; Sollogoub, M. *Chem. Eur. J.* **2007**, *13*, 8847–8857.
- (8) Galantini, L.; Jover, A.; Leggio, C.; Mejjide, F.; Pavel, N.V.; Tellini, V.H.S.; Tato, J.V.; Tortolini, C. *J. Phys. Chem. B* **2008**, *112*, 8536–8541.

- (9) Böhm, I.; Isenbügel, K.; Ritter, H.; Branscheid, R.; Kolb, U. *Angew. Chem. Int. Ed.* **2011**, *50*, 7896–7899.
- (10) Li, C.; Luo, G.-F.; Wang, H.-Y.; Zhang, J.; Gong, Y.-H.; Cheng, S.-X.; Zhuo, R.-X.; Zhang, X.-Z. *J. Phys. Chem. C* **2011**, *115*, 17651–17659.
- (11) Layre, A.-M.; Volet, G.; Wintgens, V.; Amiel, C. *Biomacromolecules* **2009**, *10*, 3283–3289.
- (12) Osman, S.K.; Brandl, F.P.; Zayed, G.M.; Tefmar, J.K.; Göpferich, A.M. *Polymer* **2011**, *52*, 4806–4812.
- (13) (a) Koopmans, C.; Ritter, H. *Macromolecules* **2008**, *41*, 7418–7422. (b) Li, L.; Guo, X.; Wang, J.; Liu, P.; Prudhomme, R.K.; May, B.L.; Lincoln, S.L. *Macromolecules* **2008**, *41*, 8677–8681.
- (14) (a) Charlot, A.; Auzély-Velty, R. *Macromolecules* **2007**, *40*, 9555–9563. (b) Charlot, A.; Auzély-Velty, R. *Macromolecules* **2007**, *40*, 1147–1158.
- (15) Van der Heyden, A.; Wilczewski, M.; Labbé, P.; Auzély, R. *Chem. Commun.* **2006**, 3220–3222.
- (16) (a) Goto, H.; Furusho, Y.; Yashima, E. *J. Am. Chem. Soc.* **2007**, *129*, 109–112. (b) Zawko, S.A.; Truong, Q.; Schmidt, C.E. *J. Biomed. Mater. Res. A* **2008**, *87*, 1044–1052. (c) Bernet, D.B.; Isenbügel, K.; Ritter, H. *Macromol. Rapid Commun.* **2011**, *32*, 397–403.
- (17) (a) Kaftan, O.; Tumbiolo, S.; Dubreuil, F.; Auzély-Velty, R.; Fery, A.; Papastavrou, G. *J. Phys. Chem. B* **2011**, *115*, 7726–7735. (b) Harada, A.; Kobayashi, R.; Takashima, Y.; Hashidzume, A.; Yamaguchi, H. *Nat. Chem.* **2010**, *3*, 34–37.
- (18) (a) Karakasyan, C.; Sébille, B.; Millot, M.C. *J. Chromatogr. B* **2006**, *845*, 200–204. (b) Rozou, S.; Raftopoulos, P.; Hatziantoniou, S.; Antoniadou-Vyza, E. *J. Sep. Sci.* **2009**, *32*, 3521–3528.
- (19) (a) van Bommel, K.J.C.; Metselaar, G.A.; Verboom, W.; Reinhoudt, D.N. *J. Org. Chem.* **2001**, *66*, 5405–5412. (b) Cromwel, W.C.; Bystrom, K.; Efting, M.R. *J. Phys. Chem.* **1985**, *89*, 326–332. (c) Prashar, D.; Shi, Y.; Bandyopadhyay, D.; Dabrowiak, J.C.; Luk, Y.-Y. *Bioorg. Med. Chem. Lett.* **2011**, *21*, 7421–7425. (d) Machut-Binkowski, C.; Hapiot, F.; Ceccelli, R.; Martin, P.; Monflier, E. *J. Incl. Phenom. Macrocycl. Chem.* **2007**, *57*, 567–572.
- (20) (a) Otyepka, M.; Kryštof, V.; Havlíček, L.; Singlerová, V.; Strnad, M.; Koča, J. *J. Med. Chem.* **2000**, *43*, 2506–2513. (b) Mor, M.; Lodola, A.; Rìvara, S.; Vacondio, F.; Duranti, A.; Tontini, A.; Sanchini, S.; Piersanti, G.; Clapper, J.R.; King, A.R.; Tarzia, G.; Piomelli, D. *J. Med. Chem.* **2008**, *51*, 3487–3498.
- (21) Vícha, R.; Potáček, M. *Tetrahedron* **2005**, *61*, 83–88.
- (22) Seong, H.R.; Kim, D.-S.; Kim, S.-G.; Choi, H.-J.; Ahn, K.H. *Tetrahedron Lett.* **2004**, *45*, 723–727.
- (23) Vaultier, M.; Knouzi, N.; Carrie, R. *Tetrahedron Lett.* **1983**, *24*, 763–764.
- (24) Koziara, A.; Osowska-Pacewicz, K.; Zawadzki, S.; Zvierzak, A. *Synthesis* **1985**, 1985, 202–204.
- (25) Bayley, H.; Standing, D.N.; Knowles, J.R. *Tetrahedron Lett.* **1978**, *19*, 3633–3634.
- (26) Lin, W.; Zhang, X.; He, Z.; Jin, Y.; Gong, L.; Mi, M. *Synth. Commun.* **2002**, *32*, 3279–3284.
- (27) Kamal, A.; Ramana, K.V.; Ankati, H.B.; Ramana, A.V. *Tetrahedron Lett.* **2002**, *43*, 6861–6863.
- (28) (a) Rolla, F. *J. Org. Chem.* **1982**, *47*, 4327–4329. (b) Boyer, J.H.; Ellzey, S.E. Jr. *J. Org. Chem.* **1958**, *23*, 127–129. (c) Aelterman, W.; Tehrani, K.A.; Coppens, W.; Huybrechts, T.; Kimpe, N.; Tourwé, D.; Declercq, J.-P. *Eur. J. Org. Chem.* **1999**, 1999, 239–250.
- (29) Kamal, A.; Laxman, E.; Arifuddin, M. *Tetrahedron Lett.* **2000**, *41*, 7743–7746.
- (30) Kazemi, F.; Kiasat, A.R.; Sayyahi, S. *Phosphor. Sulfur Silicon Relat. Elem.* **2004**, *179*, 1813–1817.
- (31) (a) Hirose, K. *J. Incl. Phenom. Macrocycl. Chem.* **2001**, *39*, 193–209. (b) Fielding, L. *Tetrahedron* **2000**, *56*, 6151–6170.
- (32) Rekharsky, M.V.; Inoue, Y. *Chem. Rev.* **1998**, *98*, 1875–1917, and references therein.
- (33) Carrazana, J.; Jover, A.; Mejjide, F.; Soto, V.H.; Tato, J.V. *J. Phys. Chem. B* **2005**, *109*, 9719–9726.
- (34) Vícha, R.; Rouchal, M.; Kozubková, Z.; Kuřitka, I.; Marek, R.; Branná, P.; Čmelík, R. *Supramol. Chem.* **2011**, *23*, 663–677.
- (35) (a) Leclercq, L.; Schmitzer, A.R. *J. Phys. Org. Chem.* **2009**, *22*, 91–95. (b) Tellini, V.H.S.; Jover, A.; Galantini, L.; Mejjide, F.; Tato, J.V. *Acta Crystallogr., Sect. B: Struct. Sci.* **2004**, *60*, 204–210. (c) Taura, D.; Taniguchi, Y.; Hashidzume, A.; Harada, A. *Macromol. Rapid Commun.* **2009**, *30*, 1741–1744. (d) Liu, H.; Zhang, Y.; Hu, J.; Li, C.; Liu, S. *Macromol. Chem. Phys.* **2009**, *210*, 2125–2137.
- (36) Martin, G.E.; Crouch, R.C. *J. Nat. Prod.* **1991**, *54*, 1–70.
- (37) Kay, L.E.; Keifer, P.; Saarinen, T. *J. Am. Chem. Soc.* **1992**, *114*, 10663–10665.
- (38) Lo Fiego, M.J.; Lockhart, M.T.; Chopa, A.B. *J. Organomet. Chem.* **2009**, *694*, 3674–3678.

4.3

Determination of Intrinsic Binding Modes by Mass Spectrometry:
Gas-Phase Behavior of Adamantylated Bisimidazolium Guests
Complexed to Cucurbiturils

Jarmila Černochová, Petra Branná, Michal Rouchal, Petr Kulhánek, Ivo Kuřitka, Robert Vícha*

Chemistry – A European Journal **2012**, *18*, 13633–13637

Determination of Intrinsic Binding Modes by Mass Spectrometry: Gas-Phase Behavior of Adamantylated Bisimidazolium Guests Complexed to Cucurbiturils

Jarmila Černochová,^[a, b] Petra Branná,^[a] Michal Rouchal,^[a] Petr Kulhánek,^[c]
 Ivo Kuřitka,^[b] and Robert Vícha*^[a]

The chemistry of cucurbit[*n*]urils (CBs) inclusion complexes with various ligands has been extensively studied in the condensed phase.^[1] The joint development of mass spectrometry (MS) techniques has provided insight into the intrinsic binding behavior of these host–guest systems readily available in the gas phase.^[2] These MS data have been used to examine self-sorting pseudorotaxane aggregates^[3] or distinguish a pseudorotaxane arrangement for the studied complexes. Depending on the initial concentrations, the formation of a 1:1 or 2:1 aggregates of butane-1,4-diamine and CB6 have been observed in the gas phase. Whereas the 1:1 complex adopted a pseudorotaxane arrangement that resulted in loss of guest and simultaneous extensive fragmentation of the CB6 cage under collision-induced dissociation (CID) conditions, the 2:1 portal-bound aggregate solely underwent facile loss of one guest.^[4] Correspondingly, the aggregates of CB6 with phenylenediamine isomers have been examined to show that *o*- and *m*-isomers preferentially bound on the exterior, whereas *p*-isomer was buried in the CB6 cavity, in a pseudorotaxane fashion.^[5] Additionally, the suppression of fragmentation channels of the ethylenediamine Ni complex after its inclusion into the CB8 cavity has been observed under CID conditions.^[6] Furthermore, the CID was used to distinguish rotaxane with phenolic axel and tetralactam macrocyclic wheel, in which the axel centerpiece was cleaved, from nonspecific unthreaded aggregate which decomposed to the wheel and axel.^[7]

In some cases of multiply charged aggregates, the CID led to the electrostatic repulsion-driven cleavage of an axel with retention of pseudorotaxane arrangement of host and guest residue as it has been demonstrated for the supramolecular aggregates of molecular tweezers containing dendritic viologen dications^[8a,b] or crown-ether/ammonium rotaxanes.^[8c] The selective binding of CB6 to lysine residues and the subsequent removal of a lysine fragment–CB6 complex was recently introduced as a probe to determine the structure of small proteins.^[9]

Formation of inclusion complexes of various adamantane derivatives with CBs in solution has been well documented. Almost ideally sphere-shaped adamantane cage perfectly fits the hydrophobic interior cavity of CB7 to form highly stable complexes. Typical values of binding constants (e.g., $1.7 \cdot 10^{14} \text{ M}^{-1}$ for 1-adamantylammonium with CB7 or $5 \cdot 10^{15} \text{ M}^{-1}$ for dication of *N*-(2-aminoethyl)-1-adamantylamine with CB7) allow such adamantane derivatives to be classed as ultrahigh affinity guests for CB7 along with bicyclo[2.2.2]octane and ferrocene derivatives.^[10] As the CBs cavity is a magnetic shielding region, the considerable up-field shifts of resonances for the adamantane protons indicate the preferable positioning of the adamantane cage inside the cavity.^[10,11] On the other hand, CB8 with larger cavity binds adamantane derivatives with reduced affinity (a typical binding constant for CB8 with 1-adamantylammonium is $8.2 \cdot 10^8 \text{ M}^{-1}$) and the lower homologue CB6 does not include adamantane cage.^[12] Nevertheless, this specificity allows to design an interesting self-sorting multi-component systems^[11] or utilize the adamantane derivatives as competitive controllers of aggregation processes.^[12]

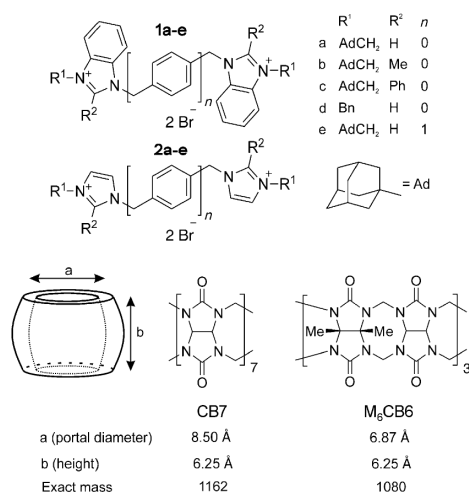
Imidazolium-based ionic liquids with various length of alkyl chains demonstrate different stoichiometry (1:1 or 2:1) with CB6 as well as two distinct binding modes differing in the imidazolium unit penetration depth.^[13] Bisimidazolium (BIM) salts with short terminal methyl substituents and *p*-xylylene spacer between imidazolium rings form a 1:1 aggregates with CB7 or CB8 in water with binding constants of about $2\text{--}3 \cdot 10^6 \text{ M}^{-1}$. In these complexes, the aromatic spacer occupies the interior of CB cavity and charged imidazolium rings cap both CB portals.^[14] It has been described, that complexation of α, α' -bis(3-(1-methylimidazolium))-*p*-xylylene dication inside the CB7 cavity significantly decrease the H/

[a] J. Černochová, P. Branná, Dr. M. Rouchal, Dr. R. Vícha
 Department of Chemistry, Faculty of Technology
 Tomas Bata University in Zlín
 Náměstí T. G. Masaryka 275, 762 72 Zlín (Czech Republic)
 Fax: (+420)576-031-560
 E-mail: rvicha@ft.utb.cz

[b] J. Černochová, Dr. I. Kuřitka
 Polymer Centre, Faculty of Technology
 Tomas Bata University in Zlín
 Náměstí T. G. Masaryka 275, 762 72 Zlín (Czech Republic)

[c] Dr. P. Kulhánek
 Central European Institute of Technology (CEITEC)
 Masaryk University, Kamenice 5, 625 00 Brno (Czech Republic)

Supporting information for this article is available on the WWW under <http://dx.doi.org/10.1002/chem.201201444>.



Scheme 1. Structures and dimensions^[17] of the bisimidazolium salts and cucurbiturils used in this work.

D exchange rate for the N–CH–N protons due to H-bonding to the CB7 portal carbonyl oxygen atoms.^[15] Additionally, the positioning of the CB7 unit on the initially unfavored dicationic binding site of the BIM **2d** (for the structure, see Scheme 1) was observed as a result of a cooperative supramolecular interaction between CB7 and β -cyclodextrin units in the ternary complex.^[16a] Upon the ESI-MS data, the similar dicationic binding site was suggested to be complexed to the CB7 due to high initial CB7 concentration.^[16b]

Herein, we describe the consecutive fragmentation of CB-complexed BIM guest dications, that is, cleavage of the covalent C–N and C–C bonds, while retaining the supramolecular interactions between the charged guest residue and the CB molecule. In addition to the unprecedented gas-phase reactivity (to the best of our knowledge), we demonstrate that analysis of the ESI-MS spectra of host–guest systems may serve as a tool for estimating the ability of CBs to slip over the molecular axel.

We first analyzed MeOH/H₂O (1:1, v:v) solutions containing only BIM dibromides (Scheme 1). Figure 1a shows that five significant ions were observed in the positive-ion mode ESI-MS spectra for compound **2a** and assigned through a detailed investigation using tandem mass spectrometry and CID experiments. The fragmentation of the ion at m/z 223 (MS²) created two product ions at m/z 297 and 149 (Figure 1b). Further fragmentation of m/z 297 (MS³) led to the parallel neutral loss of imidazole, diazine, or diimidazolymethane to yield the ions at m/z 229, 217, or 149, respectively (Figure S7c in the Supporting Information). We therefore assigned the ion at m/z 223 to the doubly charged molecular BIM ion and the ions at m/z 297 and 149 to its singly charged fragments that form during the ESI process. The loss of the singly charged adamantylmethyl cation (m/z 149) will hereinafter be referred to as “149” fragmentation. In addition, the supramolecular associate between BIM and Br[–]

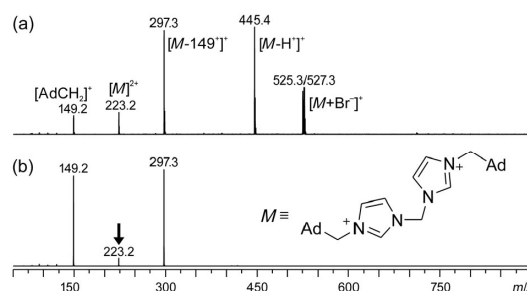


Figure 1. Positive-ion mode ESI mass spectra (full scan) of compound **2a** in a MeOH/H₂O (1:1, v:v) solution. a) First-order mass spectra, b) MS² of m/z 223. The assignments for the observed signals are shown in brackets. The ion being fragmented in the tandem mass spectra is marked with a bold, downward arrow.

was observed based on the ⁷⁹Br and ⁸¹Br isotopologue ion pair at m/z 525 and 527. This association loses a neutral HBr molecule to produce the sole singly charged N-heterocyclic carbene^[18] observed at m/z 445 (Figure S7d in the Supporting Information).

We subsequently analyzed 25 μ M mixtures of the BIM ligands and CBs (Scheme 1) in a 50 μ M solution of NaCl in water. In the spectra of the BIM/CB7 mixtures, we initially focused on the fragmentation of the doubly charged ions from the 1:1 complexes [BIM·CB]²⁺. Figure 2c and d show that, for compound **1c** with CB7, the fragmentation of the 1:1 complex at m/z 930 forms three ions at m/z 549, 1163, and 1311. Based on the corresponding MS spectra for the individual BIM and CB7 compounds, we assigned these signals to the singly charged residue of **1c** arising from “149” fragmentation, the singly charged association of CB7·H⁺ and the singly charged CB7·AdCH₂⁺, respectively. The ion at m/z 1311 loses a neutral AdCH fragment and forms CB7·H⁺ at m/z 1163 after further fragmentation (MS³). Therefore, the observed fragmentation for BIM **1c** complexed to CB7 is essentially the identical to that of free BIM (compare Figure S16b in the Supporting Information and Figure 2d).

In contrast, we obtained completely different results for the mixture of **2a** and CB7 (Figure 2a and b). In the MS² spectrum for this complex, we observed two ions at m/z 730 and 656 formed from the parent ion [BIM·CB7]²⁺ at m/z 804. Subsequent fragmentation of the ion at m/z 730 (MS³) led to the sole formation of the ion at m/z 656. This may be rationalized as the sequential loss of neutral 1-adamantylcarbene fragment (or its isomer)^[19] from both ends of the BIM scaffold to yield the doubly charged aggregate of the CB7 and BIM residue. This release of neutral AdCH fragments (exact mass of m/z 148) will be hereinafter referred to as the “148” fragmentation.

All other examined adamantylated BIMs displayed at least one (but usually exactly one) of these fragmentation pathways and no additional significant signals were observed. Little variations in signal intensities can be reasonably attributed to the different axel bulkiness which influen-

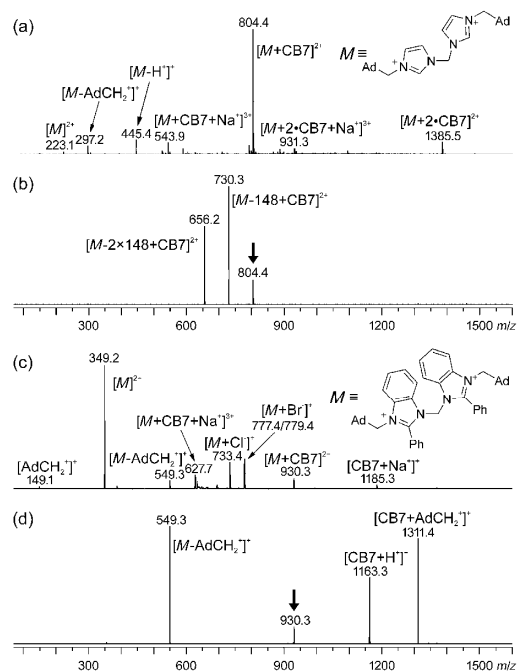


Figure 2. Positive-ion mode ESI mass spectra (full scan) of aqueous solutions of **2a**-CB7 and **1e**-CB7. a) First-order mass spectra of **2a**-CB7, b) MS² of *m/z* 804, c) first-order mass spectra of **1e**-CB7, d) MS² of *m/z* 930. The assignments for the observed signals are shown in the brackets. The fragmented ions in the tandem mass spectra are marked with bold, downward arrows.

ces the activation barriers to the slipping of CB7 between particular binding sites. Thus, the intensity of the second “148” fragmentation product signals was rather lowered in the case of BIM **2b**, **1e**, or **2e** and completely disappeared in the case of BIM **1a** or **1b**. Additionally, the CID (MS²) of doubly charged aggregates of the BIM **1a** or **1b** with CB7 resulted in products of “149” fragmentation accompanied by products of one “148” fragmentation. Comparing the intensities of the corresponding signals (Figure S40 and S41 in the Supporting Information), we may see that the **1a**-CB7 complex was predominantly cleaved via the “148” fragmentation in contrast to the **1b**-CB7. The complexes of CB7 and BIM **1e** or **2e** (Figure S43 and S47 in the Supporting Information) displayed fragmentation pattern similar to those observed for the corresponding methylene-bridged BIMs and the additional hypothetical binding site on the aromatic bridge did not affect fragmentation pattern.

The ¹H NMR spectra recorded for the mixtures of BIMs with CB7 in D₂O indicated formation of inclusion complexes with pseudorotaxane geometry (Figure S60 in the Supporting Information). The considerable upfield shift of all adamantane signals hand in hand with diminishing of signals of free BIM when the CB7 molar fraction reached of 0.7 evidenced that both terminal adamantane cages were

successively complexed to the CB7 interior cavity to form the 1:1 or 1:2 aggregates depending on the CB7 concentration. In contrast, the downfield shift of signals of methylene or *p*-xylylene bridges suggested the location of the central part of BIM close to the CB7 portal. Considering previously discussed binding constants for similar structure motifs with CBs, we assume that binding of CB7 at adamantane site is strongly favored and observation of any other potential arrangements is disabled using NMR. However, this finding does not contradict the formation of pseudorotaxane complexes with different geometry under treatment in the gas phase.

We propose that the aggregates evidenced in solution are transferred to the gas phase using ESI to observe corresponding signals in the first-order mass spectra. We believe that the CB host cannot reach the opposite end of the guest skeleton by walking “outside” of the guest molecule without decomposing the supramolecular complex. Therefore, the presence of substituents with varying bulk results in three distinct situations (Figure 3), as indicated via further frag-

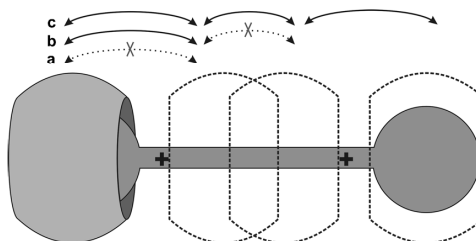


Figure 3. Schematic drawing of the slipping modes of the CB unit over the BIM dication.

mentation analyses: 1) The CB is bound to the end of the BIM molecule and cannot slip over the imidazolium unit. Only the products of “149” fragmentation are observed. Typical examples of such BIM salts are **1c** or **2c** (Figure 2d and Figure S45 in the Supporting Information). 2) The CB may slip over the imidazolium unit once bound to the BIM but cannot easily reach the opposite end of the BIM. In such cases we observed products from both “149” and “148” fragmentations. However, the “148” fragmentation occurred only once. In other words, only one adamantylmethyl substituent can be released in this manner. Typical examples of such BIM salts are **1a** or **1b** (Figures S40 and S41 in the Supporting Information). 3) The CB can freely slip over the BIM skeleton, and the products of “148” fragmentation were predominantly observed. Typical examples of such BIM salts are **2a**, **1e**, **2b**, or **2e** (Figure 2b and Figures S43, S44, and S47 in the Supporting Information).

We next focused on the fragmentation analysis of 2:1 aggregates of CB with BIM. With the exception of compounds **1a** and **2a**, the signals obtained for the 2:1 aggregates were not observed for the equimolar aqueous solutions of CB and BIM in the presence of NaCl. The transfer of the 2:1 aggre-

gates from solution to the gas phase was supported by excluding NaCl from the tested mixture and enhancing the mole fraction of CB in the solution. The 2:1 aggregates were typically observed as either doubly charged ions or their triply charged Na^+ associations. A further CID experiment led to the loss of the CB unit to form the doubly charged 1:1 complex with nearly identical fragmentation patterns to those previously described (Figures S48–S57 in the Supporting Information). However, for BIMs **2a** and **2b**, the fragmentation of the doubly charged 2-CB7-BIM at m/z 1385 and m/z 1399 yielded an unexpected pair of ions at m/z 1311 and 1237 and m/z 1325 and 1251, respectively (Figures S53 and S54 in the Supporting Information). We assigned these ions to the doubly charged products of the sequential “148” fragmentation complexed to two CB7 units. The 2:1 aggregates of two CB7 and doubly protonated diimidazolymethane with signals at m/z 1237 and 1251 further fragmented (MS^4) to yield signals at m/z 1311 and 1339, respectively. In both cases, these ions were accompanied with a signal at m/z 1163. We interpreted this as an electrostatic repulsion-driven cleavage of the 2:1 complex to form a $[\text{CB7-H}]^+$ ion at m/z 1163 and the singly charged aggregates of the CB7 and corresponding singly protonated diimidazolymethane at m/z 1311 and 1339, respectively.

To examine the scope of the described phenomenon, we analyzed mixtures of the benzylated BIMs **1d** and **2d** with CB7 and $\text{Me}_6\text{CB6}$. Typically, in the MS spectrum of **2d** we observed ions at m/z 409/411, 329, 239, and 91, which we assigned to $[\text{BIM}+\text{Br}]^+$, $[\text{BIM-H}]^+$, $[\text{BIM-Bn}]^+$ and Bn^+ (Figure S25 in the Supporting Information), respectively. Under the same experimental conditions, we observed two additional signals at m/z 746 and 505 when analyzing the equimolar mixture of **2d** and CB7. Upon further fragmentation analysis, we assigned these signals to the $[\text{CB7}\cdot\text{BIM}]^{2+}$ and $[\text{CB7}\cdot\text{BIM}\cdot\text{Na}]^{3+}$ aggregates, respectively. The former ion decomposed into the fragments observed at m/z 253, 707, 1161, and 1401 (Figure S46b in the Supporting Information). The assignment of the ion at m/z 1161 is discussed below and the rest were assigned to $[\text{BIM-77}]^+$, $[\text{CB7}+\text{BIM-78}]^{2+}$, and $[\text{CB7}+\text{BIM-Bn}]^+$, respectively. As can be clearly observed, the presence of CB7 promoted alternative fragmentation pathways involving the loss of a neutral fragment. We can conclude that CB7 clearly changed the fragmentation mechanism and supported the charge retention on the axel residue during the fragmentation process. With a view to extension of our work to other CB homologue, we analyzed mixtures of BIM salts **1d** and **2d** with $\text{Me}_6\text{CB6}$, a water-soluble analogue of CB6. Signals for $[\text{BIM}+\text{Me}_6\text{CB6}]^{2+}$ were clearly observed and fragmented (Figures S58 and S59 in the Supporting Information) to yield ions assigned to $[\text{BIM-Bn}]^+$, $[\text{Me}_6\text{CB6}+\text{BIM-Bn}]^+$, $[\text{Me}_6\text{CB6}+\text{Bn}]^+$ at m/z 1171 and the ion at m/z 1079 (see below). These results indicate that $\text{Me}_6\text{CB6}$ can form supra-molecular complexes with benzylated BIM but cannot slip over the BIM skeleton to provide the alternative fragmentations contrary to CB7, which has a larger internal cavity diameter.

Finally, we would like to note the unusual forms observed of the CBs. In some cases, the complex between the CB7 and the charged BIM fragments decompose to neutral BIM residues and a CB ion at m/z 1161. Similarly, the fragment at m/z 1079 was observed when mixtures containing $\text{Me}_6\text{CB6}$ and a suitable ligand were analyzed. Figure 4 shows the obtained tandem mass spectrum for the mixture of CB7 with **1a**. The ion at m/z 1559 was obtained through sequential MS^2 experiments beginning with the ion at m/z 855 (doubly charged CB7-BIM), which produced the minor ion at m/z 1559 under CID conditions (Figure S40b in the Supporting Information). We assigned this ion to $[\text{CB7}+\text{BIM-AdCH}_2]^+$ and a further fragmentation (Figure S40c in the Supporting Information) led to the loss of a neutral dibenzimidazolymethane unit to yield $[\text{CB7}+\text{AdCH}_2]^+$ at m/z 1311. The parallel fragmentation of m/z 1559 led to the loss of neutral adamantylmethylbenzimidazole and the ion at m/z 1293. Subsequent fragmentation yielded the ion at m/z 1161 (Figure S40d in the Supporting Information). The suggested pathway was supported by the further isolation and fragmentation analyses of the ions at m/z 1311 and 1293. Using these data, we were able to assign the ions at m/z 1293 and 1161 to the singly charged complex of CB7 and benzimidazolymethyl and the singly charged CB7 without a single hydrogen atom, respectively. We can speculate that latter ion is possibly formed by a hydride transfer from the neutral CB7 molecule to the benzimidazolymethyl cation. To support this idea, the structure and formation of the $[\text{CB7-H}]^+$ cation was further studied using a computational chemistry framework (for details and analysis, see the Supporting information). Density functional calculations indicated that the reaction depicted in Figure 4 is favorable towards the products by -160 kJ mol^{-1} . It can be expected that the transfer probably occurs within the CB7-benzimidazolymethyl cation complex. Indeed, its predicted structure shows reasonable mutual orientation of both donor and acceptor atoms of hydride ion with atom-to-atom distance of 3.5 Å.

In conclusion, we have demonstrated that CBs may dramatically change the fragmentation pathways of axel mole-

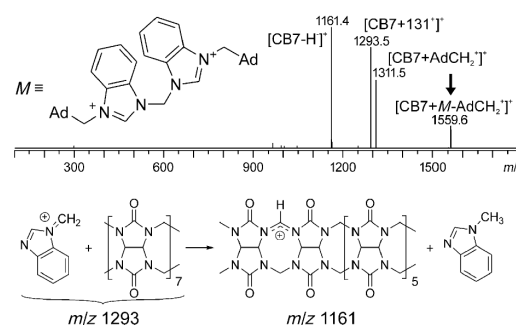


Figure 4. Tandem mass spectra (MS^3) of m/z 1559 (top) and a schematic representation of the final step in the proposed pathway toward m/z 1161 product ion (bottom).

cules in the gas phase. Whereas sole bisimidazolium dication decompose to two singly charged fragments in accordance with electrostatic repulsion, some complexed dication release neutral fragments to form doubly charged complex of CB and axel residue. Furthermore, latter fragmentation occurred only when the slippage of the CB unit over the axel was sterically allowed. This phenomenon has general importance for the description of binding modes using mass spectrometry. We are currently preparing a set of BIM ligands with a spacer of various lengths bearing a steric hindrance between the imidazolium rings to clarify the mechanism of unusual “148” fragmentation. In addition, we have demonstrated the ability of CBs to act as a hydride donor in the gas phase. This property of CBs, as soon as proved in solution, may open a new way towards functionalized CBs.

Acknowledgements

We would like to thank to Dr. Vladimír Šindelář (Department of Chemistry, Faculty of Science, Masaryk University, Brno, Czech Republic) for the kind gift of the CBs used in this study. This work was financially supported by the Internal Founding Agency of Tomas Bata University in Zlín, project No. IGA/FT/2012/016 and project CZ.1.05/1.1.00/02.0068 financed by the European Regional Development Fund at the CEITEC - Central European Institute of Technology. Access to the MetaCentrum computing facilities was provided under the program “Projects of Large Infrastructure for Research, Development, and Innovations” LM2010005, which is funded by the Ministry of Education, Youth, and Sports of the Czech Republic.

Keywords: adamantane · cucurbituril · host–guest systems · imidazolium salts · supramolecular chemistry

- [1] a) W.-H. Huang, S. Liu, L. Isaacs, in *Modern Supramolecular Chemistry* (Eds.: F. Diederich, P. J. Stang, R. R. Tykwinski) Wiley-VCH: Weinheim, 2008, pp. 113–142; b) J. Lagona, P. Mukhopadhyay, S. Chakrabarti, L. Isaacs, *Angew. Chem.* 2005, 117, 4922–4949; *Angew. Chem. Int. Ed.* 2005, 44, 4844–4870; c) S. Liu, C. Ruspic, P. Mukhopadhyay, S. Chakrabarti, P. Y. Zavalij, L. Isaacs, *J. Am. Chem. Soc.* 2005, 127, 15959–15967; d) A. C. Bhasikuttan, H. Pal, J. Mohanty, *Chem. Commun.* 2011, 47, 9959–9971; e) E. Masson, X. Ling, R. Joseph, L. Kyeremeh-Mensah, X. Lu, *RSC Adv.* 2012, 2, 1213–1247; f) L. Isaacs, *Chem. Commun.* 2009, 619–629; H.-J. Buschmann, *Isr. J. Chem.* 2011, 51, 533–536; g) D. Das, O. A. Scherman, *Isr. J. Chem.* 2011, 51, 537–550.
- [2] a) C. A. Schalley, A. Springer, *Mass Spectrometry and Gas-Phase Chemistry of Non-Covalent Complexes*, John Wiley & Sons, New York, 2009; b) F. Yang, D. V. Dearden, *Isr. J. Chem.* 2011, 51, 551–558; c) B. Baytekin, H. T. Baytekin, C. A. Schalley, *Org. Biomol. Chem.* 2006, 4, 2825–2841; d) I. Osaka, M. Kondou, N. Selvapalam, S. Samal, K. Kim, M. V. Rekharsky, Y. Inoue, R. Arakawa, *J. Mass Spectrom.* 2006, 41, 202–207; e) J. P. Da Silva, N. Jayaraj, S. Jockusch, N. J. Turro, V. Ramamurthy, *Org. Lett.* 2011, 13, 2410–2413.
- [3] a) W. Jiang, Q. Wang, I. Linder, F. Klautzsch, C. A. Schalley, *Chem. Eur. J.* 2011, 17, 2344–2348; b) S. Deroo, U. Rauwald, C. V. Robinson, O. A. Scherman, *Chem. Commun.* 2009, 644–646.
- [4] H. Zhang, E. S. Paulsen, K. A. Walker, K. E. Krakowiak, D. V. Dearden, *J. Am. Chem. Soc.* 2003, 125, 9284–9285.
- [5] D. V. Dearden, T. A. Ferrell, M. C. Asplund, L. W. Zilch, R. R. Julian, M. F. Jarrold, *J. Phys. Chem. A* 2009, 113, 989–997.
- [6] T. Mitkina, V. Fedin, R. Liusar, I. Sorribes, C. Vicent, *J. Am. Soc. Mass Spectrom.* 2007, 18, 1863–1872.
- [7] P. Ghosh, G. Federwisch, M. Kogej, C. A. Schalley, D. Haase, W. Saak, A. Lützen, R. M. Gschwind, *Org. Biomol. Chem.* 2005, 3, 2691–2700.
- [8] a) C. A. Schalley, C. Verhaelen, F. G. Klärner, U. Hahn, F. Vögtle, *Angew. Chem.* 2005, 117, 481–485; *Angew. Chem. Int. Ed.* 2005, 44, 477–480; b) Z. Qi, C. A. Schalley, *Supramol. Chem.* 2010, 22, 672–682; c) W. Jiang, C. A. Schalley, *J. Mass Spectrom.* 2010, 45, 788–798.
- [9] S. W. Heo, T. S. Choi, K. M. Park, Y. H. Ko, S. B. Kim, K. Kim, H. I. Kim, *Anal. Chem.* 2011, 83, 7916–7923.
- [10] S. Moghaddam, C. Yang, M. Rekharsky, Y. H. Ko, K. Kim, Y. Inoue, M. K. Gilson, *J. Am. Chem. Soc.* 2011, 133, 3570–3581.
- [11] a) P. Mukhopadhyay, P. Y. Zavalij, L. Isaacs, *J. Am. Chem. Soc.* 2006, 128, 14093–14102; b) Z.-J. Ding, H.-Y. Zhang, L.-H. Wang, F. Ding, Y. Liu, *Org. Lett.* 2011, 13, 856–859.
- [12] a) X. Lu, E. Masson, *Langmuir* 2011, 27, 3051–3058; b) D. Jiao, F. Biedermann, F. Tian, O. A. Scherman, *J. Am. Chem. Soc.* 2010, 132, 15734–15743; c) S. Gadde, E. K. Batchelor, J. P. Weiss, Y. Ling, A. E. Kaifer, *J. Am. Chem. Soc.* 2008, 130, 17114–17119; d) A. E. Kaifer, W. Li, S. Silvi, V. Sindelar, *Chem. Commun.* 2012, 48, 6693–6695.
- [13] a) L. Liu, N. Zhao, O. A. Scherman, *Chem. Commun.* 2008, 1070–1072; b) V. Kolman, R. Marek, Z. Strelcova, P. Kulhanek, M. Necas, J. Svec, V. Sindelar, *Chem. Eur. J.* 2009, 15, 6926–6931.
- [14] D. Jiao, F. Biedermann, O. A. Scherman, *Org. Lett.* 2011, 13, 3044–3047.
- [15] R. Wang, L. Yuan, D. H. Macartney, *Chem. Commun.* 2006, 2908–2910.
- [16] a) L. Ledercq, N. Noujeim, S. H. Sanon, A. R. Schmitzer, *J. Phys. Chem. B* 2008, 112, 14176–14184; b) S. Samsam, L. Ledercq, A. R. Schmitzer, *J. Phys. Chem. B* 2009, 113, 9493–9498.
- [17] a) D.-H. Yu, X.-L. Ni, Z.-C. Tian, Y.-Q. Zhang, S.-F. Xue, Z. Tao, Q.-J. Zhu, *J. Mol. Struct.* 2008, 891, 247–253; b) J. W. Lee, S. Samal, N. Selvapalam, H.-J. Kim, K. Kim, *Acc. Chem. Res.* 2003, 36, 621–630.
- [18] Y. E. Corilo, F. M. Nachtigall, P. V. Abdelnur, G. Ebeling, J. Dupont, M. N. Eberlin, *RSC Advances* 2011, 1, 73–78.
- [19] M. Farcasiu, D. Farcasiu, R. T. Conlin, M. Jones, P. R. Schleyer, *J. Am. Chem. Soc.* 1973, 95, 8207–8209.

Received: April 26, 2012

Revised: August 3, 2012

Published online: September 11, 2012

4.4


Gas-phase fragmentation of 1-adamantylbisimidazolium salts
and their complexes with cucurbit[7]uril studied
using selectively ^2H -labeled guest molecules.

Andrea Čablová, Michal Rouchal, Barbora Hanulíková, Jan Vícha, Lenka Dastychová,
Zdeňka Prucková, Robert Vícha*

Rapid Communications in Mass Spectrometry **2017**, *31*, 1510–1518

RESEARCH ARTICLE

Gas-phase fragmentation of 1-adamantylbisimidazolium salts and their complexes with cucurbit[7]uril studied using selectively ^2H -labeled guest molecules

Andrea Čablová¹ | Michal Rouchal¹ | Barbora Hanulíková² | Jan Vícha²  | Lenka Dastychová¹ | Zdeňka Prucková¹ | Robert Vícha¹

¹Department of Chemistry, Faculty of Technology, Tomas Bata University in Zlín, Zlín, Vavrečkova 275, 760 01 Zlín, Czech Republic

²Center of Polymer Systems, Tomas Bata University in Zlín, třída Tomáše Bati 5678, 760 01, Zlín, Czech Republic

Correspondence

R. Vícha, Department of Chemistry, Faculty of Technology, Tomas Bata University in Zlín, Vavrečkova 275, 760 01 Zlín, Czech Republic. Email: rvicha@ft.utb.cz

Funding information

Internal Founding Agency of Tomas Bata University, Grant/Award Number: IGA/FT/2017/001; Ministry of Education, Youth and Sports of the Czech Republic, Program NPU I, Grant/Award Number: LO1504; Czech Science Foundation, Grant/Award Number: 16-05691S

Rationale: Bisimidazolium salts (BIMs) represent an interesting family of ditopic ligands that are used in the construction of supramolecular systems with hosts based on cyclodextrins or cucurbit[n]urils. Understanding the fragmentation mechanism of individual BIMs and how this mechanism changes after complexation with cucurbit[n]urils can bring new insight into the intrinsic host-guest relationship, thereby allowing utilization of mass spectrometry to describe binding behavior.

Methods: Selectively ^2H -labeled bisimidazolium salts were prepared and fully characterized by spectroscopic methods. All MSⁿ experiments were conducted in the positive-ion mode using an electrospray ionization (ESI) ion-trap mass spectrometer. The structures of the proposed fragments were supported by theoretical optimizations performed at the B3LYP/6-31G(d) level of density functional theory (DFT) using the Spartan'14 program.

Results: Using selectively deuterium-labeled isotopologues of two adamantylated bisimidazolium salts and DFT calculations, we describe the fragmentation pathways of bisimidazolium salts. The release of two important adamantane moieties, $[\text{C}_{11}\text{H}_{17}]^+$ and $\text{C}_{11}\text{H}_{16}$, from M^{2+} was determined, although the former was strongly preferred. In contrast, when M^{2+} was complexed with CB7, the neutral loss of the $\text{C}_{11}\text{H}_{16}$ fragment was favored. The fragmentation pattern strongly depended on the steric hindrance of the M^{2+} guest against slippage of the CB7 unit over the guest molecular axle.

Conclusions: The structures of two adamantane-based fragments and the mechanisms of their formation were rationalized. Two distinct geometric arrangements for the adamantane cage inside the CB7 cavity were hypothesized to explain the differences in the fragmentation patterns for guests with minimal, moderate, and high steric hindrance. This finding brings new insight into the understanding of intrinsic behavior of the adamantane-based guests inside the CB7 cavity.

1 | INTRODUCTION

Bisimidazolium salts represent an intriguing family of compounds that are used, for instance, in host-guest supramolecular chemistry.^{1–7} In addition to the well-established and extensively studied imidazolium-based ionic liquids, compounds consisting of more than one imidazolium core can serve as multitopic guests. In particular, compounds that consist of hydrocarbon cage scaffolds, such as adamantane, diamantane, bicyclo[2.2.2]octane or ferrocene, can be employed as key components in complex supramolecular systems due to the extraordinary high affinity of these guest towards some macrocyclic hosts, including cucurbit[7]uril and β -cyclodextrin.^{8–11}

Another interesting feature of the imidazolium core originates from the relative acidity of hydrogen at the N=CH–N position. In addition to the rapid exchange in protic media, which can be modulated by complexation inside the macrocycle cavity,^{12,13} this proton can be abstracted to produce so-called *N*-heterocyclic carbenes (NHCs). Subsequently, the interactions of free electron pairs localized on the C2 carbon with various transition metals afford coordination complexes, which are well documented in recent literature.^{14–18} Many of these complexes have been successfully employed in various synthetic protocols. With the exception of the structures containing bulky substituents,¹⁹ the NHCs are usually highly reactive; thus, their direct observation is obstructed. Despite the inaccessibility of neutral

carbene species for mass spectrometry, the NHCs tagged with anionic²⁰ or cationic²¹ motifs can be easily observed. In the latter case, the bisimidazolium and trisimidazolium salts were studied. In such structures, one imidazolium core was transformed into an NHC, and the remaining imidazoliums allowed the detection of the resulting ions by means of mass spectrometry.

As mentioned above, cationic moieties in combination with an adjacent, suitable lipophilic scaffold form highly stable, specific aggregates with cucurbit[n]urils in solution.²² These species can be efficiently transferred into the gas phase using the electrospray technique for study using mass spectrometry.²³ Over the past decade, several intriguing papers have been published in this field. For instance, the CB6-induced selective fragmentation of proteins at lysine residues under collision-induced dissociation allows the structural determination of small proteins.²⁴ Another example in which pseudorotaxane-like and external binding modes were distinguished by gas-phase reactivity of CB6 and 1,4-diaminobutane aggregates.²⁵ Finally, it has been demonstrated that the stabilization of cationic intermediates *via* ion-dipole interactions between cationic species and cucurbit[n]uril portal(s) or other suitable electron-donating motifs plays a crucial role in fragmentation processes.²⁶

It has been previously reported⁴ that the complexation of the adamantane binding site of bisimidazolium salts inside the CB7 cavity changes the preferred fragmentation pathway. We demonstrated that the fragmentation pattern correlates with the ability of the CB7 unit to slip over the guest molecular axle. In this study, we elaborate on a previously described phenomenon and suggest the fragmentation pathways of free and complexed BIMs in detail. The structures of the guests and host are given in Figure 1.

2 | EXPERIMENTAL

2.1 | Materials

All deuterium-labeled reagents and solvents, i.e., LiAD₄ (96 atom % D), CD₂Br₂ (99 atom % D), DCl in D₂O (35 wt. %, 99 atom % D), D₂O (99.9 atom % D), and [D₄]methanol (99.8 atom % D), were obtained from Sigma-Aldrich. The deuterium-labeled compounds **1α**, **2α**, **1γ**, and **2γ** were prepared according to procedures that were described previously for non-labeled species.⁴ The Greek letters α, β, and γ specify the labeled positions, as depicted in Figure 1 and Scheme 1. The structures of all intermediates and final products were confirmed using ¹H NMR and ¹³C NMR spectrometry (for spectra, see Figures S42–S49, supporting information). The compounds **1β** and **2β** were prepared *in situ* by H/D exchange in D₂O.

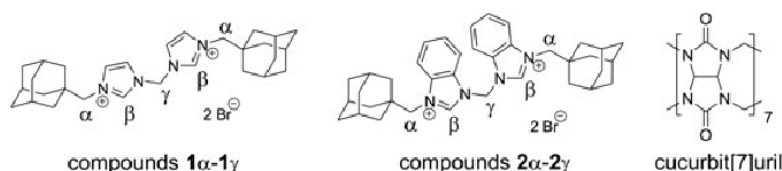
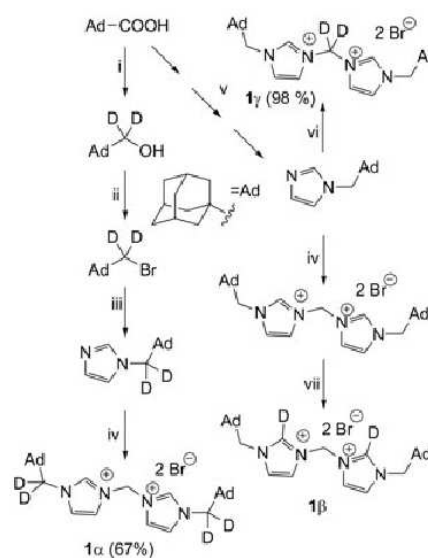


FIGURE 1 Structures of guests and host used in this study. The positions in which the compounds **1** and **2** were D-labeled are assigned with Greek characters



SCHEME 1 Preparation of deuterium-labeled imidazolium salts **1α**, **1β**, and **1γ**. Greek characters denote the position of D-labeling as depicted in Figure 1. Reaction conditions: (i) LiAD₄, DEE, reflux, 8 h, 86%; (ii) CBr₄, PPh₃, DCM, 20 °C, 24 h, 85%; (iii) imidazole, NaH, DMF, 80–90 °C, 200 h, 78–80%; (iv) neat CH₂Br₂, 70–80 °C, 100 h; (v) according to a previously reported procedure;⁴ (vi) neat CD₂Br₂, 80–90 °C, 24 h; (vii) *in situ* D₂O, 25 °C, 30 min

2.2 | Mass spectrometry

The electrospray ionization mass spectra (ESI-MS) were recorded using an amaZon X ion-trap mass spectrometer (Bruker Daltonics, Bremen, Germany) equipped with an ESI source. All experiments were conducted in the positive-ion polarity mode. The instrumental conditions used to measure the single bisimidazolium salts and their cucurbit[7]uril mixtures were different; therefore, they are described separately. *Single bisimidazolium salts*: Individual samples (with a concentration of 500 ng cm⁻³) were infused into the ESI source in methanol/water (1:1, v/v) solutions (in the case of non-labeled salts and compounds **1α**, **1γ**, **2α**, and **2γ**) using a syringe pump with a constant flow rate of 4 μL·min⁻¹. In the case of compounds **1β** and **2β** the solutions for MS analysis were prepared by 1:100 dilution of the stock solution in D₂O with D₂O/CD₃OD (1:1, v/v) or MeCN, respectively. The other instrumental conditions were as follows: an electrospray voltage of -4.2 kV, capillary exit voltage of 140 V, drying gas temperature of 220 °C, drying gas flow rate of 6.0 dm³·min⁻¹ and nebulizer pressure of 55.16 Pa. *Host-guest complexes*: An aqueous solution of the guest molecule (12.5 μM), cucurbit[7]uril (12.5 μM), was infused into the

ESI source at a constant flow rate of $4 \mu\text{L}\cdot\text{min}^{-1}$ (the D_2O solution of both host and guest molecules was used in the case of compounds **1 β** and **2 β** , respectively). The other instrumental conditions were as follows: an electrospray voltage of -4.0 kV , capillary exit voltage of $20\text{--}140 \text{ V}$, drying gas temperature of $300 \text{ }^\circ\text{C}$, drying gas flow rate of $6.0 \text{ dm}^3\cdot\text{min}^{-1}$ and nebulizer pressure of 206.84 kPa . Nitrogen was used as the nebulizing and drying gas for all experiments. Tandem mass spectra were collected using collision-induced dissociation (CID) with helium as the collision gas after the isolation of the required ions.

2.3 | Theoretical calculations

Calculations were performed using the Spartan'14 software (Wavefunction, Irvine, CA, USA).²⁷ The equilibrium geometries and energies of the optimized benzoimidazolium and imidazolium salts were determined by density functional theory (DFT) calculations on the level of the B3LYP (Becke-3-Lee-Young-Parr) model and the 6-31G* polarization basis set. Multiplicity was set to singlet in all cases and the charge was adjusted to neutral, cation or dication according to the particular molecules. All calculations were set in a vacuum with no constrained bonds or angles.

3 | RESULTS AND DISCUSSION

3.1 | Chemistry

The α -tetradeuterated compounds were prepared from commercially available adamantane-1-carboxylic acid, which was reduced by LiAlD_4 to produce the corresponding primary alcohol. This alcohol was transformed into 1-(bromomethyl)adamantane, coupled with sodium (benzo)imidazolide, and then quaternized with methylene dibromide. The γ -labeled compounds were prepared according to essentially the same protocol, except CD_2Br_2 was used instead of CH_2Br_2 in the final step. This final step was performed at the millimolar scale in 1 mL of neat CD_2Br_2 . The remaining CD_2Br_2 was recovered by microdistillation under reduced pressure and trapped using liquid nitrogen. Despite several attempts to prepare β -labeled salts in solid form using various combinations of media (D_2O , CD_3OD) and acids (DCl , HCOOD), we obtained products with unsatisfactory degrees of H/D exchange according to the mass spectra. Finally, we prepared compounds **1 β** and **2 β** *in situ* by dissolving non-labeled **1** or **2** in D_2O . The H/D exchange was equilibrated for 30 min at room temperature and obtained solution was analyzed by ESI-MS. The complete layouts of the synthetic pathways towards compounds **1 ϵ** , **1 β** , and **1 γ** are given in Scheme 1. The yields of compounds **2 α** and **2 γ** were 80% and 96% , respectively.

3.2 | Fragmentation analyses of compounds 1 and 2

In the first-order mass spectra of both bisimidazolium salts, five important signals were observed, as displayed in Figure 2A for non-labeled compound **2**. The base signal was attributed to the M^{2+} cation. The electrostatic repulsion likely drives the cleavage of the M^{2+} dication into two singly charged fragments $[\text{C}_{11}\text{H}_{17}]^+$ (149 m/z ; the m/z values refer hereafter to the non-labeled structures, if not mentioned

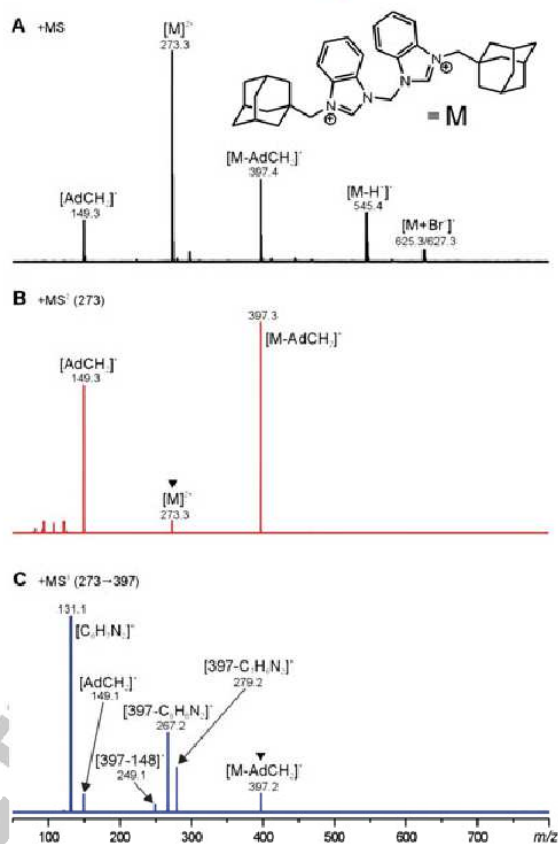
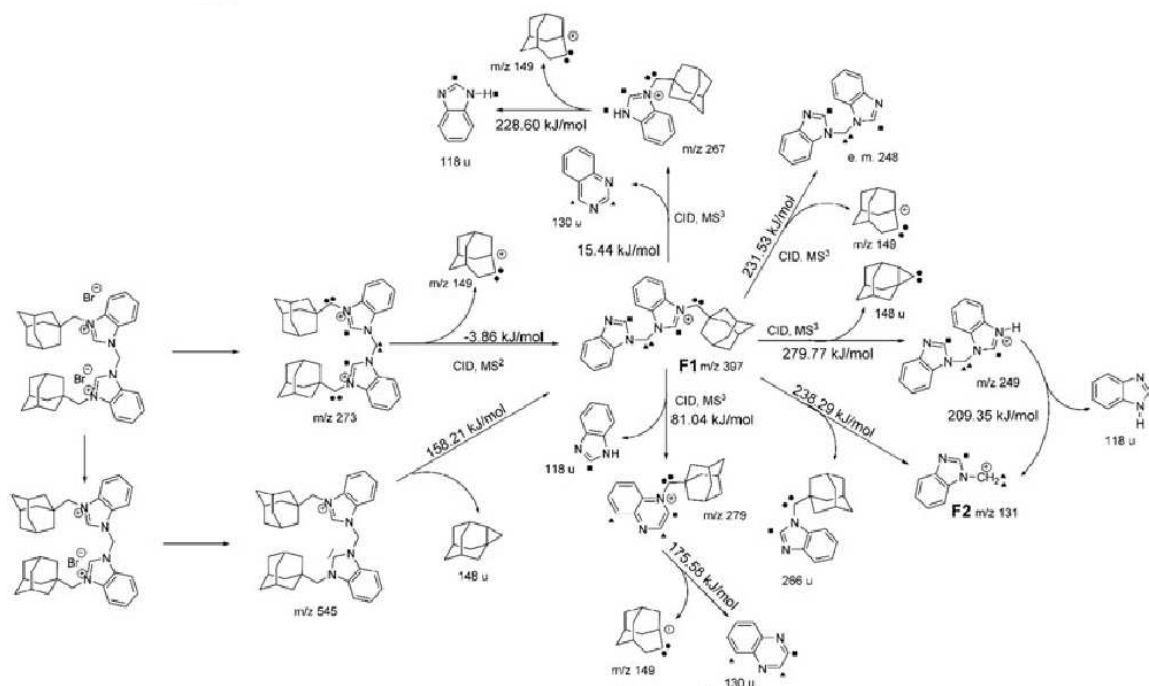


FIGURE 2 The positive-ion ESI mass spectra of an aqueous solution of **2**. (A) First-order mass spectra, (B) MS^2 of m/z 273.3, and (C) MS^2 of m/z 397.4. The assignments for observed signals are shown in brackets. The fragment ions in the tandem mass spectra are marked with a black downward-facing triangle [Color figure can be viewed at wileyonlinelibrary.com]

elsewhere) and the remainder of the molecule. This process obviously occurred during the spraying and drying of the sample. We were unable to tune the spraying conditions to suppress these signals. In addition, the signal of the $[\text{M}^{2+}+\text{Br}]^+$ aggregate and the signal related to the product of HBr elimination (m/z 545) were both observed. This process yielding a *N*-heterocyclic carbene has been previously documented.^{4,20,21} Because the fragmentation of imidazolium salts is very similar to that of benzimidazolium salts, we discuss only the fragmentation of **2** for clarity and conciseness. However, the important differences between imidazolium- and benzimidazolium-based species are noted. In addition, we prepared three selectively labeled isotopologues for each bisimidazolium salt to enable a detailed description of the fragmentation pathways. The respective labeled positions, i.e., AdCD_2^- , $\text{N}=\text{CD}-\text{N}$, and $\text{N}-\text{CD}_2-\text{N}$, are hereafter assigned as α , β , and γ , respectively. Initially, we analyzed the fragmentation pathway of the dication M^{2+} (for the corresponding MS^2 spectrum for compound **2**, see Figure 2B). The important fragmentation pathways discussed in this text are displayed in Scheme 2.

Under the CID conditions, the molecular dication M^{2+} (m/z 273) decomposed solely into the two fragments described above, i.e.,



SCHEME 2 Proposed fragmentation pathways for compound 2. Distribution of D-labeling is denoted with small circles, squares, and triangles to indicate initial α , β , and γ positions, respectively. Free energy changes obtained from DFT calculations at the B3LYP/6-31G* level of theory are given above each reaction arrow

$[C_{11}H_{17}]^+$ (m/z 149) and the singly charged residue of the molecule (m/z 397). Because we observed no transfer of labeling (Figures S25, S28, and S33, supporting information), we inferred that the AdCH₂-N bond was simply cleaved by shifting its electron pair onto the nitrogen atom to saturate the positive charge. Similar electrostatic repulsion-driven cleavage has been previously reported.²⁶ One remark regarding the identity of $[C_{11}H_{17}]^+$ cation should be given. Although the initial form of this fragment is probably a 1-adamantylmethyl cation, it is reasonable to expect the rapid rearrangement of this unstable primary cation to a more stable, likely tertiary, cationic species. The computed free energies of four reasonable structures that match the formula $[C_{11}H_{17}]^+$ are shown in Figure 3. It can be seen that the most stable cation is 3-methyladamantane-1-yl. However, to the best of our knowledge, there is no precedence in the literature that describes the transformation of 1-adamantylmethyl to 3-methyladamantane-1-yl. In contrast, it is well known that the homoadamantane-1-yl cation is

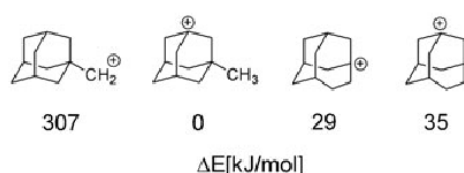
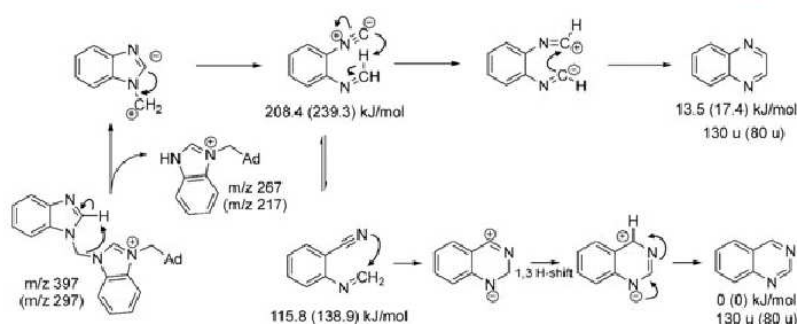


FIGURE 3 Plausible structures of the $[C_{11}H_{17}]^+$ cation, with relative free energies from DFT calculations at the B3LYP/6-31G* level of theory

readily formed from 1-adamantylmethyl upon solvolysis.²⁸ Therefore, we assumed that the $[C_{11}H_{17}]^+$ fragment was homoadamantane-1-yl in this study.

Upon further CID analysis, the m/z 397 ion displayed five independent fragmentation pathways (Figures 2C, S19, and S20, supporting information). The most abundant fragment, m/z 131, retained one D-atom from the β position and two D-atoms from the γ position, whereas no transfer from the α position was observed. Accordingly, we attributed this signal to the benzimidazol-1-ylmethyl cation, the formation of which was accompanied by the neutral loss of 1-(1-adamantyl)benzimidazole. It should be noted that analogous fragmentation was not observed in the case of compound 1.

The second highly abundant peak in the MS² spectrum of the m/z 397 ion was observed at m/z 267 (Figure 2C) and was assigned to the 1-(1-adamantylmethyl)benzimidazolium cation. The proton required to maintain the single positive charge within this structure was likely abstracted from the β position of the adjacent imidazole ring to produce a neutral fragment, C₈H₆N₂ (130 u). When 2 β was examined, this cation was observed at m/z 269, and two D-atoms were present (see Figure S28, supporting information). As displayed in Scheme 3, the initially formed dipolar structure could be stabilized via ring opening to produce 2-methylideneaminobenzoisocyanide. This structure can either reconstitute a heteroaromatic ring (i.e., to form quinoxaline) or undergo a well-known rearrangement towards a much more stable corresponding benzonitrile,²⁹ which can further form quinazoline. Considering the calculated free energies (see Scheme 3), we inferred that both 1 and 2 produce a 1,3-diazine species in this step. This



SCHEME 3 Structure rationalization of the neutral loss within the m/z 397 \rightarrow 267 fragmentation pathway of compound 2. Relative DFT computed energies are given. Values for the imidazole analogue are given in brackets

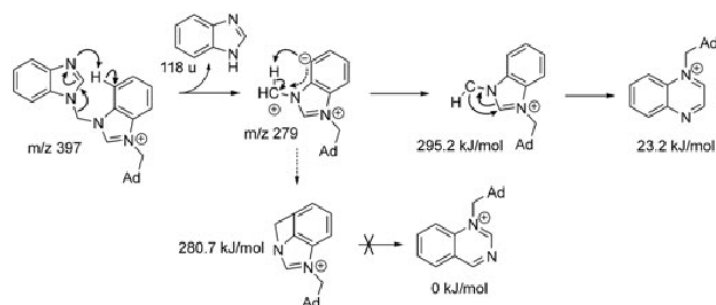
fragmentation pathway ends with the decomposition of the m/z 267 ion to yield $[C_{11}H_{17}]^+$ and neutral benzimidazole (Figure S20, supporting information).

The most interesting result was the fragment observed at m/z 279 (Figure 2C). This singly charged fragment could be formed from m/z 397 via the neutral loss of benzimidazole (Figure S20, supporting information). Thus, one proton must be transferred from 1-adamantylmethylbenzimidazole to the adjacent benzimidazole moiety. As the fragmentation of labeled 2 unambiguously shows, this proton was not taken from any labeled positions (see Figures S25, S28, and S32, supporting information). In addition, the m/z 279 ion further decomposed to yield $[C_{11}H_{17}]^+$ (with corresponding labeling), indicating that the adamantylmethyl moiety remained intact. Thus, the proton was clearly abstracted from the heterocyclic ring. The use of the β -labeled compound proved that the proton was not released from the β position and, thus, had to be released from the benzene ring. It is not completely clear whether the heterocyclic moiety $C_8H_6N_2$, which is formed here, is of the same chemical nature as that formed via m/z 397 \rightarrow 267 (Figure S20, supporting information). However, the mechanism is likely different and, in this case, involves the benzene ring. Scheme 4 displays the possible stabilization of the cationic structure formed within the m/z 397 \rightarrow 279 release of benzimidazole. We supposed that a proton was abstracted from the *ortho*-position; thus, such a species could be stabilized either by the formation of a new four-membered ring or carbene (Scheme 4). Because of the high free energy of tricyclic structures and the lack of a reasonable stabilization pathway, we supposed that the carbene

was an intermediate that subsequently rearranged to the quinoxalium cation. Interestingly, the imidazolium derivative 1 displayed essentially the same behavior according to the mass spectra, although its aromatic system lacked the fused benzene ring. In this case, the proton was likely released from position 4 or 5 of the imidazolium ring. Contrary to compound 2, two stabilization pathways can be suggested in the case of 1, as depicted in Figure S17b (supporting information). Considering the DFT computed energies, we supposed that the final m/z 229 structure is likely a 1-(1-adamantylmethyl)pyrimidinium cation.

The remaining two minor fragmentation pathways are accompanied by the release of the adamantane moiety in two different forms. The fragment observed at m/z 149 may be the product of subsequent cleavage of either the m/z 267 or m/z 279 ion (see above). However, $[C_{11}H_{17}]^+$ was also unambiguously released from the M^{2+} ion; thus, the repetition of this cleavage should be considered.

The last observed fragmentation of the m/z 397 ion, which resulted in the production of the m/z 249 ion (Figure 2) can be rationalized by the release of a neutral $C_{11}H_{16}$ moiety. Therefore, one proton was transferred from $AdCH_2$ to the benzimidazolium moiety. Because subjecting the α -labeled target ion (i.e., m/z 399) to CID led to the formation of a doubly labeled adamantane fragment (see Figure S25, supporting information), we concluded that the H-atoms from the $Ad-CH_2$ methylene group did not participate in this event; instead, the H-atom required for the m/z 249 ion was likely abstracted from the Ad cage. Therefore, we considered this neutral fragment $C_{11}H_{16}$ (148 u) to be the tetracyclic hydrocarbon depicted in Scheme 2. It



SCHEME 4 Structure rationalization of the m/z 279 fragment formed within the m/z 397 \rightarrow 279 fragmentation pathway of compound 2. Relative DFT computed energies are given

should be noted that the hypothetical carbene Ad-C-H formed via the abstraction of a proton from the methylene group is approximately 150 kJ/mol less stable than the tetracyclic derivative. This final mentioned pathway was not observed in the case of compound **1**.

The second examined signal in the first-order mass spectra of compound **2** was a cluster related to the $[M^{2+}\text{-Br}]^+$ aggregate observed at m/z 625/627 (Figure 2A). Upon CID analysis, this ion released neutral HBr to produce a singly charged fragment at m/z 545. The H-atom was unambiguously abstracted from the β -position, as suggested by the loss of m/z 81 from $[^{79}\text{Br}, \beta\beta\text{-D}_2]M^{2+}$ (for the spectrum, see Figure S26, supporting information).

Finally, we subjected the m/z 545 ion (i.e., $[M^{2+}\text{-H}]^+$) to CID and observed two independent fragmentation pathways leading to the fragments at m/z 397 and 427, respectively (Figures S18 and S19, supporting information). The former fragment is likely explained by the neutral loss of $\text{C}_{11}\text{H}_{16}$ as discussed above. The latter pathway (i.e., m/z 545 \rightarrow 427) led to the ion observed at m/z 427, which differed from the target ion by 118 u. We speculated that the neutral loss of benzimidazole occurred. However, the mechanism by which a central part of the target ion is removed, which requires a large reorganization of the molecular skeleton, is unclear. However, it was demonstrated by further CID that the m/z 427 ion can lose two Ad

units sequentially (Figure S19, supporting information). Due to the lack of an unambiguous explanation, these fragmentation pathways are not included in Scheme 4. In addition, it should be noted that all pathways that include NHC were accompanied by the wide redistribution of deuterium labeling to produce isotopological clusters instead of the single mass signals upon further CID analysis. The deuterium labeling was redistributed over the entire molecule backbone, including at least one position of the adamantane cage.

3.3 | Fragmentation of BIMs in complex with CB7

The binding behavior of the non-labeled guests **1** and **2** towards CB7 was investigated using ^1H NMR spectroscopy prior to the MS studies. Both the guests displayed the slow exchange mode on the NMR time-scale and significant upfield shift of the adamantane signals indicated positioning of the adamantane cage inside the CB7 cavity. In addition, the sequential binding of two CB7 to form the final $1/2@CB7_2$ complex was observed within a titration of guest solution with an excess of CB7. No other binding modes were detected via NMR spectrometry and the binding behaviors of the guests **1** and **2** with CB7 was essentially the same.

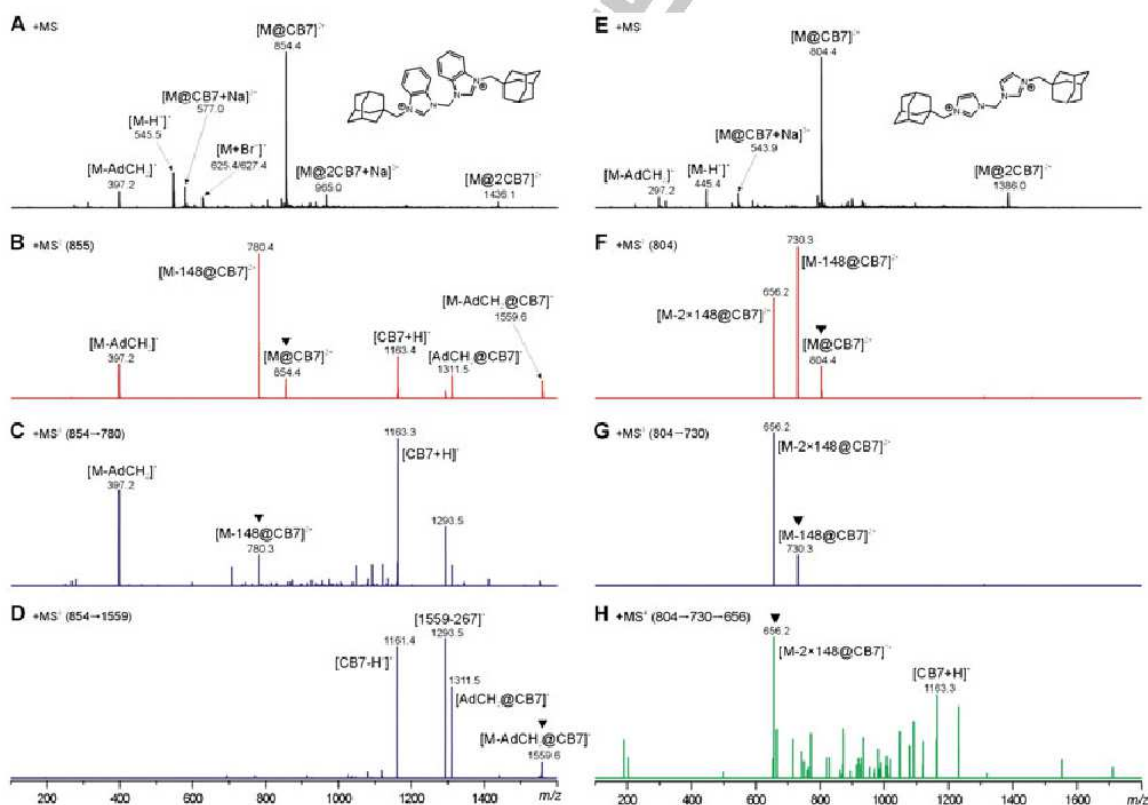


FIGURE 4 The positive-ion ESI mass spectra of an aqueous solution of **2@CB7** (A–D) and **1@CB7** (E–H) in a molar ratio of 1:1. (A, E) First-order mass spectra, (B) MS^2 of m/z 854.5, (C) MS^3 of m/z 780.3, (D) MS^3 of m/z 1559.6, (F) MS^2 of m/z 804.4, (G) MS^3 of m/z 730.3, and (H) MS^3 of m/z 656.2. The assignments for the observed signals are shown in brackets. The fragment ions in the tandem mass spectra are marked with black downward-facing triangles [Color figure can be viewed at wileyonlinelibrary.com]

As has been described previously,⁴ the adamantylated bisimidazolium salts included inside the CB7 cavity displayed two distinct initial fragmentations depending on their molecular structure. The first fragmentation, hereafter referred to as a "149 fragmentation", is related to the release of $[C_{11}H_{12}]^+$ to produce two singly charged fragments. This behavior, which is likely driven by an electrostatic repulsion, can be expected for dications and is characteristic of strongly hindered molecules. The second pathway, hereafter referred to as a "148 fragmentation", begins with the release of a neutral fragment, $C_{11}H_{16}$ (for supposed tetracyclic structure, see Scheme 2; for related discussion, see section 3.2), to yield a doubly charged residue. This 148 fragmentation is typical for axle ligands with a negligible barrier to slippage of the CB7 unit. Interestingly, the guest **1** (not hindered) displayed two subsequent 148 fragmentations beginning with $M^{2+}@CB7$, whereas the guest **2** (moderately hindered) displayed only one 148 fragmentation and some alternate pathways. These differences can be clearly seen in Figure 4. It should be noted that a CB7 complex with highly hindered guest, which was derived from the compound **2** by substitution with a phenyl residue in the β position, did not display any 148 fragmentation, as demonstrated previously.⁴ The fact that 148 fragmentation was not observed in the case of non-complexed M^{2+} justifies our supposition that this pathway is significantly

supported by CB7. We considered two possible arrangements of the $1@CB7$ complex leading to the 148 fragmentation. In the first initial geometry, the CB7 unit can be positioned in the middle of the guest, i.e., with the central charged bisimidazolium part inside the CB7 cavity, to assist in the two stepwise neutral 148 losses. However, theoretical calculations on the stability of CB7 complexes with the two respective residues formed by the first (R1) and the second (R2) 148 fragmentation indicated that this possibility is unlikely. For structures of R1 and R2, see Figure S50 (supporting information). There are two important findings against the positioning of the CB7 unit at the central part of the guest **1**. As can be seen in Figure S50 (supporting information), the residue R2 is too short to allow effective interactions of both the imidazolium units with two opposite CB7 portals. In addition, the positioning of R2 inside the CB7 cavity led to significant deformation of the CB7 macrocycle. Due to these circumstances, the energy of an external complex (for structure, see Figure S50A, supporting information) was about 46 kJ/mol lower than that of the inclusion complex (Figure S50B, supporting information). The second computed residue R1 consists of the central bisimidazolium unit and one terminal adamantane site. Optimization of a complex of R1 with CB7 was started from two initial arrangements with the CB7 unit at adamantane or bisimidazolium site, respectively. Whereas the former arrangement

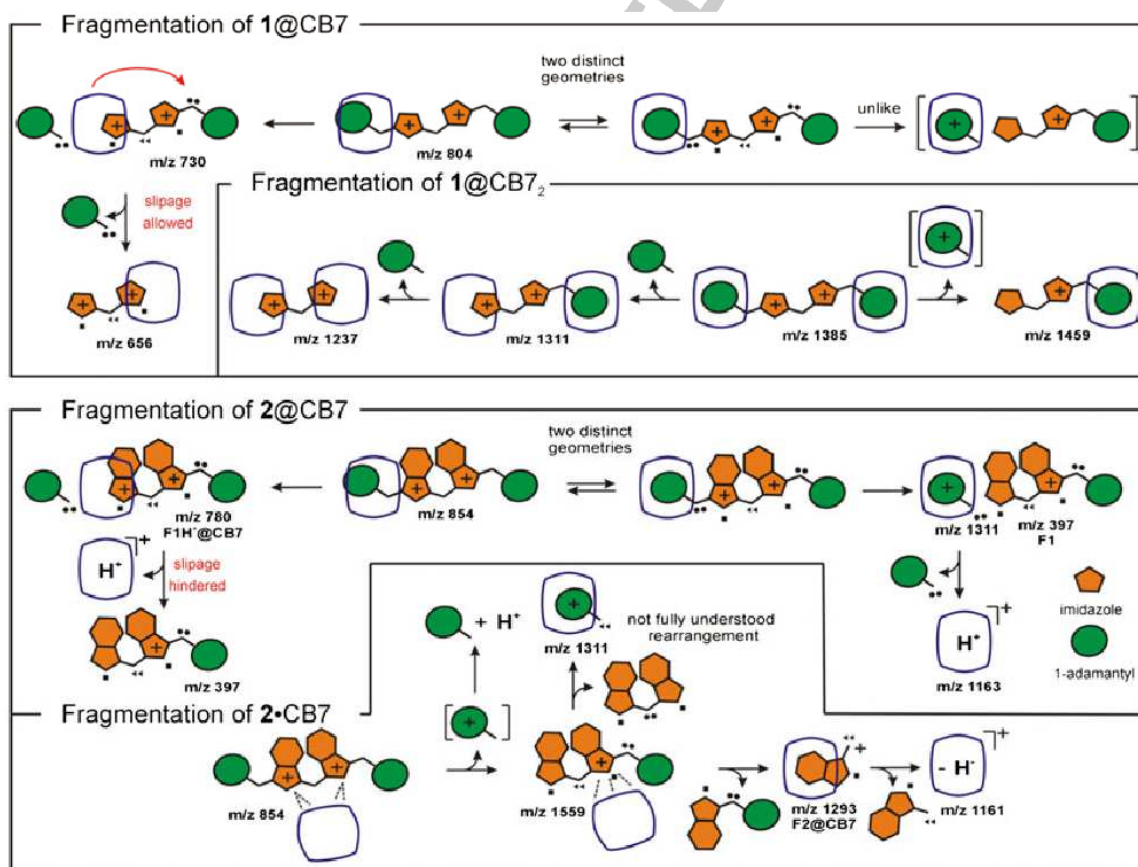


FIGURE 5 Proposed fragmentation pathways for complexes of CB7 with **1** or **2**. Distribution of D-labeling is denoted with small circles, squares, and triangles to indicate the initial α , β , and γ positions, respectively. For structures of F1 and F2, see Scheme 4. [Color figure can be viewed at wileyonlinelibrary.com]

rapidly converged to energy minimum, the latter did not reach any reasonable geometry within 500 iteration steps. Accordingly, we concluded that the positioning of the CB7 unit at the central bisimidazolium part is strongly non-preferred. Therefore, the complexes 1@CB7 and R1@CB7 likely adopted a geometry with the adamantane site occupied by the CB7 unit prior the 148 fragmentation. On the other hand, we assume that two different positions of the adamantane cage inside the CB7 unit resulted in the 148 and 149 fragmentation, respectively. We can speculate that the adamantane cage adopts an 'ideal' position inside the CB7 cavity in the first geometry, whereas the CB7 unit is shifted slightly towards the central part of the axle in the second geometry. In the former case, the 149 fragmentation occurs to release the CB7 unit together with the AdCH_2^+ fragment (likely as an inclusion aggregate). Thus, no further influence of CB7 on the axle residue is possible. In contrast, there are two ways in which the system can develop after the first 148 fragmentation. If the CB7 unit can easily reach the opposite terminal Ad site, the second 148 fragmentation occurs to produce a doubly charged bisimidazolium residue (R2) complexed to CB7. Because the bisimidazolium dication is too short to be efficiently stabilized inside the CB7 cavity by interactions of both cationic rings with the opposite CB7 portals, we considered this aggregate to be an external complex. In addition to the abovementioned computations, this hypothesis is supported by previous observation⁴ of the bisimidazolium residue complexed with two CB7 units when 1^{2+} @CB7₂ was subjected to CID (for the schematic drawing, see Figure 5). In this case, the bisimidazolium residue was likely linked to two CB7 units *via* ion-dipole interactions. Note that in this case the slippage of the CB7 unit to the second guest terminal is blocked by the second CB7 macrocycle. Therefore, we infer that the CB7 unit induces the 148 fragmentation staying at the adamantane site from which the neutral 148 fragment is released.

If CB7 cannot freely move over the molecular axle, the first 148 fragmentation is followed by the release of protonated CB7. It should be noted that any D-labeled target ion exclusively produced protonated CB7. This observation implies the migration of an H-atom from the Ad cage to the N-atom of the bisimidazolium residue within the 148 fragmentation step, followed by the subsequent abstraction of this proton by the CB7 unit with no participation of the H/D-atoms at positions α , μ , or γ .

The final fragmentation pathway of M^{2+} -CB7 that resulted in F1-CB7 was typical for hindered guest 2 (for the F1 structure, see Scheme 2). Considering the further fragmentation of F1-CB7, we inferred that the initial complex was likely arranged in an external manner (the external binding is symbolized by "." used instead of "@"). In the MS³ spectra, we observed signals of three product ions that can be assigned to $[\text{CB7-H}]^+$ (m/z 1161), F2@CB7, and AdCH_2^+ @CB7, respectively (for the F2 structure, see Scheme 2; for the spectrum, see Figure 4). We supposed that F1-CB7 decomposes in two distinct manners, as depicted in Figure 5. Note that the mechanism which leads to the AdCH_2^+ @CB7 involves an exchange of the methylene bridges, as implied by the D-labeling distribution (see Figures S39 and S41, supporting information). Although this mechanism is not completely clear, there is a significant difference from the cleavage of M^{2+} @CB7 into AdCH_2^+ @CB7 and F1, in which no redistribution of D-atoms was observed. This observation and the existence of two distinct

pathways leading to complexes between CB7 and fragments from the opposite ends of the F1 ion support our hypothesis that the nature of the aggregate F1-CB7 is different than that of M^{2+} @CB7, i.e., the aggregate is likely an external complex.

Finally, the second pathway of F1-CB7 fragmentation led to F2@CB7, which can consequently decompose to produce neutral 1-methylbenzimidazole and the $[\text{CB7-H}]^+$ cation. The last mentioned step has been previously supported by molecular modeling.⁴

4 | CONCLUSIONS

Some details of the fragmentation pathways of adamantylated bisimidazolium salts have been clarified using a series of selectively D-labeled isotopologues. Two important fragmentation pathways were studied by treating compounds 1 and 2 under CID conditions. The first fragmentation comprises electrostatic repulsion-driven C-N bond cleavage to produce $[\text{C}_{11}\text{H}_{17}]^+$ (149 u, 149 fragmentation) and a singly charged residue from the molecular dication. In contrast, the neutral $\text{C}_{11}\text{H}_{16}$ (148 u, 148 fragmentation) fragment is released from M^{2+} to produce a doubly positively charged residue within the second distinct fragmentation. Upon comparison of the tandem mass spectra of the non-labeled and selectively labeled compounds and the molecular modeling data, we suggest that the first fragment is likely the homoadamantane-1-yl cation while the second fragment resulting from neutral loss is likely tetracyclo[4.3.1.1^{4,8}.0^{1,3}]undecane.

The most important result obtained from the CID analyses of CB7 complexes with guests 1 and 2 is the suggestion of two distinct arrangements for CB7 at the terminal adamantane site. The existence of these two modes can explain the behavior of moderately hindered guests, such as compound 2. In the case of edge structures, i.e., non-hindered compound 1 and the previously reported, strongly hindered 2-phenylbenzimidazolium analogue,⁴ only the 148 and 149 fragmentations were observed, respectively. It should be noted that two 148 fragmentations and only one 149 fragmentation were always observed for these respective guests. In contrast, the complexes of CB7 with moderately hindered guests (e.g., 2) provide three independent fragmentation pathways. The first and second observed pathways can be related to the expected electrostatic repulsion, which produces $[\text{C}_{11}\text{H}_{17}]^+$ and minor external complex decomposition, respectively. Observation of the third (i.e., 148) pathway implies that there must be some binding mode in which the CB7 unit is significantly shifted towards the central part of the guest, thus resulting in the formation of the neutral $\text{C}_{11}\text{H}_{16}$ fragment instead of the 149 fragmentation. However, in this case, there is no chance to reach the opposite terminal adamantane site (the second 148 fragmentation was not observed). These important results improve our understanding of how the bulky, almost round-shaped adamantane can move inside the tight CB7 cavity.

ACKNOWLEDGEMENTS

This work was financially supported by the Internal Funding Agency of Tomas Bata University in Zlín (Project No. IGA/FT/2017/001) (to RV, MR, LD, and AC), by the Ministry of Education, Youth and Sports of the Czech Republic, Program NPU I (LO1504) (to BH), and by the Czech Science Foundation (Grant No. 16-05691S) (to JV).

REFERENCES

- Pan M, Xue M. Synthesis of a pillar[5]arene with both hydroxyl and methoxycarbonyl-methoxy groups and its host-guest complexation with a bis[imidazolium] salt. *Chin J Chem*. 2014;32:128.
- Nan Z, Lloyd GO, Scherman OA. Monofunctionalised cucurbit[6]uril synthesis using imidazolium host-guest complexation. *Chem Commun*. 2012;48:3070.
- Branná P, Rouchal M, Prucková Z, et al. Rotaxanes capped with host molecules: supramolecular behavior of adamantylated bisimidazolium salts containing a biphenyl centerpiece. *Chem Eur J*. 2015;21:11712.
- Černochová J, Branná P, Rouchal M, Kulhánek P, Kuřitka I, Vícha R. Determination of intrinsic binding modes by mass spectrometry: gas-phase behavior of adamantylated bisimidazolium guests complexed to cucurbiturils. *Chem Eur J*. 2012;18:13633.
- Jiao D, Biedermann F, Scherman OA. Size selective supramolecular cages from aryl-bisimidazolium derivatives and cucurbit[8]uril. *Org Lett*. 2011;13:3044.
- Noujeim N, Jouvelet B, Schmitzer AR. Formation of inclusion complexes between 1, 1'-dialkyl-3, 3'-(1, 4-phenylene) bisimidazolium dibromide salts and cucurbit[7]uril. *J Phys Chem B*. 2009;113:16159.
- Samsam S, Leclercq L, Schmitzer AR. Recognition of 1,4-xylylene binding sites in polyimidazolium cations by cucurbit[7]uril: toward pseudorotaxane assembly. *J Phys Chem B*. 2009;113:9493.
- Rekharsky MV, Mori T, Yang C, et al. A synthetic host-guest system achieves avidin-biotin affinity by overcoming enthalpy-entropy compensation. *Proc Natl Acad Sci USA*. 2007;104:20737.
- Moghaddam S, Yang C, Rekharsky MV, et al. New ultrahigh affinity host-guest complexes of cucurbit[7]uril with bicyclo[2.2.2]octane and adamantane guests: thermodynamic analysis and evaluation of M2 affinity calculations. *J Am Chem Soc*. 2011;133:3570.
- Cao L, Šekutor M, Zavallj PY, Mlinarić-Majerski K, Glaser R, Isaacs L. Cucurbit[7]uril guest pair with an attomolar dissociation constant. *Angew Chem Int Ed*. 2014;53:988.
- Šekutor M, Molčanov K, Cao L, Isaacs L, Glaser R, Mlinarić-Majerski K. Design, synthesis, and X-ray structural analyses of diamantane diammonium salts: guests for cucurbit[n]uril (CB[n]) hosts. *Eur J Org Chem*. 2014;2533.
- Wang R, Yuan L, Macartney DH. Inhibition of C(2)-H/D exchange of a bis[imidazolium] dication upon complexation with cucurbit[7]uril. *Chem Commun*. 2006;2908.
- Leclercq L, Schmitzer AR. Supramolecular encapsulation of 1,3-bis(1-adamantyl)imidazolium chloride by β -cyclodextrins: towards inhibition of C(2)-H/D exchange. *J Phys Org Chem*. 2009;22:91.
- Peris E. Polyaromatic N-heterocyclic carbene ligands and π -stacking: catalytic consequences. *Chem Commun*. 2016;52:5777.
- Flanigan DM, Romanov-Michallidis F, White NA, Rovis T. Organocatalytic reactions enabled by N-heterocyclic carbenes. *Chem Rev*. 2015;115:9307.
- Levin E, Ivry E, Diesendruck CE, Lemcoff NG. Water in N-heterocyclic carbene-assisted catalysis. *Chem Rev*. 2015;115:4607.
- Ramasamy B, Ghosh P. The developing concept of bifunctional catalysis with transition metal N-heterocyclic carbene complexes. *Eur J Inorg Chem*. 2016;1448.
- Ezugwu CI, Kabira NA, Yusubov M, Verpoort F. Metal-organic frameworks containing N-heterocyclic carbenes and their precursors. *Coord Chem Rev*. 2016;307:183.
- Arduengo AJ III, Harlow RL, Kline M. A stable crystalline carbene. *J Am Chem Soc*. 1991;113:361.
- Lalli PM, Rodrigues TS, Arouca AM, Eberlin MN, Neto BAD. N-Heterocyclic carbenes with negative-charge tags: direct sampling from ionic liquid solutions. *RSC Adv*. 2012;2:3201.
- Corlío YE, Nachtigall FM, Abdelnur PV, Ebeling G, Dupont J, Eberlin MN. Charge-tagged N-heterocyclic carbenes. *RSC Adv*. 2011;1:73.
- Assaf KI, Nau WM. Cucurbiturils: from synthesis to high-affinity binding and catalysis. *Chem Soc Rev*. 2015;44:394-418.
- Yang F, Dearden DV. Gas phase cucurbit[n]uril chemistry. *Isr J Chem*. 2011;51:551-558.
- Heo SW, Choi TS, Park KM, et al. Host-guest chemistry in the gas phase: selected fragmentations of CB[6]-peptide complexes at lysine residues and its utility to probe the structures of small proteins. *Anal Chem*. 2011;83:7916.
- Zhang H, Paulsen ES, Walker KA, Krakowiak KE, Dearden DV. Cucurbit[6]uril pseudorotaxanes: distinctive gas-phase dissociation and reactivity. *J Am Chem Soc*. 2003;125:9284.
- Jiang W, Schalley CA. Tandem mass spectrometry for the analysis of self-sorted pseudorotaxanes: the effects of Coulomb interactions. *J Mass Spectrom*. 2010;45:788.
- Shao Y, Molnar LF, Jung Y, et al. Advances in methods and algorithms in a modern quantum chemistry program package. *Phys Chem Chem Phys*. 2006;8:3172.
- Nordlander JE, Jindal SP, von Schleyer PR, Fort RC Jr, Harper JJ, Nicholas RD. Solvolysis of 1-adamantylcarbonyl and 3-homoadamantyl derivatives. Mechanism of the neopentyl cation rearrangement. *J Am Chem Soc*. 1966;88:4475.
- Rüchardt C, Meier M, Haaf K, Pakusch J, Wolber EKA, Müller B. The isocyanide-cyanide rearrangement; mechanism and preparative applications. *Angew Chem Int Ed*. 1991;30:893.

SUPPORTING INFORMATION

Additional Supporting Information may be found online in the supporting information tab for this article.

How to cite this article: Čablová A, Rouchal M, Hanulíková B, et al. Gas-phase fragmentation of 1-adamantylbisimidazolium salts and their complexes with cucurbit[7]uril studied using selectively ^2H -labeled guest molecules. *Rapid Commun Mass Spectrom*. 2017;1-9. <https://doi.org/10.1002/rcm.7919>

4.5

Cooperative Binding of Cucurbit[*n*]urils and β -Cyclodextrin to Heteroditopic
Imidazolium-Based Guests

Petra Branná, Jarmila Černochová, Michal Rouchal, Petr Kulhánek, Martin Babinský, Radek
Marek, Marek Nečas, Ivo Kuřitka, Robert Vícha*

The Journal of Organic Chemistry **2016**, *81*, 9595–9604

Cooperative Binding of Cucurbit[*n*]urils and β -Cyclodextrin to Heteroditopic Imidazolium-Based Guests

Petra Branná,[†] Jarmila Černochová,^{†,‡} Michal Rouchal,[†] Petr Kulhánek,[§] Martin Babinský,[§] Radek Marek,^{§,||} Marek Nečas,^{§,||} Ivo Kuřitka,[‡] and Robert Vícha^{*,†}

[†]Department of Chemistry, Faculty of Technology, Tomas Bata University in Zlín, Vavrečkova 275, 760 01 Zlín, Czech Republic

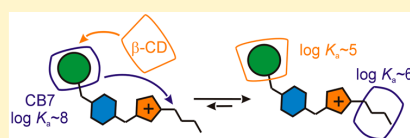
[‡]Polymer Centre, Tomas Bata University in Zlín, Vavrečkova 275, 760 01 Zlín, Czech Republic

[§]CEITEC-Central European Institute of Technology, Faculty of Science, Masaryk University, Kamenice 5, 625 00 Brno, Czech Republic

^{||}Department of Chemistry, Faculty of Science, Masaryk University, Kamenice 5, 625 00 Brno, Czech Republic

Supporting Information

ABSTRACT: Imidazolium-based guests containing two distinct binding epitopes are capable of binding β -cyclodextrin and cucurbit[6/7]uril (CB) simultaneously to form heteroternary 1:1:1 inclusion complexes. In the final configuration, the hosts occupy binding sites disfavored in the binary complexes because of the chemically induced reorganization of the intermediate 1:1 aggregate. In addition, the reported guests are capable of binding two CBs to form either 1:2 or 1:1:1 ternary assemblies despite consisting of a single cationic moiety. Whereas the adamantane site binds CB solely via hydrophobic interactions, the CB unit at the butyl site is stabilized by a combination of hydrophobic and ion–dipole interactions.



INTRODUCTION

Recently, biomimetic systems have been extensively examined because they can serve either as model systems for more complex interactions in biological chemistry or as components for constructing molecular devices. In this regard, molecules with multiple-binding epitopes play a very important role. Considering that host–guest systems are the most frequently employed approach, both hosts and guests can be designed to contain multiple-binding motifs. However, augmenting the host binding capacity is limited to either an enlargement of the single-site host interior to bind more than one guest¹ or linking two² or more³ cavity motifs via appropriate covalent bridges. Although the latter approach led to impressive demonstrations of macroscopic recognition based on host–guest interactions,⁴ all of the host sites in such a system are essentially independent. In addition, the only host with cooperating cavities has been reported by Isaacs and co-workers.⁵ This intriguing member of the cucurbituril family, *ns*-CB10, contains two distinct interior binding sites within one large cavity and exhibits homotropic allostery because of its ability to accommodate its cavity shape for the first bound guest. In contrast to the hosts, the guest molecules can be designed to contain an essentially unlimited number of binding sites,⁶ and subsequent binding of host molecules at adjacent positions can be influenced by host–host attractive⁷ or repulsive⁸ interactions or guest preorganization.⁹

Among other hosts, cucurbit[*n*]urils¹⁰ (CB*n*s) and cyclodextrins¹¹ (CDs) have attracted considerable attention within the scientific community. Because the macrocycles of the most prominent members of the cyclodextrin family (i.e., α -, β -, and

γ -CD) consist of six, seven, and eight D-glucopyranose units, respectively, linked via $\alpha(1\rightarrow4)$ glycosidic bonds, they are fully biocompatible and have consequently been used in several applications over the past decades in the pharmaceutical and food industries, cosmetics, and wrapping materials.¹² Because of the presence of nonpolar interior cavities and hydrophilic hydroxylated rims, CDs bind neutral guests to form water-soluble inclusion complexes with up to micromolar dissociation constants.¹³ Cucurbit[*n*]urils are macrocyclic oligomers of glycoluril units doubly linked by methylene bridges. They were rediscovered for modern chemistry by Mock¹⁴ and Kim,¹⁵ who repeated the original procedure developed by Behrend¹⁶ to isolate CB6 and prepare higher homologues with $n > 6$. These rigid molecules with a barrel-like hydrophobic cavity and two symmetry-equivalent rims lined with carbonyl groups are ideally structured to form inclusion complexes with nonpolar cationic guests that are held together by hydrophobic and ion–dipole interactions. In particular, dicationic guests derived from ferrocene¹⁷ or the cage hydrocarbons adamantane,¹⁸ diamantane,¹⁹ and bicyclo[2.2.2]octane¹⁸ have been reported to form ultrastable aggregates with CB7, having association constants of up to 10^{17} M^{-1} , which exceed the binding strength of the well-known avidin–biotin pair. This outstanding selectivity gave rise to the design of novel thermodynamically or kinetically driven self-sorting systems in which guests with multiple-binding epitopes play a crucial role. The pH-responsive self-sorting aggregation processes of complex mixtures consisting of CB

Received: June 29, 2016

Published: September 23, 2016

and β -CD hosts and ditopic adamantyl(alkyl)ammonium guests have been described by Issacs and co-workers.²⁰ The same group has reported an interesting dynamic behavior of a system comprised of CB6, CB7, and *trans*-cyclohexane-1,4-diammonium and adamantanealkyl ammonium guests. The former guest and CB6 formed an extraordinarily stable assembly with a half-life of 26 years, whereas the adamantane-based guests displayed very high affinity for CB7.²¹ Subsequently, Kaifer and co-workers have described an adamantane-ferrocene ditopic guest that formed two distinct inclusion complexes with CB7 that evolved toward a thermodynamically preferred adamantane-bound adduct within 10 h.²² In addition to the most frequently used alkylammonium and pyridinium cations, dialkylimidazolium salts have deservedly attracted the attention of supramolecular chemists because of their catalytic capacity²³ and biological activity²⁴ and as a source of N-heterocyclic carbene ligands.²⁵

Employing multitopic guests, we describe various chemo-responsive reorganizations as hosts that competed for different binding sites. However, in the final complexes, the individual preferences of the hosts determined which binding sites were occupied. We were intrigued to examine whether small synthetic guests consisting of two different binding epitopes can overcome the individual preference of the first host by offering a second site when the initial binary complex is transformed into a heteroternary complex during the addition of the second host. Therefore, we prepared a series of new guests consisting of one adamantane-based binding site and one butyl binding site and investigated their binding behaviors in binary and ternary systems by means of NMR spectroscopy, titration calorimetry, mass spectrometry, and molecular modeling.

RESULTS AND DISCUSSION

Synthesis of Guests 1–7. The adamantylated imidazolium/benzimidazolium salts 1–7 (Figure 1) were prepared via

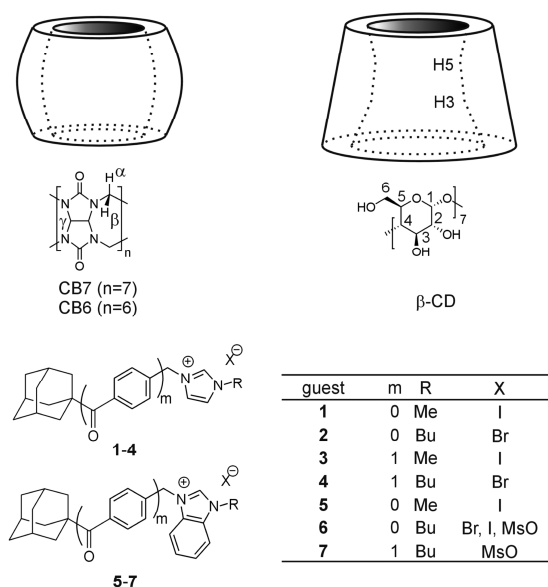


Figure 1. Structures of the guests and hosts used in this work.

the two-step procedure shown in Scheme S1. Initially, the corresponding adamantyl-bearing bromides reacted with imidazole or benzimidazole under base conditions for N1 alkylation with typical yields of 45–95%. The final quaternization was performed in neat alkyl halide or butyl mesylate. Whereas oily products had to be purified by column chromatography, solid salts were easily precipitated from the reaction mixture with diethyl ether or THF, washed with plenty of solvent, and used without further purification. The solid-state structures of 2^+I^- and 2^+MsO^- were determined via X-ray diffraction analysis (see the Supporting Information for further details). Because the prepared (benz)imidazolium salts were rather hygroscopic, the samples for characterization and binding studies were dried in vacuum at 50–60 °C to constant weight and stored under an inert atmosphere.

Binary Systems with β -CD. Initially, we investigated the binding behavior of guests 1–7 with CB6, CB7, and β -CD using 1H NMR spectroscopy. It is well established that the guest protons inside the CB cavity are shielded (upfield shift), whereas the protons located outside the cavity, close to its portal, are deshielded (downfield shift).^{1b,10a} In contrast, the interior of the β -CD cavity has, in general, only a weak deshielding effect on the atoms of the encapsulated guest, as has been demonstrated for various adamantane guests.^{2a,b,d,26} Accordingly, NMR spectroscopy is very useful tool for determining the predominant binding site of the host–guest interaction. All of the examined guest/ β -CD systems followed the fast-exchange regime on the NMR time scale (at defined conditions), and thus, only a single set of signals was observed for each titration. The maximal complexation-induced downfield shift of approximately 0.22 ppm for adamantane bridgehead H atoms, which was observed for all of the examined guests (1–7), unambiguously implies that β -CD binds the adamantane moiety to form an inclusion complex. The 1:1 stoichiometry of these complexes was estimated by 1H NMR titrations, as shown for guests 1, 2, and 4 in Figure S36. Additional evidence indicating the inclusion of the adamantane moiety in the CD cavity was obtained using two-dimensional (2D) ROESY experiments. We clearly observed interactions between the H atoms of the adamantane scaffold and the inner cyclodextrin H atoms at positions 3 and 5. An example of such interactions observed in the ROESY spectrum of a 1:1 mixture of guest 2 with β -CD is given in Figure S36. The formation of 1:1 complexes was further evidenced by isothermal titration calorimetry (ITC). In addition, the values of the obtained binding constants on the order of 10^4 – 10^5 M⁻¹ (see Table 1, entries 1–8) are typical for cyclodextrin inclusion aggregates with adamantane-based guests in aqueous solutions.¹³ Note that the binding strength is essentially unaffected by the replacement of imidazolium with the much more sterically hindered benzimidazolium. This β -CD binding versatility with averaged K_{imid}/K_{bimid} values of 1.05 strongly contrasts with the results obtained for CB7, which is 1000 times more selective (see below). Considering the similar cavity dimensions of CB7 and β -CD, we attribute the binding properties of β -CD to its greater flexibility, which permits ample space for both cationic structural motifs. In addition, β -CD displayed appreciably higher affinities for guests 4 and 7, in which the methylene bridge between the adamantane cage and the heterocyclic cation was replaced with the longer carbonylbenzyl moiety.

Binary Systems with CB6 and CB7. Contrary to β -CD, CB6 and CB7 bind guests 1–7 in the slow-exchange regime, and two sets of 1H NMR signals corresponding to free and

Table 1. Stoichiometry Parameters (n), Association Constants (K_a), and Standard Gibbs Energies (ΔG°) Determined for Binary Systems by ITC Experiments at 303 K

entry	guest	host	n	K_a (M^{-1})	$-\Delta G^\circ$ (kJ mol $^{-1}$)
1	2 ⁺ Br ⁻	β -CD ^a	1.02 ± 0.03	$(4.49 \pm 0.07) \times 10^4$	26.99 ± 0.42
2	2 ⁺ Br ⁻	β -CD ^b	1.03 ± 0.02	$(4.03 \pm 0.05) \times 10^4$	26.71 ± 0.33
3	4 ⁺ Br ⁻	β -CD ^a	0.98 ± 0.03	$(4.60 \pm 0.05) \times 10^5$	32.85 ± 0.36
4	4 ⁺ Br ⁻	β -CD ^b	1.00 ± 0.01	$(4.14 \pm 0.09) \times 10^5$	32.58 ± 0.71
5	1 ⁺ T ⁻	β -CD ^a	1.00 ± 0.03	$(6.07 \pm 0.06) \times 10^4$	27.75 ± 0.27
6	6 ⁺ Br ⁻	β -CD ^a	0.99 ± 0.03	$(3.80 \pm 0.07) \times 10^4$	26.57 ± 0.49
7	7 ⁺ MsO ⁻	β -CD ^a	0.95 ± 0.03	$(5.38 \pm 0.09) \times 10^5$	33.24 ± 0.56
8	5 ⁺ T ⁻	β -CD ^a	1.00 ± 0.02	$(5.43 \pm 0.10) \times 10^4$	27.46 ± 0.51
9	2 ⁺ Br ⁻	CB7 ^{a,c}	1.01 ± 0.03	$(4.08 \pm 0.12) \times 10^{11}$	67.35 ± 1.98
10	2 ⁺ Br ⁻	CB7 ^{b,c}	1.02 ± 0.04	$(3.14 \pm 0.20) \times 10^{10}$	60.89 ± 3.84
11	4 ⁺ Br ⁻	CB7 ^a	0.73 ± 0.02, 1.34 ± 0.04	$(2.27 \pm 0.06) \times 10^6$, $(8.97 \pm 0.11) \times 10^5$	48.47 ± 1.28, 34.53 ± 0.42
12	4 ⁺ Br ⁻	CB7 ^b	0.64 ± 0.01, 0.70 ± 0.01	$(9.03 \pm 0.12) \times 10^7$, $(3.93 \pm 0.07) \times 10^6$	46.15 ± 0.61, 32.45 ± 0.58
13	1 ⁺ T ⁻	CB7 ^{a,c}	1.00 ± 0.01	$(3.68 \pm 0.21) \times 10^{12}$	72.89 ± 4.12
14	3 ⁺ T ⁻	CB7 ^{a,d}	1.04 ± 0.03	$(2.69 \pm 0.11) \times 10^8$	48.90 ± 2.07
15	6 ⁺ Br ⁻	CB7 ^{a,e}	1.02 ± 0.03	$(7.15 \pm 0.39) \times 10^8$	51.36 ± 2.77
16	7 ⁺ MsO ⁻	CB7 ^a	0.69 ± 0.03, 1.31 ± 0.02	$(1.59 \pm 0.03) \times 10^8$, $(2.28 \pm 0.03) \times 10^5$	47.57 ± 0.90, 31.08 ± 0.41
17	5 ⁺ T ⁻	CB7 ^{a,e}	0.99 ± 0.03	$(2.97 \pm 0.15) \times 10^9$	54.95 ± 2.83
18	2 ⁺ Br ⁻	CB6 ^b	1.05 ± 0.01	$(2.99 \pm 0.05) \times 10^6$	31.76 ± 0.53
19	4 ⁺ Br ⁻	CB6 ^b	0.95 ± 0.04	$(1.43 \pm 0.03) \times 10^6$	35.70 ± 0.75
20	6 ⁺ Br ⁻	CB6 ^b	0.97 ± 0.03	$(4.18 \pm 0.07) \times 10^4$	26.81 ± 0.45
21	7 ⁺ MsO ⁻	CB6 ^b	0.98 ± 0.03	$(2.43 \pm 0.05) \times 10^5$	31.24 ± 0.64

^aPerformed in water. ^bPerformed in a 2.5 mM NaCl aqueous solution. ^c1,6-Hexanediamine-2HCl competitor. ^dDopamine-HCl competitor. ^eL-Phenylalanine competitor. Titrations performed in triplicate.

complexed guests were observed. Because of the different cavity diameters,¹⁵ CB7 can form a complex with both of the adamantyl and butyl moieties, whereas the binding of CB6 is limited to the linear butyl chain. These assumptions are consistent with our observations. The addition of CB7 to a solution of guest 1 or 5, which possesses only an adamantane binding site, led to a significant shielding of the adamantane protons. This result indicates the formation of 1/5@CB7^{Ad} aggregates, as shown for 1 in Figure S38. (For the sake of clarity, the specific host position will be hereafter indicated by a superscripted “Ad” or “Bu” for the adamantyl or butyl binding site, respectively.) In contrast, we did not observe any complexation-induced NMR shift (CIS) during the titrations of guests 1 and 5 with CB6 in a 50 mM NaCl aqueous solution. The structures of guests 2 and 6 consist of two different butyl and adamantyl binding sites accessible to CB7. However, we observed shielding of only the adamantane protons (see Table S2). This suggests that CB7 predominantly binds adamantane inside its cavity with the butyl chain protruding outward toward the external environment. Because CB6 has a cavity that is narrower than that of CB7 and cannot confine the bulky adamantane, the inverse geometries for the 2/6-CB6 assemblies with the butyl residue included inside the CB6 cavity were indicated by the strong shielding of the butyl protons (see Figure S39).

Subsequently, we examined the complexation of guests 1, 2, 5, and 6 with CB6 and CB7 in terms of titration calorimetry to support a 1:1 stoichiometry. The ITC results are summarized in Table 1 (entries 9–21). We observed a surprisingly large number of variations in the binding strengths of imidazolium and benzimidazolium salts with CB7. In contrast, complexes formed between these guests and β -CD (see above) or CB6 display similar stabilities. For instance, the association constant for 2@CB7^{Ad} is 570 times higher than that for 6@CB7^{Ad}, whereas 2@CB6^{Bu} has a K_a value that is only 7 times higher

than that of 6@CB6^{Bu}. (For further details, compare entries 9 and 15 and entries 18 and 20, respectively, in Table 1.) A similar disfavoring of the benzimidazolium cation was observed for 1@CB7^{Ad} and 5@CB7^{Ad} (Table 1, entries 13 and 17, respectively). Considering these observations, we attribute the differences in binding strengths to the inability of the rigid CB7 portal to accommodate the benzimidazolium cation efficiently because the bulky adamantane cage hinders guest shifting along the virtual c_7 -symmetry axis of CB7. Note that distinct binding modes were reported for the imidazolium salts substituted with linear alkyl chains with different lengths, with the aromatic cationic moiety more or less buried in the CB6 cavity.²⁷ In contrast to this flexible binding model, it is reasonable to expect that the movement of the guest along the c_7 axis is significantly restricted with increased bulkiness.

Noteworthy results were obtained with the longer imidazolium salts 4 and 7. In an equimolar mixture of the respective guest and CB7, strong shielding of the adamantyl protons corresponding to the complexation of the adamantane cage inside the CB7 cavity was accompanied by weak but clear shielding of the butyl protons, as depicted in Figure S40. The observed CISs are summarized in Table S2. There can be two reasonable explanations for this observation. As discussed below in more detail, one molecule of guest 4 or 7 can simultaneously bind two molecules of CB7 at the adamantane and butyl binding sites. Thus, in an equimolar mixture, two distinct 1:1 complexes (i.e., 4@CB7^{Ad/Bu} or 7@CB7^{Ad/Bu}) are present in a fast equilibrium, which results in a time-averaged ¹H NMR spectrum. The second explanation is that the guest binds CB7 selectively at the adamantane site and the free portion of the long molecule is folded outside the cavity to an external shielding region. We strongly favor the latter hypothesis considering that 4@CB7^{Ad} is approximately 14 kJ mol⁻¹ lower in energy than 4@CB7^{Bu} and strongly predominates in an equilibrium mixture at 30 °C (Table 1,

entry 11). In addition, very similar CISs were observed for the guest 4/CB6 mixture. In this instance, the strong shielding of all of the butyl protons indicates that the butyl chain is inside the CB6 cavity. The small shielding of the adamantane protons can be attributed to the folding of the Ad cage back to the macrocycle exterior because the adamantane moiety is too bulky to fit inside CB6.

To further clarify this situation, we calculated the spatial distribution of isotropic magnetic shielding using a nucleus-independent chemical shielding (NICS) approach²⁸ around CBn using the methodology described in the Supporting Information. The slices through the volumetric NICS data computed for CB6 and CB7 (see Figure S86) clearly show that, apart from the expected strong shielding inside the cavity, there is also a weakly shielded region located outside the macrocycle between the carbonyl portal and the equatorial plane. Thus, any part of guest 4 located in this region will experience a weak (0.1–0.2 ppm) shielding at its atomic nuclei, which supports the hypothesis regarding back folding of guest 4 onto the exterior of CB. This bent back folding of guest 4 in complex with CB7 was further supported by molecular dynamics (MD) simulations. Figure 2 shows the superposition of snapshots

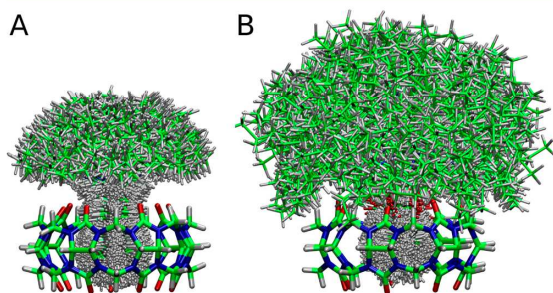


Figure 2. Overlap of guest (A) 2 and (B) 4 conformers complexed with CB7 every 1 ns from the last 900 ns of molecular dynamics simulations. Only one structure of CB7 is shown for the sake of clarity. The adamantane moiety of 2 and 4 is located inside the CB7 cavity.

from MD simulations for complexes of guests 2 and 4 with CB7. Clearly, the longer and more flexible chain of 4 can reach the external shielding region. Representative conformers of 4 and 2 superimposed with a SIMS slice for CB7 are shown in Figure S94. Additionally, the slight increase in the respective affinities of CB6 for 4 and 7 compared to those for 2 and 6 (Table 1, entries 18 and 19 and entries 20 and 21, respectively) may be attributed to the nonspecific interaction of the folded guest molecule with the CB6 exterior. However, a significant shielding of the butyl protons in the mixture of 4 and CB7 was observed as the fraction of CB7 exceeded the 1:1 ratio. The assumption that this shielding can be attributed to the formation of a 1:2 aggregate of $4@(\text{CB7}^{\text{Ad}}, \text{CB7}^{\text{Bu}})$ was supported by ITC measurements in which two slopes could be clearly distinguished, indicating the presence of two distinct binding sites with respective association constants on the order of 10^8 and 10^5 M^{-1} (see Table 1, entry 11, and Figure 3). Combining the NMR and ITC results, we attributed the stronger binding event to the complexation of the adamantane site and the weaker binding event to the encapsulation of the butyl chain because the latter association constant is in good agreement with that published for 1-butyl-3-methylimidazolium with CB7.²⁹ The contribution of other binding modes (e.g.,

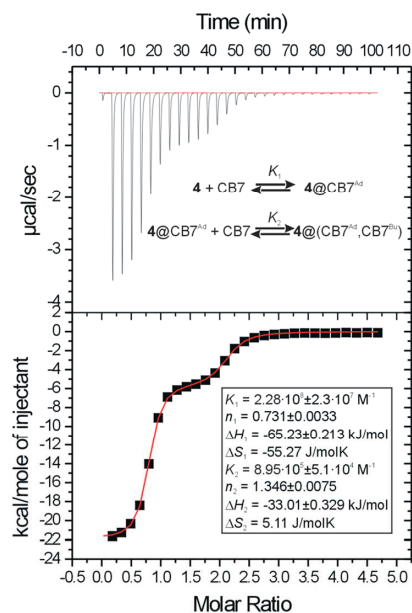


Figure 3. ITC of the complexation of 4^{Br^-} with CB7 in water at 303 K. Curve fitting was performed using the two sets of sites model.

with a phenyl ring positioned inside the CB7 cavity) was excluded by using model guest 3, which clearly displayed the formation of a 1:1 complex of $3@(\text{CB7}^{\text{Ad}})$ (Table 1, entry 14). In clear contrast to the 1/5 and 2/6 pairs of guests with CB7, the binding strength at the adamantane site in the 4/7 pair is not influenced by the chemical nature of the cation (see Table 1, entries 11 and 16). In addition, the corresponding association constants match those reported by Isaacs and co-workers for noncharged adamantane-based guests.³⁰ Thus, we may conclude that the ion–dipole interaction does not contribute significantly to the binding of CB7 to the adamantane site of 4. This observation is crucial for the ability of guests 4 and 7 to simultaneously bind two cucurbituril macrocycles. To the best of our knowledge, these homoternary $4/7@(\text{CB7}^{\text{Ad}}, \text{CB7}^{\text{Bu}})$ and heteroternary $4/7@(\text{CB7}^{\text{Ad}}, \text{CB6}^{\text{Bu}})$ aggregates are the first well-documented complexes with two CB units compactly arranged around a single cationic moiety.

All of the discussed binary aggregates were detected using ESI-MS techniques with the exception of $6@(\text{CB6})$. The ESI-MS spectra are given in Figures S71–S85.

Ternary Systems of 2 and 4 with β -CD, CB7, and CB6.

In the next step, we examined the guest's ability to form ternary systems with two different macrocycles using representative guests 2 and 4. To examine the binding ability of 2, a mixture containing 2 and CB6 in a 1:1 molar ratio in 50 mM NaCl in D_2O was initially taken and examined by means of ^1H NMR titration. In this solution, the predominant arrangement is the $2@(\text{CB6}^{\text{Bu}})$ inclusion complex as discussed above, the formation of which is evident in Figure 4 (lines 1–3). In addition, lines 4–6 in Figure 4 show that the stepwise addition of a β -CD stock solution in 50 mM NaCl has a marginal effect on the positions of the butyl signals, whereas the protons of the adamantane cage experience a significant deshielding. These observations are consistent with the formation of the ternary

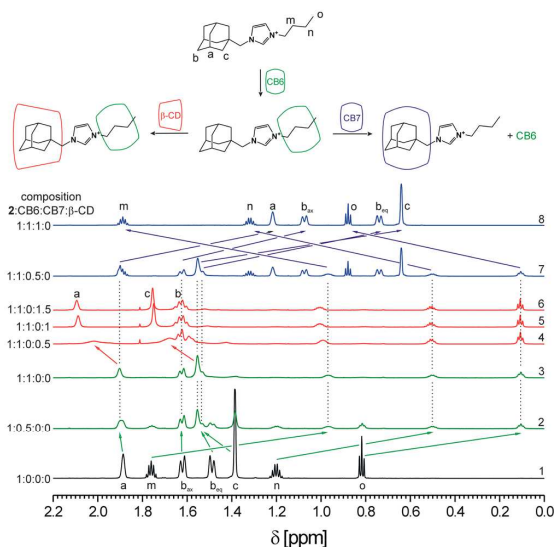


Figure 4. ^1H NMR spectra (700 MHz, 50 mM NaCl in D_2O , 303 K) of mixtures of **2** with CB7, β -CD, and/or CB6. The molar ratios of the mixture components are given above each line. The signal assignment is based on 2D NMR spectra.

assembly $2@(\text{CB6}^{\text{Bu}}, \beta\text{-CD}^{\text{Ad}})$, whose geometry is schematically drawn in Figure 4.

In such a compact arrangement, the steric repulsion between the proximate CD and CB units could decrease the stability of the complex. Nevertheless, as we demonstrated using ITC, the ternary complex can be further stabilized by the formation of transient $\text{O}-\text{H}\cdots\text{O}$ hydrogen bonds between the OH groups of β -CD and the carbonyl oxygen atoms located on the CB portal. This additional stabilization energy, which amounts to -3.12 kJ mol^{-1} , can be calculated as the difference between the Gibbs energy obtained for the formation of $2@(\beta\text{-CD}^{\text{Ad}}, \text{CB6}^{\text{Bu}})$ (see Table 1, entry 1, and Table 2, entry 1). During an independent titration of a $2@(\text{CB6}^{\text{Bu}})$ solution with CB7, we observed a substantial shift of both the adamantane and butyl resonances. Whereas the H atoms of the adamantane cage were significantly shielded, the butyl protons were deshielded (Figure 4, lines 7 and 8). Because there is a lack of any attractive force between the two CB units due to a strong electrostatic repulsion between the two portals and as the binding strength of CB7 at the adamantane site is much higher than that for CB6 at the butyl site ($K_{\text{CB7}}/K_{\text{CB6}} = 1.05 \times 10^5$), we may conclude that CB6^{Bu} was displaced from its initial position by CB7^{Ad} . Subsequently, we titrated an

equimolar mixture of **2** and CB7 ($2@(\text{CB7}^{\text{Ad}})$ predominates in this solution) with β -CD. We observed significant deshielding of the imidazole H2 and H4 protons, AdCH_2 , and $\text{N}(\text{CH}_2)_2\text{Et}$, whereas the imidazole H5 protons and $\text{N}(\text{CH}_2)_2\text{Et}$ were shielded (see Table S2). This observation can be rationalized by the formation of the ternary aggregate $2@(\text{CB7}^{\text{Ad}}, \beta\text{-CD}^{\text{Bu}})$. The association constant for this process ($K_a = 3.1 \times 10^3 \text{ M}^{-1}$) was calculated via NMR titration (see Figure S43). We were not able to determine the association constant using ITC because of poor quality data, even after employing the highest available concentrations. In summary, guest **2** is capable of forming ternary aggregates with one CB and one β -CD unit, whereas a ternary complex consisting of two CB units was not observed.

An examination of ternary systems with guest **4** began with an equimolar solution of **4** and CB7 in which complex $4@(\text{CB7}^{\text{Ad}})$ predominated (shielding effect in Figure 5, lines 1–3).

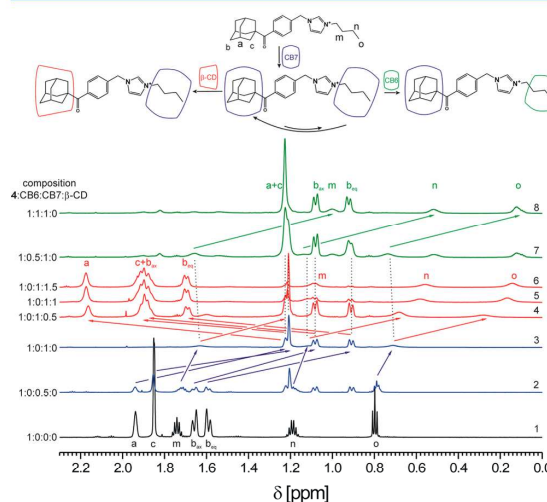


Figure 5. ^1H NMR spectra (700 MHz, 50 mM NaCl in D_2O , 303 K) of mixtures of guest **4** with CB7, β -CD, and/or CB6. The molar ratios of the mixture components are given above each line. The signal assignment is based on 2D NMR spectra.

Subsequent addition of CB6 led to a significant shielding of the butyl protons, whereas the positions of the adamantane NMR resonances remained essentially unaffected (Figure 5, lines 7 and 8). Total strong shielding of both the adamantane and butyl protons indicates the formation of the heteroternary complex $4@(\text{CB7}^{\text{Ad}}, \text{CB6}^{\text{Bu}})$. As was discussed in the previous section, the binding of CB7 at the adamantane site is driven

Table 2. Stoichiometry Parameters (n), Experimental Association Constants (K^{exp}), and Standard Gibbs Energies (ΔG°) Determined for Stepwise Complexation Reactions by ITC Experiments at 303.15 K

entry	guest	host	n	K^{exp} (M^{-1})	$-\Delta G$ (kJ mol^{-1})	$\Delta\Delta G^{\text{ad}}$ (kJ mol^{-1})
1	$2@(\text{CB6})$	$\beta\text{-CD}^{\text{b}}$	0.99 ± 0.02	$(1.39 \pm 0.06) \times 10^5$	29.83 ± 0.64	-3.12 ± 0.72
2	$4@(\text{CB6})$	$\beta\text{-CD}^{\text{b}}$	1.03 ± 0.02	$(7.95 \pm 0.05) \times 10^5$	34.23 ± 0.47	-1.65 ± 0.85
3	$4@(\text{CB7})$	$\beta\text{-CD}^{\text{c}}$	1.04 ± 0.03	$(3.10 \pm 0.03) \times 10^4$	26.05 ± 0.50	-7.17 ± 0.87
4	$4@(\text{CB7})$	CB6^{b}	1.03 ± 0.02	$(4.66 \pm 0.07) \times 10^5$	32.88 ± 0.64	2.82 ± 0.95

^a $\Delta\Delta G^\circ$ values were calculated as the difference between the ΔG° of the complexed guest titration and the ΔG° of the corresponding binary titrations. ^bPerformed in a 2.5 mM NaCl aqueous solution. ^cPerformed in 2.5 mM NaCl in D_2O . The 1:1 **4**:CB7 ratio was verified before titration using ^1H NMR. Titrations were performed in triplicate.

primarily by hydrophobic interactions, leaving the butylimidazolium site free for an ion–dipole interaction with CB6. Considering the gains in energy for the formation of $4@CB6^{Bu}$ and $4@(\text{CB7}^{Ad}, \text{CB6}^{Bu})$ (Table 1, entry 19, and Table 2, entry 4), the free energy of such a ternary complex is approximately 3 kJ mol^{-1} higher than the value expected for a system consisting of two independent sites. This energy difference can probably be attributed to the electrostatic repulsion between the CB7 and CB6 portals. Finally, during the titration of the $4@CB7^{Ad}$ complex with β -CD, we observed a significant deshielding of the adamantane protons coupled with a simultaneous NMR shielding of the butyl chain atoms (Figure 5, lines 4–6). This observation can be rationalized in the following terms. As mentioned above, CB7 can bind both the butyl and adamantyl moieties of 4. However, in the 1:1 mixture in a 50 mM NaCl solution at 30°C , $4@CB7^{Ad}$ greatly predominates (for the corresponding ΔG , see entry 12 of Table 1). β -Cyclodextrin can also encapsulate both the adamantane cage and the butyl chain of 4 in a manner similar to that of CB7. Using titration calorimetry, we have determined the binding constant for 4 and β -CD to be $4.14 \times 10^5 \text{ M}^{-1}$ in a 2.5 mM NaCl aqueous solution (Table 1, entry 4). The combined ITC and NMR data clearly indicate a strong preference for a $4@(\beta\text{-CD}^{Ad})$ complex. Although it is reasonable to suppose weak binding of β -CD at the Bu site of 4, we can exclude such a system from further discussion because the corresponding binding constant is substantially lower than that for the Ad site. Thus, both β -CD and CB7 compete for the adamantane binding site with individual binding constants of 4.14×10^5 and $9.03 \times 10^7 \text{ M}^{-1}$, respectively. Notably, the NMR data indicated the expulsion of CB7 from its preferred position at the adamantane site. It is clear that the displacement of CB7 into the bulk solution is unlikely because such an event is penalized thermodynamically by $\sim 16 \text{ kJ mol}^{-1}$. However, CB7 can encapsulate the less preferred butyl chain with an approximate 35 kJ mol^{-1} gain in free energy. If this additional energy gain is considered, the overall process leading to the formation of the predominant $4@(\beta\text{-CD}^{Ad}, \text{CB7}^{Bu})$ aggregate is thermodynamically favored with a theoretical net free energy gain of $\sim 19 \text{ kJ mol}^{-1}$. Note that the experimental value of the overall energy gain obtained from the direct titration of $4@CB7^{Ad}$ with β -CD (Table 2, entry 3) is larger by approximately 7 kJ mol^{-1} . We can attribute this additional stabilization of the ternary complex to the attractive interactions between the CB7 and β -CD rims via direct or water-mediated O–H...O hydrogen bonds.

Still, a final question concerning the possible formation mechanism of $4@(\beta\text{-CD}^{Ad}, \text{CB7}^{Bu})$ remains. In the following, we discuss the two alternative pathways that begin with the $4@CB7^{Ad}$ complex as depicted in Figure 6. The first pathway involves the dissociation of $4@CB7^{Ad}$ into free CB7 and guest 4 followed by the sequential binding of β -CD and CB7 at the adamantane and butyl sites, respectively. The particular order of these two binding events should be of little importance because of the very similar relative free energies of formation of $4@CB7^{Bu}$ and $4@(\beta\text{-CD}^{Ad})$. The key step of the second pathway consists of the displacement of CB7 over the guest molecule toward the nonpreferred butyl site, which is accompanied by the binding of β -CD at the adamantane site. Given the energy difference between the C and B states, the $A \rightarrow C$ pathway is strongly disfavored because the concentration of C is much lower than that of B. According to the Boltzmann distribution, the equilibrium population is more than 99.9999% of B at the expense of C considering only these two species. From a kinetic

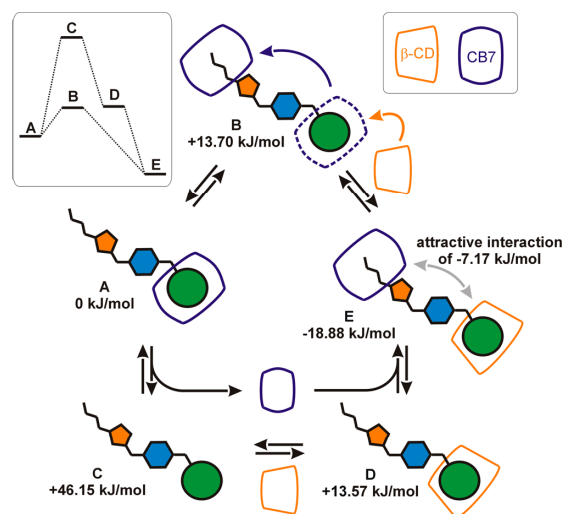


Figure 6. Possible pathways for the formation of the ternary complex $4@(\text{CB7}^{Bu}, \beta\text{-CD}^{Ad})$. The relative free energies associated with the individual binding events were obtained from ITC experiments (2.5 mM NaCl solution, 303 K).

point of view, the most important energetic barrier is associated with the displacement of the adamantane cage through the CB7 portal. Nevertheless, both pathways result in CB7 surrendering the adamantane binding site by either leaving and entering the bulk solution or sliding toward the butyl binding site. Thus, we may conclude that the only significant difference between the $A \rightarrow C \rightarrow D \rightarrow E$ and $A \rightarrow B \rightarrow E$ pathways lies in the energetic barrier arising from the steric hindrance associated with shuttling CB7 over the guest molecule. With regard to this, we have demonstrated previously that such movement of CB7 along guest molecules bearing similar adamantylated bisimidazolium-based structures is possible in the gas phase, even when the cationic moiety is derived from the more sterically hindered benzimidazolium core.³¹

Moreover, we have prepared separately adamantane-terminated dumbbell-like guests based on imidazolium salts bearing an additional central binding site for β -CD. When both of the terminal adamantane sites were occupied by CB7, the central site became inaccessible to β -CD.³² This suggests that the replacement of CB7 at the adamantane site with β -CD is very unlikely. In addition, we employed MD simulations to demonstrate that the shuttling of CB7 between the adamantane and butyl sites of 4 is feasible. Initially, we positioned the CB7 unit at the butyl site and let the system develop. CB7 remained at the butyl site for 450 ns before moving to the middle phenyl site for the next 50 ns. Finally, CB7 shifted to the Ad until the end of the simulation (i.e., 500 ns). It is not surprising that only the shifting of the CB7 unit from the weaker to stronger binding site, if any, is observed within the MD simulation. However, it is reasonable to expect that the movement of CB7 is reversible. An analysis of the MD simulation can be seen in Figure S89. On this basis, we infer that the formation of $4@(\text{CB7}^{Bu}, \beta\text{-CD}^{Ad})$ from $4@CB7^{Ad}$ and β -CD can result from a chemically induced reorganization of the starting complex (i.e., $A \rightarrow B \rightarrow E$) rather than a sequence of binding and dissociation events (i.e., $A \rightarrow C \rightarrow D/B \rightarrow E$). In addition to these two pathways, participation of other species that are

present in small portions in the real complex mixture should be taken into account (i.e., free **4**, **4**@CB7^{bu}, and **4**@CB7₂).

Finally, the formation of the discussed ternary assemblies was confirmed in aqueous solutions using ESI-MS techniques (for comments and spectra, see the Supporting Information).

CONCLUSIONS

We synthesized four members of a new guest family (**2**, **4**, **6**, and **7**) with structures that combine the advantages of the adamantane cage and the imidazolium moiety. The supra-molecular affinity for CB6, CB7, and β -CD has been investigated with the aid of additional model guests **1**, **3**, and **5**. The combination of calorimetric titrations and ¹H NMR spectroscopy has revealed that, in aqueous solution, both β -CD and CB7 occupy predominantly the adamantane binding sites, with association constants within the ranges of 3.8×10^4 to 5.4×10^5 M⁻¹ and 1.6×10^8 to 3.7×10^{12} M⁻¹, respectively. However, CB6 was shown to bind the butyl site, with K_1 values within the range of 4.2×10^4 to 1.4×10^6 M⁻¹. In strong contrast to those of CB6^{bu} and β -CD^{Ad}, the binding strength of CB7^{Ad} was significantly reduced upon replacement of the imidazolium ring in guests **1**, **2**, **5**, and **6** (i.e., guests that contain the 1-adamantylmethyl moiety) with the benzimidazolium core. These differences can be attributed to both the inability of CB to accommodate the bulkier benzimidazolium moiety compared to β -CD and the requirement for a fixed position of the adamantane cage inside the CB7 cavity, which contrasts with the requirement for the butyl residue inside the CB6 cavity. The complete lack of CB7 selectivity toward guests **4** and **7** implies that the binding of the adamantyl group inside the CB7 cavity is driven predominantly by hydrophobic interactions, whereas the contribution of ion-dipole interactions between the imidazolium cation and the CB7 portal plays a marginal role, if any. Thus, the combination of mostly hydrophobic binding at the adamantane site with the electrostatically driven binding of the butyl chain in guests **4** and **7** allowed us to prepare compact arrangements consisting of two cucurbituril units surrounding a single imidazolium cation. Although complexes **4**/7@(CB7^{Ad},CB7^{bu}) and **4**/(CB7^{Ad},CB6^{bu}) were evidenced using ITC and NMR experiments, the calorimetric titrations demonstrated that such systems are destabilized by approximately 3 kJ mol⁻¹ with respect to the individual binary complexes, most likely because of electrostatic repulsion between the CB portals. To the best of our knowledge, these results represent the first quantification of repulsion strength between two CB units, which contributes negatively to the overall stability of ternary complexes featuring these macrocycles. In addition, we were able to determine additional energetic stabilizations of -3.1 ± 0.72 , -1.7 ± 0.85 , and -7.2 ± 0.87 kJ mol⁻¹ for complexes **2**/(β -CD^{Ad},CB6^{bu}), **4**/(β -CD^{Ad},CB6^{bu}), and **4**/(β -CD^{Ad},CB7^{bu}), respectively. The overall strength of the proposed portal-portal direct or water-mediated O-H...O hydrogen bonds is comparable to that reported by Rekharsky and co-workers^{7a} for CB6 and α/β -CD complexed with the dihexylammonium cation. The values of the respective stabilization energies confirm our assumptions based on the host and guest geometries. Thus, guest **2**, which possesses a distance between the binding sites that is shorter than that of guest **4**, allows for stronger interactions between β -CD and CB6. In addition, CB7, which has a portal wider than that of CB6, was shown to be more suitable for interaction with β -CD than with CB6 in ternary complexes with **4**.

The most interesting result of this work is the clear demonstration of the thermodynamically driven formation of the ternary aggregate **4**/(β -CD^{Ad},CB7^{bu}) that features CB7 bound to an otherwise strongly disfavored butyl chain ($K_{Ad}/K_{Bu} = 229.8$ in a 2.5 mM NaCl aqueous solution). In addition, the formation of **4**/(β -CD^{Ad},CB7^{bu}) from **4**@CB7^{Ad} involves a displacement of CB7^{Ad} by β -CD, which has an affinity for the adamantane site much lower than that of CB7 ($K_{CB7}/K_{\beta-CD} = 218.1$ for the Ad site in a 2.5 mM NaCl aqueous solution). However, the energy loss related to such a displacement is compensated by the subsequent binding of CB7 to the butyl chain, which leads to an overall energetic gain of -26 kJ mol⁻¹ and makes the formation of the ternary complex thermodynamically feasible. Thus, we have demonstrated that the binding behavior of multitopic guests in complex mixtures is driven by the overall energetic effect and does not always conform to the initial expectations based on knowledge of the individual binary systems. While this concept is commonly found in biological systems and complements the work of Ding et al.³³ describing self-sorting of CB8, β -CD, and the 1,6-dihydroxynaphthalene-adamantylated viologen CT complex, herein we have presented the first example of such behavior in assemblies formed by low-molecular weight synthetic guests with β -CD and CB7.

EXPERIMENTAL SECTION

General Methods. Guests **1**–**7** were prepared according to a previously published method.³² Preparation of compounds **8** and **10** has been described previously.³¹ Hosts CB6, CB7, and β -CD were purchased from commercial sources. β -CD was dried prior to use under reduced pressure at 50 °C to a constant weight. The concentrations of the CB7 solutions were determined by ITC with L-Phe as the standard. NMR spectra were recorded on a 700 MHz instrument equipped with a room-temperature (¹H, ¹³C, ¹⁵N) inverse triple-resonance probe. One-dimensional (1D) proton spectra were recorded at 303 K using a 7.0 kHz spectral width and a 3.3 kHz transmitter offset. Data were collected in 8–32 scans using a 1.5 s recycle delay, and 16k complex points were recorded per scan. The FIDs were apodized by a square cosine window function, zero filled to 32k complex points, and Fourier transformed to yield the resulting spectra. The 2D ROESY spectra were recorded using a spectral width of 7.0 kHz and a transmitter offset of 3.3 kHz in both dimensions and employing 150–400 ms continuous wave spinlock during the mixing period. A total of 2k complex points were collected in the t2 dimension and a total of 512 t1 increments were recorded using 16–32 scans per increment and 1.5 s recycle delay. The raw data were apodized by a squared cosine window function, zero filled to 4096 t2 and 2048 t1 points and Fourier transformed to yield the resulting 2D spectra. The residual HDO signal in both the 1D and 2D ROESY experiments was suppressed by employing presaturation during the recycle delay. No time-dependent changes in signal intensities were observed when ¹H NMR titration experiments were performed. The association constants and thermodynamic parameters for the complexation of guests **1**–**7** with CB7, CB6, and/or β -CD were determined by ITC. A solution of the host in water or in 2.5 mM NaCl was placed in the sample cell, to which a solution of the guest was added in a series of 20–30 injections (10 μ L). The concentrations of the CB6, CB7, and β -CD solutions were determined via ITC using 1,6-hexanediamine-2HCl and 1-adamantaneamine-HCl. For the ternary systems, a solution of an equimolar mixture of the guest and host in the sample cell was titrated with a solution of the second host. The heat evolved was recorded at 303 K. The net heat effect was obtained by subtracting the heat of guest dilution from the overall observed heat effect. The association constants exceeding 10⁷ M⁻¹ were determined by the multistep competition method as described by Rekharsky et al.^{17a} 1,6-Hexanediamine-2HCl with a K_a (H₂O) of 2.05×10^9 M⁻¹ and a K_a (2.5 mM NaCl) of 2.97×10^8 M⁻¹, dopamine-HCl with a K_a (H₂O) of 4.58

$\times 10^5 \text{ M}^{-1}$, and L-phenylalanine with a $K_{\text{c}}(\text{H}_2\text{O})$ of $9.86 \times 10^5 \text{ M}^{-1}$ and a $K_{\text{c}}(2.5 \text{ mM NaCl})$ of $3.01 \times 10^5 \text{ M}^{-1}$ were used as the competitors. The complexation enthalpies for the multistep titration experiments were calculated as a sum of enthalpies for each complexation step. The values of K obtained from competitive titrations were verified using different concentrations of competitors. The typical ITC thermograms are shown in Figure 3 and in Figures S48–S70.

General Procedure for Preparation of 1–7 Bromides and Iodides. Imidazole 8 or 9 or benzoimidazole 10 or 11 (1 equiv, see the Supporting Information for structures) was dissolved in the corresponding haloalkane (60 equiv) under an inert atmosphere. The mixture was refluxed until the starting material was consumed. After residual haloalkane had been removed under reduced pressure, the crude product was washed several times with diethyl ether. Solid products were used without further purification after being dried *in vacuo*. Oily products were purified by successive column chromatography using silica gel and 1:1 (v/v) petroleum ether/AcOEt and 1:1 (v/v) $\text{CHCl}_3/\text{MeOH}$ solvents.

General Procedure for Preparation of 6 and 7 Mesylates. Benzoimidazole 9 or 10 (1 equiv) was dissolved in dry toluene (2 equiv), and butyl mesylate (2–3 equiv) was added at room temperature. The mixture was refluxed and monitored by TLC. When no further progress was observed, the toluene was removed *in vacuo*, and the resulting slurry was washed several times with diethyl ether. Products were purified as mentioned above.

1-(1-Adamantylmethyl)-3-methylimidazolium iodide (1⁺). The iodide of 1⁺ was isolated as pale yellow crystalline powder (131 mg, 87% yield) using 90 mg (0.42 mmol) of 8. Mp: 123–127 °C. Anal. Calcd for $\text{C}_{12}\text{H}_{23}\text{IN}_2$ (358.26): C, 50.29; H, 6.47; N, 7.82. Found: C, 49.93; H, 6.52; N, 8.03. $^1\text{H NMR}$ (300 MHz, CDCl_3): δ 1.51 (s, 6H), 1.55–1.70 (m, 6H), 2.00 (s, 3H), 4.00 (s, 2H), 4.14 (s, 3H), 7.30 (s, 1H), 7.62 (s, 1H), 9.90 (s, 1H). $^{13}\text{C}\{^1\text{H}\}$ NMR (75 MHz, CDCl_3): δ 27.9, 34.1, 36.4, 37.3, 39.8, 61.6, 123.4, 123.9, 137.5. IR (KBr): 3483(m), 3398(m), 3138(w), 3074(m), 2900(s), 2848(s), 2677(w), 2657(w), 1618(w), 1562(m), 1452(m), 1425(w), 1342(w), 1209(w), 1169(s), 1136(w), 1107(w), 833(m), 810(m), 781(w), 752(m), 719(w), 665(m), 621(m) cm^{-1} . ESI-MS: m/z 231.1 $[\text{M}]^+$ (100%).

1-(1-Adamantylmethyl)-3-butylimidazolium Bromide (2⁺Br). The bromide of 2⁺ was isolated as tan highly viscous oil (238 mg, 79% yield) using 186 mg (0.86 mmol) of 8. Anal. Calcd for $\text{C}_{18}\text{H}_{29}\text{BrN}_2$ (353.34): C, 61.19; H, 8.27; N, 7.93. Found: C, 61.36; H, 8.22; N, 8.21. $^1\text{H NMR}$ (300 MHz, CDCl_3): δ 0.94 (t, $J = 7.2$ Hz, 3H), 1.37 (m, 2H), 1.50 (s, 6H), 1.62 (m, 6H), 1.91 (m, 2H), 1.99 (s, 3H), 4.02 (s, 2H), 4.39 (t, $J = 7.3$ Hz, 2H), 7.27 (s, 1H), 7.52 (s, 1H), 10.26 (s, 1H). $^{13}\text{C}\{^1\text{H}\}$ NMR (75 MHz, CDCl_3): δ 13.7, 19.7, 28.0, 32.4, 34.2, 36.5, 40.0, 50.2, 61.7, 121.9, 124.1, 137.1. IR (KBr): 3464(s), 3410(s), 3132(w), 3069(w), 2958(w), 2903(s), 2848(m), 2677(w), 2658(w), 1633(w), 1561(m), 1453(m), 1370(w), 1316(w), 1162(s), 1135(w), 1106(w), 773(w), 755(w), 717(w), 665(w) cm^{-1} . ESI-MS: m/z 625.3 $[2\text{-M}^+ + ^{79}\text{Br}]^+$ (8%), 273.3 $[\text{M}]^+$ (100%).

1-[4-(1-Adamantylcarbonyl)benzyl]-3-methylimidazolium iodide (3⁺). The iodide of 3⁺ was isolated as pale yellow crystalline powder (196 mg, 83% yield) using 164 mg (0.51 mmol) of 9. Mp: 162–167 °C. Anal. Calcd for $\text{C}_{22}\text{H}_{27}\text{IN}_2\text{O}$ (462.37): C, 57.15; H, 5.89; N, 6.06. Found: C, 57.02; H, 5.91; N, 6.17. $^1\text{H NMR}$ (300 MHz, $\text{DMSO}-d_6$): δ 1.69 (s, 6H), 1.89 (s, 6H), 2.01 (s, 3H), 3.87 (s, 3H), 5.49 (s, 2H), 7.46 (d, $J = 7.5$ Hz, 2H), 7.58 (d, $J = 7.2$ Hz, 2H), 7.74 (s, 1H), 7.82 (s, 1H), 9.24 (s, 1H). $^{13}\text{C}\{^1\text{H}\}$ NMR (75 MHz, $\text{DMSO}-d_6$): δ 27.4, 35.8, 35.9, 38.3, 46.0, 51.4, 122.4, 124.0, 127.4, 127.8, 136.7, 136.8, 139.2, 208.7. IR (KBr): 3164(m), 3135(m), 3056(s), 2971(w), 2911(s), 2850(s), 2677(w), 2656(w), 1735(w), 1671(s), 1608 (w), 1573(m), 1558(m), 1450(m), 1412(w), 1269(m), 1240(m), 1171(s), 1024(w), 987(m), 967(w), 952(w), 834(m), 754(m), 730(m), 692(w), 670(w), 610(m) cm^{-1} . ESI-MS: m/z 335.3 $[\text{M}]^+$ (100%).

1-[4-(1-Adamantylcarbonyl)benzyl]-3-butylimidazolium Bromide (4⁺Br). The bromide of 4⁺ was isolated as tan viscous oil (129 mg, 43% yield) using 212 mg (0.66 mmol) of 9. Anal. Calcd for $\text{C}_{22}\text{H}_{33}\text{BrN}_2\text{O}$ (457.45): C, 65.64; H, 7.27; N, 6.12. Found: C, 65.82; H, 7.35; N, 5.97. $^1\text{H NMR}$ (300 MHz, CDCl_3): δ 0.94 (t, $J = 7.2$ Hz,

3H), 1.35 (m, 2H), 1.72 (m, 6H), 1.87–1.94 (m, 2 + 6H), 2.05 (s, 3H), 4.28 (t, $J = 7.2$ Hz, 2H), 5.70 (s, 2H), 7.35 (s, 1H), 7.44 (s, 1H), 7.50 (d, $J = 8.1$ Hz, 2H), 7.59 (d, $J = 8.4$ Hz, 2H), 10.57 (s, 1H). $^{13}\text{C}\{^1\text{H}\}$ NMR (75 MHz, CDCl_3): δ 13.6, 19.7, 28.2, 32.2, 36.6, 39.1, 47.2, 50.2, 52.9, 122.2, 128.1, 128.9, 135.3, 137.3, 140.8, 210.0. IR (KBr): 3432(s), 3131(w), 3063(w), 2906(s), 2850(m), 2678(w), 2658(w), 1668(m), 1609(w), 1561(m), 1453(m), 1411(w), 1271(m), 1237(m), 1160(m), 988(w), 930(w), 765(w), 684(w), 617(w) cm^{-1} . ESI-MS: m/z 833.4 $[2\text{-M}^+ + ^{79}\text{Br}]^+$ (3%), m/z 377.3 $[\text{M}]^+$ (100%).

1-(1-Adamantylmethyl)-3-methylbenzoimidazolium iodide (5⁺). The iodide of 5⁺ was isolated as colorless crystalline powder (125 mg, 83% yield) using 98 mg (0.37 mmol) of 10. Mp: 115–120 °C. Anal. Calcd for $\text{C}_{16}\text{H}_{23}\text{IN}_2$ (408.32): C, 55.89; H, 6.17; N, 6.86. Found: C, 55.55; H, 6.17; N, 7.03. $^1\text{H NMR}$ (300 MHz, $\text{DMSO}-d_6$): δ 1.56–1.67 (m, 12H), 1.95 (s, 3H), 4.11 (s, 3H), 4.23 (s, 2H), 7.67–7.70 (m, 2H), 8.01–8.03 (m, 1H), 8.12–8.14 (m, 1H), 9.64 (s, 1H). $^{13}\text{C}\{^1\text{H}\}$ NMR (75 MHz, $\text{DMSO}-d_6$): δ 27.4, 33.3, 34.3, 35.9, 39.0, 57.0, 113.4, 114.1, 126.2, 126.4, 131.5, 132.3, 143.2. IR (KBr): 3467(m), 3442(m), 3134(w), 3010(w), 2902(s), 2848(m), 1618(w), 1566(m), 1487(w), 1456(m), 1344(w), 1313(w), 1275(w), 1209(w), 1024(w), 845(w), 762(m), 750(w), 569(w), 428 (w) cm^{-1} . ESI-MS: m/z 281.2 $[\text{M}]^+$ (100%).

1-(1-Adamantylmethyl)-3-butylbenzoimidazolium Bromide (6⁺Br). The bromide of 6⁺ was isolated as colorless crystalline powder (279 mg, 92% yield) using 200 mg (0.75 mmol) of 10. Mp: 208–212 °C. Anal. Calcd for $\text{C}_{22}\text{H}_{31}\text{BrN}_2$ (403.40): C, 66.50; H, 7.75; N, 6.94. Found: C, 66.27; H, 7.83; N, 7.05. $^1\text{H NMR}$ (300 MHz, CDCl_3): δ 0.96 (t, $J = 7.2$ Hz, 3H), 1.43 (m, 2H), 1.54–1.69 (m, 12H), 1.99–2.06 (m, 5H), 4.31 (s, 2H), 4.68 (t, $J = 7.5$ Hz, 2H), 7.61–7.74 (m, 4H), 11.17 (s, 1H). $^{13}\text{C}\{^1\text{H}\}$ NMR (75 MHz, CDCl_3): δ 13.7, 19.9, 28.0, 31.5, 35.2, 36.4, 40.4, 47.6, 58.7, 113.1, 114.0, 127.0, 127.2, 131.0, 132.9, 143.6. IR (KBr): 3454(m), 3387(m), 3129(w), 3056(w), 3029(w), 2964(m), 2904(s), 2849(m), 2789(w), 2679(w), 1614(w), 1564(s), 1480(w), 1458(m), 1428(m), 1386(m), 1369(w), 1346(w), 1316(w), 1278(w), 1230(w), 1212(w), 762(s), 616(w) cm^{-1} . ESI-MS: m/z 725.3 $[2\text{-M}^+ + ^{79}\text{Br}]^+$ (10%), m/z 323.2 $[\text{M}]^+$ (100%).

1-(1-Adamantylmethyl)-3-butylbenzoimidazolium Iodide (6⁺). The iodide of 6⁺ was isolated as colorless crystalline powder (128 mg, 86% yield) using 89 mg (0.33 mmol) of 10. Mp: 202–204 °C. Anal. Calcd for $\text{C}_{22}\text{H}_{31}\text{IN}_2$ (450.40): C, 58.67; H, 6.94; N, 6.22. Found: C, 58.43; H, 6.86; N, 6.23. $^1\text{H NMR}$ (300 MHz, CDCl_3): δ 0.98 (t, $J = 7.2$ Hz, 3H), 1.46 (m, 2H), 1.55–1.66 (m, 12H), 2.01–2.09 (m, 5H), 4.33 (s, 2H), 4.68 (t, $J = 7.5$ Hz, 2H), 7.63–7.79 (m, 4H), 10.91 (s, 1H). $^{13}\text{C}\{^1\text{H}\}$ NMR (75 MHz, CDCl_3): δ 13.7, 19.9, 28.0, 31.5, 35.2, 36.4, 40.5, 47.6, 58.7, 113.2, 114.1, 127.2, 127.4, 131.0, 132.8, 142.6. IR (KBr): 3126(w), 3023(w), 2994(w), 2965(m), 2901(s), 2847(m), 2676(w), 2657(w), 1612(w), 1563(s), 1488(w), 1459(m), 1430(m), 1367(w), 1347(w), 1315(w), 1277(w), 1207(w), 1180(w), 1022(w), 758(s), 615(w), 571(w) cm^{-1} . ESI-MS: m/z 773.3 $[2\text{-M}^+ + \text{I}]^+$ (21%), m/z 323.3 $[\text{M}]^+$ (100%).

1-(1-Adamantylmethyl)-3-butylbenzoimidazolium Mesylate (6⁺MsO). The mesylate of 6⁺ was isolated as colorless crystalline powder (57 mg, 36% yield) using 100 mg (0.38 mmol) of 10. Mp: 195–198 °C. Anal. Calcd for $\text{C}_{23}\text{H}_{34}\text{N}_2\text{O}_3\text{S}$ (418.59): C, 65.99; H, 8.19; N, 6.69. Found: C, 66.17; H, 8.12; N, 6.92. $^1\text{H NMR}$ (300 MHz, CDCl_3): δ 0.98 (t, $J = 7.5$ Hz, 3H), 1.45 (m, 2H), 1.56–1.71 (m, 12H), 2.01–2.07 (m, 5H), 2.80 (s, 3H), 4.28 (s, 2H), 4.64 (t, $J = 7.2$ Hz, 2H), 7.59–7.71 (m, 4H), 10.57 (s, 1H). ^{13}C NMR (75 MHz, CDCl_3): δ 13.6, 19.9, 28.1, 31.5, 35.2, 36.5, 39.8, 40.4, 47.5, 58.6, 113.0, 114.0, 126.8, 126.9, 131.2, 133.0, 144.7. IR (KBr): 3121(w), 3103(w), 3027(w), 2960(w), 2906(s), 2849(m), 2677(w), 1638(w), 1614(w), 1561(m), 1484(w), 1459(w), 1429(w), 1385(w), 1344(w), 1318(w), 1279(w), 1207(s), 1145(w), 1044(s), 1021(w), 772(s), 672(w), 617(w), 553(m) cm^{-1} . ESI-MS: m/z 741.4 $[2\text{-M}^+ + \text{MsO}]^+$ (2%), m/z 323.3 $[\text{M}]^+$ (100%).

1-[4-(1-Adamantylcarbonyl)benzyl]-3-butylbenzoimidazolium Mesylate (7⁺MsO). The mesylate of 7⁺ was isolated as colorless crystalline powder (24 mg, 17% yield) using 100 mg (0.27 mmol) of 11. Mp: 193–198 °C. Anal. Calcd for $\text{C}_{30}\text{H}_{38}\text{N}_2\text{O}_3\text{S}$ (522.70): C,

68.93; H, 7.33; N, 5.36. Found: C, 69.07; H, 7.39; N, 5.12. ^1H NMR (300 MHz, CDCl_3): δ 0.98 (t, $J = 6.9$ Hz, 3H), 1.45 (m, 2H), 1.71 (m, 6H), 1.92–2.03 (m, 11H), 2.82 (s, 3H), 4.57 (t, $J = 6.9$ Hz, 2H), 5.89 (s, 2H), 7.50–7.70 (m, 8H), 10.98 (s, 1H). ^{13}C NMR (75 MHz, CDCl_3): δ 13.6, 20.0, 28.2, 31.4, 36.6, 39.1, 39.8, 47.1, 47.8, 51.0, 113.2, 114.0, 127.2, 127.4, 128.1, 128.2, 131.5, 131.7, 135.2, 140.5, 144.0, 209.8. IR (KBr): 3125(w), 3059(w), 2931(s), 2907(s), 2852(m), 2680(w), 2659(w), 1690(m), 1611(w), 1561(m), 1481(w), 1454(w), 1431(w), 1380(w), 1346(w), 1273(w), 1208(s), 1194(s), 1116(w), 1059(m), 1045(m), 989(w), 952(w), 932(w), 854(w), 809(w), 761(m), 670(w), 634(w), 611(w), 555(w), 536(w) cm^{-1} . ESI-MS: m/z 949.4 [$2\text{-M}^+ + \text{MsO}^-$] (11%), m/z 427.3 [M^+] (100%).

General Procedure for Preparation of 9 and 11. Benzimidazole or imidazole (1 equiv) was dissolved in dry DMF (150 equiv), and *N*-ethyl-*N*-isopropylpropan-2-amine (1.5 equiv) and 1-adamantyl 4-bromomethylphenyl ketone (1.1 equiv) were added at room temperature. The mixture was vigorously stirred under an inert atmosphere at 100 °C for 5 days. The resulting slurry was poured into crushed ice and extracted with CH_2Cl_2 . Collected organic portions were washed with water and brine and dried over Na_2SO_4 . Solvents were distilled off in vacuum, and residual DMF was removed via azeotropic distillation with CH_2Cl_2 . Crude material was purified on column [silica gel, 1:1 (v/v) petroleum ether/ethyl acetate].

1-[4-(1-Adamantylcarbonyl)benzyl]-1H-imidazole (9). Compound 9 was isolated as pale yellow oil in a yield of 328 mg (65%) using 573 mg (1.72 mmol) of starting bromide. Anal. Calcd for $\text{C}_{25}\text{H}_{28}\text{N}_2\text{O}$ (320.43): C, 78.71; H, 7.55; N, 8.74. Found: C, 78.83; H, 7.52; N, 8.51. ^1H NMR (300 MHz, CDCl_3): δ 1.71–1.81 (m, 6H), 2.00 (s, 6H), 2.09 (s, 3H), 5.28 (s, 2H), 7.00 (s, 1H), 7.23–7.28 (overlapped signals, 3H), 7.56 (d, $J = 8.4$ Hz, 2H), 8.22 (s, 1H). ^{13}C NMR (75 MHz, CDCl_3): δ 28.3, 36.7, 39.2, 47.2, 50.8, 119.6, 127.0, 128.1, 129.4, 137.5, 138.1, 139.8, 209.6. IR (KBr): 3111(w), 2905(s), 2850(s), 2679(w), 2658(w), 1667(s), 1609(m), 1506(m), 1452(m), 1412(w), 1345(w), 1271(s), 1234(s), 1177(m), 1106(w), 1076(m), 1030(w), 988(m), 954(w), 930(w), 834(w), 815(w), 794(w), 733(m), 663(m) cm^{-1} . GC-MS (EI): m/z 320 (5%), 293 (12%), 292 (50%), 136 (11%), 135 (100%), 118 (9%), 107 (14%), 93 (24%), 91 (9%), 90 (13%), 89 (8%), 81 (9%), 79 (27%), 77 (9%), 67 (11%), 55 (7%), 41 (8%).

1-[4-(1-Adamantylcarbonyl)benzyl]-1H-benzimidazole (11). Compound 11 was isolated as pale yellow crystalline powder in a yield of 218 mg (44%) using 497 mg (1.49 mmol) of starting bromide. Mp: 126–131 °C. Anal. Calcd for $\text{C}_{25}\text{H}_{28}\text{N}_2\text{O}$ (370.49): C, 81.05; H, 7.07; N, 7.56. Found: C, 80.94; H, 7.09; N, 7.38. ^1H NMR (300 MHz, CDCl_3): δ 1.68–1.78 (m, 6H), 1.96–1.97 (m, 6H), 2.06 (s, 3H), 5.42 (s, 2H), 7.20 (d, $J = 8.4$ Hz, 2H), 7.27–7.32 (overlapped signals, 3H), 7.52 (d, $J = 7.2$ Hz, 2H), 7.86 (m, 1H), 8.15 (s, 1H). ^{13}C NMR (300 MHz, CDCl_3): δ 28.3, 36.7, 39.2, 47.1, 48.6, 110.1, 120.7, 122.7, 123.5, 126.7, 128.2, 134.0, 137.8, 139.7, 143.3, 144.0, 209.5. IR (KBr): 3436(w), 3118(w), 3100(w), 3057(w), 3037(w), 3025(w), 2930(s), 2900(s), 2850(s), 2675(w), 2658(w), 1943(w), 1906(w), 1793(w), 1718(w), 1670(s), 1617(w), 1561(w), 1494(s), 1460(m), 1446(m), 1411(w), 1373(m), 1349(m), 1316(w), 1274(m), 1240(m), 1205(w), 1179(m), 1111(w), 1050(w), 1020(w), 986(m), 930(m), 887(w), 845(w), 864(w), 845(w), 821(w), 789(w), 756(s), 722(w), 683(w), 640(w), 608(w), 581(w) cm^{-1} . GC-MS (EI): m/z 371 (8%), 370 (28%), 343 (15%), 342 (55%), 225 (6%), 208 (6%), 136 (11%), 135 (100%), 131 (6%), 119 (8%), 107 (13%), 93 (25%), 91 (12%), 90 (16%), 89 (12%), 81 (8%), 79 (26%), 77 (10%), 67 (11%), 55 (8%), 41 (6%).

Computational Details. The nucleus-independent chemical shielding (NICs²⁸) was calculated on geometry-optimized structures of β -CD, CB6, and CB7 at the PBE0³⁵/6-311G**³⁵ level of theory using the Gaussian 09.A2³⁶ software package. PyMOL³⁷ and VMD³⁸ were used to visualize the computed data. Molecular dynamics of individual complexes were performed in the AMBER 12 package³⁹ using GAFF⁴⁰ and GLYCAM06⁴¹ force fields. Production simulations at 300 K and 1 bar in an explicit water environment were 1 μs long. See the Supporting Information for further details.

■ ASSOCIATED CONTENT

● Supporting Information

The Supporting Information is available free of charge on the ACS Publications website at DOI: 10.1021/acs.joc.6b01564.

^1H and ^{13}C NMR spectra of the new compounds 1–7, crystallographic data for 6^{T^-} and $6^{\text{M}^{\text{SO}^-}}$, mass spectra of the free guests and their complexes, ^1H NMR and ITC data related to the titration experiments, and computational details (PDF)

Crystallographic data (CIF)

■ AUTHOR INFORMATION

Corresponding Author

*E-mail: rvicha@ff.utb.cz.

Notes

The authors declare no competing financial interest.

■ ACKNOWLEDGMENTS

This work was financially supported by the Internal Funding Agency of Tomas Bata University in Zlín (IGA/FT/2016/001 to P.B., M.R., and R.V.), by the Czech Science Foundation (16-05961S to R.M.), and by the Ministry of Education, Youth and Sports of the Czech Republic under Project CEITEC 2020 (LQ1601 to P.K.). Computational resources were provided by the CESNET LM2015042 and the CERIT Scientific Cloud LM2015085 under the program “Projects of Large Research, Development, and Innovations Infrastructures”.

■ REFERENCES

- (1) (a) Jiao, D.; Biedermann, F.; Schermer, O. A. *Org. Lett.* **2011**, *13*, 3044–3047. (b) Ku, Y. H.; Kim, E.; Hwang, I.; Kim, K. *Chem. Commun.* **2007**, 1305–1315. (c) Urbach, A. R.; Ramalingam, V. *Isr. J. Chem.* **2011**, *51*, 664–678. (d) Das, D.; Schermer, O. A. *Isr. J. Chem.* **2011**, *51*, 537–550. (e) Jiang, W.; Wang, Q.; Linder, I.; Klautzsch, F.; Schalley, C. A. *Chem. - Eur. J.* **2011**, *17*, 2344–2348. (f) Liu, Y.; Fang, R.; Tan, X.; Wang, Z.; Zhang, X. *Chem. - Eur. J.* **2012**, *18*, 15650–15654.
- (2) (a) Ohga, K.; Takashima, Y.; Takahashi, H.; Kawaguchi, Y.; Yamaguchi, H.; Harada, A. *Macromolecules* **2005**, *38*, 5897–5904. (b) Hasegawa, Y.; Miyauchi, M.; Takashima, Y.; Yamaguchi, H.; Harada, A. *Macromolecules* **2005**, *38*, 3724–3730. (c) Wittenberg, J. B.; Zavalij, P. Y.; Isaacs, L. *Angew. Chem., Int. Ed.* **2013**, *52*, 3690–3694. (d) Takashima, Y.; Yuting, Y.; Otsubo, M.; Yamaguchi, H.; Harada, A. *Berstein J. Org. Chem.* **2012**, *8*, 1594–1600.
- (3) (a) Böhm, I.; Isenbügel, K.; Ritter, H.; Branscheid, R.; Kolb, U. *Angew. Chem., Int. Ed.* **2011**, *50*, 7896–7899. (b) Bertrand, B.; Stenzel, M.; Fleury, E.; Bernard, J. *Polym. Chem.* **2012**, *3*, 377–383. (c) Charlot, A.; Auzély-Velty, R. *Macromolecules* **2007**, *40*, 1147–1158.
- (4) (a) Harada, A.; Kobayashi, R.; Takashima, Y.; Hashidzume, A.; Yamaguchi, H. *Nat. Chem.* **2011**, *3*, 34–37. (b) Zheng, Y.; Hashidzume, A.; Harada, A. *Macromol. Rapid Commun.* **2013**, *34*, 1062–1066.
- (5) (a) Huang, W.-H.; Liu, S.; Zavalij, P. Y.; Isaacs, L. *J. Am. Chem. Soc.* **2006**, *128*, 14744–14745. (b) Nally, R.; Isaacs, L. *Tetrahedron* **2009**, *65*, 7749–7754. (c) Lemaire, V.; Carroy, G.; Poussiguet, F.; Chirof, F.; De Winter, J.; Isaacs, L.; Dugourd, P.; Cornil, J.; Gerbaux, P. *ChemPlusChem* **2013**, *78*, 959–969.
- (6) (a) Buschmann, H.-J. *Isr. J. Chem.* **2011**, *51*, 533–536. (b) Girek, T. *J. Inclusion Phenom. Macrocyclic Chem.* **2013**, *76*, 237–252. (c) Kim, K. *Chem. Soc. Rev.* **2002**, *31*, 96–107. (d) Sforazzini, G.; Kahnt, A.; Wykes, M.; Sprafke, J. K.; Brovelli, S.; Montarnal, D.; Meinardi, F.; Cacialli, F.; Beljonne, D.; Albinsson, B.; Anderson, L. H. *J. Phys. Chem. C* **2014**, *118*, 4553–4566. (e) Buschmann, H.-J.; Wego, A.; Jansen, K.; Schollmeyer, E.; Döpp, D. *J. Inclusion Phenom. Mol. Recognit. Chem.* **2005**, *53*, 183–189.

- (7) (a) Rekharsky, M. V.; Yamamura, H.; Kawai, M.; Osaka, I.; Arakawa, R.; Sato, A.; Ko, Y. H.; Selvapalam, N.; Kim, K.; Inoue, Y. *Org. Lett.* **2006**, *8*, 815–817. (b) Leclercq, L.; Noujeim, N.; Sanon, S. H.; Schmitzer, A. R. *J. Phys. Chem. B* **2008**, *112*, 14176–14184.
- (8) (a) Wyman, I. W.; Macartney, D. H. *J. Org. Chem.* **2009**, *74*, 8031–8038. (b) Sinha, M. K.; Reany, O.; Yefet, M.; Botoshansky, M.; Keinan, E. *Chem. - Eur. J.* **2012**, *18*, 5589–5605.
- (9) Samsam, S.; Leclercq, L.; Schmitzer, A. R. *J. Phys. Chem. B* **2009**, *113*, 9493–9498.
- (10) (a) Isaacs, L. *Chem. Commun.* **2009**, 619–629. (b) Masson, E.; Ling, X.; Joseph, R.; Kyeremeh-Mensah, L.; Lu, X. *RSC Adv.* **2012**, *2*, 1213–1247. (c) Huang, W.-H.; Liu, S.; Isaacs, L. *Cucurbit[n]urils*. In *Modern Supramolecular Chemistry: Strategy for Macrocyclic Synthesis*; Diederich, F., Stang, P. J., Tykwinski, R. R., Eds.; Wiley-VCH: Weinheim, Germany, 2008; pp 113. (d) Barrow, S. J.; Kasper, S.; Rowland, M. J.; del Barrio, J.; Scherman, O. A. *Chem. Rev.* **2015**, *115*, 12320–12406.
- (11) (a) Harada, A.; Takashima, Y. *Chem. Rev.* **2013**, *13*, 420. (b) Harada, A.; Takashima, Y.; Nakahata, M. *Acc. Chem. Res.* **2014**, *47*, 2128–2140.
- (12) Hashimoto, H. *CyD applications in food, cosmetic, toiletry, textile and wrapping material fields*. In *Cyclodextrins and Their Complexes*; Dodziuk, H., Ed.; Wiley-VCH: Weinheim, Germany, 2006; pp 452.
- (13) Rekharsky, M. V.; Inoue, Y. *Chem. Rev.* **1998**, *98*, 1875–1918.
- (14) Freeman, W. A.; Mock, W. L.; Shih, N.-Y. *J. Am. Chem. Soc.* **1981**, *103*, 7367–7368.
- (15) Kim, J.; Jung, I. S.; Kim, S. Y.; Lee, E.; Kang, J. K.; Sakamoto, S.; Yamaguchi, K.; Kim, K. *J. Am. Chem. Soc.* **2000**, *122*, 540–541.
- (16) Behrend, R.; Meyer, E.; Rusche, F. *Liebigs Ann. Chem.* **1905**, *339*, 1–37.
- (17) (a) Rekharsky, M. V.; Mori, T.; Yang, C.; Ko, H. K.; Selvapalam, N.; Kim, H.; Sobransingh, D.; Kaifer, A. E.; Liu, S.; Isaacs, L.; Chen, W.; Moghaddam, S.; Gilson, M. K.; Kim, K.; Inoue, Y. *Proc. Natl. Acad. Sci. U. S. A.* **2007**, *104*, 20737–20742. (b) Yi, S.; Li, W.; Nieto, D.; Cuadrado, I.; Kaifer, A. E. *Org. Biomol. Chem.* **2013**, *11*, 287–293.
- (18) Moghaddam, S.; Yang, C.; Rekharsky, M.; Ko, Y. H.; Kim, K.; Inoue, Y.; Gilson, M. K. *J. Am. Chem. Soc.* **2011**, *133*, 3570–3581.
- (19) Cao, L.; Šekutor, M.; Zavalij, P. Y.; Mlinarić-Majerski, K.; Glaser, R.; Isaacs, L. *Angew. Chem., Int. Ed.* **2014**, *53*, 988–993.
- (20) Chakrabarti, S.; Mukhopadhyay, P.; Lin, S.; Isaacs, L. *Org. Lett.* **2007**, *9*, 2349–2352.
- (21) Mukhopadhyay, P.; Zavalij, P. Y.; Isaacs, L. *J. Am. Chem. Soc.* **2006**, *128*, 14093–14102.
- (22) Tootoonchi, M. H.; Yi, S.; Kaifer, A. E. *J. Am. Chem. Soc.* **2013**, *135*, 10804–10809.
- (23) (a) Wei-Li, D.; Bi, J.; Sheng-Lian, L.; Xu-Biao, L.; Xin-Man, T.; Chak-Tong, A. *Catal. Sci. Technol.* **2014**, *4*, 556–562. (b) Ruan, J.; Xiao, J. *Acc. Chem. Res.* **2011**, *44*, 614–626. (c) Headley, A. D.; Ni, B. *Aldrichimica Acta* **2007**, *40*, 107–117. (d) Lee, S. *Chem. Commun.* **2006**, 1049–1063.
- (24) Riduan, S. N.; Zhang, Y. *Chem. Soc. Rev.* **2013**, *42*, 9055–9070.
- (25) (a) Cavell, K. *Dalton Trans.* **2008**, 6676–6685. (b) Legrand, F.-X.; Ménand, M.; Sollogoub, M.; Tilloy, S.; Monflier, E. *New J. Chem.* **2011**, *35*, 2061–2065.
- (26) (a) Rouchal, M.; Matelová, A.; de Carvalho, F. P.; Bemat, R.; Gribić, D.; Kuřitka, I.; Babinský, M.; Marek, R.; Čmelík, R.; Vicha, R. *Supramol. Chem.* **2013**, *25*, 349–361. (b) Vicha, R.; Rouchal, M.; Kozubková, Z.; Kuřitka, I.; Marek, R.; Branná, P.; Čmelík, R. *Supramol. Chem.* **2011**, *23*, 663–677.
- (27) (a) Kolman, V.; Marek, R.; Štřelcová, Z.; Kulhánek, P.; Nečas, M.; Švec, J.; Šindelář, V. *Chem. - Eur. J.* **2009**, *15*, 6926–6931. (b) Zhao, N.; Liu, L.; Biedermann, F.; Scherman, O. A. *Chem. - Asian J.* **2010**, *5*, 530–537. (c) Liu, L.; Zhao, N.; Scherman, O. A. *Chem. Commun.* **2008**, 1070–1072. (d) Liu, L.; Nouvel, N.; Scherman, O. A. *Chem. Commun.* **2009**, 3243–3245.
- (28) (a) Schleyer, P. v. R.; Maerker, C.; Dransfeld, A.; Jiao, H.; Hommes, N. J. R. v. E. *J. Am. Chem. Soc.* **1996**, *118*, 6317–6318. (b) Babinský, M.; Bouzková, K.; Pipiška, M.; Novosadová, L.; Marek, R. *J. Phys. Chem. A* **2013**, *117*, 497–503. (c) Bouzková, K.; Babinský, M.; Novosadová, L.; Marek, R. *J. Chem. Theory Comput.* **2013**, *9*, 2629–2638.
- (29) Wintgens, V.; Biczók, L.; Miskolczy, Z. *Supramol. Chem.* **2010**, *22*, 612–618.
- (30) Liu, S.; Ruspic, C.; Mukhopadhyay, P.; Chakrabarti, S.; Zavalij, P. Y.; Isaacs, L. *J. Am. Chem. Soc.* **2005**, *127*, 15959–15967.
- (31) Černochová, J.; Branná, P.; Rouchal, M.; Kulhánek, P.; Kuřitka, I.; Vicha, R. *Chem. - Eur. J.* **2012**, *18*, 13633–13637.
- (32) Branná, P.; Rouchal, M.; Prucková, Z.; Dastyčová, L.; Lenobel, R.; Pospíšil, T.; Maláč, K.; Vicha, R. *Chem. - Eur. J.* **2015**, *21*, 11712–11718.
- (33) Ding, Z.-J.; Zhang, H.-Y.; Wang, L.-H.; Ding, F.; Liu, Y. *Org. Lett.* **2011**, *13*, 856–859.
- (34) (a) Perdew, J. P.; Ernzerhof, M.; Burke, K. *J. Chem. Phys.* **1996**, *105*, 9982–9985. (b) Adamo, C.; Barone, V. *J. Chem. Phys.* **1999**, *110*, 6158–6170.
- (35) Krishnan, R.; Binkley, J. S.; Seeger, R.; Pople, J. A. *J. Chem. Phys.* **1980**, *72*, 650–654.
- (36) Frisch, M. J.; Trucks, G. W.; Schlegel, H. B.; Scuseria, G. E.; Robb, M. A.; Cheeseman, J. R.; Scalmani, G.; Barone, V.; Mennucci, B.; Petersson, G. A.; Nakatsuji, H.; Caricato, M.; Li, X.; Hratchian, H. P.; Izmaylov, A. F.; Bloino, J.; Zheng, G.; Sonnenberg, J. L.; Hada, M.; Ehara, M.; Toyota, K.; Fukuda, R.; Hasegawa, J.; Ishida, M.; Nakajima, T.; Honda, Y.; Kitao, O.; Nakai, H.; Vreven, T.; Montgomery, J. A., Jr.; Peralta, J. E.; Ogliaro, F.; Bearpark, M.; Heyd, J. J.; Brothers, E.; Kudin, K. N.; Staroverov, V. N.; Kobayashi, R.; Normand, J.; Raghavachari, K.; Rendell, A.; Burant, J. C.; Iyengar, S. S.; Tomasi, J.; Cossi, M.; Rega, N.; Millam, J. M.; Klene, M.; Knox, J. E.; Cross, J. B.; Bakken, V.; Adamo, C.; Jaramillo, J.; Gomperts, R.; Stratmann, R. E.; Yazyev, O.; Austin, A. J.; Cammi, R.; Pomelli, C.; Ochterski, J. W.; Martin, R. L.; Morokuma, K.; Zakrzewski, V. G.; Voth, G. A.; Salvador, P.; Dannenberg, J. J.; Dapprich, S.; Daniels, A. D.; Farkas, Ö.; Foresman, J. B.; Ortiz, J. V.; Cioslowski, J.; Fox, D. J. *Gaussian 09*, revision A.2; Gaussian Inc.: Wallingford, CT, 2009.
- (37) *The PyMOL Molecular Graphics System*, version 1.6.0; Schrödinger, LLC, 2013.
- (38) Humphrey, W.; Dalke, A.; Schulten, K. *J. Mol. Graphics* **1996**, *14*, 33–38.
- (39) Case, D.; Darden, T.; Cheatham, T.; Simmerling, C.; Wang, J.; Duke, R.; Luo, R.; Walker, R.; Zhang, W.; Merz, K.; Roberts, B.; Hayik, S.; Roitberg, A.; Seabra, G.; Swails, J.; Goetz, A.; Kolossvary, I.; Wong, K.; Paesani, F.; Vanicek, J.; Wolf, R.; Liu, J.; Wu, X.; Brozell, S.; Steinbrecher, T.; Gohlke, H.; Cai, Q.; Ye, X.; Wang, J.; Hsieh, M.; Cui, G.; Roe, D.; Mathews, D.; Seetin, M.; Salomon-Ferrer, R.; Sagui, C.; Babin, V.; Luchko, T.; Gusarov, S.; Kovalenko, A.; Kollman, P. *AMBER 12*; University of California: San Francisco, 2012.
- (40) Wang, J. M.; Wolf, R. M.; Caldwell, J. W.; Kollman, P. A.; Case, D. A. *J. Comput. Chem.* **2004**, *25*, 1157–1174.
- (41) Kirschner, K. N.; Yongye, A. B.; Tschampel, S. M.; González-Outeiriño, J.; Daniels, C. R.; Foley, B. L.; Woods, R. J. *J. Comput. Chem.* **2008**, *29*, 622–655.

4.6

Adamantylated trisimidazolium-based tritopic guests
and their binding properties towards cucurbit[7]uril and β -cyclodextrin

Shantanu Ganesh Kulkarni, Zdeňka Prucková, Michal Rouchal, Lenka Dastychová, Robert Vícha *

Journal of Inclusion Phenomena and Macrocyclic Chemistry **2016**, 84, 11–20



Adamantylated trisimidazolium-based tritopic guests and their binding properties towards cucurbit[7]uril and β -cyclodextrin

Shantanu Ganesh Kulkarni¹ · Zdeňka Prucková¹ · Michal Rouchal¹ · Lenka Dastychová¹ · Robert Vícha¹

Received: 24 September 2015 / Accepted: 26 October 2015 / Published online: 3 November 2015
© Springer Science+Business Media Dordrecht 2015

Abstract Two new homotritopic guests based on tris(benz)imidazolium salts with adamantane binding sites were prepared. NMR and calorimetric titration experiments revealed that each of the three sites independently binds β -cyclodextrin (β -CD) or cucurbit[7]uril (CB7) units to form binary host–guest complexes with 1:3 stoichiometry. The association constants for the single binding site for β -CD and CB7 were determined using titration calorimetry and are in the order of 10^5 and 10^{9-10} dm³ mol⁻¹, respectively. In addition, both guests were able to form ternary systems with β -CD and CB7 in ratios of 1:1:2 and 1:2:1, respectively.

Keywords Adamantane · Multitopic guests · Imidazolium salts · Binding properties · Host–guest systems

Introduction

In the past decades, significant efforts have been made to construct complex supramolecular systems with various promising properties and/or functions. Besides micelles, dendritic polymers, and membrane vesicles, hydrogels have been designed to store, deliver or release active compounds under the control of external stimuli such as

pH, light, temperature or concentration of additional compounds [1–8]. Because the host–guest concept is one of the most popular approaches in this research area [9], either the guest or the host binding motifs are used for the preparation of the building blocks. Thus, both can be grafted onto a suitable polymer backbone, and supramolecular aggregates are formed via intermolecular interactions between two chains [10–15]. Another strategy is to use a host- or guest-modified polymer and a complementary low-molecular-weight linker [16]. Furthermore, supramolecular polymeric aggregates were constructed using either low-molecular-weight homoditopic guests and host “monomers” or heteroditopic building blocks containing both host and guest motifs [17–23]. As an extension of these well-documented approaches, tritopic building blocks were used for the construction of branched supramolecular polymers [24, 25], star-like structures [26, 27], and hydrogels [28–30].

There are two very popular families of hosts, namely cyclodextrins (CDs) [31–36] and cucurbit[n]urils (CBns) [37–39], each having particular advantages. The interest of scientific community is justified, inter alia, by biocompatibility of CDs and outstanding affinity of CBs, particularly CB7, towards some cationic guests derived from ferrocene [40], bicyclo[2.2.2]octane [41], adamantane [41], or diamantane [42]. Cationic moieties are frequently based on alkylammonium, pyridinium or imidazolium salts. However, imidazolium salts have some additional advantages as they display catalytic activity [43–47] and an ability to be transformed into *N*-heterocyclic carbenes to coordinate metals [48–53].

Herein, we report the convenient synthesis and binding properties of homotritopic, virtually *C*₃-symmetrical guests with 1-adamantylmethylimidazolium binding sites, which have the potential to be used as supramolecular cross-linkage agents.

Electronic supplementary material The online version of this article (doi:10.1007/s10847-015-0577-9) contains supplementary material, which is available to authorized users.

✉ Robert Vícha
rvicha@ft.utb.cz

¹ Department of Chemistry, Faculty of Technology, Tomas Bata University in Zlín, Vavrečkova 275, 760 01 Zlín, Czech Republic

Results and discussion

Chemistry

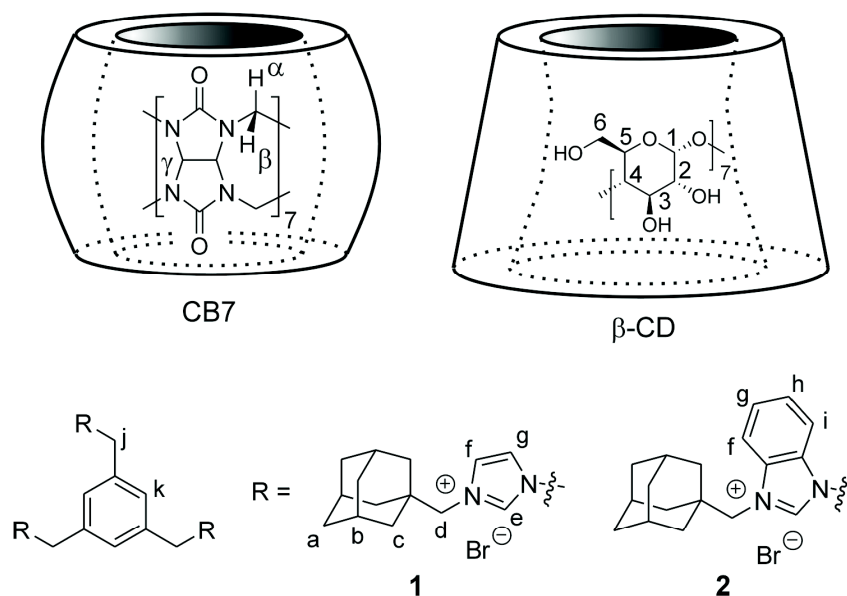
Compounds **1** and **2** (for structures, see Fig. 1) were prepared via a conventional quaternization reaction using commercially available 1,3,5-tris(bromomethyl)benzene and 1-(1-adamantylmethyl)(benz)imidazole. The synthesis of the latter starting material has been described elsewhere [54]. Although the preparation of **1** and **2** was typically smooth and with satisfactory yields, it should be noted that the resulting material sometimes contained a small portion of intermediates with one or two unchanged bromomethyl groups. This inconvenience was clearly detected by ESI-MS analysis. In such cases, all the material was further treated in toluene with an excess of the corresponding (benz)imidazole precursor to complete the formation of the desired product. The resulting compounds **1** and **2** were dried in vacuo to constant weight; however, the elemental analyses revealed that some water was still present, and compounds **1** and **2** should be considered to be tetrahydrate and pentahydrate, respectively. This material was used for further binding studies, and the water molecules were taken into account.

Binary systems

First, we investigated the individual binding behaviors of **1** and **2** towards CB7. The ^1H NMR spectra recorded during the titration of a solution of guest **1** in D_2O with CB7 are

stacked in Fig. 2 and display two sets of signals for the complexed and free guest (i.e., a slow exchange regime). It is clearly seen that the signal of H(k) on the central benzene ring was shifted downfield (Fig. 2a), whereas all the Ad signals were shifted upfield (Fig. 2b). Considering known magnetic anisotropy of CB7 [55], this observation implies that the Ad cage was included into the CB7 cavity, and therefore that the central benzene ring was positioned at the CB7 portal. Such an arrangement was supported by a ROESY spectrum recorded for a solution containing 3 equivalents (eq) of CB7. Figure 2c unambiguously shows cross-peaks related to the intermolecular interaction between the H(α) of CB7 and H(k) and H(g) from the central part of guest **1**. In addition to the binding mode of the **1**@CB7 complex, the stoichiometry can be estimated based on the ^1H NMR titration data. Because the signals of the free guest disappeared at the expense of the signals of complexed guest when 3 eq of CB7 were added, the formation of aggregate **1**@CB7₃ can be assumed. Note that there is only one set of signals in the spectrum of a sample containing a 1:3 mixture of **1** and CB7. To support our assumption, it can be rationalized based on the virtual C_3 symmetry of the predominant complex **1**@CB7₃ that all three binding sites in guest **1** are essentially independent. Subsequently, we studied the interaction between **1** and CB7 by means of isothermal titration calorimetry (ITC). The observation of a one-slope binding isotherm fitted to a One Set of Sites model further supports the independent behavior of each binding site. Because we have titrated the solution of CB7/competitor with a solution of guest **1**, the

Fig. 1 Structures of the trisimidazolium guest and host molecules



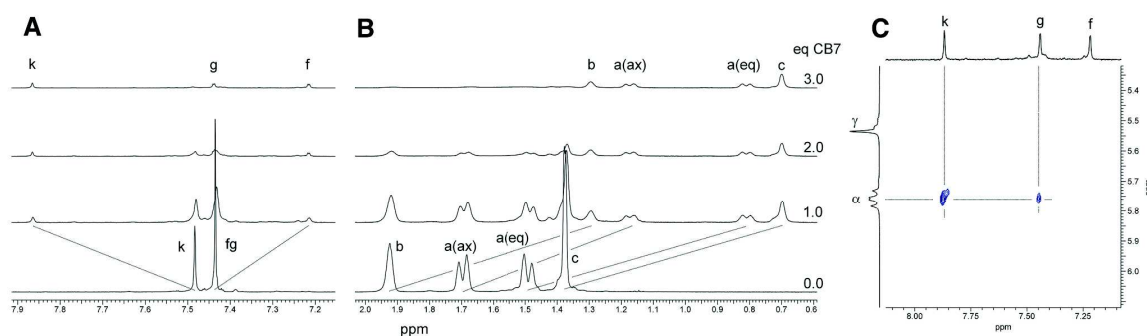


Fig. 2 Stacking plot of a portion of the ^1H NMR spectra for **1** and CB7 (a, b). A portion of the ROESY spectrum of a 1:3 mixture of **1** and CB7 (c). For signal assignment, see Fig. 1

value of the parameter $n \sim 0.33$ agrees with a stoichiometry of 1:3 in favor of CB7. The value of the association constant of the single Ad binding site, determined to be $4.8 \times 10^{10} \pm 5.6 \times 10^6 \text{ dm}^3 \text{ mol}^{-1}$, corresponds to that published for similar single cationic adamantane-based guests [41]. The thermodynamic parameters are summarized in Table 1.

Similar results were obtained for guest **2** and CB7. The only notable difference is that the binding strength of one site of **2** with CB7 is 74 times lower than that of **1** (see Table 1). This observation can be reasonably explained by the higher steric hindrance of the benzimidazolium cation in the CB7 portal.

As β -CD is the second geometrically reasonable host molecule for our guests, we continued our study by examining its binding properties towards guest **1**. Because the guest **1** interacts with β -CD in a fast exchange regime on the NMR timescale, only one set of ^1H NMR signals was observed during the titration experiment, and the continuous variations method had to be used separately for the determination of the stoichiometry of the complex. The Job plot for **1** and β -CD is displayed in Fig. 3c. The position of the curve maximum was observed for $x_{\text{guest}} = 0.25$ and matches the expectation for a 1:3 complex. Figure 3a shows the changes in the chemical shifts of selected H-atoms of guest **1** during the titration with β -CD in D_2O . The signals of H-atoms positioned inside the β -CD cavity are generally known to be shifted downfield [56]. As seen in Fig. 3a, the

adamantane H-atoms are markedly deshielded. Additionally, the ROESY spectrum (Fig. 3b) was recorded for a mixture containing **1** and β -CD in a 1:5 molar ratio to observe the intermolecular interactions between adamantane hydrogen atoms H(a), H(b), and H(c) and inner β -CD hydrogen atoms H(3) and H(5). Therefore, we can deduce from the ^1H NMR titration experiment and ROESY spectrum that the adamantane cage was included into the β -CD cavity to form the **1**@ β -CD $_3$ complex, similarly to **1**@CB7 $_3$. The above-mentioned inferences based on the NMR data are in good agreement with results from the titration calorimetry experiments. As it can be seen in Table 1, β -CD forms a 3:1 aggregate with both guest **1** and **2**. Note that, contrarily to the CB7 complexes, there is only an insubstantial difference between the association constants of **1** and **2** with β -CD. Because the glucose units in the β -CD macrocycle are linked by only one line of O-bridges in contrast to the couples of methylene bridges in CB7, the β -CD molecule is much more flexible than CB7. Therefore, β -CD better accommodates bulkier guest molecules, *i.e.*, the replacement of imidazolium with benzimidazolium has no significant impact on the binding strength.

Ternary systems

When we ascertained the formation of 1:3 binary aggregates consisting of guests **1** or **2** and β -CD or CB7, we

Table 1 ITC-determined values of the thermodynamic parameters for the interactions of **1** and **2** with CB7 and β -CD

Guest	Host	K [$\text{dm}^3 \text{ mol}^{-1}$] ^a	$-\Delta\text{H}$ [kJ mol^{-1}]	$-\Delta\text{S}$ [$\text{J mol}^{-1}\text{K}^{-1}$]	n
1	β -CD	$1.02 \times 10^5 \pm 1.29 \times 10^3$	85.7 ± 5.4	186.7	$0.367 \pm 1 \times 10^{-3}$
2	β -CD	$1.21 \times 10^5 \pm 1.19 \times 10^3$	98.8 ± 0.3	228.6	$0.312 \pm 1 \times 10^{-3}$
1	CB7 ^b	$4.84 \times 10^{10} \pm 5.63 \times 10^6$	173.8 ± 1.0	369.0	$0.391 \pm 1 \times 10^{-3}$
2	CB7 ^c	$6.52 \times 10^8 \pm 1.23 \times 10^6$	187.2 ± 1.7	450.8	$0.373 \pm 2 \times 10^{-3}$

^a The K values are reported for the single binding site

^b L-phenylalanine

^c 1-butyl-3-methylimidazolium bromide was used as a competitor

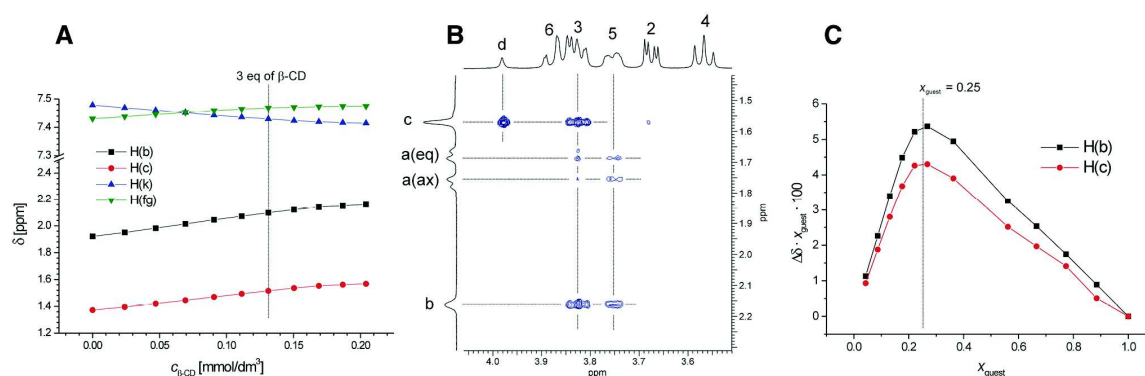


Fig. 3 A plot of the complexation-induced ¹H NMR shifts of selected H-atoms of **1** against the concentration of β -CD (a). A portion of the ROESY spectrum of a 1:3 mixture of **1** and β -CD (b). Job plot for **1** and β -CD based on ¹H NMR data (c). For signal assignment, see Fig. 1

turned our attention to the ternary systems containing a guest and all the combinations of the β -CD and CB7 hosts. Because we revealed that the behavior of **1** and **2** is very similar, we will focus on the behavior of guest **1** in following discussion. First, we attempted to prepare the mixture with predominating **1**@(β -CD, CB7)₂ complex in D₂O. As described above, it is easy to follow the degree of occupation of the Ad sites by CB7 units with ¹H NMR. Thus, we titrated a solution of **1** with CB7 until the ratio of the normalized integral intensity of the signal of the complexed and free guest reached a value of 2.0. In such a solution, two-thirds of total amount of binding sites were occupied and **1**@CB7₂ complex predominated. It should be noted that minor portions of free **1**, **1**@CB7, and **1**@CB7₃ can be also present, however, only one set of signals for bound and one set of signals for free Ad binding sites was observed in the ¹H NMR spectrum. Consecutively, we added a solution of β -CD in a stepwise manner to reveal whether the remaining Ad binding sites can be complexed by β -CD. As seen in Fig. 4a, the addition of β -CD led to the downfield shift of the signals of the Ad that is not complexed to CB7. Considering the above-discussed binding behavior of **1** and β -CD, this observation suggests the inclusion of the remaining adamantane cage into the β -CD cavity. The ROESY spectrum recorded for a 1:2:2 mixture of **1**, β -CD, and CB7 supports this suggestion by displaying cross-peaks related to the intermolecular interaction of the adamantane cage and β -CD (Fig. 4b).

Similarly, we prepared mixture in D₂O containing a ternary aggregate **1**@(β -CD₂, CB7) predominantly. First, we titrated a solution of **1** with CB7 to obtain a mixture in which a third of Ad sites were occupied by CB7, i.e., **1**@CB7 predominated. The consecutive addition of the β -CD solution led to the significant deshielding of the H-atoms of the adamantane cage that was not yet included into CB7. Similarly to the previous case, the ROESY

spectrum of the mixture containing a 1:3:1 solution of **1**, CB7, and β -CD revealed the intermolecular interactions between the inner β -CD protons and the Ad cage (Fig. 5c). These observations are consistent with our expectation that the free Ad positions can be occupied by β -CD units. However, the above-mentioned results do not imply that all free Ad sites were occupied by β -CD. Therefore, we constructed a Job plot where one component was the mixture of **1** and CB7 (1:1) and the second was β -CD. As shown in Fig. 5a, we observed a maximum on the Job plot at $x_{\beta\text{-CD}} = 0.33$, evidencing the occupation of all of the free Ad sites. Thus, we assume that the **1**@(β -CD₂,CB7) complex predominated in the mixture in addition to minor portions of **1**@(β -CD,CB7₂), **1**@ β -CD₃, and **1**@CB7₃.

Finally, we confirmed by means of ¹H NMR that all the ternary complexes consisting of guest **1** or **2** and β -CD and CB7 can be converted to **1**@CB7₃ and **2**@CB7₃ by addition of a sufficient amount of CB7 into the solution. Considering the respective selectivity of **1** and **2** towards β -CD/CB7 (expressed as $K_{\beta\text{-CD}} \times K_{\text{CB7}}^{-1}$) of 2.1×10^{-6} and 1.9×10^{-4} , it is not surprising that β -CD was readily replaced by CB7 units when CB7 was added. Although such a result was expected, it is important to acknowledge that the replacement process was fast on the NMR time-scale. Additionally, we performed a competitive experiment using ITC. We placed the $0.54 \text{ mmol dm}^{-3}$ CB7 solution into cell and we added the mixture containing **1** ($1.60 \text{ mmol dm}^{-3}$) and β -CD ($15.4 \text{ mmol dm}^{-3}$) portion wise. According to the Rekharsky approach [40], the single site association constant for **1**@CB7₃ was calculated to be of $2.95 \times 10^{10} \text{ dm}^3 \text{ mol}^{-1}$. This K value is in very good agreement with that obtained via competitive titration described above (see Table 1). The stoichiometric parameter $n = 0.37$ suggest the replacement of β -CD units by CB7 at all of the binding sites. Accordingly, guests **1** and **2** can be considered to be supramolecular cross-linkers for β -

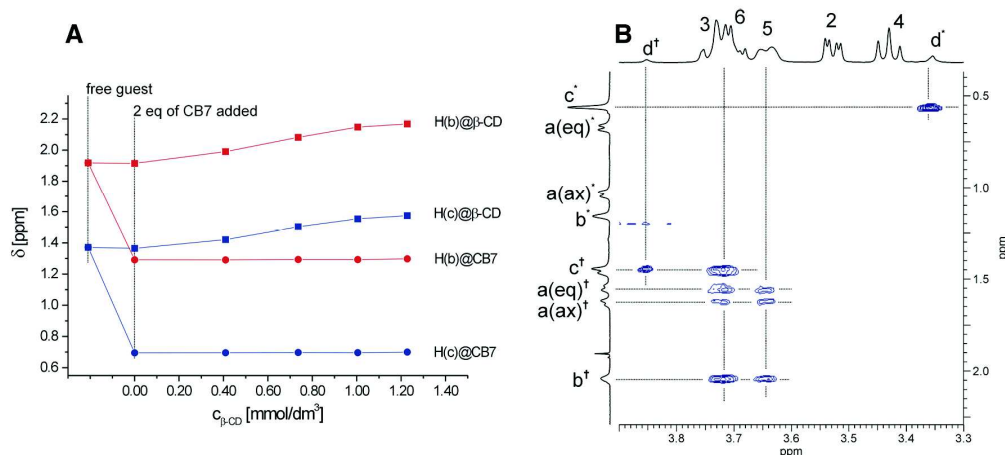


Fig. 4 A plot of the complexation-induced ^1H NMR shifts of selected H-atoms of **1** against the concentration of β -CD (a). A portion of the ROESY spectrum of a 1:2:2 mixture of **1**, CB7, and β -CD (b). For

signal assignment, see Fig. 1. * and † assign signals to the guests bound to CB7 and β -CD, respectively

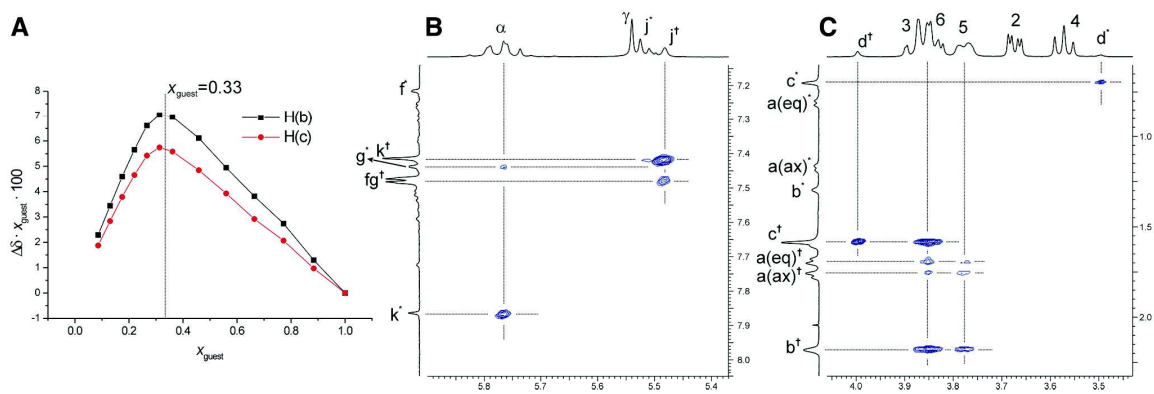


Fig. 5 Job plot for **1**@CB7 as a “guest” and β -CD based on ^1H NMR data (a). A portion of the ROESY spectrum of a 1:3:1 mixture of **1**, CB7, and β -CD (b, c). For signal assignment, see Fig. 1. * and † assign signals to the guest bound to CB7 and β -CD, respectively

CD-modified polymer chains, and CB7 can be considered to be an efficient disturbing agent. The examined complexation modes of **1**, β -CD, and CB7 are outlined in Fig. 6.

Mass spectrometry

In addition to the NMR and ITC measurements, we attempted to confirm the presence of the considered aggregates in aqueous solution by means of electrospray ionization mass spectrometry (for details, see the “Experimental section” section). In the mixture of a particular guest and CB7 in a molar ratio of 1:3, we observed minor signals (22 and 18 % for ligand **1** and **2**, respectively) related to the $[\text{G}^{3+}\cdot 3\text{CB7}]^{3+}$ aggregates; however, the base

peaks were assigned as $[\text{G}^{3+}\cdot 3\text{CB7}\cdot \text{H}^+]^{4+}$. Moreover, a $[\text{G}^{3+}\cdot 3\text{CB7}\cdot 2\text{H}^+]^{5+}$ aggregate was observed in the case of ligand **2**. Subsequently, we analyzed mixtures of guest **1** or **2** with 5 eq of β -CD to observe the signals related to $[\text{G}^{3+}\cdot \beta\text{-CD}]^{3+}$, $[\text{G}^{3+}\cdot 2\beta\text{-CD}]^{3+}$, and $[\text{G}^{3+}\cdot 3\beta\text{-CD}]^{3+}$. All of these aggregates consecutively released neutral β -CD units upon collision-induced dissociation (CID) treatment.

Finally, we turned our attention to the aqueous mixtures containing ligand **1** or **2**, CB7, and β -CD. The above-discussed $\text{G}^{3+}\cdot \text{CB7}_n\cdot \beta\text{-CD}_m$ ($n, m = 1$ or 2) ternary aggregates were unambiguously detected when a mixture of the guest with 1 eq of CB7 and 5 eq of β -CD in water was analyzed. The representative ESI-MS result for the ternary mixture is depicted in Fig. 7a. The three groups of signals related to the complexes of **1** with one, two, or three host

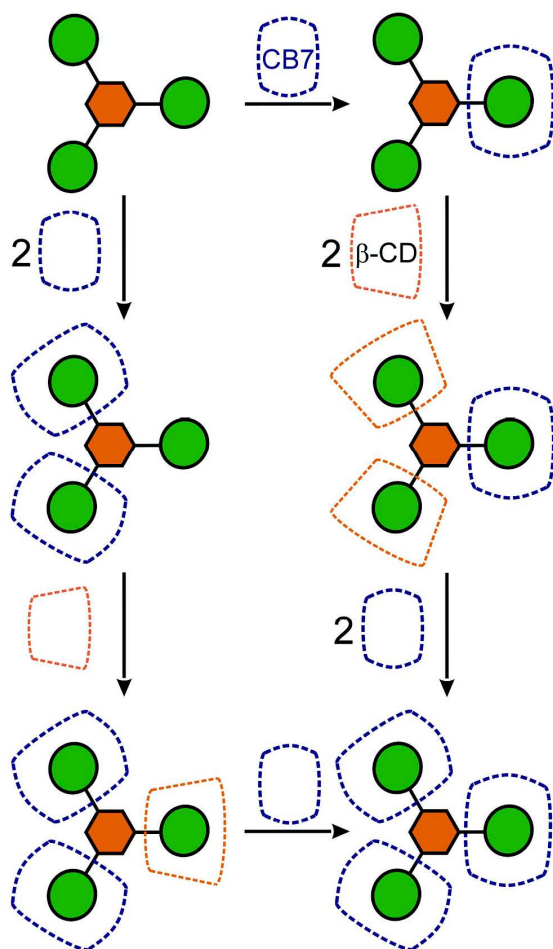


Fig. 6 Supramolecular aggregates and their transformation considered upon ^1H NMR data

molecules can be clearly seen along with the signals of the free guest and hosts. Under CID conditions, the aggregates **1**-CB7-2 β -CD and **1**-2CB7- β -CD released a neutral β -CD unit to produce **1**-CB7 and **1**-2CB7, respectively (see Fig. 7B and 7C). Further CID treatment of these aggregates led to the decomposition of either the guest or the host molecules.

Conclusion

In conclusion, we describe herein a synthetic procedure towards new C_3 -symmetrical homotritypic guests based on imidazolium cations and adamantane binding sites. We demonstrated using ^1H NMR spectrometry that guests **1** and **2** form 1:3 complexes with CB7 or β -CD. Using isothermal titration calorimetry, we determined the

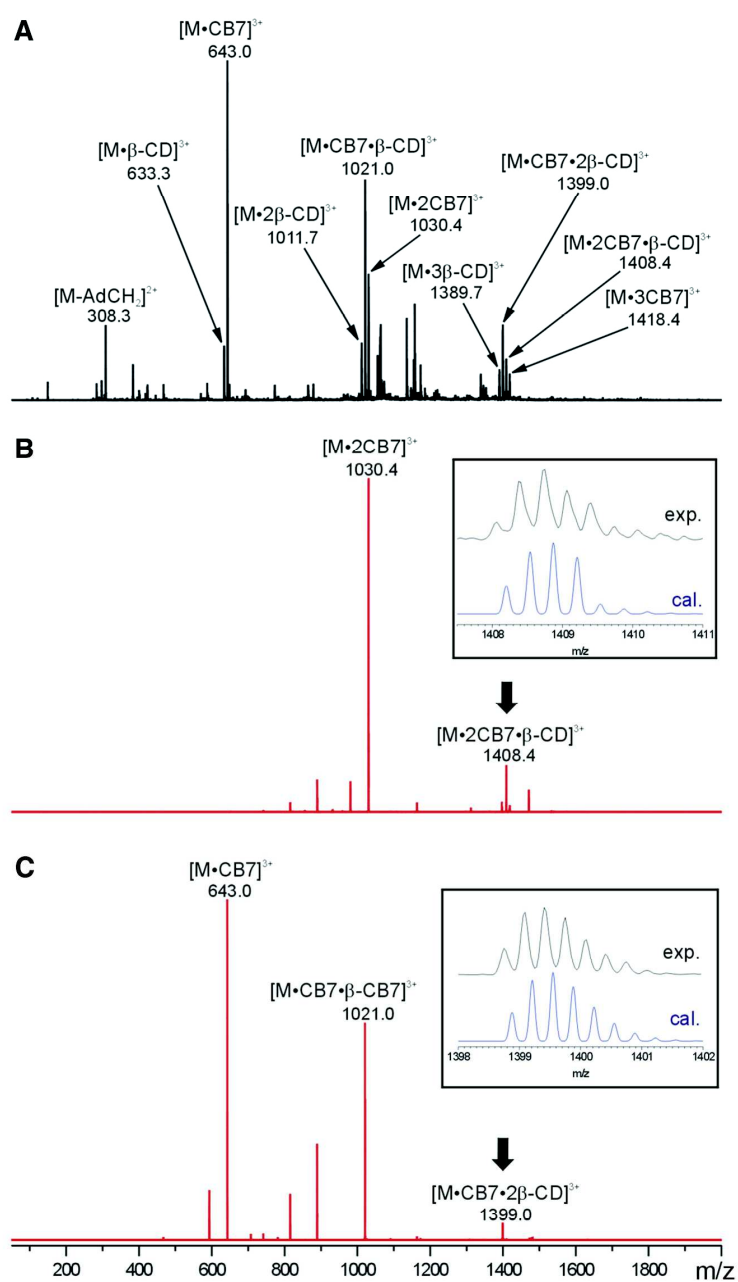
association constants of the guests with β -CD and CB7 to be in the order of 10^5 and $10^{9-10} \text{ dm}^3 \text{ mol}^{-1}$, respectively. Furthermore, we demonstrated the formation of ternary aggregates with all the mutual combinations of β -CD and CB7 based on both ligands **1** and **2** (i.e., $\text{G} @ (\beta\text{-CD}, \text{CB7}_2)$ and $\text{G} @ (\beta\text{-CD}_2, \text{CB7})$). Finally, we demonstrated that the β -CD units in any of the examined aggregates can be readily replaced by CB7. The thermodynamic selectivity of guest **1** and **2** towards β -CD/CB7 was determined to be of 2.1×10^{-6} and 1.9×10^{-4} . In our future work, we will test the guests **1** and **2** as cross-linkage agents for cyclodextrin-modified polymers. Considering the mentioned selectivity, we believe that the preferred host CB7 can be used as a modulator of the cross-linkage process to finely tune physical properties of final hydrogels.

Experimental section

General

All solvents, reagents and starting compounds (if not mentioned otherwise) were of analytical grade, purchased from commercial sources and used without further purification. 1-(1-Adamantylmethyl)imidazole and 1-(1-adamantylmethyl)benzimidazole were prepared as described previously [54]. Melting points were measured on a Kofler block and are uncorrected. Elemental analyses (C, H and N) were determined with a Thermo Fisher Scientific Flash EA 1112. NMR spectra were recorded at 303 K on a Bruker Avance III 500 spectrometer operating at frequencies of 500.11 MHz (^1H) and 125.77 MHz (^{13}C) and on a Bruker Avance III 300 spectrometer operating at frequencies of 300.13 MHz (^1H) and 75.77 MHz (^{13}C). ^1H - and ^{13}C -NMR chemical shifts were referenced to the signal of the solvent [^1H : $\delta(\text{residual HDO}) = 4.70 \text{ ppm}$, $\delta(\text{residual DMSO-}d_5) = 2.50 \text{ ppm}$; ^{13}C : $\delta(\text{DMSO-}d_6) = 39.52 \text{ ppm}$]. The spin-lock for ROESY was adjusted to 400 ms. The signal multiplicity is indicated by “s” for singlet, “d” for doublet, and “um” for unresolved multiplet. IR spectra were recorded using a Smart OMNI-Transmission Nicolet iS10 spectrophotometer. Samples were measured in KBr pellets. Electrospray mass spectra (ESI-MS) were recorded using an amaZon X ion-trap mass spectrometer (Bruker Daltonics, Bremen, Germany) equipped with an electrospray ionization source. All the experiments were conducted in the positive-ion polarity mode. The instrumental conditions used to measure the single imidazolium salts and their mixtures with the host molecules were different; therefore, they are described separately. *Single imidazolium salts*: Individual samples (with concentrations of $0.5 \mu\text{g cm}^{-3}$) were infused into the ESI source in methanol:water (1:1, v:v) solutions using a syringe pump

Fig. 7 ESI–MS spectra of the mixture of **1**, CB7, and β -CD in a 1:1:5 molar ratio in water. The positive ion first-order mass spectrum (a); ESI–MS/MS spectrum of ions at m/z 1408 (b) and 1399 (c). Precursor ions are marked with a *bold downward arrow*. *Inserted boxes* display the experimental and calculated [57] precursor ions



with a constant flow rate of $4 \mu\text{l min}^{-1}$. The other instrumental conditions were as follows: an electrospray voltage of -4.2 kV , a capillary exit voltage of 140 V , a drying gas temperature of $220 \text{ }^\circ\text{C}$, a drying gas flow rate of $6.0 \text{ dm}^3 \text{ min}^{-1}$ and a nebulizer pressure of 55.16 kPa . *Host–guest complexes*: An aqueous solution of the guest molecule ($6.25 \mu\text{M}$) and the corresponding host molecule

(3.0 eq of CB7 and 5.0 eq of β -CD, respectively) for the binary complexes or an aqueous solution of the guest molecule ($6.25 \mu\text{M}$), CB7 (1.0 eq), and β -CD (5.0 eq) for the ternary complexes was infused into the ESI source at a constant flow rate of $4 \mu\text{l min}^{-1}$. The other instrumental conditions were as follows: an electrospray voltage of -4.0 kV , a capillary exit voltage of 140 up to -50 V , a

drying gas temperature of 300 °C, a drying gas flow rate of 6.0 dm³ min⁻¹, and a nebulizer pressure of 206.84 kPa. Nitrogen was used as both the nebulizing and drying gas for all of the experiments. Tandem mass spectra were collected using CID with He as the collision gas after the isolation of the required ions. Isothermal titration calorimetry measurements were carried out in H₂O using a VP-ITC MicroCal instrument at 303 K. The concentrations of the host in the cell and the guest in the microsyringe were approximately 0.13–0.15 and 0.46–0.50 mM, respectively. The raw experimental data were analyzed with the MicroCal ORIGIN software. The heats of dilution were taken into account for each guest compound. The data were fitted to a theoretical titration curve using the ‘One Set of Binding Sites’ model. A 1-methyl-3-butylimidazolium bromide and an α -phenylalanine with respective association constants of 1.17×10^7 and 6.72×10^6 dm³ mol⁻¹ were used as competitors [40].

General procedure for the preparation of guests 1 and 2

1,3,5-Tris(bromomethyl)benzene (TBMB) (0.10 g, 0.28 mmol) was dissolved in 3 cm³ of dry toluene and 3.2 equivalents of 1-adamantylmethylimidazole/benzimidazole were added. The mixture was stirred for several hours at 100 °C until the starting TBMB disappeared according to TLC. The crude product was precipitated by freshly distilled dry THF and separated by centrifugation. The solid material was triturated with THF several times, isolated by centrifugation, and dried under vacuum to a constant weight.

$\alpha, \alpha', \alpha''$ -Tris(3-(1-(1-adamantylmethyl)imidazolium))-mesitylene tribromide (1)

$\alpha, \alpha', \alpha''$ -Tris(3-(1-(1-adamantylmethyl)imidazolium))mesitylene tribromide (1) was isolated as a colorless microcrystalline powder with a yield of 0.30 g (99 % with respect to TBMB). Mp = 204–206 °C, Anal. Calcd for C₅₁H₆₉Br₃N₆·4H₂O (1077.91) C, 56.83 %; H, 7.20 %; N, 7.80 %; found C, 57.12 %; H, 7.19 %; N, 7.53 %. ¹H NMR (DMSO-*d*₆): δ = 1.45 (um, 18H, Hc), 1.55 (um, 9H, Ha_{eq}), 1.67 (um, 9H, Ha_{ax}), 1.96 (um, 9H, Hb), 3.98 (s, 6H, Hd), 5.52 (s, 6H, Hj), 7.62 (s, 3H, Hk), 7.71 (um, 3H, Hf), 7.90 (um, 3H, Hg), 9.50 (um, 3H, He) ppm. ¹³C NMR (DMSO-*d*₆): δ = 27.4 (Cb), 33.2 (Cc—C), 36.0 (Ca), 38.9 (Cc), 51.3 (Cj), 59.9 (Cd), 122.0 (Cg), 124.3 (Cf), 128.8 (Ck), 136.2 (Cj—C), 136.9 (Ce) ppm. IR (KBr): 651(m), 750(m), 876(w), 1105(m), 1134(m), 1157(s), 1176(m), 1449(s), 1559(s), 2846(s), 2902(s), 3065(m), 3127(m), 3415(bs) cm⁻¹. ESI-MS: m/z 149.3 [AdCH₂]⁺, 255.3 M³⁺, 308.3 [M³⁺–149⁺]²⁺, 382.4 [M³⁺–H⁺]²⁺, 422.3 [M³⁺+⁷⁹Br⁻]²⁺.

$\alpha, \alpha', \alpha''$ -Tris(3-(1-(1-adamantylmethyl)benzo[d]imidazolium))-mesitylene tribromide (2)

$\alpha, \alpha', \alpha''$ -Tris(3-(1-(1-adamantylmethyl)benzo[d]imidazolium))-mesitylene tribromide (2) was isolated as a colorless microcrystalline powder with a yield of 0.24 g (69 % with respect to TBMB). Mp = 273–275 °C, Anal. Calcd for C₆₃H₇₅Br₃N₆·5H₂O (1246.10) C, 60.72 %; H, 6.88 %; N, 6.74 %; found C, 60.64 %; H, 6.64 %; N, 6.53 %. ¹H NMR (DMSO-*d*₆): δ = 1.55–1.57 (um, 27H, Hc, Ha_{eq}), 1.65 (um, 9H, Ha_{ax}), 1.95 (um, 9H, Hb), 4.34 (s, 6H, Hd), 5.81 (s, 6H, Hj), 7.47 (dd, *J* = 7.9, 3H, Hh), 7.64 (dd, *J* = 8.0, 3H, Hg), 7.82 (d, *J* = 8.4, 3H, Hi), 7.88 (s, 3H, Hk), 8.14 (d, *J* = 8.5, 3H, Hf), 10.20 (s, 3H, He) ppm. ¹³C NMR (DMSO-*d*₆): δ = 27.4 (Cb), 34.3 (Cc—C), 35.9 (Ca), 39.1 (Cc), 49.3 (Cj), 57.3 (Cd), 113.5 (Cf), 114.4 (Ci), 126.2 (Ch), 126.5 (Cg), 128.7 (Ck), 130.2 (Cf—C), 132.6 (Ci—C), 135.6 (Cj—C), 143.2 (Ce) ppm. IR (KBr): 1177(m), 1200(m), 1344(m), 1366(m), 1426(m), 1448(m), 1559(s), 2846(s), 2901(s), 3405(bs) cm⁻¹. ESI-MS; m/z 149.1 [AdCH₂]⁺, 305.2 M³⁺, 383.3 [M³⁺–AdCH₂]²⁺, 497.3 [M³⁺+⁷⁹Br⁻]²⁺.

Acknowledgments This work was supported by the Internal Funding Agency of the Tomas Bata University in Zlín under Grant IGA/FT/2015/005.

References

- Xing, M., Yanli, Z.: Biomedical applications of supramolecular systems based on host–guest interactions. *Chem. Rev.* **115**, 7794–7839 (2015)
- Li, M., Zhou, C., Quanzhu, Y., Xiaogang, Y., Chao, Z., Liqiong, L.: Polymeric supramolecular materials and their biomedical applications. *Curr. Org. Chem.* **18**, 1937–1947 (2014)
- Wang, D., Tong, G., Dong, R., Zhou, Y., Shen, J., Zhu, X.: Self-assembly of supramolecularly engineered polymers and their biomedical applications. *Chem. Commun.* **50**, 11994–12017 (2014)
- Dong, R., Zhou, Y., Zhu, X.: Supramolecular dendritic polymers: from synthesis to applications. *Acc. Chem. Res.* **47**, 2006–2016 (2014)
- Hu, J., Liu, S.: Engineering responsive polymer building blocks with host–guest molecular recognition for functional applications. *Acc. Chem. Res.* **47**, 2084–2095 (2014)
- Zhang, J., Ma, P.X.: Cyclodextrin-based supramolecular systems for drug delivery: recent progress and future perspective. *Adv. Drug. Deliv. Rev.* **65**, 1215–1233 (2013)
- Kejik, Z., Kaplanek, R., Briza, T., Kralova, J., Martasek, P., Kral, V.: Supramolecular approach for target transport of photodynamic anticancer agents. *Supramol. Chem.* **24**, 106–116 (2012)
- De Greef, T.F.A., Smulders, M.M.J., Wolfs, M., Schenning, A.P.H.J., Sijbesma, R.P., Meijer, E.W.: Supramolecular polymerization. *Chem. Rev.* **109**, 5687–5754 (2009)
- Dong, S., Bo, Z., Wang, F., Huang, F.: Supramolecular polymers constructed from macrocycle-based host–guest molecular recognition motifs. *Acc. Chem. Res.* **47**, 1982–1994 (2014)
- Charlot, A., Velty, R.A.: Novel hyaluronan-based supramolecular assemblies stabilized by multivalent specific interactions:

- rheological behavior in aqueous solution. *Macromolecules* **40**, 9555–9563 (2007)
11. Layre, A.M., Volet, G., Wintgens, V., Amiel, C.: Associative network based on cyclodextrin polymer: a model system for drug delivery. *Biomacromolecules* **10**, 3283–3289 (2009)
 12. Li, L., Guo, X., Wang, J., Liu, P., Frud'homme, R.K., May, B.L., Lincoln, S.F.: Polymer networks assembled by host–guest inclusion between adamantyl and β -cyclodextrin substituents on poly(acrylic acid) in aqueous solution. *Macromolecules* **41**, 8677–8681 (2008)
 13. Heyden, A.V., Wilczewski, M., Labbe, P., Auzely, R.: Multilayer films based on host–guest interactions between biocompatible polymers. *Chem. Commun.* 3220–3222 (2006)
 14. Charlot, A., Vely, R.A.: Synthesis of novel supramolecular assemblies based on hyaluronic acid derivatives bearing bivalent β -cyclodextrin and adamantane moieties. *Macromolecules* **40**, 1147–1158 (2007)
 15. Li, C., Luo, G.F., Wang, H.Y., Zhang, J., Gong, Y.H., Cheng, S.X.: Host–guest assembly of pH-responsive degradable microcapsules with controlled drug release behavior. *J. Phys. Chem.* **115**, 17651–17659 (2011)
 16. Bistri, O., Mazeau, K., Vely, R.A., Sollogoub, M.: A hydrophilic cyclodextrin duplex forming supramolecular assemblies by physical cross-linking of a biopolymer. *Chem. Eur. J.* **13**, 8847–8857 (2007)
 17. Nally, R., Isaacs, L.: Toward supramolecular polymers incorporating double cavity cucurbituril hosts. *Tetrahedron* **65**, 7249–7258 (2009)
 18. Liu, Y., Fang, R., Tan, X., Wang, Z., Zhang, X.: Supramolecular polymerization at low monomer concentrations: enhancing intermolecular interactions and suppressing cyclization by rational molecular design. *Chem. Eur. J.* **18**, 15650–15654 (2012)
 19. Galantini, L., Jover, A., Leggio, C., Mejjide, F., Pavel, N.V., Tellini, V.H.S., Tato, J.V., Tortolini, C.: Early stages of formation of branched host–guest supramolecular polymers. *J. Phys. Chem. B* **112**, 8536–8541 (2008)
 20. Leggio, C., Anselmi, M., Nola, A.D., Galantini, L., Jover, A., Mejjide, F., Pavel, N.V., Tellini, V.H.S., Tato, J.V.: Study on the structure of host–guest supramolecular polymers. *Macromolecules* **40**, 5899–5906 (2007)
 21. Hasegawa, Y., Miyachi, M., Takashima, Y., Harada, A.: Supramolecular polymers formed from β -cyclodextrins dimer linked by poly(ethylene glycol) and guest dimers. *Macromolecules* **38**, 3724–3730 (2005)
 22. Krishnan, R., Gopidas, K.: β -Cyclodextrin as an end-to-end connector. *J. Phys. Chem. Lett.* **2**, 2094–2098 (2011)
 23. Ohga, K., Takashima, Y., Takahashi, H., Kawaguchi, Y., Yamaguchi, H., Harada, A.: Preparation of supramolecular polymers from a cyclodextrin dimer and ditopic guest molecules: control of structure by linker flexibility. *Macromolecules* **38**, 5897–5904 (2005)
 24. Miyawaki, A., Takashima, Y., Yamaguchi, H., Harada, A.: Branched supramolecular polymers formed by bifunctional cyclodextrin derivatives. *Tetrahedron* **64**, 8355–8361 (2008)
 25. Bohm, I., Isenbugel, K., Ritter, H., Branscheid, R., Kolb, U.: Cyclodextrin and adamantane host–guest interactions of modified hyperbranched poly(ethylene imine) as mimetics for biological membranes. *Angew. Chem. Int. Ed.* **50**, 7896–7899 (2011)
 26. Schmidt, B.V.K.J., Rudolph, T., Hetzer, M., Ritter, H., Schacher, F.H., Barner-Kowollik, C.: Supramolecular three-armed star polymers via cyclodextrin host–guest self-assembly. *Polym. Chem.* **3**, 3139–3145 (2012)
 27. Bednařková, T., Tošner, Z., Horský, J., Jindřich, J.: Synthesis of C_3 -symmetric tri(alkylamino) guests and their interaction with cyclodextrins. *J. Incl. Phenom. Macrocycl. Chem.* **81**, 141–152 (2015)
 28. Takashima, Y., Yuting, Y., Otsubo, M., Yamaguchi, H., Harada, A.: Supramolecular hydrogels formed from poly(viologen) cross-linked with cyclodextrin dimers and their physical properties. *Beilstein J. Org. Chem.* **8**, 1594–1600 (2012)
 29. Osman, S.K., Brandl, F.P., Zayed, G.M., Tebmer, J.K., Gopferich, A.M.: Cyclodextrin based hydrogels: inclusion complex formation and micellization of adamantane and cholesterol grafted polymers. *Polymer* **52**, 4806–4812 (2011)
 30. Koopmans, C., Ritter, H.: Formation of physical hydrogels via host–guest interactions of β -cyclodextrin polymers and copolymers bearing adamantyl groups. *Macromolecules* **41**, 7418–7422 (2008)
 31. Crini, G.: Review: a history of cyclodextrins. *Hist. Cyclodextr. Chem. Rev.* **114**, 10940–10975 (2014)
 32. Del Valle, E.M.M.: Cyclodextrins and their uses: a review. *Process Biochem.* **39**, 1033–1046 (2004)
 33. Kraus, T.: Modified cyclodextrins with pendant cationic and anionic moieties as hosts for highly stable inclusion complexes and molecular recognition. *Curr. Org. Chem.* **15**, 802–814 (2011)
 34. Bricout, H., Hapiot, F., Ponchel, A., Tilloy, S., Monflier, F.: Chemically modified cyclodextrins: an attractive class of supramolecular hosts for the development of aqueous biphasic catalytic processes. *Sustainability* **1**, 924–945 (2009)
 35. Brewster, M.E., Loftsson, T.: The use of chemically modified cyclodextrins in the development of formulations for chemical delivery systems. *Pharmazie* **57**, 94–101 (2002)
 36. Hattori, K., Ikeda, H.: Modification reactions of cyclodextrins and the chemistry of modified cyclodextrins. In: Dodziuk, H. (ed.) *Cyclodextrins and their complexes*, pp. 31–64. Wiley-VCH, Weinheim (2006)
 37. Isaacs, L.: Cucurbit[n]urils: from mechanism to structure and function. *Chem. Commun.* 619–629 (2009)
 38. Isaacs, L.: Stimuli responsive systems constructed using cucurbit[n]uril-type molecular containers. *Acc. Chem. Res.* **47**, 2053–2062 (2014)
 39. Kaifer, A.E.: Toward reversible control of cucurbit[n]uril complexes. *Acc. Chem. Res.* **47**, 2160–2167 (2014)
 40. Rekharsky, M.V., Mori, T., Yang, C., Ko, Y.H., Selvapalam, N., Kim, H., Sobransingh, D., Kaifer, A.E., Liu, S., Isaacs, L., Chen, W., Moghaddam, S., Gilson, M.K., Kim, K., Inoue, Y.: A synthetic host–guest system achieves avidin–biotin affinity by overcoming enthalpy–entropy compensation. *Proc. Natl. Acad. Sci. USA* **104**, 20737–20742 (2007)
 41. Moghaddam, S., Yang, C., Rekharsky, M.V., Ko, Y.H., Kim, K., Inoue, Y., Gilson, M.K.: New ultrahigh affinity host–guest complexes of cucurbit[7]uril with bicyclo[2.2.2]octane and adamantane guests: thermodynamic analysis and evaluation of M2 affinity calculations. *J. Am. Chem. Soc.* **133**, 3570–3581 (2011)
 42. Cao, L., Šekutor, M., Zavalij, P.Y., Mlinarić-Majerski, K., Glaser, R., Isaacs, L.: Cucurbit[7]uril-guest pair with an attomolar dissociation constant. *Angew. Chem. Int. Ed.* **53**, 988–993 (2014)
 43. Agrigento, P., Al-Amsyar, S.M., Soree, B., Taherimehr, M., Gruttaduria, M., Aprile, C., Pescarmona, P.P.: Synthesis and high-throughput testing of multilayered supported ionic liquid catalysts for the conversion of CO₂ and epoxides into cyclic carbonates. *Catal. Sci. Tech.* **4**, 1598–1607 (2014)
 44. Ghosh, D., Lee, J.Y., Liu, C.Y., Chiang, Y.H., Lee, H.M.: Direct C–H arylations of unactivated arenes catalyzed by amido-functionalized imidazolium salts. *Adv. Synth. Catal.* **356**, 406–410 (2014)
 45. Byeun, A., Baek, K., Han, M.S., Lee, S.: Palladium-catalyzed C–S bond formation by using *N*-amido imidazolium salts as ligands. *Tetrahedron Lett.* **54**, 6712–6715 (2013)
 46. Myles, L., Gore, R.G., Gathergood, N., Connon, S.J.: A new generation of aprotic yet Brønsted acidic imidazolium salts: low toxicity, high recyclability and greatly improved activity. *Green Chem.* **15**, 2740–2746 (2013)

47. Li, H., Chen, J., Hua, L., Qiao, Y., Yu, Y., Pan, Z., Yang, H., Hou, Z.: Polyoxometalate and copolymer-functionalized ionic liquid catalyst for esterification. *Pure Appl. Chem.* **84**, 541–551 (2012)
48. Wang, Y., Robinson, G.H.: *N*-Heterocyclic carbene—main-group chemistry: a rapidly evolving field. *Inorg. Chem.* **53**, 11815–11832 (2014)
49. Hopkinson, M.N., Richter, C., Schedler, M., Glorius, F.: An overview *N*-heterocyclic carbenes. *Nature* **510**, 485–496 (2014)
50. Riener, K., Haslinger, S., Raba, A., Hogerl, M.P., Cokoja, M., Herrmann, W.A., Kuhn, F.E.: Chemistry of iron *N*-heterocyclic carbene complexes: syntheses, structures, reactivities, and catalytic applications. *Chem. Rev.* **114**, 5215–5272 (2014)
51. Chauhan, P., Enders, D.: *N*-Heterocyclic carbene catalyzed activation of esters: a new option for asymmetric domino reactions. *Angew. Chem. Int. Ed.* **53**, 1485–1487 (2014)
52. Ranganath, K.V.S., Onitsuka, S., Kumar, A.K., Inanaga, J.: Recent progress of *N*-heterocyclic carbenes in heterogeneous catalysis. *Catal. Sci. Tech.* **3**, 2161–2181 (2013)
53. Rovis, T., Nolan, S.P.: Stable carbenes: from ‘laboratory curiosities’ to catalysis mainstays. *Synlett* **24**, 1188–1189 (2013)
54. Černochová, J., Bránná, P., Rouchal, M., Kulhánek, P., Kuřitka, I., Vicha, R.: Determination of intrinsic binding modes by mass spectrometry: gas-phase behavior of adamantylated bisimidazolium guests complexed to cucurbiturils. *Chem. Eur. J.* **18**, 13633–13637 (2012)
55. Zhao, N., Liu, L., Biedermann, F., Scherman, O.A.: Binding studies on CB[6] with a series of 1-alkyl-3-methylimidazolium ionic liquids in an aqueous system. *Chem. Asian. J.* **5**, 530–537 (2010)
56. Schneider, H.-J., Hacket, F., Rüdiger, V.: NMR studies of cyclodextrins and cyclodextrin complexes. *Chem. Rev.* **98**, 1755–1785 (1998)
57. Patiny, L., Borel, A.: ChemCalc: a building block for tomorrow’s chemical infrastructure. *J. Chem. Inf. Model.* **53**, 1223–1228 (2013)

4.7

Rotaxanes Capped with Host Molecules: Supramolecular Behavior of
Adamantylated Bisimidazolium Salts Containing a Biphenyl Centerpiece

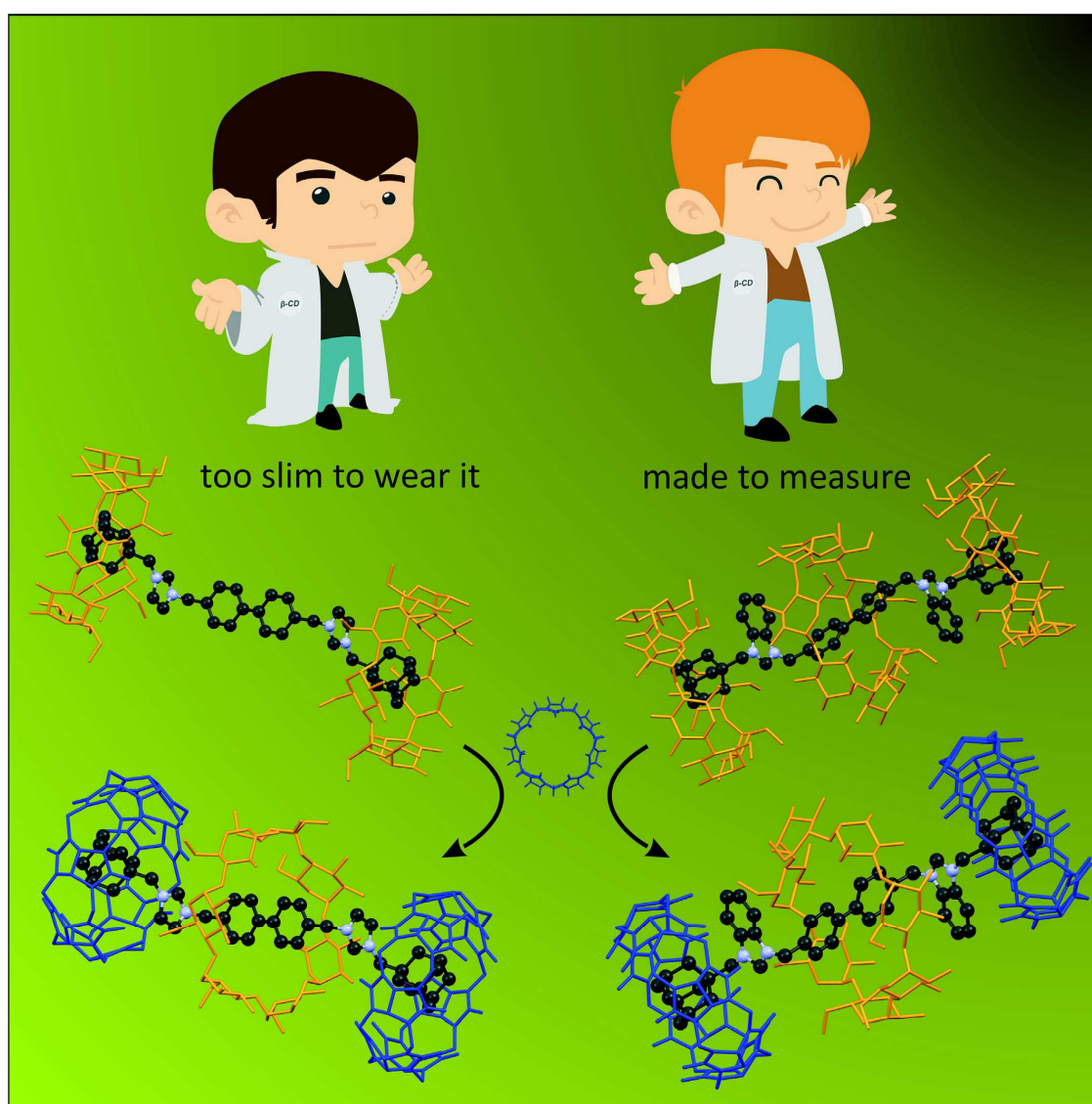
Petra Branná, Michal Rouchal, Zdeňka Prucková, , Lenka Dastychová, René Lenobel, Tomáš
Pospíšil, Kamil Maláč, Robert Vícha*

Chemistry – A European Journal **2015**, *21*, 11712–11718

Rotaxanes | *Hot Paper*

Rotaxanes Capped with Host Molecules: Supramolecular Behavior of Adamantylated Bisimidazolium Salts Containing a Biphenyl Centerpiece

Petra Branná,^[a] Michal Rouchal,^[a] Zdeňka Prucková,^[a] Lenka Dastychová,^[a] René Lenobel,^[b] Tomáš Pospíšil,^[c] Kamil Maláč,^[d] and Robert Vícha^{*[a]}



Abstract: Bisimidazolium salts with one central biphenyl binding site and two terminal adamantyl binding sites form water-soluble binary or ternary aggregates with cucurbit[7]uril (CB7) and β -cyclodextrin (β -CD) with rotaxane and pseudorotaxane architectures. The observed arrangements

result from cooperation of the supramolecular stopper binding strength and steric barriers against free slippage of the CB7 and β -CD host molecules over the bisimidazolium guest axle.

Introduction

The cucurbit[*n*]urils^[1] (CBns) and cyclodextrins^[2] (CDs) represent the two best-established families of hosts used for the construction of supramolecular systems. The structure of CD macrocycles consists of D-glucopyranoside units linked via $\alpha(1\rightarrow4)$ glycosidic bonds, forming a bottomless-cap-like cylindrical shape (Figure 1). The nonpolar cavity lined with polar hydroxy groups facilitates the inclusion of nonpolar guests within CDs with up to micromolar dissociation constants.^[3] The barrel-shaped CB molecules are composed of glycoluril units joined by pairs of methylene bridges (Figure 1). The combination of the nonpolar cavity of a CB and symmetrically equivalent portals rimmed with carbonyl groups allows an extraordinary binding affinity and selectivity, particularly towards cationic guests derived from ferrocene,^[4] the cage hydrocarbon bicyclo[2.2.2]octane,^[5] adamantane,^[5] or diamantane.^[6] The hydroxy groups on the rims of CDs can significantly participate in the stabilization of CD–CD or CB–CD aggregates via O–H...O interactions. In contrast, there is strong electrostatic repulsion between the portals of the two CB units that destabilizes arrangements with short portal–portal distances, either in pure water or metal salt solutions. However, metal cation-mediated attractive interactions between the portals of two CB units have rarely been reported in aqueous solutions containing a large excess of metal ions^[7] or in the gas phase.^[8]

Because the portals of CBs are complementary to those of cyclodextrins, H-bonds stabilize the ternary aggregates in

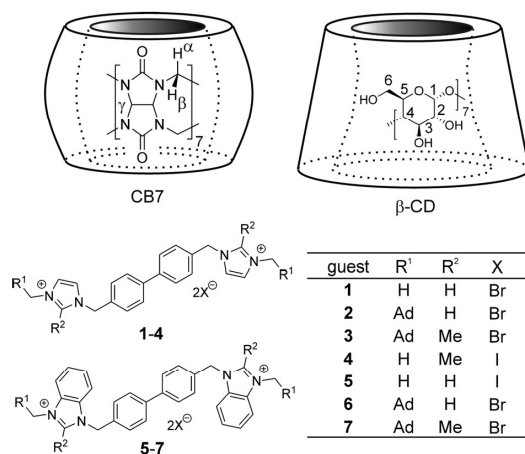


Figure 1. Structures of the bisimidazolium guests and host molecules used in this work.

a pseudorotaxane manner, in which the macrocycles surround one^[9] or two^[10] cationic centers. Even non-ionic polyethylene-glycol has been reported to thread α -CD or CB6 and α -CD units in a random order.^[11]

It should also be noted that many oligo/polypseudorotaxanes consisting solely of CB units and an axle molecule have been prepared. However, in all of these cases, each CB unit was bound to the single-cationic binding site^[12] or, more frequently, to the double-cationic site,^[13] to reduce the electrostatic repulsion between two adjacent CB portals. Recently, several multitopic guests have been used for construction of intriguing supramolecular systems under thermodynamic^[14] or kinetic^[15] control.

In our ongoing work, we aim to utilize imidazolium-based guests in supramolecular systems. Imidazolium salts, compared with the most frequently used ammonium and pyridinium salts, offer additional benefits because they can provide catalytic functions or can be transformed into N-heterocyclic carbenes to form organometallic complexes. Herein, we report a binding study of four members of a new guest family (Figure 1) that form binary and ternary (pseudo)rotaxane aggregates with CB7 and β -CD.

Results and Discussion

Rather surprisingly, there has, to our knowledge, only been one report on the supramolecular behavior of a 4,4'-biphenylene bisimidazolium salt; specifically, **1** with CB8.^[16] Owing to

[a] P. Branná, Dr. M. Rouchal, Dr. Z. Prucková, Dr. L. Dastychová, Dr. R. Vicha
Department of Chemistry
Tomas Bata University in Zlín, Faculty of Technology
Nám. T. G. Masaryka 275, 762 76 Zlín (Czech Republic)
E-mail: rvicha@ft.utb.cz

[b] Dr. R. Lenobel
Department of Protein Biochemistry and Proteomics
Palacký University, Faculty of Science
Centre of the Region Haná for Biotechnological and Agricultural Research
Šlechtitelů 27, 783 71 Olomouc-Holice (Czech Republic)

[c] Dr. T. Pospíšil
Department of Chemical Biology, Palacký University, Faculty of Science
Centre of the Region Haná for Biotechnological and Agricultural Research
Šlechtitelů 11, 783 71 Olomouc (Czech Republic)

[d] Dr. K. Maláč
Centre of Polymer Systems, Tomas Bata University in Zlín
Nad Ovčírnou 275, 760 01 Zlín (Czech Republic)

Supporting information for this article is available on the WWW under <http://dx.doi.org/10.1002/chem.201501353> and contains the experimental and synthetic details, ¹H and ¹³C NMR spectra of bisimidazolium salts 1–7, mass spectra of the free guests and their CB7 and β -CD complexes, and computational details.

this lack of information, we prepared three guests, **1**, **4** and **5** (Figure 1), incorporating a central biphenyl binding site (BiPh) and explored their binding properties towards CB7 and β -CD by means of ^1H NMR spectroscopy and titration calorimetry (ITC). According to the NMR data, guests **1** and **4** form inclusion complexes with β -CD in the fast-exchange regime, whereas guest **5** displays slow exchange (see the Supporting Information, Figures S22, S43, and S48). The ITC measurements confirmed the 1:1 stoichiometry and revealed that the binding strength positively correlates with the bulkiness of the cationic moiety (see Table 1).

Table 1. ITC-determined values of K_s and the complex stoichiometry for the interactions of **1–5** with CB7 and β -CD.

Guest	CB7		β -CD	
	K_s [M^{-1}]	n ^[a]	K_s [M^{-1}]	n ^[a]
1	4.22×10^6	1.00	3.57×10^3	1.04
2	1.35×10^{12} ^[b]	0.56	9.20×10^4	0.49
3	1.15×10^{12} ^[b]	0.50	9.87×10^4	0.44
4	–	–	5.72×10^3	0.99
5	4.43×10^6	1.01	1.01×10^4	1.06

[a] The molar fraction of the guest relative to that of the host; [b] 1-methyl-3-butylimidazolium bromide was used as a competitor.

In contrast, CB7 binds to all of the BiPh guests in the slow-exchange regime. The shielding of aromatic and methylene protons accompanied by the deshielding of methyl protons implies the inclusion of the biphenyl moiety within the CB7 cavity. According to ITC data, CB7 forms 1:1 complexes with ligands **1** and **5** with essentially the same stability (Table 1). Although the ITC data obtained for the titration of CB7 with **4** fit the Two Sets of Sites model, the final stoichiometry was 1:1 (see the Supporting Information, Figure S45). Thus, we suppose that external and inclusion complexes are in equilibrium in a solution containing an excess of CB7. However, the 1:1 inclusion complex **4**@CB7 far outweighs the external complex in a solution with an excess of guest **4**, as is evident from the NMR titration data (see the Supporting Information, Figure S44). Accordingly, we can conclude that the 4,4'-biphenylene scaffold linked by methylenes with two imidazolium, 2-methylimidazolium, or benzimidazolium cations represents a capable binding site for β -CD and CB7.

We have also investigated ternary systems of our ligands starting with compound **2**. The NMR and ITC data suggest that ligand **2** forms a binary complex with CB7 as well as with β -CD in a 1:2 stoichiometry with two host molecules occupying the terminal adamantyl sites (Ad; see the Supporting Information, Figures S27, S28, and S32). The superscript index Ad or BiPh will be used hereafter to assign the positioning of CB7 or β -CD in the complex.

The ternary aggregate **2**@(CB7^{Ad}, β -CD^{Ad}) was formed when an equimolar mixture of **2** and CB7 in D_2O was titrated with β -CD. In complex **2**@CB7, one Ad site is included inside the CB7 cavity (strongly shielded Ad protons), whereas the second Ad is free (see the Supporting Information, Figure S29). Subse-

quently, the addition of a β -CD solution led to the deshielding of the free Ad protons as the second Ad cage was included within the β -CD cavity. In the next titration experiment, the mixing mode was changed. We prepared an initial solution containing guest **2** and 3.2 equivalents of β -CD, in which the complex **2**@ β -CD₂^{Ad} predominates (Figure 2, line ii), and we subsequently added a solution of CB7. The appearance of signals of significantly shielded Ad H atoms at the expense of those related to the β -CD-bound Ad cage (Figure 2, lines iii–v) implies the replacement of the β -CD units at the Ad site with CB7. Interestingly, a new set of β -CD signals arose during this titration, as demonstrated in Figure 2 for β -CD H1, and, in addition, the BiPh signals were split into two sets (see the Supporting Information, Figure S30). The 0.98 molar ratio of guest **2** and minor β -CD was calculated from the normalized integral intensity of the Ad H_b and the minor β -CD H1 signals. Subsequent 2D DOSY-NMR spectroscopy revealed that there are two forms of β -CD differing in their diffusion coefficients D . The minor β -CD had the same D value as the ligand **2** and CB7 (for DOSY spectrum, see the Supporting Information, Figure S31). These observations can be reasonably explained by the trapping of β -CD at the BiPh site in a rotaxane manner to form a ternary aggregate **2**@(CB7₂^{Ad}, β -CD^{BiPh}) with two CB7 caps at

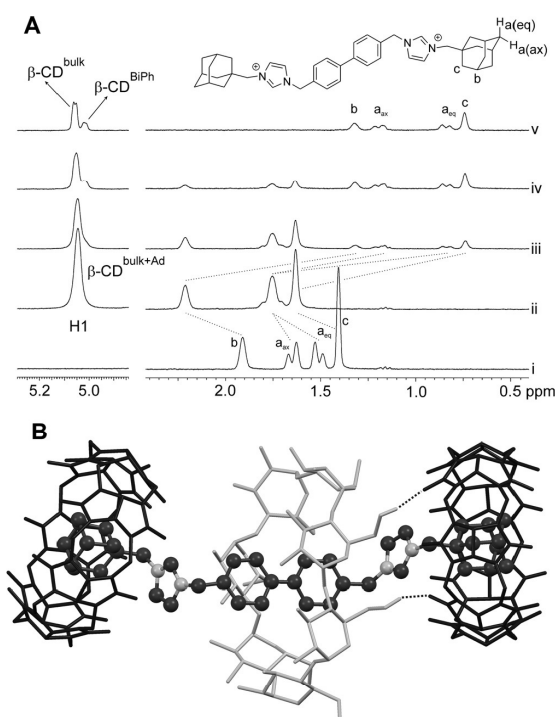


Figure 2. A) Stacking plot of a portion of the ^1H NMR spectra recorded in D_2O at 303 K. Molar fractions of **2**, β -CD and CB7: i) 1.00, 0.00, 0.00; ii) 0.25, 0.75, 0.00; iii) 0.21, 0.68, 0.11; iv) 0.18, 0.56, 0.26; v) 0.16, 0.52, 0.32. B) Representative snapshot of the **2**@(CB7₂^{Ad}, β -CD^{BiPh}) complex. CB7 and β -CD are drawn in black and gray, respectively. Hydrogen atoms not participating in H-bonds (dotted lines) are omitted for clarity.

the terminal Ad sites. The molecular dynamic calculations revealed that the narrower rim of the β -CD cavity, which is occupied with secondary OH groups, most likely interacts with the CB7 portal by H-bonds to keep the β -CD unit slightly shifted from the central position (for the representative geometry, see Figure 2B). It is important to note that the β -CD^{BiPh} signal appeared as a shoulder on the major β -CD H1 signal from the early stages of the titration experiment. Thus, the ternary aggregate $2@(\text{CB7}^{\text{Ad}}, \beta\text{-CD}^{\text{BiPh}}, \beta\text{-CD}^{\text{Ad}})$ rather than $2@(\text{CB7}^{\text{Ad}}, \beta\text{-CD}^{\text{Ad}})$ should be considered as an intermediate in this process. We employed the last mixing mode to reveal the stability of the $2@(\text{CB7}_2^{\text{Ad}}, \beta\text{-CD}^{\text{BiPh}})$ aggregate. We prepared a solution of **2** with 2 equivalents of CB7, in which the complex $2@(\text{CB7}_2^{\text{Ad}})$ predominates, and we subsequently added 5 equivalents of β -CD. The ^1H NMR spectra of this system were recorded within four months and no splitting of any of the signals was observed as the β -CD units were disabled to reach the BiPh site. During this time, the sample was stored at room temperature, and all of the components remain unchanged according to the ^1H NMR spectra. Thus, we may conclude that, under our experimental conditions, CB7 at the Ad site displays very slow exchange and serves as an efficient supramolecular cap that is useful for the preparation of rotaxane arrangements. However, we performed an ITC experiment (see the Supporting Information, Figure S33) employing the second mixing mode described above, which revealed that the stability of the ternary aggregate $2@(\text{CB7}_2^{\text{Ad}}, \beta\text{-CD}^{\text{BiPh}})$ is slightly lower than that calculated from the ΔG of the individual binding events. When the mixture of **2** and 5 equivalents of β -CD were placed into the reaction cell and titrated with a solution of CB7 in water, ΔG_{exp} for each Ad binding site was determined to be $-46.03 \text{ kJ mol}^{-1}$. In contrast, ΔG_{calcd} calculated from the formation of $1@(\beta\text{-CD}^{\text{BiPh}})$, $2@(\text{CB7}^{\text{Ad}})$, and $2@(\beta\text{-CD}_2^{\text{Ad}})$, is $-51.90 \text{ kJ mol}^{-1}$. The lowering of the complex stability by $11.74 \text{ kJ mol}^{-1}$ can be attributed to the steric hindrance of the host molecules and/or to the loss in entropy.

Continuing our study, we examined the binding ability of **6** (Figure 3). Because the guest **6** is less soluble in water, we started the NMR titration experiment by the addition of 4.2 equivalents of β -CD into a dispersion of **6** in D_2O to obtain a clear solution (the second mixing mode described above). In contrast to the corresponding spectrum of the $2/\beta$ -CD mixture, splitting of β -CD H1 and the guest aromatic signals was observed (see Figure 3, line ii, and Figure S53 in the Supporting Information). Because the adamantyl signals are simultaneously deshielded, we attribute these observations to the formation of the binary complex $6@(\beta\text{-CD}_2^{\text{Ad}}, \beta\text{-CD}^{\text{BiPh}})$, in which the two β -CDs at terminal Ad sites are in fast

equilibrium with β -CD in the bulk solution, whereas the β -CD at the central BiPh is bound in a slow-exchange regime. This explanation was supported by the molar ratio of **6** to the minor β -CD (0.97), which was calculated from intensities of the corresponding ^1H NMR signals. We have shown that this complex is stable even at 60°C (Figure 3, line iii). The subsequent addition of a solution of CB7 (Figure 3, lines iv–vi) led to the significant deshielding of the Ad H atoms as both β -CDs at terminal Ad sites were replaced with CB7 units to produce the ternary aggregate $6@(\text{CB7}^{\text{Ad}}\text{CB7}_2^{\text{Ad}}, \beta\text{-CD}^{\text{BiPh}})$. Note that the signal of β -CD H1 was slightly shifted downfield as the surrounding environment changed. In summary, guest **6** is able to bind not only two CB7 units and one β -CD unit, but even, in contrast to guest **2**, three β -CD units. This latter mentioned ability can be attributed to the higher steric hindrance of the central BiPh site. To examine the scope and limitations of the phenomenon described above, we employed two further guests, **3** and **7**, which are derived from guests **2** and **6**, respectively, by replacing the H-atom at position 2 of the imidazolium ring with a methyl group. Guest **3** is capable of forming the ternary aggregate $3@(\text{CB7}^{\text{Ad}}, \beta\text{-CD}^{\text{BiPh}})$, whereas the complex $3@(\beta\text{-CD}_2^{\text{Ad}}, \beta\text{-CD}^{\text{BiPh}})$ was not detected (see the Supporting Information, Figure S38), similarly to guest **2**. In contrast, the most hindering guest **7** did not bind either CB7 or β -CD at the central BiPh site, according to the NMR data. Thus, only the binary complexes $7@(\text{CB7}_2^{\text{Ad}})$ and $7@(\beta\text{-CD}_2^{\text{Ad}})$ or the ternary complex $7@(\text{CB7}^{\text{Ad}}, \beta\text{-CD}^{\text{Ad}})$ can be prepared.

Finally, we employed ESI mass spectrometry (MS) to support our inferences based on the ITC and NMR data (for details, see the Supporting Information). The water solutions of equimolar mixtures of guests **1–7** and host CB7 or β -CD were examined to observe the signals related to the $[\text{guest-host}]^{2+}$. Subsequently, mixtures of guests **2**, **3**, **6**, and **7** with a 5 equivalents of β -CD were analyzed. Three types of complexes $[\text{guest-}\beta\text{-CD}_n]^{2+}$, where $n = 1, 2$ or 3 , were detected. However, the signal of $[\text{2-}\beta\text{-CD}_3]^{2+}$ was of very low intensity in comparison to those of the other guests (for the spectra, see the Supporting Information). Finally, 3 equivalents of CB7 were added into the solu-

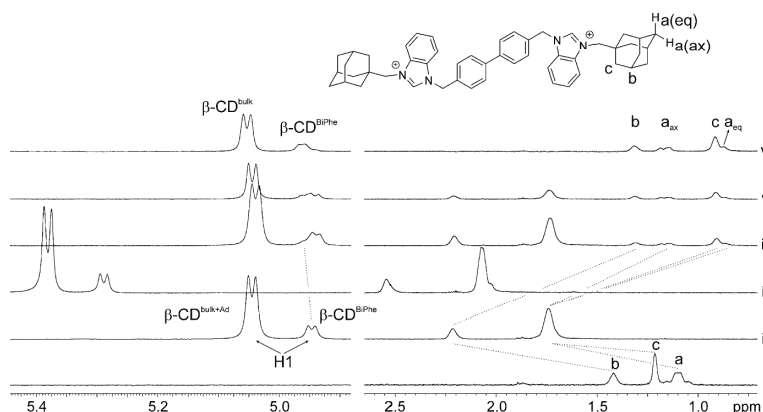


Figure 3. Stacking plot of a portion of the ^1H NMR spectra recorded in D_2O at 303 K or 333 K for line iii. Molar fractions of **6**, β -CD and CB7: i) 1.00, 0.00, 0.00; ii) and iii) 0.19, 0.81, 0.00; iv) 0.17, 0.74, 0.09; v) 0.16, 0.68, 0.16; vi) 0.14, 0.58, 0.28.

tions mentioned above, and, for all of the guests, the resulting mixtures gave rise to signals related to the ternary aggregates $[\text{guest}(\beta\text{-CD}, \text{CB}_7)]^{2+}$. The assignment of these signals was supported by HRMS. The detection of ternary complexes for all of the examined guests was rather surprising in light of the data obtained from NMR spectroscopy and ITC analysis. However, it should be kept in mind that MS allows the detection of aggregates weakly populated in solution. A typical result of the MS measurements for guest **2** is depicted in Figure 4.

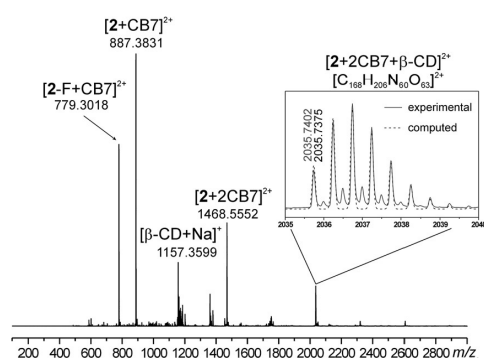


Figure 4. The positive-ion ESI high-resolution mass spectrum (full scan) of an aqueous solution of **2** (12.5 μM), CB7 (37.5 μM), and $\beta\text{-CD}$ (62.5 μM). The inset displays the experimental and computed^[17] lines. F = 1-(1-adamantylmethyl)imidazole neutral fragment.

Using an ion-trap MS device, we have isolated the cations $[\text{guest}(\beta\text{-CD}, \text{CB}_7)]^{2+}$ and treated them under collision-induced dissociation conditions. Interestingly, these aggregates did not dissociate sooner than when rather high resonance energy was applied to yield signals related to the $[\text{guest-CB}_7]^{2+}$. In another words, the initial ternary aggregate lost a neutral $\beta\text{-CD}$ unit, which was assumed to be bound at the central BiPh site. The applied energy was comparable with that used for cleavage of $[\beta\text{-CD-Na}]^+$ to glucose units and much higher than the energy needed for the decomposition of nonspecific aggregates studied in our laboratory (e.g., adamantane derivatives with $\alpha\text{-CD}$). As the CB7 unit is unlikely to thread through the $\beta\text{-CD}$ cavity, we can conclude that the $\beta\text{-CD}$ was likely released by the destruction of its macrocycle, whereas the CB7 units remained firmly bound at the Ad sites.

Conclusion

We can conclude that the 4,4'-biphenylene bisimidazolium moiety (BiPh) represents an interesting binding site that is capable of forming inclusion complexes with $\beta\text{-CD}$ and CB7 with association constants of approximately 10^{3-4} and 10^6 M^{-1} , respectively. We have prepared four new multitopic guests, in which a BiPh site was combined with two symmetrically equivalent adamantyl sites, displaying high affinities towards CB7 (up to approximately 10^{12} M^{-1}). These guests were used for the preparation of binary 1:2 and 1:3 pseudorotaxanes with $\beta\text{-CD}$ and ternary rotaxane-like aggregates with CB7 and $\beta\text{-CD}$ with

a stoichiometry of 1:1:1 or 1:2:1 (guest/CB7/ $\beta\text{-CD}$). The interesting result of this work is the demonstration that the central BiPh is more capable of binding the $\beta\text{-CD}$ unit when surrounded by rather sterically hindering cationic moieties, e.g., **6** binds three $\beta\text{-CD}$ units, whereas **2** binds only two $\beta\text{-CD}$ units. In our future work, we will elaborate the utilization of guests **1–7** in multicomponent responsive systems.

Experimental Section

General information: Unless otherwise stated, all of the starting materials, reagents and solvents (HPLC-MS grade) were purchased from commercial sources and used without further purification. 1-Adamantylbromomethane, 1-(1-adamantylmethyl)imidazole, 1-(1-adamantylmethyl)-2-methylimidazole, 1-(1-adamantylmethyl)-2-methylbenzimidazole, and 1-(1-adamantylmethyl)benzimidazole were prepared according to procedures previously published.^[18] Melting points were measured by using a Kofler block and are uncorrected. Elemental analyses (C, H, and N) were performed on a Thermo Fisher Scientific Flash EA 1112. ^1H and ^{13}C NMR spectra were recorded on a Bruker Avance III 300/500 spectrometer operating at frequencies of 300.13/500.13 MHz (^1H) and 75.77/125.77 MHz (^{13}C). ^1H NMR and ^{13}C NMR chemical shifts were referenced to the solvent signals (^1H : $\delta(\text{residual H}_2\text{O}) = 4.70$ ppm, $\delta(\text{residual } [\text{D}_6]\text{DMSO}) = 2.50$ ppm, $\delta(\text{residual } \text{CD}_3\text{HOD}) = 3.31$ ppm; ^{13}C : $\delta([\text{D}_6]\text{DMSO}) = 39.52$ ppm, $\delta(\text{CD}_3\text{OD}) = 49.15$ ppm). 2D NMR spectra and related 1D NMR spectra were recorded on a JEOL ECA-500 spectrometer operating at frequencies of 500.16 MHz (^1H) and 125.76 MHz (^{13}C). All NMR spectra were measured at 303 K. For NMR spectra including signal assignment, see the Supporting Information. The IR spectra were recorded using KBr discs with a Matteson 3000 FT-IR instrument. The electrospray mass spectra (ESI-MS) were recorded using an amaZon X ion-trap mass spectrometer (Bruker Daltonics, Bremen, Germany) equipped with an electrospray ionization source. HRMS measurements were performed on an ultrahigh-resolution quadrupole time-of-flight instrument (UHR-Q-TOF maXis, Bruker Daltonics, Bremen, Germany) equipped with an electrospray ionization source. The association constants and thermodynamic parameters for the complexation of guests **1–7** with CB7 and $\beta\text{-CD}$ were determined by titration calorimetry using a MicroCal VP-ITC instrument. Association constants exceeding 10^8 M^{-1} were determined by a multistep competition method, as described by Rekharsky et al.^[9] The compound 1-butyl-3-methylimidazolium bromide, with $K_a = 1.13 \times 10^7 \text{ M}^{-1}$, was used as a competitor. The data were analyzed by MicroCal Origin software. The complexation enthalpies for the multistep titration experiments were calculated as a sum of the enthalpies for each complexation step. The values of K and n were determined in multiple measurements and agreed within $\pm 5\%$.

Synthesis of the dibromides 1–3, 6, and 7: The corresponding 1-alkylbenzimidazole or 1-alkylimidazole (2.5–3.0 equiv.) was dissolved in dry toluene (60 equiv.) and 4,4'-bis(bromomethyl)biphenyl (BMB; 1 equiv.) was added at room temperature. The mixture was stirred under inert atmosphere at 80–110 $^\circ\text{C}$ and monitored by TLC. When the starting material (BMB) was consumed, the reaction mixture was allowed to cool down to room temperature, and the crude product was precipitated by the addition of freshly distilled THF. The solid material was triturated with plenty of THF by using the sequence of centrifugation and dispersion under sonication. The resultant microcrystalline powder was dried under vacuum to a constant weight.

4,4'-Bis((3-methyl-1*H*-imidazolium-1-yl)methyl)biphenyl dibromide 1: Compound **1** was prepared from BMB (0.1220 g, 0.36 mmol). The product was obtained as a colorless microcrystalline powder (178 mg, 99%). M.p. = 104–109 °C; ¹H NMR (500 MHz, [D₆]DMSO): δ = 3.88 (s, 6H), 5.51 (s, 4H), 7.55 (d, *J* = 8.5 Hz, 4H), 7.73 (d, *J* = 8.0 Hz, 4H), 7.76 (d, *J* = 1.5 Hz, 2H), 7.87 (d, *J* = 1.5 Hz, 2H), 9.36 ppm (s, 2H); ¹³C{¹H} NMR (125 MHz, [D₆]DMSO): δ = 35.9, 51.4, 122.3, 124.0, 127.2, 129.0, 134.3, 136.7, 139.7 ppm; IR (KBr): 3421, 3386, 3102, 3072, 3019, 1577, 1561, 1503, 1451, 1175, 831, 779, 749, 670, 628 cm⁻¹; MS (ESI): *m/z* (%): 425.2 [*M* + ⁷⁹Br]⁺ (3), 343.3 [*M* - H⁺]⁺ (4), 261.3 (4), 172.2 [*M*]²⁺ (29), 131.3 (100); elemental analysis calcd (%) for C₂₂H₂₀Br₂N₄·2.3H₂O: C 48.42, H 5.28, N 10.27; found C 48.70, H 5.20, N 9.96.

4,4'-Bis((3-(1-adamantylmethyl)-1*H*-imidazolium-1-yl)methyl)biphenyl dibromide 2: Compound **2** was prepared from BMB (0.1260 g, 0.37 mmol). The product was obtained as a colorless microcrystalline powder (273 mg, 95%). M.p. = 322–325 °C; ¹H NMR (500 MHz, [D₆]DMSO): δ = 1.44 (m, 12H), 1.56 (m, 6H), 1.68 (m, 6H), 1.97 (m, 6H), 3.94 (s, 4H), 5.52 (s, 4H), 7.52 (d, *J* = 8.0 Hz, 4H), 7.70 (s, 2H), 7.74 (d, *J* = 8.5 Hz, 4H), 7.87 (s, 2H), 9.22 ppm (s, 2H); ¹³C{¹H} NMR (125 MHz, CD₃OD/CDCl₃): δ = 28.8, 34.5, 37.0, 40.5, 53.7, 62.4, 122.8, 125.4, 128.8, 129.9, 133.8, 137.4, 142.0 ppm; IR (KBr): 3422, 3062, 2904, 2849, 1557, 1451, 1160, 756, 644 cm⁻¹; MS (ESI): *m/z* (%): 306.3 [*M*]²⁺ (100); elemental analysis calcd (%) for C₄₂H₅₀Br₂N₄·1.2H₂O: C 63.51, H 6.90, N 7.05; found C 63.87, H 6.88, N 6.87.

4,4'-Bis((3-(1-adamantylmethyl)-2-methyl-1*H*-imidazolium-1-yl)methyl)biphenyl dibromide 3: Compound **3** was prepared from BMB (0.1260 g, 0.37 mmol). The product was obtained as a colorless microcrystalline powder (275 mg, 93%). M.p. = 321–324 °C; ¹H NMR (500 MHz, [D₆]DMSO): δ = 1.54 (m, 18H), 1.67 (m, 6H), 1.96 (m, 6H), 2.65 (s, 6H), 3.92 (s, 4H), 5.50 (s, 4H), 7.43 (d, *J* = 8.5 Hz, 4H), 7.63 (d, *J* = 1.5 Hz, 2H), 7.74 (d, *J* = 8.5 Hz, 4H), 7.83 ppm (d, *J* = 2.0 Hz, 2H); ¹³C{¹H} NMR (125 MHz, [D₆]DMSO): δ = 10.4, 27.4, 34.5, 35.9, 39.0, 50.4, 58.4, 121.1, 123.4, 127.2, 128.4, 133.8, 139.4, 144.8 ppm; IR (KBr): 3422, 2904, 2847, 1526, 1453, 767, 746 cm⁻¹; MS (ESI): *m/z* (%): 320.3 [*M*]²⁺ (100); elemental analysis calcd (%) for C₄₄H₅₆Br₂N₄·1.1H₂O: C 64.40, H 7.15, N 6.83; found C 64.79, H 7.29, N 7.04.

4,4'-Bis((3-(1-adamantylmethyl)-1*H*-benzimidazolium-1-yl)methyl)biphenyl dibromide 6: Compound **6** was prepared from BMB (0.2001 g, 0.59 mmol). The product was obtained as a pale violet microcrystalline powder (436 mg, 85%). M.p. > 330 °C; ¹H NMR (500 MHz, CD₃OD/CDCl₃): δ = 1.61 (m, 18H), 1.74 (m, 6H), 2.02 (m, 6H), 4.25 (s, 4H), 5.81 (s, 4H), 7.52 (d, *J* = 8.0 Hz, 4H), 7.63 (m, 8H), 7.80 (d, *J* = 8.1 Hz, 2H), 7.89 (d, *J* = 8.2 Hz, 2H), 9.84 ppm (s, 2H); ¹³C{¹H} NMR (125 MHz, CD₃OD/CDCl₃): δ = 28.9, 35.7, 37.0, 51.5, 59.5, 114.5, 115.1, 128.2, 128.3, 128.9, 129.5, 131.9, 133.4, 134.0, 141.9, 143.1 ppm; IR (KBr): 3422, 3023, 2902, 2846, 1558, 1449, 1432, 1381, 1367, 1345, 1200, 1180, 774 cm⁻¹; MS (ESI): *m/z* (%): 356.3 [*M*]²⁺ (100); elemental analysis calcd (%) for C₅₀H₅₆Br₂N₄·H₂O: C 67.41, H 6.56, N 6.29; found C 67.54, H 6.54, N 6.01.

4,4'-Bis((3-(1-adamantylmethyl)-2-methyl-1*H*-benzimidazolium-1-yl)methyl)biphenyl dibromide 7: Compound **7** was prepared from BMB (0.0802 g, 0.24 mmol). The product was obtained as a colorless microcrystalline powder (109 mg, 51%). M.p. > 330 °C; ¹H NMR (500 MHz, CD₃OD/CDCl₃): δ = 1.64 (m, 18H), 1.73 (m, 6H), 2.02 (m, 6H), 2.96 (s, 6H), 4.25 (s, 4H), 5.80 (s, 4H), 7.29 (d, *J* = 8.5 Hz, 4H), 7.62 (m, 8H), 7.80 (d, *J* = 7.6 Hz, 2H), 7.89 ppm (d, *J* = 7.2 Hz, 2H); ¹³C{¹H} NMR (125 MHz, CD₃OD/CDCl₃): δ = 12.8, 29.0, 37.0, 37.6, 41.7, 49.6, 58.2, 113.6, 115.3, 127.7, 128.1, 128.3, 128.9, 132.2, 133.4, 133.8, 141.6, 152.8 ppm; IR (KBr): 3422, 2903, 2849,

1521, 1472, 1415, 787, 778 cm⁻¹; MS (ESI): *m/z* (%): 370.3 [*M*]²⁺ (100); elemental analysis calcd (%) for C₅₂H₆₀Br₂N₄·3.5H₂O: C 64.79, H 7.01, N 5.81; found C 64.79, H 7.29, N 6.02.

General procedure for the synthesis of the diiodides 4 and 5: 4,4'-bis((2-methyl-1*H*-imidazol-1-yl)methyl)biphenyl or 4,4'-bis((1*H*-imidazol-1-yl)methyl)biphenyl (1 equiv.) was dissolved in methyl iodide (100 equiv.) under an inert atmosphere. The mixture was refluxed until the starting material was consumed. After the removal of residual methyl iodide under reduced pressure, the crude product was triturated with freshly distilled diethyl ether or THF several times. Solid products were dried under vacuum and used without further purification.

4,4'-Bis((3-methyl-2-methyl-1*H*-imidazolium-1-yl)methyl)biphenyl diiodide 4: Compound **4**, prepared from biphenyl precursor (0.095 g, 0.28 mmol), was obtained as a pale yellow microcrystalline powder (147 mg, 85%). M.p. = 289–294 °C; ¹H NMR (500 MHz, [D₆]DMSO): δ = 2.64 (s, 6H), 3.79 (s, 6H), 5.48 (s, 4H), 7.44 (d, *J* = 8.5 Hz, 4H), 7.69 (d, *J* = 2.1 Hz, 2H), 7.71 (d, *J* = 8.4 Hz, 4H), 7.76 ppm (d, *J* = 2.1 Hz, 2H); ¹³C{¹H} NMR (125 MHz, [D₆]DMSO): δ = 9.6, 34.9, 50.2, 121.2, 122.7, 127.2, 128.4, 134.0, 139.4, 144.6 ppm; IR (KBr): 3417, 3084, 3069, 1588, 1536, 1503, 1448, 1405, 1377, 1276, 1241, 1169, 807, 759, 662, 477 cm⁻¹; MS (ESI): *m/z* (%): 499.1 [*M* + ¹²⁶I]⁺ (3), 275.2 (7), 186.1 [*M*]²⁺ (100), 138.1 (53), 97.1 (4); elemental analysis calcd (%) for C₂₄H₂₈I₂N₄·0.5H₂O: C 45.37, H 4.60, N 8.82; found C 45.66, H 4.60, N 8.75.

4,4'-Bis((3-methyl-1*H*-benzimidazolium-1-yl)methyl)biphenyl diiodide 5: Compound **5**, prepared from biphenyl precursor (0.0548 g, 0.13 mmol), was obtained as a pale yellow microcrystalline powder (84 mg, 91%). M.p. = 271–274 °C; ¹H NMR (500 MHz, [D₆]DMSO): δ = 4.11 (s, 6H), 5.82 (s, 4H), 7.59–7.71 (m, 12H), 7.98 (d, *J* = 8.0 Hz, 2H), 8.04 (d, *J* = 8.0 Hz, 2H), 9.86 ppm (s, 2H); ¹³C{¹H} NMR (125 MHz, [D₆]DMSO): δ = 33.5, 49.4, 113.7, 113.8, 126.6, 126.6, 127.2, 128.9, 130.7, 132.0, 133.5, 139.6, 142.9 ppm; IR (KBr): 3429, 3029, 3019, 1568, 1461, 1453, 772, 759 cm⁻¹; MS (ESI): *m/z* (%): 222.2 [*M*]²⁺ (100); elemental analysis calcd (%) for C₃₀H₂₈I₂N₄·H₂O C 50.30, H 4.22, N 7.82; found C 50.58, H 4.11, N 7.93.

Acknowledgements

The authors gratefully acknowledge the internal funding agency of Tomas Bata University in Zlín (project No. IGA/FT/2015/005) for financial support. Access to computing and storage facilities owned by parties and projects contributing to the National Grid Infrastructure MetaCentrum, provided under the program "Projects of Large Infrastructure for Research, Development, and Innovations" (LM2010005), is greatly appreciated.

Keywords: cucurbituril • cyclodextrins • host–guest systems • rotaxanes • supramolecular chemistry

- [1] a) J. Kim, I.-S. Jung, S.-Y. Kim, E. Lee, J.-K. Kang, S. Sakamoto, K. Yamaguchi, K. Kim, *J. Am. Chem. Soc.* **2000**, *122*, 540–541; b) S. Liu, C. Ruspic, P. Mukhopadhyay, S. Chakrabarti, P. Y. Zavalij, L. Isaacs, *J. Am. Chem. Soc.* **2005**, *127*, 15959–15967; c) L. Isaacs, *Chem. Commun.* **2009**, 619–629; d) H.-J. Buschmann, *Isr. J. Chem.* **2011**, *51*, 533–536; e) D. Das, O. A. Scherman, *Isr. J. Chem.* **2011**, *51*, 537–550; f) J. Lagona, P. Mukhopadhyay, S. Chakrabarti, L. Isaacs, *Angew. Chem. Int. Ed.* **2005**, *44*, 4844–4870; *Angew. Chem.* **2005**, *117*, 4922–4949; g) A. C. Bhasikuttan, H. Pal, J. Mohanty, *Chem. Commun.* **2011**, 47, 9959–9971; h) E. Masson, X. Ling, R. Joseph, L. Kyeremeh-Mensah, X. Lu, *RSC Adv.* **2012**, *2*, 1213–1247.

- [2] a) *Cyclodextrins and Their Complexes* (Ed.: H. Dodziuk), Wiley-VCH: Weinheim, **2006**; b) G. Crini, *Chem. Rev.* **2014**, *114*, 10940–10975; c) E. M. M. Del Valle, *Process Biochem.* **2004**, *39*, 1033–1046.
- [3] M. V. Rekharsky, Y. Inoue, *Chem. Rev.* **1998**, *98*, 1875–1917.
- [4] M. V. Rekharsky, T. Mori, C. Yang, H. K. Ko, N. Selvapalam, H. Kim, D. So-bransingh, A. E. Kaifer, S. Liu, L. Isaacs, W. Chen, S. Moghaddam, M. K. Gilson, K. Kim, Y. Inoue, *Proc. Natl. Acad. Sci. USA* **2007**, *104*, 20737–20742.
- [5] S. Moghaddam, C. Yang, M. V. Rekharsky, Y. H. Ko, K. Kim, Y. Inoue, M. K. Gilson, *J. Am. Chem. Soc.* **2011**, *133*, 3570–3581.
- [6] L. Cao, M. Šekutor, P. Y. Zavalij, K. Mlinarić-Majerski, R. Glaser, L. Isaacs, *Angew. Chem. Int. Ed.* **2014**, *53*, 988–993; *Angew. Chem.* **2014**, *126*, 1006–1011.
- [7] S. D. Choudhury, J. Mohanty, H. Pal, A. C. Bhasikuttan, *J. Am. Chem. Soc.* **2010**, *132*, 1395–1401.
- [8] J. P. Da Silva, N. Jayaraj, S. Jockusch, N. J. Turro, V. Ramamurthy, *Org. Lett.* **2011**, *13*, 2410–2413.
- [9] M. V. Rekharsky, H. Yamamura, M. Kawai, I. Osaka, R. Arakawa, A. Sato, Y. H. Ko, S. K. Kim, Y. Inoue, *Org. Lett.* **2006**, *8*, 815–818.
- [10] L. Leclercq, N. Noujeim, S. H. Sanon, A. R. Schmitzer, *J. Phys. Chem. B* **2008**, *112*, 14176–14184.
- [11] a) A. Harada, M. Kamachi, *Macromolecules* **1990**, *23*, 2821–2823; b) H.-J. Buschmann, A. Wego, K. Jansen, E. Schollmeyer, D. Döpp, *J. Inclusion Phenom. Macrocyclic Chem.* **2005**, *53*, 183–189.
- [12] a) M. K. Sinha, O. Reany, M. Yefet, M. Botoshansky, E. Keinan, *Chem. Eur. J.* **2012**, *18*, 5589–5605; b) I. W. Wyman, D. H. Macartney, *J. Org. Chem.* **2009**, *74*, 8031–8038; c) S. He, C. Zhou, H. Zhang, *J. Inclusion Phenom. Macrocyclic Chem.* **2013**, *76*, 333–344.
- [13] a) S. Samsam, L. Leclercq, A. R. Schmitzer, *J. Phys. Chem. B* **2009**, *113*, 9493–9498; b) K. Kim, *Chem. Soc. Rev.* **2002**, *31*, 96–107; c) A. T. Buck, J. T. Paletta, S. A. Khidrangala, C. L. Beck, A. H. Winter, *J. Am. Chem. Soc.* **2013**, *135*, 10594–10597; d) G. Celtek, M. Artar, O. A. Scherman, D. Tuncel, *Chem. Eur. J.* **2009**, *15*, 10360–10363; e) M. V. Rekharsky, H. Yamamura, T. Mori, A. Sato, M. Shiro, S. V. Lindeman, R. Rathore, K. Shiba, Y. H. Ko, N. Selvapalam, K. Kim, Y. Inoue, *Chem. Eur. J.* **2009**, *15*, 1957–1965; f) L. Cera, C. A. Schalley, *Chem. Sci.* **2014**, *5*, 2560–2567.
- [14] a) V. Sindelar, S. Silvi, A. E. Kaifer, *Chem. Commun.* **2006**, 2185–2187; b) D. Tuncel, Ö. Özsar, H. B. Tiftik, B. Salih, *Chem. Commun.* **2007**, 1369–1371; c) N. Noujeim, L. Leclercq, A. Schmitzer, *J. Org. Chem.* **2008**, *73*, 3784–3790; d) Z.-J. Ding, H.-Y. Zhang, L.-H. Wang, F. Ding, Y. Liu, *Org. Lett.* **2011**, *13*, 856–859.
- [15] a) P. Mukhopadhyay, P. Y. Zavalij, L. Isaacs, *J. Am. Chem. Soc.* **2006**, *128*, 14093–14102; b) M. H. Tootoonchi, S. Yi, A. E. Kaifer, *J. Am. Chem. Soc.* **2013**, *135*, 10804–10809; c) X. Lu, E. Masson, *Langmuir* **2011**, *27*, 3051–3058; d) D. Jiao, F. Biedermann, F. Tian, O. A. Scherman, *J. Am. Chem. Soc.* **2010**, *132*, 15734–15743; e) S. Gadde, E. K. Batchelor, J. P. Weiss, Y. Ling, A. E. Kaifer, *J. Am. Chem. Soc.* **2008**, *130*, 17114–17119; f) A. E. Kaifer, W. Li, S. Silvi, V. Sindelar, *Chem. Commun.* **2012**, 48, 6693–6695.
- [16] D. Jiao, F. Biedermann, O. A. Scherman, *Org. Lett.* **2011**, *13*, 3044–3047.
- [17] L. Patiny, A. Borel, *J. Chem. Inf. Model.* **2013**, *53*, 1223–1228.
- [18] a) S. Shahane, L. Toupet, C. Fischmeister, C. Bruneau, *Eur. J. Inorg. Chem.* **2013**, 54–60; b) M. Bochmann, G. Wilkinson, B. G. Young, *J. Chem. Soc. Dalton Trans.* **1980**, 1879–1887; c) J. Černochová, P. Branná, M. Rouchal, P. Kulhánek, I. Kuřitka, R. Vícha, *Chem. Eur. J.* **2012**, *18*, 13633–13637.

Received: April 7, 2015

Published online on July 3, 2015

4.8

An Adamantane-Based Disubstituted Binding Motif
with Picomolar Dissociation Constants for Cucurbit[*n*]urils in Water
and Related Ternary Aggregates

Eva Babjaková, Petra Branná, Magdalena Kuczyńska, Michal Rouchal, Zdeňka Prucková, Lenka
Dastychová, Jan Vícha, Robert Vícha*

RSC Advances **2016**, *6*, 105146–105153

Cite this: *RSC Adv.*, 2016, 6, 105146

An adamantane-based disubstituted binding motif with picomolar dissociation constants for cucurbit[*n*]urils in water and related quaternary assemblies†

E. Babjaková,^a P. Branná,^a M. Kuczyńska,^a M. Rouchal,^a Z. Prucková,^a L. Dastychová,^a J. Vícha^b and R. Vícha^{*a}

A non-axial centerpiece based on 1,3-disubstituted adamantane was designed, and three new guests were prepared. In the structure of the heterotopic guests, the central adamantane site was combined with two terminal butyl or 1-adamantyl sites. The new central binding motif displayed an extraordinarily high affinity towards CB8 ($K_a = (5.3 \pm 0.3) \times 10^{12} \text{ M}^{-1}$ in water) to allow formation of quaternary assemblies with geometries which are dependent on the nature of macrocycles. Based on the individual binding strengths, the replacement of CB7 by CB8 led to inverse arrangements of the quaternary assemblies; *i.e.*, β -CD is capped at the central site by two CB7 units, while the CB8 prefers the central site to be capped with two β -CD units.

Received 21st September 2016
Accepted 24th October 2016

DOI: 10.1039/c6ra23524g

www.rsc.org/advances

Introduction

The inclusion complexes of cucurbit[*n*]uril (CB*n*) macrocycles and cationic guests that are derived from cage hydrocarbons or ferrocene have attracted significant interest in host-guest chemistry over the past two decades due to their outstanding stability.^{1–5} CB*n* is a rigid barrel-like shaped molecule with a non-polar cavity and two symmetric portals that are rimmed with carbonyl groups. Therefore, the best suited guests for CB*n* hosts consist of a hydrophobic central part to fill the cavity and two cationic substituents that are oriented along an axis to enable ion-dipole interactions with the opposite portals. Thus, it is not surprising that the strongest inclusion complex that has been reported to date was for 4,9-bis(trimethylammonium)-diamantane with CB7.^{6,7} In contrast to diamantane and other extensively used scaffolds, bicyclo[2.2.2]octane⁸ and ferrocene,⁹ which can bear two substituents that are located essentially along the axis, the two substituents at the adamantane (Ad) bridgehead positions adopt a tetrahedral orientation with an angle of 109.5°. To the best of our knowledge, there are only three examples of 1,3-disubstituted Ad dicationic guests for which the binding strengths with CB7 and CB8 have been reported.^{10,11} 1,3-Bis(trimethyl-ammonium)adamantane diiodide has K_a values with CB7 and CB8 of $6.42 \times 10^4 \text{ M}^{-1}$ (in 50 mM

$\text{CD}_3\text{CO}_2\text{Na}/\text{D}_2\text{O}$) and $1.11 \times 10^{11} \text{ M}^{-1}$ (in 50 mM $\text{CD}_3\text{CO}_2\text{Na}/\text{D}_2\text{O}$), respectively. Adamantane-1,3-diamine and 1,3-bis(4,5-dihydro-1*H*-imidazol-2-yl)adamantane have K_a values with CB7 of $2.06 \times 10^8 \text{ M}^{-1}$ (in 50 mM $\text{CD}_3\text{CO}_2\text{Na}/\text{D}_2\text{O}$) and $1 \times 10^4 \text{ M}^{-1}$ (in water), respectively (the K_a values with CB8 were not reported). It should be noted that the binding strengths of these dicationic guests towards CB7 are significantly lower than those of corresponding singly substituted derivatives, where the magnitude of K_a reaches 10^{12} M^{-1} .^{8,10} Thus, the Ad scaffold has been employed as a terminal binding site in guest molecules that display interesting supramolecular behaviors.^{12–17} The 1,3-disubstituted Ad cage has also been incorporated into macrocyclic molecules as a bent motif which allows for the preparation of macrobicyclic derivatives of cyclen and cyclam,¹⁸ cryptands,¹⁹ macrocyclic lactams binding squaraine,²⁰ and adamantanophanes.^{21,22} 1,3-Disubstituted Ad has also been utilized as a suitable linker for quadruple H-bond-based binding motifs, which are capable of self-assembling into cyclopentameric complexes.²³ In this paper, we present the first (to the best of our knowledge) preparation of multitopic guest molecules with a central binding site derived from a 1,3-disubstituted Ad cage (Fig. 1) and describe its binding properties.

Results and discussion

As a part of our ongoing research on multitopic guests, we prepared three new ligands (5–7; Fig. 1). Commercially available dicarboxylic acid **1** was used as the starting material for the preparation of the central motif and was converted to the compound **4** by a sequence of esterification, reduction, and the Appel reaction with a high overall yield of 71%. In the final step,

^aDepartment of Chemistry, Faculty of Technology, Tomas Bata University in Zlín, Vavrečkova 275, 760 01 Zlín, Czech Republic. E-mail: rvicha@ft.uthb.cz; Tel: +420 576 031 103

^bCentre of Polymer Systems, Tomas Bata University in Zlín, třída Tomáše Bati 5678, 760 01 Zlín, Czech Republic

† Electronic supplementary information (ESI) available: ¹H and ¹³C NMR spectra, titration data, and mass spectra. See DOI: 10.1039/c6ra23524g

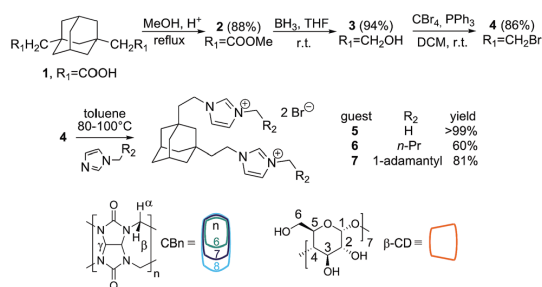


Fig. 1 Synthesis of guests 5–7 (top) and the host molecules that were used in this study (bottom).

we reacted **4** with three 1-alkylimidazoles to yield the corresponding bisimidazolium dibromides **5–7** at satisfactory overall yields of 43–70%. Compound **5** represents a model guest with only a central adamantane binding site, while guests **6** and **7** contain the additional terminal binding sites *n*-butyl and 1-adamantylmethyl, respectively, which have different affinities towards particular hosts.

To overcome the steric disadvantage of 1,3-disubstituted adamantane, we used flexible ethylene linkers between the central Ad and imidazolium units. Due to the lack of information about this binding motif, we initially focused on examining the binding behavior of model guest **5** towards hosts with suitable inner cavity dimensions; *i.e.*, CB7, CB8, and β -CD. Guest **5** interacts with β -CD following a fast exchange mode on the NMR timescale, and all of the Ad and ethylene signals are shifted downfield (see Fig. S10†). Because of the well-known magnetic anisotropy of β -CD,²⁴ we assume that the Ad cage is included in the β -CD cavity. The association constants $K_a = 1.82 \times 10^4 \text{ M}^{-1}$ (in water) and $1.71 \times 10^4 \text{ M}^{-1}$ (in 50 mM AcONa buffer), which were determined by means of isothermal titration calorimetry (ITC), are comparable to that obtained for other adamantane-based guests (Table 1).^{25,26} It should be noted that all binding experiments were initially performed in pure water or an aqueous NaCl solution because there is no need for buffering of the solutions of our permanent imidazolium cations. Nevertheless, we determined the thermodynamic parameters for the model guest **5** also in a sodium acetate buffer to enable easier comparison with previously published data (for full thermodynamic data, see Table S1†). By examining the

complexes of **5** with CB7 and CB8 using NMR titrations, we observed rapid formation of 1 : 1 complexes in slow exchange mode in both cases. In addition, a significant increase of the solubility of CB8 was observed during the titration of **5** by a fine dispersion of CB8 in 50 mM NaCl. No remaining solid CB8 was observed at the final concentration of 1.1 mM. Note in Table 1 that the guest **5** is better suited for CB8 by factor of 32.3 in water (9.7 in AcONa buffer). This observation can be likely explained by better accommodation of hindered 1,3-disubstituted adamantane scaffold by wider CB8. The strength of the **5**@CB7 complex (Table 1, for full ITC data, see Table S1†) is comparable to that of singly substituted adamantane-based guests. We speculate that the expected steric hindrance of the disubstituted Ad cage inside the CB7 cavity is compensated for by the ion-dipole interactions of two imidazolium rings with the CB7 portals.

To determine the possible orientation of guest **5** inside the hosts, we performed optimization calculations at the B3LYP/6-31G(d,p) level with a D3 dispersion correction and the COSMO solvent model (water) (for details and corresponding references, see Computational details). Fig. 2 shows top and side views of the minimized structures. Note that the Ad cage of **5** is shifted markedly from the virtual plane of the glycosidic oxygen atoms towards the primary rim of the β -CD likely due to steric hindrance between the C(6)H₂OH groups of β -CD and the imidazolium ring. In contrast to the nearly ideal symmetric geometry of CB7 in the complex **5**@CB7, with the Ad cage positioned near the center of gravity of the CB7, the Ad cage of **5** in **5**@CB8 is shifted from the central position and is accompanied by tilting of the two opposite glycoluril units.

Subsequently, the intrinsic stability of the **5** host aggregates in the gas phase was studied by ESI-MS. The $[\text{M} + \text{host}]^{2+}$ cations were isolated in an ion trap and treated under collision-induced dissociation (CID) conditions. Fig. 3 shows the plot of the relative intensity of the $[\text{M} + \text{host}]^{2+}$ signal against the CID amplitude. The observed stabilities $5\text{@CB8} \geq 5\text{@CB7} > 5\text{@}\beta\text{-CD}$ correlate well qualitatively with the association constants that were obtained by calorimetric titrations, see Table 1. For comparison, we also measured $5 \cdot \alpha\text{-CD}$, which is expected to be a weak non-specific aggregate, and $\text{Ad-NH}_3^+\text{Cl}^- \text{@CB7}$ with the previously reported value $K_a = 4.17 \times 10^{12} \text{ M}^{-1}$.¹⁰ Although the MS data correlate well with K_a , it should be noted that fragmentation upon CID conditions combines the dissociation of the supramolecular aggregate and cleavage of its molecular

Table 1 ITC-determined values of K_a^a [M^{-1}] for the interactions of **5–7** with CB6, CB7, CB8, and β -CD at 303 K

Guest	CB6	CB7	CB8	β -CD
5	nb	$(1.64 \pm 0.09) \times 10^{11b,c}$	$(5.3 \pm 0.3) \times 10^{12b,d}$	$(1.82 \pm 0.01) \times 10^{4b}$
5	nb	$(3.5 \pm 0.3) \times 10^{10c,e}$	$(3.4 \pm 0.2) \times 10^{11d,e}$	$(1.71 \pm 0.03) \times 10^{4e}$
6	$(1.23\text{--}1.36) \times 10^{6f,g}$	$(1.29 \pm 0.11) \times 10^{11b,c}$	$(3.29 \pm 0.15) \times 10^{12b,d}$	$(1.65 \pm 0.01) \times 10^{4b}$
7	nb	omb	omb	$(0.18\text{--}6.31) \times 10^{5b,f}$

^a All titrations were performed in triplicate. The K_a values are reported for a single binding site. ^b Experiments were carried out in water. ^c 1,6-Hexamethylene diamine·2HCl was used as a competitor. ^d 1-Adamantaneamine·HCl was used as a competitor. ^e Experiments were carried out in 50 mM AcONa. ^f Various fitting models were used. See Table S1 and comments in the text for detail. nb = no binding, omb = off-model binding. ^g Experiments were carried out in 2.5 mM NaCl.

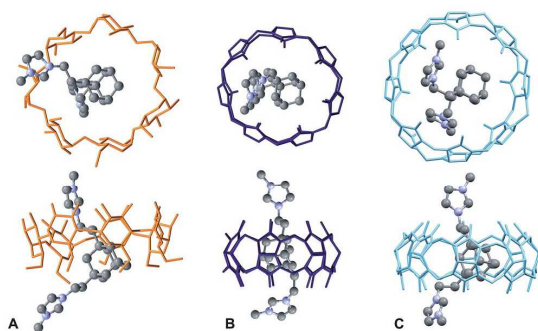


Fig. 2 Energy-minimized structures of the 5@ β -CD (A), 5@CB7 (B), and 5@CB8 (C) complexes.

components (note that Ad—NH₃⁺ is likely much more stable than 5 in the complex with CB7).

Having obtained these promising data, we examined the binding behavior of guest 6, which contains two additional terminal butyl binding sites. We use the superscripts “T” and “C” to denote the positioning of particular macrocycles at the terminal and central binding sites, respectively. The NMR and ITC data of the binary complexes of 6 with CB7, CB8, and β -CD indicate that the binding behavior of 6 is very similar to that of 5; *i.e.*, 6 forms 1 : 1 complexes with all of these macrocycles in a pseudorotaxane manner with the central Ad cage included inside the cavity. However, in complex of 6 with CB6, hosts occupy both terminal sites with K_a values similar to those of other alkylimidazolium salts²⁷ forming the 2 : 1 complex 6@CB6₂^T as ¹H NMR titration experiment clearly indicate (Fig. S14[†]). To support this hypothesis, we performed calorimetric titration of CB6 with the guest 6 which provided a single-ramp binding isotherm with inflexion at $x_6 = 0.47$. We employed “One Set of Sites” and “Two Sets of Sites” models to obtain consistent values of K_a for single terminal site ($K_a \sim 1.3 \times 10^6 \text{ M}^{-1}$, for full data, see Table S1[†]). In contrast, fitting procedure using a “Sequential Binding” model did not converge on reasonable binding parameters. Upon these findings, it can be inferred that each site binds the CB6 unit independently.

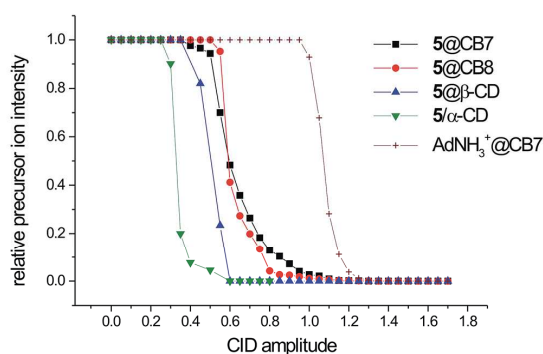


Fig. 3 Intrinsic gas-phase stability of 5@host complexes.

Subsequently, we examined whether guest 6 is capable of forming a ternary or quaternary assembly; *i.e.*, a complex with two different macrocycles. Our experiment can be followed by examining the stacked ¹H NMR spectra in Fig. 4. Initially, four molar excess of β -CD was added to the solution of guest 6 in 50 mM NaCl in D₂O (the NaCl solution was used to increase solubility of CB6). The significant downfield shift of the signals that were related to the central Ad cage implies the formation of 6@ β -CD^C. According to β -CD selectivity towards the butyl and the adamantane site ($K_{Ad}/K_{Bu} \sim 1000$), the terminal sites remained free to allow further binding. Subsequent stepwise addition of the solution of CB6 led to a small but unambiguous downfield shift of the adamantane H_i signal. In contrast, the signals of the butyl chains were markedly shifted upfield. Broadening and/or overlapping of the peaks in the range of 1.4–1.8 ppm in final stages of titration can be attributed to increase in number of the adamantane peaks (particularly H_m and H_k) as these H-atoms became non-equivalent inside the chiral CD cavity. Considering that CB6 does not bind the Ad site due to incompatible geometries, β -CD strongly prefers the Ad site, and there is no expectation of significant repulsion between the β -CD and CB6 units, the above mentioned observations can be explained by the positioning of the two CB6 units at butyl chains, whereas β -CD remained bound to the central Ad site to form quaternary assembly 6@(β -CD^C,CB6₂^T).

The second examined multiple-binding-site guest 7 consists of two high-affinity terminal Ad-based sites in addition to the title central site. Initially, its complexation by CB7 was studied. The NMR data (upfield shift of the terminal adamantane signals) clearly imply that the terminal Ad sites of 7 are occupied by CB7 to form 7@CB7^T at low CB7 concentrations and 7@CB7₂^T with excess of CB7 (see Fig. S18[†]). Simultaneously, the signals of the central adamantane hydrogen atoms were more shielded as the central adamantane cage was positioned close to the CB7 portals. Because no change of the guest signals intensities and/or positions was observed after addition of more than two equivalents of CB7, we infer that

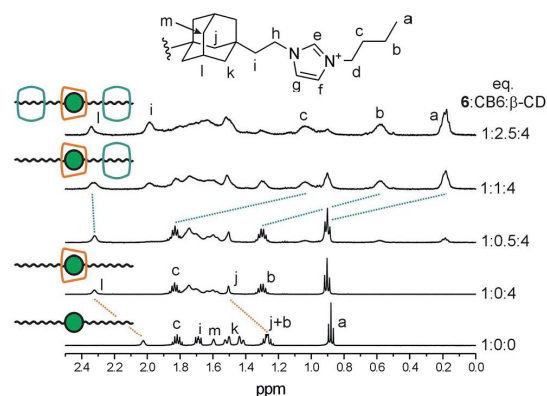


Fig. 4 Stacking plot of a portion of the ¹H NMR (500 MHz) spectra of 6 (1.83 mM) and its complexes recorded in a 50 mM NaCl solution in D₂O at 303 K.

$7@CB7_2^T$ predominated in the solution and no significant amount of $7@(CB7_2^T, CB7^C)$ and/or $7@(CB7^T, CB7^C)$ was formed. It should be noted that formation of the two last mentioned complexes is most unlikely because such complexes, with two CB units which are arranged around one cationic moiety, suffer from strong electrostatic repulsion between two adjacent CB portals. Unfortunately, determination of the association constant for terminal Ad site of the guest 7 with CB7 *via* ITC was disabled because of too long equilibration when competitor was used. Although the binding constant remained unavailable, the binding isotherm which was obtained without any competitor (see Fig. 5, left) suggests that two binding sites were occupied within a simple binding event (only one slope was observed with inflexion at $x_{CB7} \approx 2$). Combining this observation with 1H NMR data, we speculate that the ternary complex $7@CB7_2^T$ is formed with binding strength of CB7 at Ad^T significantly exceeding that at Ad^C . If the value of K_a for Ad^T site and CB7 would be lower than that for Ad^C , the occupation of the central Ad site, not the terminal one, could be expected at low CB7 concentrations. The formation of $7@CB7_2^T$ would follow only with the excess CB7. This is however not the case. Thus, we assume that the binding constant of CB7 at Ad^T is likely similar to that obtained for the model guest 1-(1-adamantylmethyl)-3-methylimidazolium iodide (AMI) and CB7 (*i.e.*, $3.7 \times 10^{12} M^{-1}$, for more information, see ref. 28). This would provide the two sequential bindings of CB7 at terminal Ad sites of the guest 7 with no substantial participation of the central site (K_a for Ad^C site of 7 could be similar to that of 5, *i.e.*, $(1.64 \pm 0.09) \times 10^{11}$

M^{-1}) as depicted in Fig. 5 (left). Subsequently, we treated the guest 7 with CB8. Unfortunately, limited solubility of CB8 disabled NMR data of sufficient quality. Although the appearing of the second set of signals of aromatic hydrogen atoms clearly indicated some binding in slow-exchange manner, the signals of adamantane hydrogen atoms became too broad to allow unambiguous assignment. Binding isotherm which was recorded for competitive calorimetric titration of CB8 with the guest 7 did not fit any available model. However, two slopes were clearly observed when titration was performed without competitor as can be seen in Fig. 5 (right). Considering binding strengths of individual sites which were obtained using model compound 5 and AMI (K_a for CB8 and AMI in water at 303 K is $(1.07 \pm 0.15) \times 10^{11} M^{-1}$), we assume that two subsequent distinct binding events took place when molar fraction of the guest was lower than 1.0. In other words, the CB8 unit was bound initially at Ad^T and then moved to Ad^C to form the complex $7@CB8^C$ predominantly. This complex was transformed with the excess CB8 to $7@CB8_2^T$ since the positioning of the two CB8 units around one cationic moiety is not preferred (Fig. 5, right). Consistent results were obtained when titrations were performed in inverse mode, *i.e.*, the host in the cell was titrated with CBn (see Fig. S23†). These observations indicate different preferences of CB7 and CB8 towards available binding sites of the guest 7 to enable preparation of quaternary complexes with various arrangements of the CDs and CBs macrocycles as demonstrated below. Finally, we examined binding behavior of 7 towards β -CD. In the 1H NMR spectra that were recorded during the titration of 7 with β -CD, significant deshielding of both the central and terminal Ad cages was observed. The Job plot that was constructed for this system suggested a stoichiometry 1 : 2 (7 : β -CD). However, the analysis of the ITC data implies that more than two binding sites can be occupied by β -CD at once (Fig. S17†).

Our previous work showed that similar guests with a biphenyl central site can form rotaxane-like complexes in which one β -CD unit is firmly trapped at the central site by two CB7 units at the terminal Ad sites.²⁸ Fig. 6 shows the 1H NMR titration experiment that confirms the ability of 7 to form a similar quaternary assembly. Initially, we added 5 eq. of β -CD to the solution of 7 in water. As discussed above, the significant downfield shift of all of the Ad signals suggests that at least two binding sites are occupied. The subsequent addition of the CB7 solution led to the large upfield shift of the terminal Ad signals, whereas the H-atoms in the central Ad cage were significantly deshielded. Because the deshielding of the central part of the guest is much higher than the deshielding that would originate solely from the portal effect of the CB7 units,^{27,29} we can conclude that this NMR experiment confirms the formation of the $7@(\beta\text{-CD}^C, CB7_2^T)$ assembly. As was demonstrated in our previous work, binding of CB7 units at both terminal sites of the tritopic Ad-terminated bisimidazolium guest disabled the central biphenyl site for β -CD.²⁸ In the case of compound 7, we observed significant deshielding of the hydrogen atoms of the central Ad cage after addition of an excess of β -CD into a solution which contained $7@CB7_2^T$. However, we observed only single set of the β -CD signals. These observations imply that

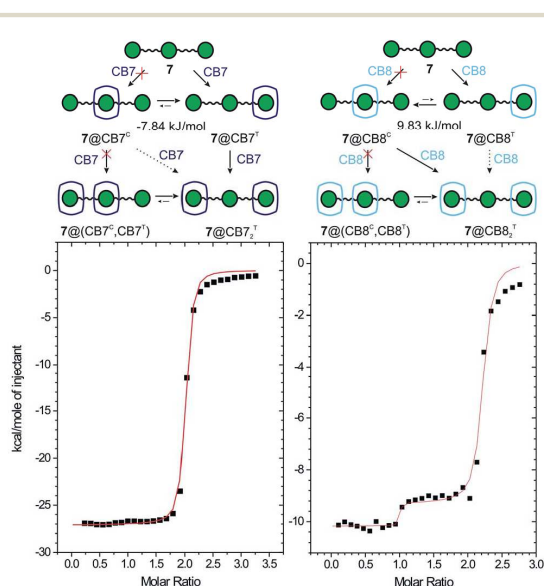


Fig. 5 Assumed binding events and binding isotherms obtained by ITC for titration of the guest 7 with CB7 (left) and with CB8 (right) (guest in the cell, host in the syringe) in water at 303 K. Unlike conversions are denoted by dotted arrows. Initial concentrations: $c_{CB7} = 0.3465$ mM, $c_7 = 0.0036$ mM; $c_{CB8} = 0.1082$ mM, $c_7 = 0.0084$ mM. Energy differences between the two distinct 1 : 1 complexes were calculated using model guests.

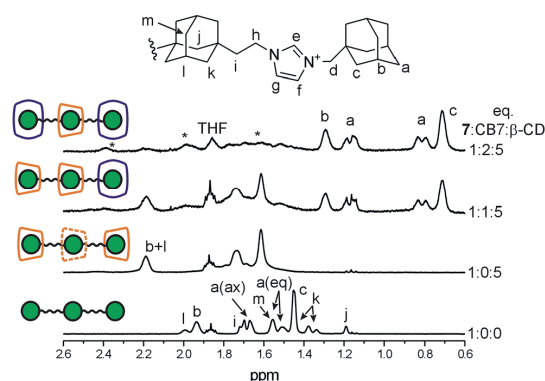


Fig. 6 Stacking plot of a portion of the ^1H NMR (500 MHz) spectra of guest 7 (1.83 mM) titrated with β -CD and CB7 in D_2O at 303 K. Signals of the central Ad deshielded by β -CD are shown with asterisks.

some non-specific aggregate ($7@CB7_2^T$)- β -CD is formed more likely than $7@(\text{CB7}_2^T, \beta\text{-CD}^C)$.

The binding data of 5 suggests a high affinity of the central site in guest 7 towards CB8. In addition, as discussed above, CB8 slightly prefers the central site over the terminal site. Subsequently, we performed ^1H NMR titrations to determine whether guest 7 can form quaternary assemblies with the CB8 unit that is trapped at the central site. Although guest 7 interacts with CB8 in water, the broadening of the shielded proton signals does not allow unambiguous assignment of the signals (Fig. 7). It should be noted that during this stage of the experiment, some CB8 remained undissolved. After the subsequent addition of an excess of β -CD, the sharp signals of the central Ad appeared. Compared to the spectrum of the free guest, the signals of the central Ad are shielded, whereas the terminal Ad signals are deshielded. These observations can be rationalized by the predominant formation of complex $7@(\beta\text{-CD}_2^T, \text{CB8}^C)$. In other words, the CB8 unit is fixed at the central binding site with two β -CDs that are positioned at the terminal sites. The molar fraction of the CB8-complexed guest was calculated immediately after the addition of β -CD using signal b (overlapping

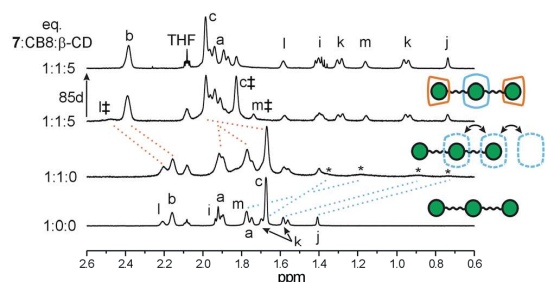


Fig. 7 Stacking plot of a portion of the ^1H NMR (500 MHz) spectra of guest 7 (1.83 mM) titrated with β -CD and CB8 in 50 mM NaCl solution in D_2O at 323 K. The signals of $7@CB8$ and $7@(\beta\text{-CD}_2)$ are denoted by * and ‡, respectively.

signals of all of the terminal Ad; Fig. 7) and signals i–m (related to the central Ad that was complexed with CB8) to be 0.51. However, the fraction of this quaternary assembly increased to 0.84 after 85 days of standing at room temperature. This increase can be attributed to the CB8 slow dissolving rather than slow equilibration process because of only one set of signals for CB8 was observed in the ^1H NMR spectra. These CB8 signals displayed the same diffusion coefficient in a DOSY experiment as signals of the guest (see Fig. S20a in the ESI†). Additional support for the complex hypothesized above can clearly be observed in a ROESY spectrum (Fig. S19†). Whereas the cross-peaks of the terminal Ad and inner β -CD H3 and H5 suggest the inclusion of terminal Ads into β -CD cavities, the positioning of the CB8 at the central Ad can be demonstrated by the intermolecular interaction of the H α from CB8 and Hc from the terminal adamantanes.

Both quaternary assemblies consisting of guest 7 (*i.e.*, $7@(\beta\text{-CD}_2^T, \text{CB8}^C)$ and $7@(\beta\text{-CD}^C, \text{CB7}_2^T)$) were detected by ESI-MS (for the spectra, see Fig. S38 and S37,† respectively). The proposed composition of these complexes was supported by a tandem mass spectra analysis that revealed subsequent releases of the host molecules.

Experimental

General

Unless otherwise stated, all of the starting material, reagents and solvents were purchased from commercial sources and used without further purification. The adamantane-1,3-diacetic acid was obtained as a gift from Provisco CS Ltd. The melting points were measured using a Kofler block and are uncorrected. The elemental analyses (C, H, N) were performed on a Thermo Fisher Scientific Flash EA 1112. The NMR spectra were recorded on Bruker 300/500 spectrometers that operate at frequencies of 300.13/500.11 MHz (^1H) and 75.77/125.77 MHz (^{13}C). ^1H and ^{13}C -NMR chemical shifts were referenced to the solvent signals [^1H : $\delta(\text{residual DMSO-}d_5) = 2.50$ ppm, $\delta(\text{HDO}) = 4.70$ ppm, $\delta(\text{residual CHCl}_3) = 7.26$ ppm; ^{13}C : $\delta(\text{DMSO-}d_6) = 39.52$ ppm, $\delta(\text{CDCl}_3) = 77.16$ ppm]. The signals were assigned as follows: s = singlet, t = triplet, and m = multiplet with J values in Hz. The IR spectra were recorded using KBr discs with a Mattson 3000 FT-IR instrument, and ν was reported in cm^{-1} . The electrospray mass spectra (ESI-MS) were recorded using an amaZon X ion-trap mass spectrometer (Bruker Daltonics, Bremen, Germany) that was equipped with an electrospray ion source. All of the experiments were conducted in the positive-ion polarity mode. The instrumental conditions that were used to measure the single imidazolium salts and their mixtures with the host molecules were different; therefore, they are described separately. Single imidazolium salts: Individual samples (with a concentration of $0.5 \mu\text{g cm}^{-3}$) were infused into the ESI source in methanol : water (1 : 1, v/v) solutions using a syringe pump with a constant flow rate of $4 \mu\text{l min}^{-1}$. The other instrumental conditions were as follows: an electrospray voltage of -4.2 kV, capillary exit voltage of 140 V, drying gas temperature of 220°C , drying gas flow rate of $6.0 \text{ dm}^3 \text{ min}^{-1}$ and nebulizer

pressure of 55.16 kPa. Host-guest complexes: An aqueous solution of the guest molecule (6.25 μM) and the corresponding host molecule (1.0–5.0 equivalents) for the binary/ternary complexes or an aqueous solution of the guest molecule (6.25 μM) and the corresponding host molecules (1.0–5.0 equivalents) for the quaternary complexes was infused into the ESI source at a constant flow rate of 4 $\mu\text{l min}^{-1}$. The other instrumental conditions were as follows: an electrospray voltage of -4.0 kV, capillary exit voltage of from -30 to 140 V, drying gas temperature of 300 $^{\circ}\text{C}$, drying gas flow rate of 6.0 $\text{dm}^3 \text{min}^{-1}$ and nebulizer pressure of 206.84 kPa. Nitrogen was used as the nebulizing and drying gases in all of the experiments. The tandem mass spectra were collected using collision-induced dissociation (CID) with He as the collision gas after isolating the required ions. The isothermal titration calorimetry measurements were carried out in H_2O using a VP-ITC MicroCal instrument at 303 K. The concentrations of the host in the cell and the guest in the microsyringe were approximately 0.35 – 0.05 and 3.50 – 0.50 mM, respectively. The exact concentrations of $\text{CB}n$ stock solutions were determined by the ITC titration of stable and non-hygroscopic guests which are known to form 1:1 complex (*i.e.*, 1-adamantaneamine·HCl for β -CD, CB7, and CB8 and 1,6-hexanediamine·2HCl for CB6; purity was checked by elemental analysis prior titration). The raw experimental data were analyzed with the MicroCal ORIGIN software. The heats of dilution of each guest compound were taken into account. The data were fitted to a theoretical titration curve using the “One Set of Sites”, “Two Sets of Sites”, or “Sequential Binding” model. 1,6-Hexanediamine·2HCl with $K_{a,\text{CB}7} = (2.05 \pm 0.09) \times 10^9 \text{ M}^{-1}$ (water) and $K_{a,\text{CB}7} = (2.84 \pm 0.22) \times 10^7 \text{ M}^{-1}$ (50 mM $\text{CH}_3\text{CO}_2\text{Na}$ buffer) and 1-adamantaneamine·HCl with $K_{a,\text{CB}8} = (2.79 \pm 0.15) \times 10^9 \text{ M}^{-1}$ and $K_{a,\text{CB}8} = (2.50 \pm 0.16) \times 10^8 \text{ M}^{-1}$ (50 mM $\text{CH}_3\text{CO}_2\text{Na}$ buffer) were used as competitors.⁹ The enthalpy for competitive experiment was calculated as a sum of enthalpies for each step in competitive sequence. These ΔH values were verified by independent titration without competitor (see, Table S1†).

1,3-Bis(2-hydroxyethan-1-yl)adamantane (3). The dimethyl dicarboxylate 2 (2.4 g, 8.6 mmol) was dissolved in 16 cm^3 of dry THF, and the reaction flask was placed into a crushed ice-water bath. The $\text{THF} \cdot \text{BH}_3$ as a 1 M THF solution (35 cm^3 , 35 mmol) was added within one hour at -5 to 0 $^{\circ}\text{C}$. Subsequently, the mixture was stirred for 1 h at -5 to 0 $^{\circ}\text{C}$ and an additional 48 h at room temperature until the starting material disappeared. The reaction was quenched with 10 cm^3 of water and 18 cm^3 of 3 M water solution of NaOH. The mixture was extracted with several portions of hexane and diethyl ether, the combined organic portions were dried over Na_2SO_4 , and the solvents were evaporated under reduced pressure. The diol 3 was isolated as a colorless crystalline powder (1.81 g, 94%) with mp = 118 – 120 $^{\circ}\text{C}$ (compared with values from the literature³⁹ of mp = 117 – 118 $^{\circ}\text{C}$). No further purification was needed. $^1\text{H NMR}$ (CDCl_3): δ 1.28 (s, 2H), 1.37–1.51 (m, 14H), 1.58 (m, 2H), 2.00 (m, 2H), 3.70 (m, 4H). ^{13}C $\{^1\text{H}\}$ NMR (CDCl_3): 29.10, 32.7, 36.6, 42.3, 47.0, 48.3, 58.9. (KBr): 3301 (m), 2907 (m), 2874 (m), 2838 (m), 1447 (m), 1035 (s), 1021 (s), 967 (w), 669 (w), 615 (m) cm^{-1} .

1,3-Bis(2-bromoethan-1-yl)adamantane (4). Diol 3 (1.82 g, 8.1 mmol) and CBr_4 (5.05 g, 15.2 mmol) were dissolved in 22 cm^3 of dry dichloromethane. Subsequently, the triphenylphosphine (4.67 g, 17.8 mmol) was added portionwise within 30 min at 0 $^{\circ}\text{C}$. The mixture was stirred at room temperature until the GC-MS analysis indicated complete consumption of the starting compound 3. The reaction was quenched with 12 cm^3 of water, the aqueous portion was extracted with CH_2Cl_2 , the collected organic portions were washed with $3 \times 15 \text{ cm}^3$ of saturated NaHCO_3 solution and dried over Na_2SO_4 , and the solvent was removed under reduced pressure. The obtained solid material was triturated with pentane several times, and the collected liquid portions were passed through a celite pad until all of the POPh_3 had been removed. The solvent was then removed under reduced pressure to obtain the crystalline product 4 (2.44 g, 86%) with mp = 45 – 48 $^{\circ}\text{C}$ (compared with the values from the literature²⁹ of 45 – 47 $^{\circ}\text{C}$). This material was used in the next step without further purification. $^1\text{H NMR}$ (CDCl_3): δ 1.26 (s, 2H), 1.45 (m, 8H), 1.58 (m, 2H), 1.74 (m, 4H), 2.04 (m, 2H), 3.39 (m, 4H). ^{13}C $\{^1\text{H}\}$ NMR (CDCl_3): δ 28.7, 28.8, 34.7, 36.4, 41.6, 47.0, 47.8. IR (KBr): 2909 (s), 2846 (s), 1446 (s), 1363 (w), 1343 (w), 1329 (m), 1239 (w), 1219 (m), 1153 (12), 662 (s), 562 (s) cm^{-1} .

General procedure for the preparation of guests 5–7

The corresponding 1-methyl, 1-butyl, and 1-(1-adamantylmethyl)imidazole (4 eq.) was dissolved in dry toluene (2 cm^3), and 1 eq. of 4 was added at room temperature. The mixture was stirred under inert atmosphere at 80 – 100 $^{\circ}\text{C}$ and monitored by thin-layer chromatography. When the starting material had been consumed, the crude product was isolated from the reaction mixture by addition of freshly distilled DEE or THF. The crude material was washed with plenty of DEE or THF under sonication and separated by centrifugation if applicable. The resultant colorless microcrystalline powder (7) or oil (5 and 6) was dried in vacuum to a constant weight; however, the elemental analyses revealed that some water and/or THF was still present. This material was used for further binding studies, and the water and/or THF molecules were taken into account.

1,3-Bis[2-(3-methylimidazolionio-1-yl)ethyl]adamantane dibromide (5). Compound 5 was prepared from 0.1 g (0.29 mmol) of dibromide 4. The product was obtained as a colorless viscous oil in the yield of $>99\%$. Anal. calcd for $\text{C}_{22}\text{H}_{34}\text{Br}_2\text{N}_4 \cdot 2\text{H}_2\text{O}$: C, 48.01%; H, 6.96%; N, 10.18%; found C, 47.93%; H, 6.96%; N, 10.33%. $^1\text{H NMR}$ ($\text{DMSO}-d_6$): δ 1.33 (s, 2H), 1.41–1.51 (m, 8H), 1.58 (m, 2H), 1.62–1.65 (m, 4H), 2.02 (m, 2H), 3.86 (s, 6H), 4.21–4.24 (m, 4H), 7.72 (m, 2H), 7.84 (m, 2H), 9.29 (s, 2H) ppm. ^{13}C $\{^1\text{H}\}$ NMR ($\text{DMSO}-d_6$): δ 28.1, 32.3, 35.6, 35.7, 40.7, 43.1, 44.4, 46.2, 122.3, 123.5, 136.5 ppm. IR (KBr): 3149 (vw), 2904 (w), 2845 (m), 1634 (s), 1572 (s), 1449 (w), 1344 (vw), 1169 (vs), 1106 (w), 851 (s), 759 (m), 667 (w), 623 (m) cm^{-1} . ESI-MS: 433.3/435.3 [$\text{M}^{2+} + \text{Br}^-$] $^+$, 353.4 [$\text{M}^{2+} - \text{H}^+$] $^+$, 271.3 [$\text{M}^{2+} - \text{C}_4\text{H}_7\text{N}_2$] $^+$, 177.2 [M] $^{2+}$, 83.3 [$\text{C}_4\text{H}_7\text{N}_2$] $^+$ m/z .

1,3-Bis[2-(3-butylimidazolionio-1-yl)ethyl]adamantane dibromide (6). Compound 6 was prepared from 0.1 g (0.29 mmol) of dibromide 4. The product was obtained as a colorless liquid in the yield of 60%. Anal. calcd for $\text{C}_{28}\text{H}_{46}\text{Br}_2\text{N}_4 \cdot 1.6\text{H}_2\text{O}$: C, 53.61;

H, 7.91%; N, 8.93%; found C, 53.69%; H, 8.18%; N, 8.54%. ^1H NMR (DMSO- d_6): δ 0.89 (t, $^3J_{\text{HH}} = 7.4$ Hz, 6H), 1.21–1.29 (m, 4H), 1.32 (s, 2H), 1.40–1.50 (m, 8H), 1.58 (m, 2H), 1.63–1.66 (m, 4H), 1.75–1.81 (m, 4H), 2.01 (m, 2H), 4.18 (t, $^3J_{\text{HH}} = 7.1$ Hz, 4H), 4.22–4.25 (m, 4H), 7.82 (m, 2H), 7.87–7.88 (m, 2H), 9.41 (s, 2H) ppm. ^{13}C $\{^1\text{H}\}$ NMR (DMSO- d_6): δ 13.2, 18.7, 28.1, 31.2, 32.3, 35.6, 40.6, 43.0, 44.5, 46.2, 48.2, 122.3, 122.5, 135.9 ppm. IR (KBr): 3134 (s), 3074 (s), 2961 (s), 2927 (sh), 2905 (s), 2873 (sh), 2847 (vs), 1628 (w), 1562 (vs), 1461 (w), 1448 (w) 1369 (w), 1162 (w), 1026 (w), 865 (s), 754 (m), 645 (w) cm^{-1} . ESI-MS: 219.3 $[\text{M}]^{2+}$ m/z .

1,3-Bis{2-[3-(1-adamantylmethyl)imidazolono-1-yl]ethyl}adamantane dibromide (7). Compound 7 was prepared from 0.1 g (0.29 mmol) of dibromide 4. The product was obtained as a colorless microcrystalline powder in the yield of 81%. Mp = 192–195 °C, anal. calcd for $\text{C}_{42}\text{H}_{62}\text{Br}_2\text{N}_4 \cdot 0.8\text{THF} \cdot \text{H}_2\text{O}$: C, 63.24; H, 8.27%; N, 6.53%; found C, 63.27%; H 8.35%; N, 6.27. ^1H NMR (DMSO- d_6): δ 1.33 (s, 2H), 1.37–1.49 (m, 8H), 1.44 (m, 12H), 1.52–1.67 (m, 12H), 1.52–1.55 (m, 2H), 1.65–1.68 (m, 4H), 1.95 (m, 6H), 1.99 (m, 2H), 3.92 (s, 4H), 4.26–4.29 (m, 4H), 7.69 (m, 2H), 7.91 (m, 2H), 9.35 (s, 2H) ppm. ^{13}C $\{^1\text{H}\}$ NMR (DMSO- d_6): δ 27.4, 28.1, 32.4, 33.1, 35.5, 36.0, 39.0, 40.6, 42.8, 44.5, 46.4, 59.8, 121.9, 124.0, 136.5 ppm. IR (KBr): 3150 (sh), 3129 (m), 3065 (s), 3040 (s), 2927 (sh), 2918 (sh), 2906 (vs), 2882 (sh), 2845 (vs), 2677 (vw), 2657 (vw), 1561 (vs), 1449 (m), 1366 (m), 1344 (w), 1315 (w), 1168 (s), 1156 (s), 1107 (w), 1067 (w), 977 (s), 837 (m), 803 (m), 783 (w), 719 (w), 664 (w), 644 (w) cm^{-1} . ESI-MS: 311.3 $[\text{M}]^{2+}$ m/z .

Computational details

Structures of 5, β -CD, CB7 and CB8 and corresponding inclusion complexes were optimized using B3LYP functional^{31,32} and standard 6-31G(d,p) basis set with COSMO (CONductor-like Screening MOdel) solvent model³³ (water). The D3 dispersion correction³⁴ was implemented during the optimizations of inclusion complexes for better description of these non-covalently bonded species.

Conclusions

In conclusion, we demonstrated that the 1,3-disubstituted adamantane scaffold that bears two imidazolium cations bonded via ethylene linkers represents an efficient binding site for β -CD, CB7, and CB8. The aggregation constants of guest 5 towards β -CD and CB7 were comparable with that obtained for singly substituted adamantane-derived guests. In addition, 5 is the non-peptide guest with the highest value of K_a observed to date ($(5.3 \pm 0.3) \times 10^{12} \text{ M}^{-1}$ in water and $(3.4 \pm 0.2) \times 10^{11} \text{ M}^{-1}$ in 50 mM $\text{CH}_3\text{CO}_2\text{Na}$ buffer) for 1 : 1 complex with CB8. Furthermore, ligands 6 and 7, which feature additional binding sites, were found to be capable of forming quaternary assemblies in a pseudorotaxane manner in a water environment. Guests 6 and 7 formed complexes with the β -CD unit at the central site capped by CB7 or CB6 at both terminal sites; i.e., $6@(\beta\text{-CD}^{\text{C}}, \text{CB6}_2^{\text{T}})$ and $7@(\beta\text{-CD}^{\text{C}}, \text{CB7}_2^{\text{T}})$. In contrast, the CB8 was predominantly trapped at the central Ad site by two β -CD units at the terminal sites; i.e., $7@(\beta\text{-CD}_2^{\text{T}}, \text{CB8}^{\text{C}})$. These findings can enable new modalities in the design and construction of supramolecular systems.

Acknowledgements

This work was financially supported by the Internal Founding Agency of Tomas Bata University in Zlín, project No. IGA/FT/2016/001, and the Czech Science Foundation grant 16-05691S to J.V. The authors thank to Lukáš Maier from Masaryk University (Brno, Czech Republic) for assistance with the NMR measurements.

Notes and references

- S. J. Barrow, S. Kasera, M. J. Rowland, J. del Barrio and O. A. Scherman, *Chem. Rev.*, 2015, **115**, 12320–12406.
- D. Shetty, J. K. Khedkar, K. M. Park and K. Kim, *Chem. Soc. Rev.*, 2015, **44**, 8747–8761.
- A. E. Kaifer, *Acc. Chem. Res.*, 2014, **47**, 2160–2167.
- L. Isaacs, *Acc. Chem. Res.*, 2014, **47**, 2052–2062.
- K. I. Assaf and W. M. Nau, *Chem. Soc. Rev.*, 2015, **44**, 394–418.
- L. Cao, M. Šekutor, P. Y. Zavalij, K. Mlinarić-Majerski, R. Glaser and L. Isaacs, *Angew. Chem., Int. Ed.*, 2014, **53**, 988–993.
- M. Šekutor, K. Molčanov, L. Cao, L. Isaacs, R. Glaser and K. Mlinarić-Majerski, *Eur. J. Org. Chem.*, 2014, 2533–2542.
- S. Moghaddam, C. Yang, M. Rekharsky, Y. H. Ko, K. Kim, Y. Inoue and M. K. Gilson, *J. Am. Chem. Soc.*, 2011, **133**, 3570–3581.
- M. V. Rekharsky, T. Mori, C. Yang, H. K. Ko, N. Selvapalam, H. Kim, D. Sobransingh, A. E. Kaifer, S. Liu, L. Isaacs, W. Chen, S. Moghaddam, M. K. Gilson, K. Kim and Y. Inoue, *Proc. Natl. Acad. Sci. U. S. A.*, 2007, **104**, 20737–20742.
- S. Liu, C. Ruspice, P. Mukhopadhyay, S. Chakrabarti, P. Zavalij and L. Isaacs, *J. Am. Chem. Soc.*, 2005, **127**, 15959–15967.
- D. S. N. Hettiarachchi and D. H. Macartney, *Can. J. Chem.*, 2006, **84**, 905–914.
- J. Gravel, J. Kempf and A. Schmitzer, *Chem.-Eur. J.*, 2015, **21**, 1–8.
- P. Mukhopadhyay, P. Y. Zavalij and L. Isaacs, *J. Am. Chem. Soc.*, 2006, **128**, 14093–14102.
- X. Lu and E. Masson, *Langmuir*, 2011, **27**, 3051–3058.
- M. H. Tootoonchi, S. Yi and A. E. Kaifer, *J. Am. Chem. Soc.*, 2013, **135**, 10804–10809.
- Z.-J. Ding, H.-Y. Zhang, L.-H. Wang, F. Ding and Y. Liu, *Org. Lett.*, 2011, **13**, 856–859.
- S. Ghosh and L. Isaacs, *J. Am. Chem. Soc.*, 2010, **132**, 4445–4454.
- S. M. Kobelev, A. D. Averin, A. K. Buryak, E. N. Savelyev, B. S. Orlinson, G. M. Butov, I. A. Novakov, F. Denat, R. Guillard and I. P. Beletskaya, *ARKIVOC*, 2012, 196–209.
- T. Š. Ramljak, I. Despotović, B. Bertoša and K. Mlinarić-Majerski, *Tetrahedron*, 2013, **69**, 10610–10620.
- C. G. Collins, A. T. Johnson, R. D. Connell, S. A. Nelson, I. Murgu, A. G. Oliver and B. D. Smith, *New J. Chem.*, 2014, **38**, 3992–3998.
- K. Mlinarić-Majerski, D. Pavlović and Ž. Marinić, *Tetrahedron Lett.*, 1996, **37**, 4829–4832.

Paper

RSC Advances

- 22 K. Mlinarić-Majerski, D. Pavlović, M. Luić and B. Kojić-Prodić, *Chem. Ber.*, 1994, **127**, 1327–1329.
- 23 H. M. Keizer, J. J. Gonzáles, M. Segura, P. Prados, R. P. Sijbesma, E. W. Meijer and J. de Mendoza, *Chem.-Eur. J.*, 2005, **11**, 4602–4608.
- 24 H.-J. Schneider, F. Hacket and V. Rüdiger, *Chem. Rev.*, 1998, **98**, 1755–1785.
- 25 M. V. Rekharsky and Y. Inoue, *Chem. Rev.*, 1998, **98**, 1875–1917.
- 26 S. G. Kulkarni, Z. Prucková, M. Rouchal, L. Dastychová and R. Vícha, *J. Inclusion Phenom. Macrocyclic Chem.*, 2016, **84**, 11–20.
- 27 N. Zhao, L. Liu, F. Biedermann and O. A. Scherman, *Chem.-Asian J.*, 2010, **5**, 530–537.
- 28 P. Branná, J. Černochová, M. Rouchal, M. Babinský, R. Marek, M. Nečas, I. Kuřitka and R. Vícha, *J. Org. Chem.*, 2016, **81**, 9595–9604.
- 29 P. Branná, M. Rouchal, Z. Prucková, L. Dastychová, R. Lenobel, T. Pospíšil, K. Maláč and R. Vícha, *Chem.-Eur. J.*, 2015, **21**, 11712–11718.
- 30 J. G. Henkel, J. T. Hane and G. Gianutsos, *J. Med. Chem.*, 1982, **25**, 51–56.
- 31 C. Lee, W. Yang and R. G. Parr, *Phys. Rev. B: Condens. Matter Mater. Phys.*, 1988, **37**, 785–789.
- 32 P. J. Stephens, F. J. Devlin, C. F. Chabalowski and M. J. Frisch, *J. Phys. Chem.*, 1994, **98**, 11623–11627.
- 33 A. Klant and G. Schürmann, *J. Chem. Soc., Perkin Trans. 2*, 1993, 799–805.
- 34 S. J. Grimme, *Comput. Chem.*, 2006, **27**, 1787–1799.

4.9

Cubane Arrives on the Cucurbituril Scene

Kristýna Jelínková, Heda Surmová, Alena Matelová, Michal Rouchal, Zdeňka Prucková, Lenka Dastychová, Marek Nečas, Robert Vícha *

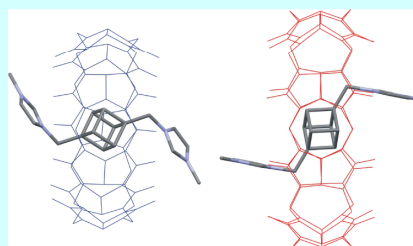
Organic Letters **2017**, *19*, 2698–2701

Cubane Arrives on the Cucurbituril Scene

Kristýna Jelínková,[†] Heda Surmová,[†] Alena Matelová,[†] Michal Rouchal,[†] Zdeňka Prucková,[†] Lenka Dastychová,[†] Marek Nečas,[‡] and Robert Vícha^{*,†}[†]Department of Chemistry, Faculty of Technology, Tomas Bata University in Zlín, Vavrečkova 275, 760 01 Zlín, Czech Republic[‡]Department of Chemistry, Faculty of Science, Masaryk University, Kamenice 5, 625 00 Brno, Czech Republic

Supporting Information

ABSTRACT: Cubane, an intriguing chemical curiosity first studied in the early 1960s, has become a valuable structural motif and has recently been involved in the structures of a great number of prospective compounds. The first dicationic supramolecular guest **5** is prepared and derived from a 1,4-disubstituted cubane moiety, and its binding behavior toward cucurbit[*n*]urils (CB*n*) and cyclodextrins (CD) is studied. The bisimidazolium salt **5** forms 1:1 inclusion complexes with CB7, CB8, and β -CD with the respective association constants $(6.7 \pm 0.5) \times 10^{11} \text{ M}^{-1}$, $(1.5 \pm 0.2) \times 10^9 \text{ M}^{-1}$, and $<10^2 \text{ M}^{-1}$ in water. The solid-state structures of the **5**@CB7 and **5**@CB8 complexes are also reported.



Cage hydrocarbons have recently been recognized as outstanding scaffolds for preparing cationic guests in supramolecular chemistry. Particularly, ammonio derivatives of adamantane,¹ adamantane,² and bicyclo[2.2.2]octane,² along with similar ferrocene³ derivatives, have displayed extraordinarily high association constants toward cucurbit[7]uril which surpass, in some cases, the tightest natural avidin–biotin complex. Simultaneously, to obtain the strongest binding by using structural modifications, high-affinity binding motifs were employed in various more complex, self-assembled supramolecular systems in an effort to create molecular tools.⁴ In this light, it is slightly surprising that derivatives of another highly symmetric, synthetically feasible cage hydrocarbon, cubane, has not attracted the interest of supramolecular chemists so far. To the best of our knowledge, there is only one report describing cubane binding sites, published by Lincoln and co-workers, who studied noncharged adamantane/cubane-cyclodextrin conjugates.⁵ Since the initial preparation of cubane by Eaton and Cole in 1964, its derivatives have been investigated in several branches of chemistry. Apart from nitrocubanes, which are well-known high-energy materials,⁶ a number of intriguing polymers,⁷ sulfides,⁸ peptides,⁹ and chiral ligands¹⁰ have been studied. Biegasiewicz et al. has published a comprehensive review of recent cubane chemistry.¹¹ In addition, Eaton suggested in 1992 that the cubane scaffold can act as a benzene bioisostere (both 1,4-disubstituted), and thus cubane can replace the potentially toxic benzene ring in drug molecules.¹² This hypothesis inspired the preparation of various bioactive compounds in which the cubane skeleton was incorporated in place of benzene.¹³ The above-mentioned examples demonstrate the recent increased interest in cubane chemistry, and extensive supramolecular studies can be expected as the next logical step. As a part of our ongoing research on cage-hydrocarbon binding motifs, we report here the first preparation of a dicationic cubane-derived guest and its

binding with cucurbit[7/8]uril (CB7/8) and β -cyclodextrin (β -CD). The structures of the studied guests and hosts are depicted in Figure 1.

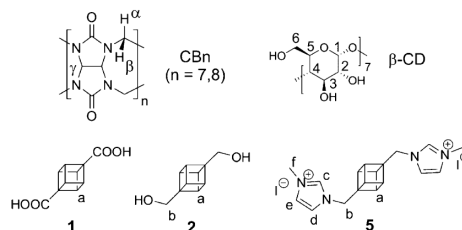


Figure 1. Structures of hosts and guests used in this study.

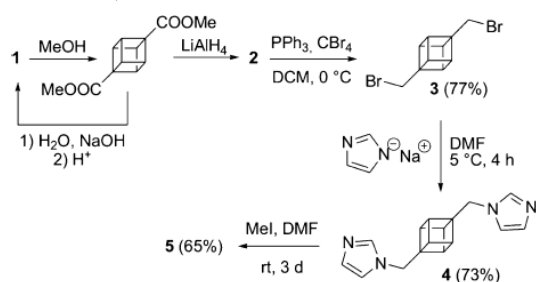
We employed the Chapman modification¹⁴ of the original Eaton and Cole's synthesis¹⁵ to prepare cubane-1,4-dicarboxylic acid (**1**), which is a key intermediate in the wide spectrum of 1,4-disubstituted cubanes. Subsequently, the acid **1** was transformed to the dibromide **3** using the sequence of Fisher esterification with MeOH, reduction, and Appel bromination, as depicted in Scheme 1. Dibromide **3** was reacted with sodium imidazolidine within 4 h at 5 °C to produce intermediate **4** in satisfactory yield. Finally, the desired guest **5** was readily obtained via quaternization with MeI. The sample of the dicarboxylic acid **1**, which was pure enough for binding studies, was obtained by hydrolysis of the sublimated dimethyl ester of acid **1**.¹⁶

We examined the supramolecular properties of **5** using ¹H NMR spectroscopy. First, we tested the ability of **5** to form

Received: April 5, 2017

Published: May 3, 2017

Scheme 1. Synthesis of Cubane-Based Dicationic Guest 5



inclusion complexes with CB7/8. The ^1H NMR spectrum of guest **5** shows three signals corresponding to aliphatic H atoms. All of these signals appear within the range 3.7–4.4 ppm due to the electron-withdrawing effects of the adjacent imidazolium cation or strained structure (Figure 2, line (iii)). It should be

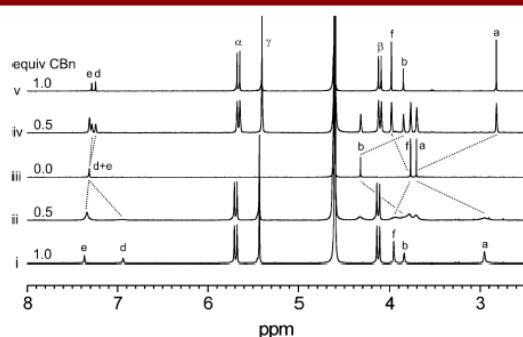


Figure 2. Stacking plot of a region of the ^1H NMR (500 MHz) spectra of guest **5** (iii) titrated with CB8 (i, ii) and CB7 (iv, v) in D_2O at 303 K. For signal assignment, see Figure 1.

noted that signal of H(c) was not observed due to rapid H/D exchange. Upon the addition of 0.5 equiv of CB7 or CB8, new sets of guest signals appeared, and the original signals of the free guest completely vanished in equimolar solutions. The strong upfield shift of the cubane CH and CH_2 signals and the simultaneous downfield shift of the CH_3 signals imply that the cubane moiety was included inside the CB_n cavity, whereas terminal methyls are positioned outside near the CB' s portals. Broadening of the guest signals during the titration of **5** with CB8 (Figure 2, line ii) can be attributed to the faster exchange compared to CB7. Similarly, the inclusion complexes of cubane-1,4-dicarboxylic acid (**1**) and diol **2** with CB7 in slow exchange mode were detected via ^1H NMR titrations (for

corresponding stacking plots, see the Supporting Information (SI), Figures S9 and S11).

To obtain comprehensive insight into the complexation ability of cubane guests, we performed ^1H NMR titrations with β -CD. The noncationic guests **1** and **2** displayed an unambiguous downfield shift of the cubane signals, indicating the formation of inclusion complexes in fast exchange mode with the cubane moiety inside the CD cavity (for the spectra, see SI, Figures S8 and S10). In contrast, the signals of the guest **5** displayed an order of magnitude smaller chemical shifts upon titration with β -CD.

Continuing our study, we determined the thermodynamic binding parameters by means of titration calorimetry (ITC). Because there is no serious need for buffering, we performed titrations of the permanently dicationic guest **5** and noncharged diol **2** in pure water to avoid competition between guest and buffer components. Nevertheless, we also provide data, which were obtained using 50 mM AcONa buffer, to allow comparison with results from other laboratories. All these titration data indicated a 1:1 binding mode. The acid **1** was titrated in 1 mM HCl (pH = 2.88) to maintain its protonated form (the dissociation constants of **1**, $\text{p}K_{\text{a},1} = 3.83$ and $\text{p}K_{\text{a},2} = 5.13$, were determined by acidimetric titration). The ITC showed no interaction of **1** with CB8, and only a relatively weak interaction (millimolar dissociation constants) with β -CD and CB7 (the K values are summarized in Table 1, and full ITC data are given in Table S4). In pure water, no complexation was detected for **1**. The diol **2** can be considered as a model compound, in which binding with CB_n 's is not affected by ion-dipole interactions between the guest and the portals of CB_n . As seen in Table 1, **2** binds CB7 and CB8 significantly more strongly than **1**; the approximate $\log K$ values in water are 8 and 4, respectively. In agreement with the well-known competition of ionic guests and metal ions for the portals of CB_n , 10 times lower binding strengths were observed in AcONa buffer. Finally, as the cationic moieties of **5** can be attracted to the portals of CB_n via ion-dipole interactions, the guest **5** displayed 10^{4-5} times stronger binding toward CB7/8 than **2**. Note that the relative increase in the binding strength is significantly higher for CB8 than that for CB7 (6.7X in water and 3.4X in AcONa buffer; the $K_{5@CB7}/K_{2@CB7}$ and $K_{5@CB8}/K_{2@CB8}$ ratios were compared). We speculate that this increase in binding strength can be attributed to the more effective involvement of imidazolium moieties through C–H \cdots O interactions within the portals or the better accommodation of guests by the wider CB8 cavity. As seen below, the X-ray data support the latter conclusion.

All the three complexes of **5**, whose formation in solution was indicated by either NMR or ITC, were detected using the ESI MS technique. The structures of the complexes with the

Table 1. ITC-Determined Values of K for the Interactions of **1**, **2**, and **5** with CB7, CB8, and β -CD at 303 K, Reported in $\text{dm}^3 \text{mol}^{-1}$ ^a

	CB7	CB8	β -CD
1 ^b	$(3.5 \pm 0.3) \times 10^3$	nb ^k	$(3.7 \pm 0.8) \times 10^3$
2 ^c	$(5.6 \pm 0.2) \times 10^{7e}$	$(2.08 \pm 0.07) \times 10^4$	$(1.62 \pm 0.04) \times 10^3$
2 ^d	$(2.19 \pm 0.02) \times 10^6$	$(1.2 \pm 0.4) \times 10^3$	$(1.66 \pm 0.02) \times 10^3$
5 ^c	$(6.0 \pm 0.6) \times 10^{11f}$	$(1.5 \pm 0.2) \times 10^{9g}$	nb ^k
5 ^d	$(6.4 \pm 0.6) \times 10^{10f}$	$(1.2 \pm 0.5) \times 10^{8g}$	nb ^k

^aThe titration experiments were performed in triplicate. ^bIn 1 mM HCl. ^cIn water. ^dIn 50 mM AcONa. ^eCyclopentanone used as competitor. ^f1,6-Hexamethylene diamine·2HCl used as competitor. ^gMethylviologen used as a competitor. ^hnb = no binding detected by ITC.

CB n hosts were determined by tandem mass spectrometry. For the corresponding spectra, see SI, Figures S15–S17.

Since we succeeded in growing single crystals of 5@CB7 and 5@CB8, we can provide direct insight into their solid-state geometries (side and front views are depicted in Figure 3). It is

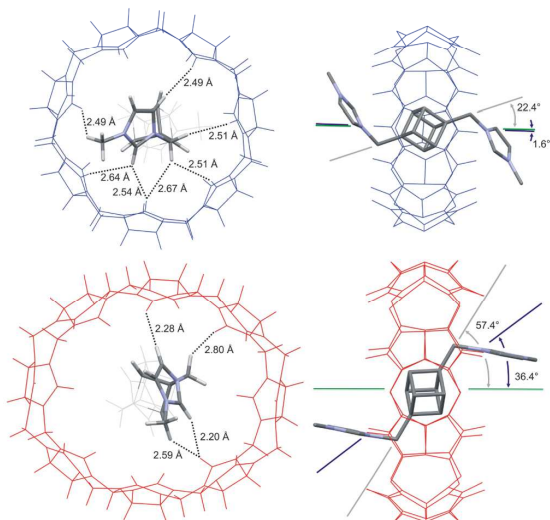


Figure 3. Solid-state structure of 5@CB7 (top) and 5@CB8 (bottom) determined by X-ray diffraction. Iodide counterions are not shown for clarity. Hydrogen short contacts within the portals are drawn with dotted lines. Gray lines are virtual axes of 1,4-disubstituted cubane moiety, blue lines go through the N atoms adjacent to the cubane moiety, and green lines go through the centers of gravity of O atoms in opposite portals.

well-known that ion–dipole interactions are one of the most important attractive forces that hold the CB n inclusion complexes together. Since the CB n 's have two identical, opposite-facing carbonyl-rimmed portals, the cage moieties, which can be disubstituted along the axis, are the most promising candidates for construction of high-affinity guests. Because of the strong rigidity of the CB n macrocycle, the distance between the two centers of positive charge in the guest molecule plays a very important role. Considering the 4,9-disubstituted diamantane to be at this point the best suited for CB7 (the N $^+$...N $^+$ distance in 4,9-bis(trimethylammonio)-diamantane (BTAD) is 7.78 Å, and the bridgehead-to-bridgehead distance is $d_{BB} = 4.64$ Å),¹ it is clear that much more compact bicyclo[2.2.2]octane ($d_{BB} = 2.60$ Å) or cubane ($d_{BB} = 2.70$ Å) moieties must be extended by suitable linkers between the hydrocarbon cage and cationic moieties to prevent the nonpreferred burying of cations deep into the portals. Unfortunately, prolongation by sp³ or sp² carbons breaks the symmetry of the axially disubstituted central hydrocarbon cage, and interactions in the portals cannot be fully established. However, this disadvantage can be partially compensated for by tilting of the hydrocarbon cage inside the CB cavity. With the above-mentioned circumstances considered, it is clear that the cubane-based bisimidazolium salts cannot overcome the superior BTAD, with its $K_{(CB7)} = 7.2 \times 10^{17}$ M⁻¹; however, cubane derivatives complement the family of high-affinity guests and are important from both a theoretical and practical point of view.

As Figure 3 shows, there are some remarkable differences in the binding of the guest 5 inside CB7 and CB8. As mentioned above, the imidazolium moieties do not match the symmetry of either the 1,4-disubstituted cubane moiety or cucurbituril. Therefore, the cubane moiety is tilted by 22.4° in the 5@CB7 complex to allow positioning the adjacent N atoms of imidazolium essentially on the virtual c_7 axis of CB7 (i.e., in the portal center). In fact, 5–7 contacts were found in which the O...H distance is lower than the sum of the van der Waals radii in each portal (full list of contacts is given in Table S2 in SI). Surprisingly, the cubane moiety is much more tilted (57.4°) in the 5@CB8 complex. The two most important consequences are that imidazolium cations are moved far from the centers of the portals and methylene bridges are buried into the cavity. Accordingly, only four short contacts (Figure 3) were found in the portal, and CB8 adopts an elliptical geometry. We infer that the 5@CB8 geometry highlights CB8's inability to bind cations in the centers of its portals.

In addition to ion–dipole interactions, which occur in the CB n portals, the dispersion forces play a significant role in complex stabilization. Although this stabilization force arises everywhere the molecular surfaces are close, the theoretical calculations suggest that short side chains that protrude from the cavity into the external environment contribute to the overall dispersive force by approximately 10–15%.¹⁷ In other words, the most significant contribution to the dispersive force is related to the stiffness of the guest inside the CB n cavity, which can be qualitatively estimated by means of Hirshfeld surface (HS) analysis. The Hirshfeld surface can be straightforwardly computed from crystallographic data and, simply said, reflects the intermolecular interactions in a very subtle way.¹⁸ Although HS is usually used for the analysis of intermolecular interactions in crystal lattices, it can also provide insight into intermolecular contacts inside macrocycle cavities. We calculated the HS for the hydrocarbon skeleton of 5 (including methylene bridges) and compared it with the HS of the diamantane moiety in the BTAD@CB7 complex, which was published by Isaacs and co-workers.¹ The side and front views of the complexes with the HS, on which the distances from the adjacent inside atoms are encoded from red (close) to blue (far), are depicted in Figure 4 (top). The fingerprints display the distance from each point on the HS toward the closest atom inside and outside the surface, which is indicative

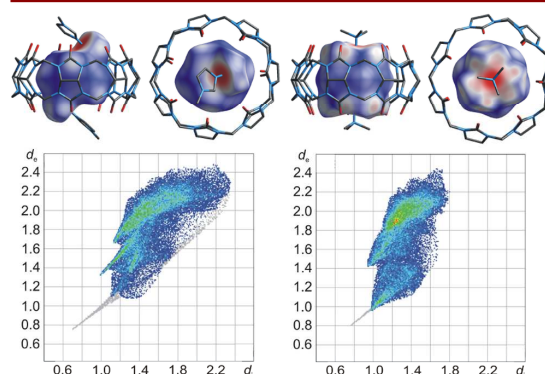


Figure 4. Hirshfeld surfaces (top and side views) and corresponding fingerprints for 5@CB7 (left) and BTAD@CB7¹ (right). Gray dots are related to the Cⁱ–N^e intramolecular covalent bonds.

Organic Letters

Letter

of guest stiffness inside the cavity. As can be clearly seen in Figure 4 (bottom), on the HS, the distances of inner atoms in the diamantane complex do not exceed 1.8 Å. In contrast, a significant number of surface points for 5@CB7 have d_i coordinates within the range of 1.80–2.35 Å. This clearly indicates that the cubane moiety does not fill the inner space of the CB7 cavity as nicely as diamantane. Therefore, it is reasonable to suppose that the contribution of dispersive forces inside the CB7 cavity is significantly lower for our cubane guest than that for the diamantane derivatives.

In conclusion, we introduced the first dicationic supra-molecular guest 5 based on a highly symmetric hydrocarbon cubane cage and investigated its ability to form host–guest complexes with CB7, CB8, and β -CD. The association constants of 5 with CB7 and CB8, i.e., $(6.0 \pm 0.6) \times 10^{11} \text{ M}^{-1}$ and $(1.5 \pm 0.2) \times 10^9 \text{ M}^{-1}$ in water, are lower than those for the strongest complex, as known to date, BTAD@CB7,¹ which is likely due to the imperfect symmetry of the imidazolium cationic moieties and lower degree of dispersive interactions of the much smaller cubane inside the CB7 cavity. However, this work demonstrates that the cubane moiety can be combined with adjacent cationic moieties to expand the family of the high-affinity guests and thus be considered in the design of multitopic guests in which binding sites with diverse properties are desired.

■ ASSOCIATED CONTENT

● Supporting Information

The Supporting Information is available free of charge on the ACS Publications website at DOI: 10.1021/acs.orglett.7b01029.

Experimental procedures and analytical data for all new compounds; NMR, ITC, and MS data for the complexes (PDF)

X-ray data for inclusion complex 5@CB7 (CIF)

X-ray data for inclusion complex 5@CB8 (CIF)

X-ray data for intermediate 4 (CIF)

■ AUTHOR INFORMATION

Corresponding Author

*E-mail: rvicha@ft.utb.cz.

ORCID

Robert Vicha: 0000-0002-5229-9863

Notes

The authors declare no competing financial interest.

■ ACKNOWLEDGMENTS

This work was financially supported by the Internal Founding Agency of Tomas Bata University in Zlín, Project No. IGA/FT/2017/001. The CIISB Research Infrastructure Project LM2015043 funded by MEYS CR is gratefully acknowledged for the financial support of the measurements at the CEITEC X-ray Diffraction and Bio-SAXS Core Facility. The authors thank Lukáš Maier from Masaryk University (Brno, Czech Republic) for assistance with the NMR measurements.

■ REFERENCES

- (1) Cao, L.; Šekutor, M.; Zavalij, P. Y.; Mlinarić-Majerski, K.; Glaser, R.; Isaacs, L. *Angew. Chem., Int. Ed.* **2014**, *53*, 988–993.
- (2) Moghaddam, S.; Yang, C.; Rekharsky, M.; Ko, Y. H.; Kim, K.; Inoue, Y.; Gilson, M. K. *J. Am. Chem. Soc.* **2011**, *133*, 3570–3581.

- (3) Rekharsky, M. V.; Mori, T.; Yang, C.; Ko, H. K.; Selvapalam, N.; Kim, H.; Sobransingh, D.; Kaifer, A. E.; Liu, S.; Isaacs, L.; Chen, W.; Moghaddam, S.; Gilson, M. K.; Kim, K.; Inoue, Y. *Proc. Natl. Acad. Sci. U. S. A.* **2007**, *104*, 20737–20742.

- (4) (a) Branná, P.; Rouchal, M.; Prucková, Z.; Dastyčová, L.; Lenobel, R.; Pospíšil, T.; Maláč, K.; Vicha, R. *Chem. - Eur. J.* **2015**, *21*, 11712–11718. (b) Sun, H.-L.; Zhang, H.-Y.; Dai, Z.; Han, X.; Liu, Y. *Chem. - Asian J.* **2017**, *12*, 265–270. (c) Yan, Z.; Huang, Q.; Liang, W.; Yu, X.; Zhou, D.; Wu, W.; Chruma, J. J.; Yang, C. *Org. Lett.* **2017**, *19*, 898–901.

- (5) May, B. L.; Clements, P.; Tsanaktsidis, J.; Easton, C. J.; Lincoln, S. F. *J. Chem. Soc., Perkin Trans. 1* **2000**, 463–469.

- (6) Lukin, K. A.; Li, J.; Eaton, P. E.; Kanomata, N.; Hain, J.; Punzalan, E.; Gilardi, R. *J. Am. Chem. Soc.* **1997**, *119*, 9591–9602.

- (7) (a) Mahkam, M.; Sanjani, N. S. *Polym. Int.* **2000**, *49*, 260–264. (b) Yeh, N.-H.; Chen, C.-W.; Lee, S.-L.; Wu, H.-J.; Chen, C.-h.; Luh, T.-Y. *Macromolecules* **2012**, *45*, 2662–2667.

- (8) Priefer, R.; Lee, Y. J.; Barrios, F.; Wosnick, J. H.; Lebus, A. M.; Farrell, P. G.; Harpp, D. N.; Sun, A.; Wu, S.; Snyder, J. P. *J. Am. Chem. Soc.* **2002**, *124*, 5626–5627.

- (9) Churches, Q. I.; Mulder, R. J.; White, J. M.; Tsanaktsidis, J.; Duggan, P. J. *Aust. J. Chem.* **2012**, *65*, 690–693.

- (10) Biegasiewicz, K. F.; Ingalsbe, M. L.; St. Denis, J. D.; Gleason, J. L.; Ho, J.; Coote, M. L.; Savage, G. P.; Priefer, R. *Beilstein J. Org. Chem.* **2012**, *8*, 1814–1818.

- (11) Biegasiewicz, K. F.; Griffiths, J. R.; Savage, G. P.; Tsanaktsidis, J.; Priefer, R. *Chem. Rev.* **2015**, *115*, 6719–6745.

- (12) Eaton, P. E. *Angew. Chem., Int. Ed. Engl.* **1992**, *31*, 1421–1436.

- (13) (a) Chalmers, B. A.; Xing, H.; Houston, S.; Clark, C.; Ghassabian, S.; Kuo, A.; Cao, B.; Reitsma, A.; Murray, C.-E. P.; Stok, J. E.; Boyle, G. M.; Pierce, C. J.; Littler, S. W.; Winkler, D. A.; Bernhardt, P. V.; Pasay, C.; De Voss, J. J.; McCarthy, J.; Parsons, P. G.; Walter, G. H.; Smith, M. T.; Cooper, H. M.; Nilsson, S. K.; Tsanaktsidis, J.; Savage, G. P.; Williams, C. M. *Angew. Chem.* **2016**, *128*, 3644–3649. (b) Wlochal, J.; Davies, R. D. M.; Burton, J. *Org. Lett.* **2014**, *16*, 4094–4097.

- (14) Chapman, N. B.; Key, J. M.; Toyne, K. J. *J. Org. Chem.* **1970**, *35*, 3860–3867.

- (15) Eaton, P. E.; Cole, T. W. *J. Am. Chem. Soc.* **1964**, *86*, 962–964.

- (16) Griffiths, J. R.; Tsanaktsidis, J.; Savage, G. P.; Priefer, R. *Thermochim. Acta* **2010**, *499*, 15–20.

- (17) Hostaš, J.; Sigwalt, D.; Šekutor, M.; Ajani, H.; Dubecký, M.; Řezáč, J.; Zavalij, P. Y.; Cao, L.; Wohlschlager, C.; Mlinarić-Majerski, K.; Isaacs, L.; Glaser, R.; Hobza, P. *Chem. - Eur. J.* **2016**, *22*, 17226–17238.

- (18) Spackman, M. A.; Jayatilaka, D. *CrystEngComm* **2009**, *11*, 19–32.



V. ZÁVĚR

Vše, co bylo v předchozích kapitolách popsáno, je minulost. Zdá se ale možné na ni navázat a minimálně některé směry dále rozvíjet. Předně je tu otázka přípravy a studia vazebných možností nových vazebných motivů. Nemám ovšem na mysli planné obměňování struktury a zkoušení všeho možného, nýbrž racionální návrhy vycházející z dosavadních zkušeností a případně molekulového modelování, přičemž hlavním cílem by měly být ligandy s výrazně diferencovanými afinitami k různým makrocyclům. Například se nabízí k vyřešení otázka, zdali je možné ještě dále zvyšovat afinitu ligandů k β -CD a případně při tom modulovat afinitu k CB_n . Aktuálně připravujeme publikaci o adamantanových ligandech s K atakujícími hodnoty okolo 10^7 M^{-1} . Rovněž velmi zajímavé, jak z teoretického, tak z praktického hlediska by mohly být ligandy odvozené od klecových uhlovodíků mající elektrondeficitní, ale nikoliv kladně nabitě skupiny atomů v místech vhodných pro interakci s CB_n portály.

Pro přípravu sebeorganizujících multitopických ligandů využitelných například pro molekulární sondy se zatím jako perspektivnější jeví lineární uspořádání vazebných motivů. Proto je nutné vypracovat obecný praktický přístup k syntéze rozmanitých heterotritopických, případně heterotetra(a více)topických ligandů. Zatím připravujeme centrální část se dvěma ekvivalentními reakčními centry, na která poté připojujeme, zpravidla v přebytku reakčního činidla, terminální vazebné motivy za vzniku ligandů typu $A-B-A$. Tento postup lze využít i pro přípravu požadovaných ligandů $A-B-C$, ovšem za předpokladu, že budeme schopni efektivně zachytit a izolovat první stupeň reakce. Jiný přístup spočívá v přípravě centrální části se dvěma odlišnými reakčními centry s různou reaktivitou vzhledem k syntonům terminálních míst. Oba tyto přístupy aktuálně experimentálně ověřujeme.

Poslední oblast, kterou považuji za velmi aktuální je studium supramolekulárního chování vhodných derivátů nových, dosud neprobádaných klecových uhlovodíků. Například nebyl dosud publikován žádný ligand odvozený od klecového uhlovodíku vhodný pro CB_6 . Přitom právě tyto ligandy, vyplňující sférickou kavitu CB_6 lépe než lineární alifatické uhlovodíky mohou poskytnout komplexy se stabilitou výrazně vyšší než je dnešních rekordních $pK(CB_6) = 10,73$ pro spermin.³³ Že není zcela vyloučené takový ligand nalézt, naznačují hodnoty PC diskutované v kapitole 3.4.

Tato habilitační práce by dost možná vypadala úplně jinak, kdyby mi můj současný zaměstnavatel, tedy Univerzita Tomáše Bati ve Zlíně, nedovolil postupně vytvořit výzkumnou skupinu zabývající se supramolekulární chemií. Chci mu tedy poděkovat za důvěru.

Nikdy bych nemohl dotáhnout do konce publikace, které jsou předmětem této habilitační práce bez kolegů Michala Rouchala, Lenky Dastychové a Zdeňky Pruckové, bez doktorandů Zuzky Kozubkové, Jarmily Černochové, Evy Babjakové, Petry Branné, Jany Hermanové, Andrei Čablové, Shantana Kulkarni, Aleny Matelové, Evy Achbergerové, Davida Gergely, Jelici Kovačević, Hedy Surmové a Kristýny Jelínkové a bez řady diplomantů, kteří se odvážili pracovat na tématech na FT UTB ne zcela obvyklých a etablovaných.

Nesmím zapomenout zmínit nemalý příspěvek kolegů z jiných pracovišť spočívající v měření RTG difrakce a analýze získaných dat Markem Nečasem (MU) a Martinem Babiakem (MU), molekulovém modelování Petrem Kulhánkem (MU), Ivem Kuřitkou (UTB), Barborou Hanulíkovou (UTB), Kamilem Maláčem (UTB) a Honzou Víchou (MU, UTB), v pomoci Lukáše Maiera (MU), Zdeňka Moravce (MU), Radka Marka (MU) a Tomáše Pospíšila (UPOL) s měřením NMR spekter, v měření ESI-MS Richardem Čmelíkem (AV ČR) a HRMS René Lenobelem (UPOL) a v zapůjčení fotochemického reaktoru Petrem Klánem (MU) bez něj bychom asi neuvařili žádný kuban.

Jitko, Dorotko, Ivánku a Emo, díky za schovívavost a trpělivost.

Nakonec jeden vzkaz Antonínovi Tálskému, který mne kdysi, zřejmě nechtě, nasměroval k chemii a v časech studií i potom všemožně podporoval. Moc si přál, abych tu habilitační práci konečně sepsal, ale na dokončení si nepočkal. Tak už je to hotové. Díky.

VI REFERENCE

- ¹ R. Vícha, M. Potáček: *Tetrahedron* **2005**, *61*, 83–88.
- ² R. Vícha, M. Nečas, M. Potáček: *Collect. Czech. Chem. Commun.* **2006**, *71*, 709–722.
- ³ R. Vícha, M. Potáček: *Chem. Listy* **2004**, *98*, 68–74.
- ⁴ R. Vícha, I. Kuřitka, M. Rouchal, V. Ježková, A. Zierhut: *ARKIVOC* **2009** (xii), 60–80.
- ⁵ (a) E. Babjaková, B. Hanulíková, L. Dastychová, I. Kuřitka, M. Nečas, R. Vícha: *J. Mol. Struct.* **2014**, *1078*, 106–113; (b) E. Babjaková, L. Dastychová, B. Hanulíková, I. Kuřitka, M. Nečas, H. Vašková, R. Vícha: *J. Mol. Struct.* **2015**, *1085*, 207–214.
- ⁶ Z. Kozubková, M. Rouchal, M. Nečas, R. Vícha: *Helv. Chim. Acta* **2012**, *95*, 1003–1017.
- ⁷ (a) L. Gřundělová, A. Mráček, R. Vícha, P. Smolka, A. Minařík, A. Gregorova: *Carbohydr. Polym.* **2015**, *119*, 142–148; (b) A. Matelová, G. Huerta-Angeles, D. Šmejkalová, Z. Brůnová, J. Dušek, R. Vícha, V. Velebný: *Carbohydr. Polym.* **2016**, *151*, 1175–1183; (c) T. Václavková, J. Růžička, M. Julinová, R. Vícha, M. Koutný: *Appl. Microbiol. Biotechnol.* **2007**, *76*, 911–917.
- ⁸ M. V. Rekharsky, Y. Inoue: *Chem. Rev.* **1998**, *98*, 1875–1918.
- ⁹ (a) S. Ain, B. Kumar, K. Pathak: *Int. J. Pharm. Chem. Biol. Sci.* **2015**, *5*, 583–593; (b) V. J. Stela, R. A. Rajewski: *Pharm. Res.* **1997**, *14*, 556–567; (c) J. Szejtli, T. Osa: *Comprehensive Supramolecular Chemistry* **1996**, *3*, 441–450.
- ¹⁰ Y. Li, J. Zhang, W. Gao, L. Zhang, Y. Pan, S. Zhang, Y. Wang: *Int. J. Mol. Sci.* **2015**, *16*, 9314–9340.
- ¹¹ W. F. De Azevedo, S. Leclerc, L. Meijer, L. Havlíček, M. Strnad, S.-H. Kim: *Eur. J. Biochem.* **1997**, *243*, 518–526.
- ¹² M. Otyepka, V. Kryštof, L. Havlíček, V. Singlerová, M. Strnad, J. Koča: *J. Med. Chem.* **2000**, *43*, 2506–2513.
- ¹³ K. Vermeulen, M. Strnad, V. Kryštof, L. Havlíček, A. Van der Aa, M. Lenjou, G. Nijs, I. Rodrigues, B. Stockman, H. van Onckelen, D. R. Van Bockstaele, Z. N. Berneman: *Leukemia* **2002**, *16*, 299–305.
- ¹⁴ D. Taura, Y. Taniguchi, A. Hashidzume, A. Harada: *Macromol. Rapid Commun.* **2009**, *30*, 1741–1744.
- ¹⁵ A. J. Arduengo III, R. L. Harlow, M. Kline: *J. Am. Chem. Soc.* **1991**, *113*, 361–363.
- ¹⁶ K. I. Assaf, W. M. Nau: *Chem. Soc. Rev.* **2015**, *44*, 394–418.
- ¹⁷ H. L. Sun, H. Y. Zhang, D. Dai, X. Han, Y. Liu: *Chem. Asian J.* **2017**, *12*, 265–270.
- ¹⁸ (a) P. Kaszynski, J. Michl: *J. Org. Chem.* **1988**, *53*, 4593–4594; (b) K. R. Mondanaro, W. P. Dailey: *Org. Syn.* **2004**, *Coll. Vol. 10*, 658; (c) J. Kaleta, C. Mazal: *Org. Lett.* **2011**, *13*, 1326–1329.
- ¹⁹ (a) S. Moghaddam, C. Yang, M. V. Rekharsky, Y. H. Ko, K. Kim, Y. Inoue, M. K. Gilson: *J. Am. Chem. Soc.* **2011**, *133*, 3570–3581; (b) N. Le Marquer, M. Y. Laurent, A. Martel: *Synthesis* **2015**, *47*, 2185–2187.
- ²⁰ (a) N. B. Chapman, J. M. Key, K. J. Toyne: *J. Org. Chem.* **1970**, *35*, 3860–3867; (b) P. E. Eaton, T. W. J. Cole: *J. Am. Chem. Soc.* **1964**, *86*, 962–964.
- ²¹ (a) F. Tureček, V. Hanuš, P. Sedmera, H. Antropiusová, K. Mach: *Collect. Czech. Chem. Commun.* **1981**, *46*, 1474–1485; (b) N. A. Fokina, B. A. Tkachenko, A. Merz, M. Serafin, J. E. P. Dahl, R. M. K. Carlson, A. A. Fokin, P. R. Schreiner: *Eur. J. Org. Chem.* **2007**, 4738–4745; (c) N. A. Fokina, B. A. Tkachenko, J. E. P. Dahl, R. M. K. Carlson, A. A. Fokin, P. R. Schreiner: *Synthesis* **2012**, *44*, 259–264.
- ²² B. J. May, P. Clements, J. Tsanaksidis, C. J. Easton, S. F. Lincoln: *J. Chem. Soc., Perkin Trans. 1* **2000**, 463–469.
- ²³ R. B. Silverman, J. P. Zhou, P. E. Eaton: *J. Am. Chem. Soc.* **1993**, *115*, 8841–8842.
- ²⁴ D. Sigwalt, M. Šekutor, L. Cao, P. Y. Zavalij, J. Hostaš, H. Ajani, P. Hobza, K. Minarič-Majerski, R. Glaser, L. Isaacs: *J. Am. Chem. Soc.* **2017**, *139*, 3249–3258.
- ²⁵ (a) D.-S. Guo, V. D. Uzunova, K. I. Assaf, A. I. Lazar, Y. Liu, W. M. Nau: *Supramol. Chem.* **2016**, *28*, 384–395; (b) T. C. Lee, E. Kalenius, A. I. Lazar, K. I. Assaf, N. Kuhnert, C. H. Grun, J. Janis, O. A. Scherman, W. M. Nau: *Nat. Chem.* **2013**, *5*, 376–382.
- ²⁶ S. Mecozzi, J. Rebek, Jr.: *Chem. Eur. J.* **1998**, *4*, 1016–1022.
- ²⁷ W. M. Nau, M. Florea, K. I. Assaf: *Isr. J. Chem.* **2011**, *51*, 559–577.
- ²⁸ Y. H. Zhao, M. H. Abraham, A. M. Zissimos: *J. Org. Chem.* **2003**, *68*, 7368–7373.

- ²⁹ J. Lagona, P. Mukhopadhyay, S. Chakrabarti, L. Isaacs: *Angew. Chem., Int. Ed. Engl.* **2005**, *44*, 4844–4870.
- ³⁰ (a) I. W. Jones, M. A. Lynn, E. A. Mash: *Tetrahedron* **2009**, *65*, 10317–10322; (b) I. W. Jones, Y. Mongushi, A. Dawson, M. D. Carducci, E. A. Mash: *Org. Lett.* **2005**, *7*, 2841–2843.
- ³¹ R. W. Weber, J. M. Cook: *Can. J. Chem.* **1978**, *56*, 189–192.
- ³² (a) N. J. Leonard, J. C. Coll: *J. Am. Chem. Soc.* 1970, *92*, 6685–6686; (b) G. S. Wayne, G. J. Snyder: *Synth. Commun.* **1995**, *25*, 3267–3270.
- ³³ M. V. Rekharsky, T. Mori, C. Yang, Y. H. Ko, N. Selvapalam, H. Kim, D. Sobransingh, A. E. Kaifer, S. Liu, L. Isaacs, W. Chen, S. Moghaddam, M. K. Gilson, K. Kim, Y. A. Inoue: *Proc. Natl. Acad. Sci. U. S. A.* **2007**, *104*, 20737–20742.